Secondary CMB Anisotropy

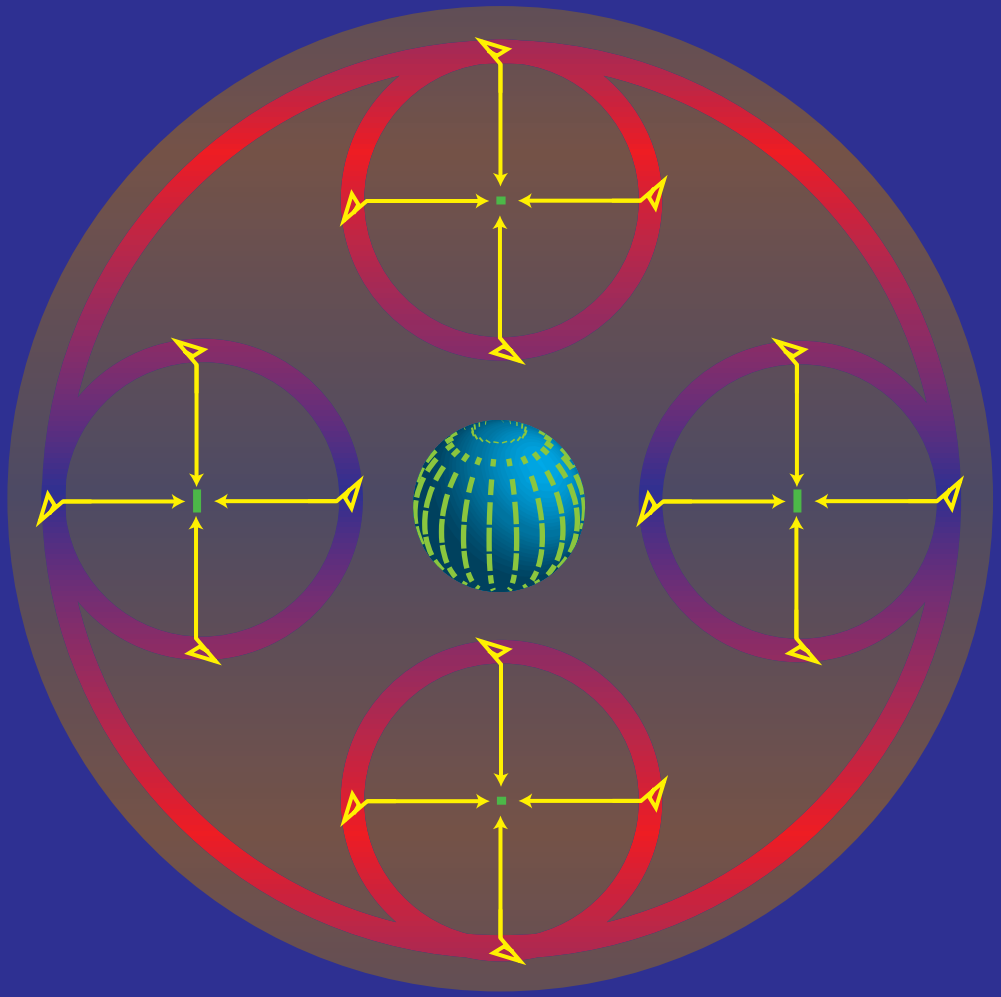

Wayne Hu

Astro 448, Fall 2012

Outline

Cabo Lectures

- Reionization
- B-modes

  Gravitational Lensing
- Cosmic Acceleration

Physics of Secondary Anisotropies

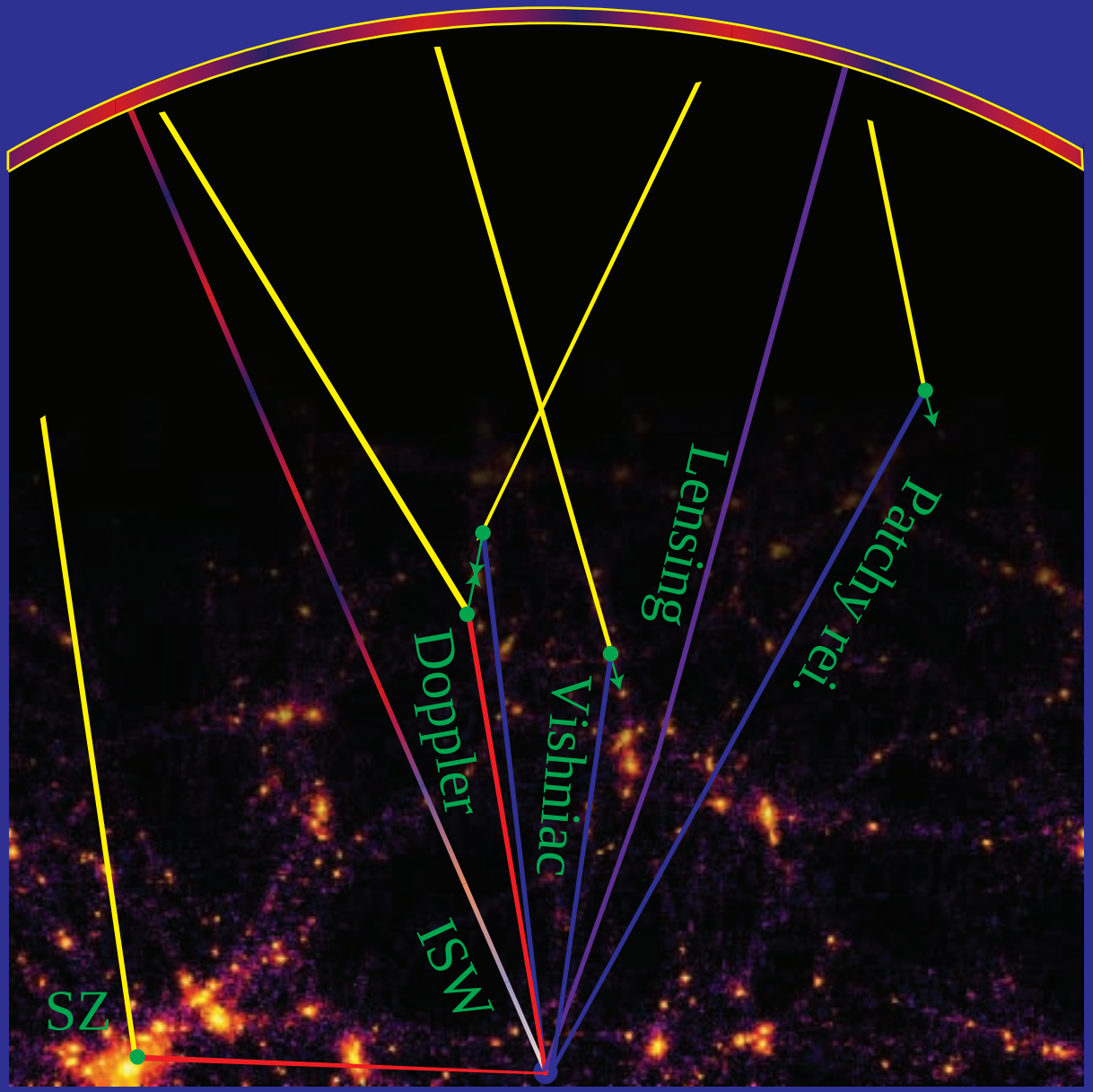

Scattering Secondaries

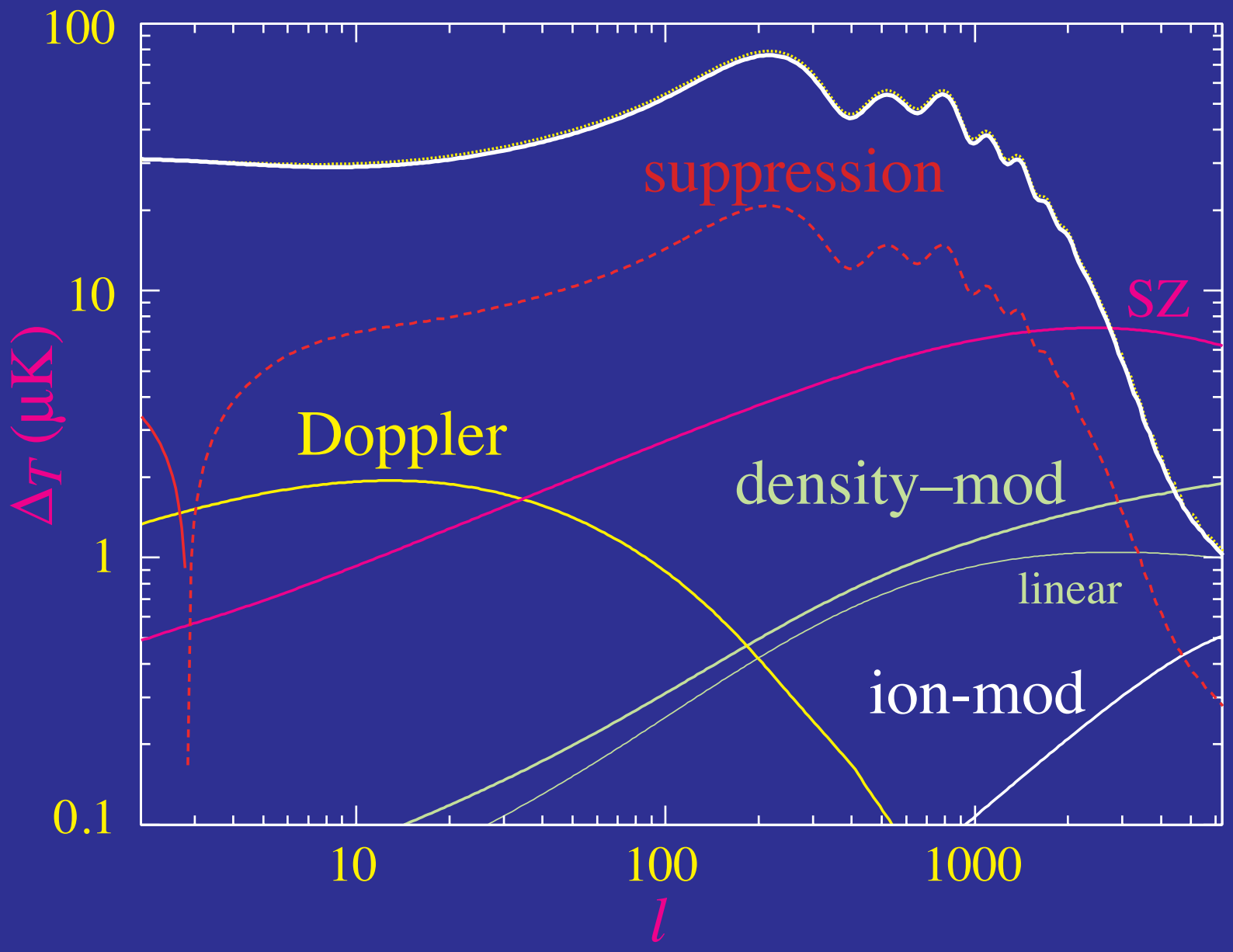

Gravitational Secondaries

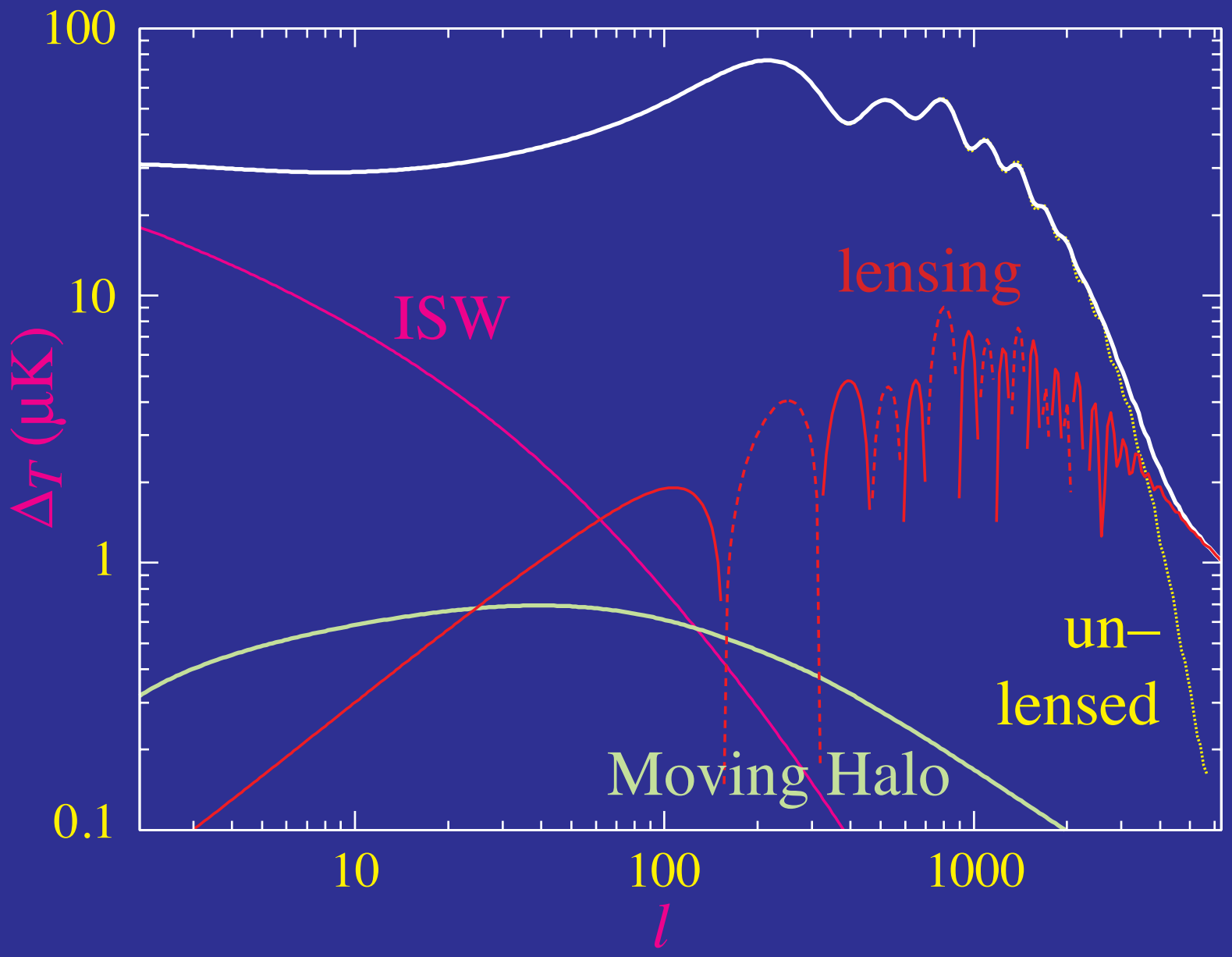

Reionization

Across the Horizon

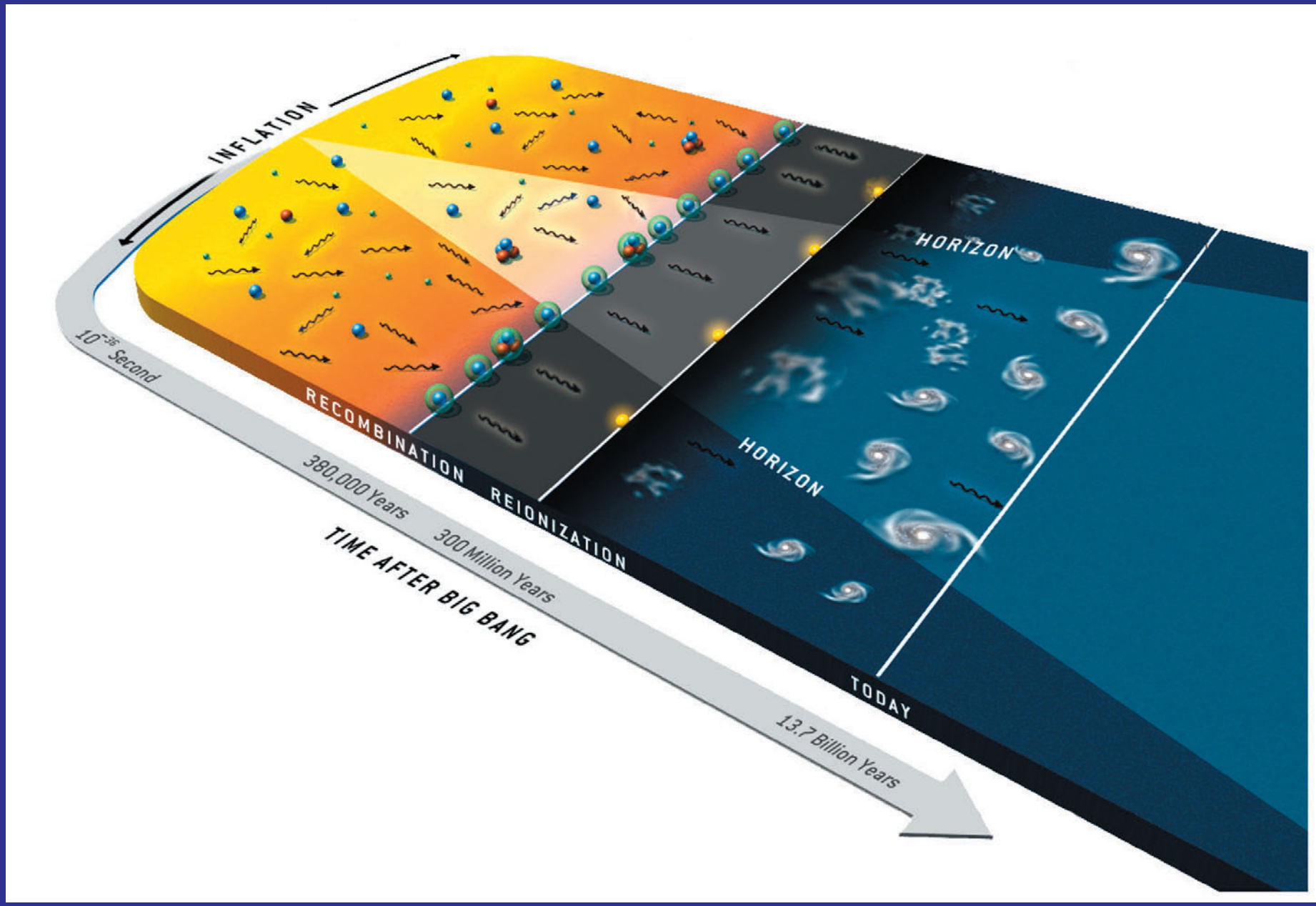

Hu & White (2004); artist:B. Christie/SciAm; available at http://background.uchicago.edu

Anisotropy Suppression

- A fraction $\tau \sim 0.1$ of photons rescattered during reionization out of line of sight and replaced statistically by photon with random temperature flucutuation - suppressing anisotropy as $e^{-\tau}$

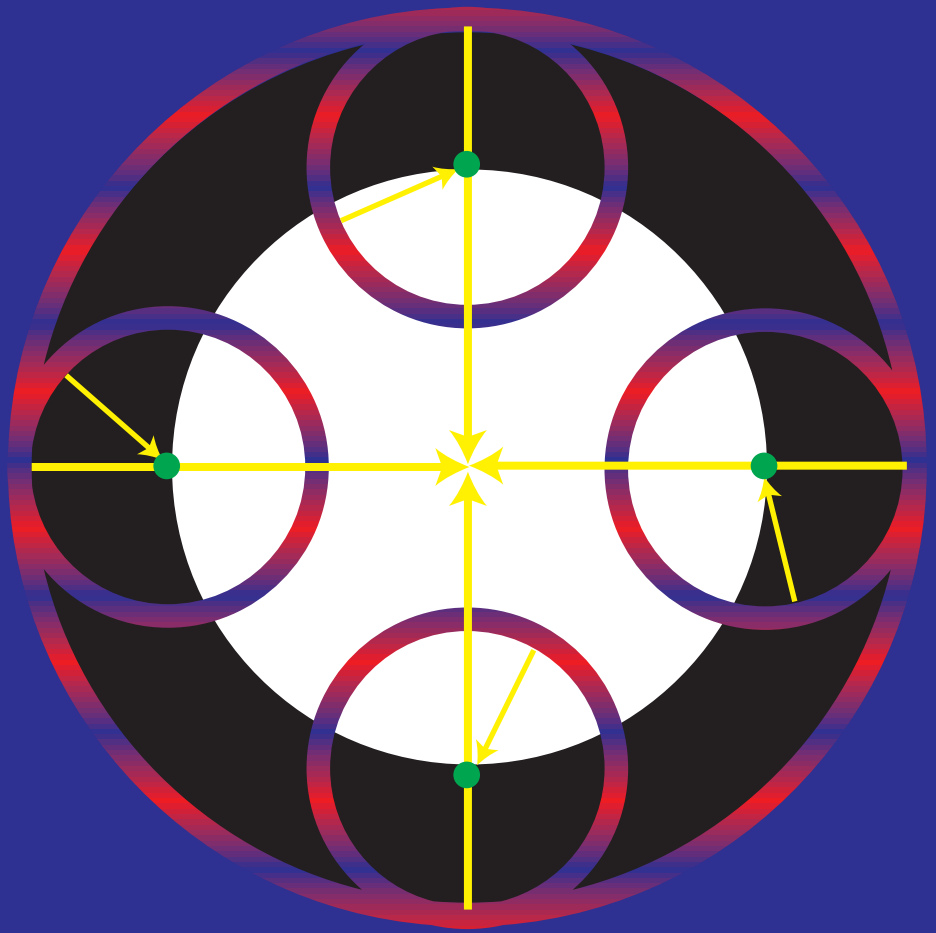

Why Are Secondaries So Smalll?

- Original anisotropy replaced by new secondary sources
- Late universe more developed than early universe

  Density fluctuations nonlinear not 10^{-5}

  Velocity field 10^{-3} not not 10^{-5}
- Shouldn't $\Delta T/T \sim \tau v \sim 10^{-4}$?
- Limber says no!
- Spatial and angular dependence of sources contributing and cancelling broadly in redshift

Integral Solution

- Formal solution to the radiative transfer or Boltzmann equation involves integrating sources across line of sight
- Linear solution describes the decomposition of the source $S_\ell^{(m)}$ with its local angular dependence and plane wave spatial dependence as seen at a distance $\mathbf{x} = D\hat{\mathbf{n}}$.
- Proceed by decomposing the angular dependence of the plane wave

$$e^{i\mathbf{k}\cdot\mathbf{x}} = \sum_\ell (-i)^\ell \sqrt{4\pi(2\ell+1)}\, j_\ell(kD) Y_\ell^0(\hat{\mathbf{n}})$$

- Recouple to the local angular dependence of G_ℓ^m

$$G_{\ell_s}^m = \sum_\ell (-i)^\ell \sqrt{4\pi(2\ell+1)}\, \alpha_{\ell_s \ell}^{(m)}(kD) Y_\ell^m(\hat{\mathbf{n}})$$

Integral Solution

- Projection kernels (monopole, temperature; dipole, doppler):

$$\ell_s = 0, \quad m = 0 \qquad \alpha^{(0)}_{0\ell} \equiv j_\ell$$

$$\ell_s = 1, \quad m = 0 \qquad \alpha^{(0)}_{1\ell} \equiv j'_\ell$$

- Integral solution: for $\Theta = \Delta T/T$

$$\frac{\Theta^{(m)}_\ell(k,0)}{2\ell+1} = \int_0^\infty dD e^{-\tau} \sum_{\ell_s} S^{(m)}_{\ell_s} \alpha^{(m)}_{\ell_s \ell}(kD)$$

- Power spectrum:

$$C_\ell = \frac{2}{\pi} \int \frac{dk}{k} \sum_m \frac{k^3 \langle \Theta^{(m)*}_\ell \Theta^{(m)}_\ell \rangle}{(2\ell+1)^2}$$

- Solving for C_ℓ reduces to solving for the behavior of a handful of sources. Straightforward generalization to polarization.

Anisotropy Suppression and Regeneration

- Recombination sources obscured and replaced with secondary sources that suffer Limber cancellation from integrating over many wavelengths of the source
- Net suppression despite substantially larger sources due to growth of structure except beyond damping tail <10’

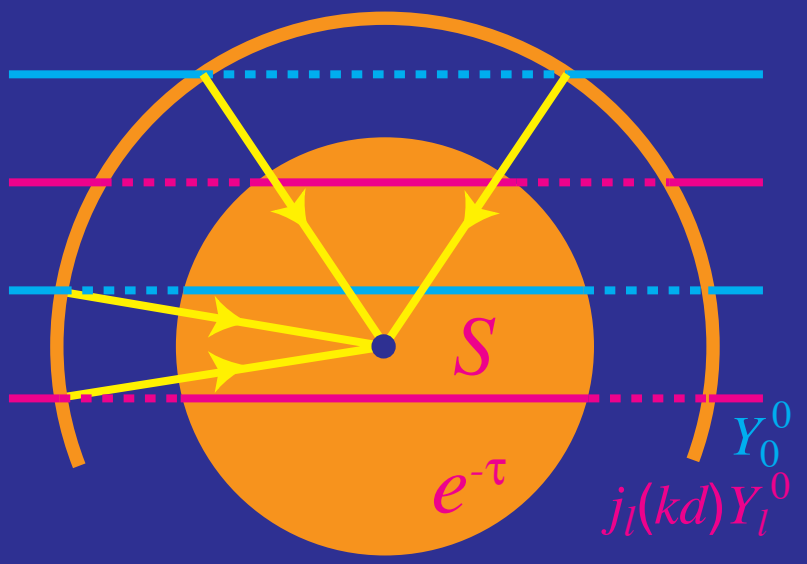

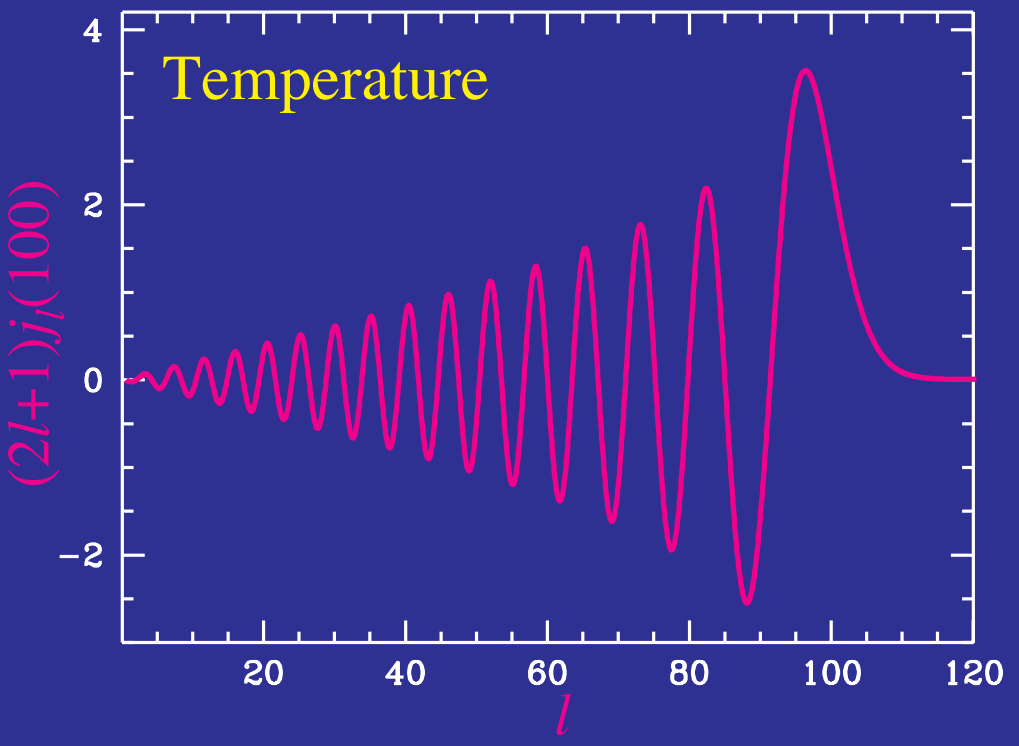

Reionization Suppression

- Rescattering suppresses primary temperature and polarization anisotropy according to optical depth, fraction of photons rescattered

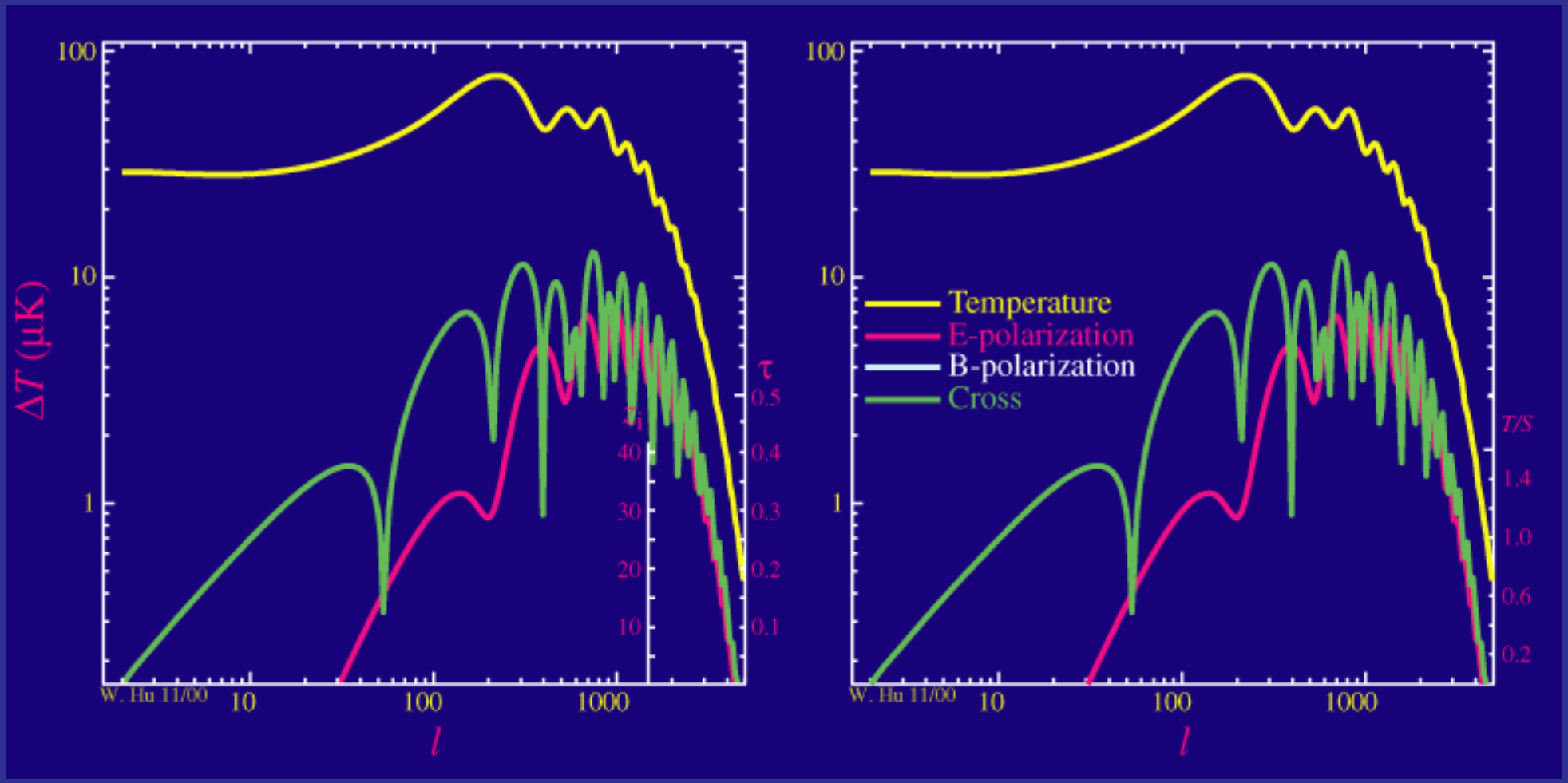

Tilt-τ Degeneracy

- Only anisotropy at reionization (high k), not isotropic temperature fluctuations (low k) - is suppressed leading to effective tilt for WMAP (not Planck)

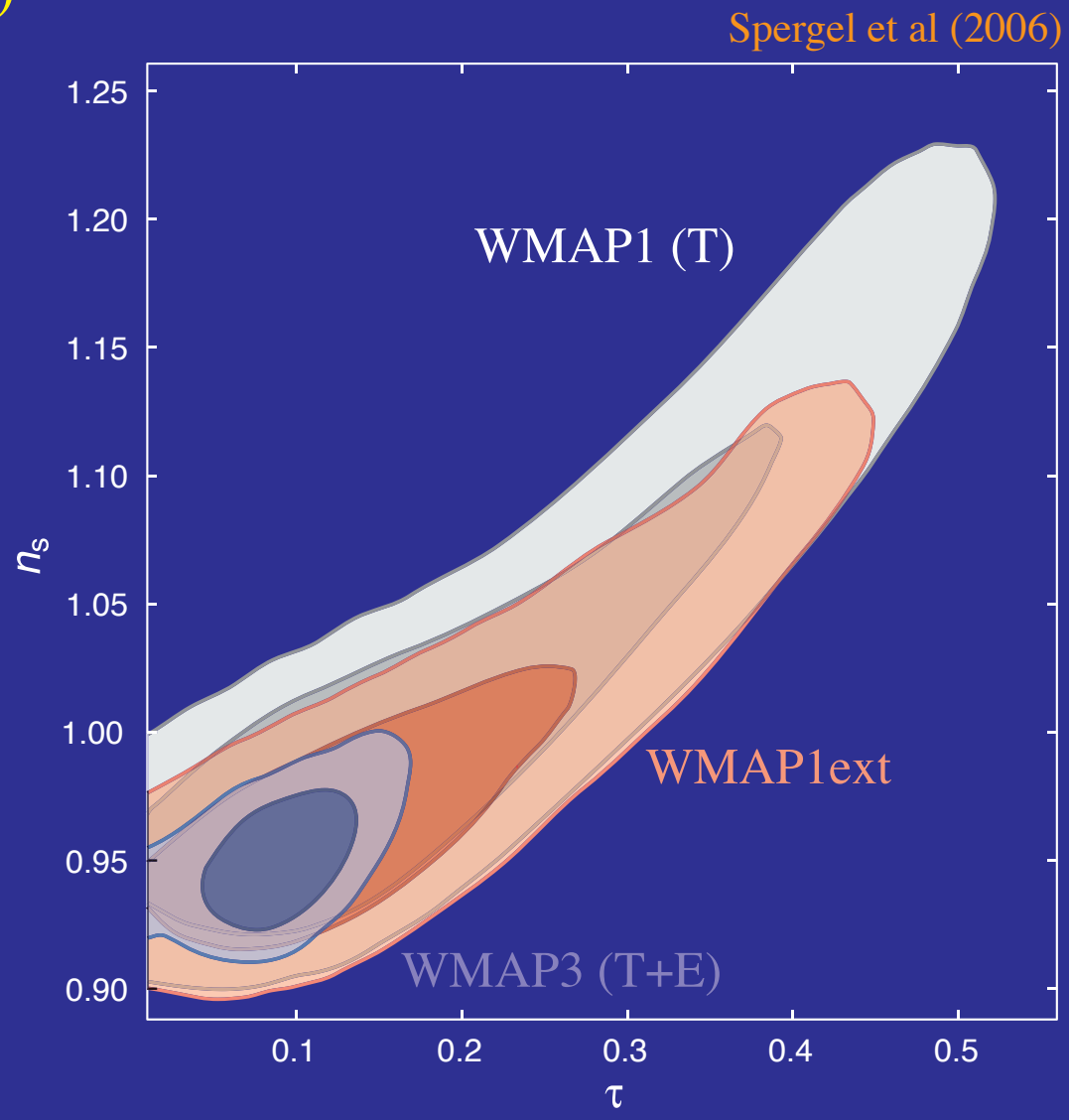

Doppler Effect

Scattering Secondaries

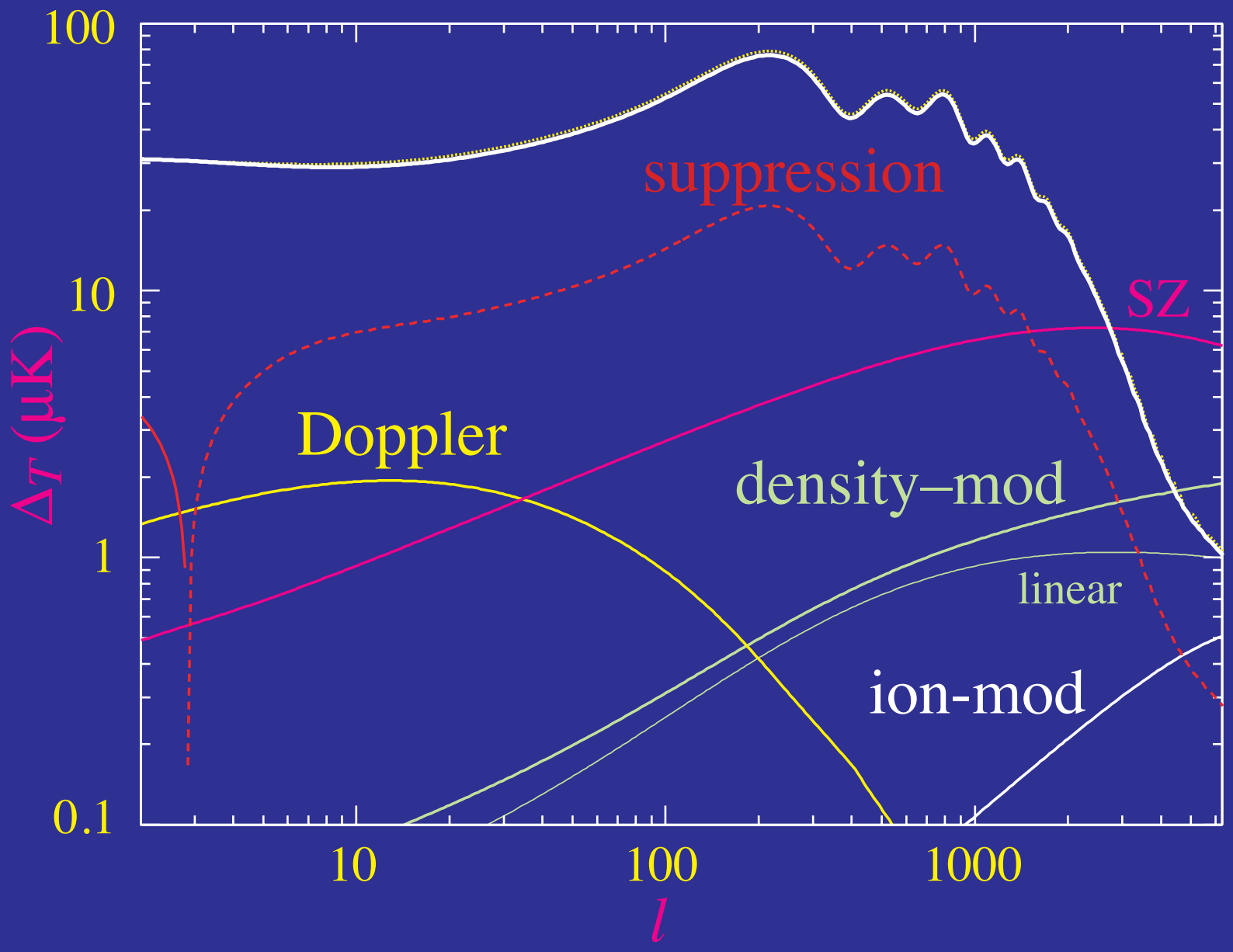

Doppler Effect in Limber Approximation

- Only fluctuations transverse to line of sight survive in Limber approx but linear Doppler effect has no contribution in this direction

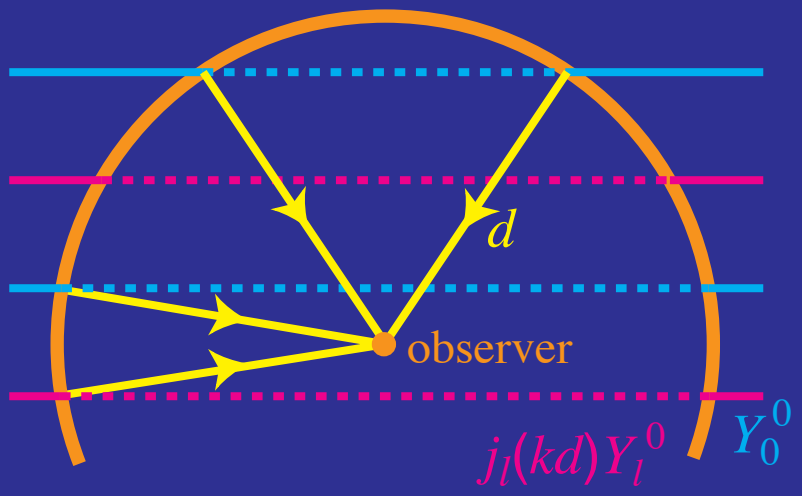

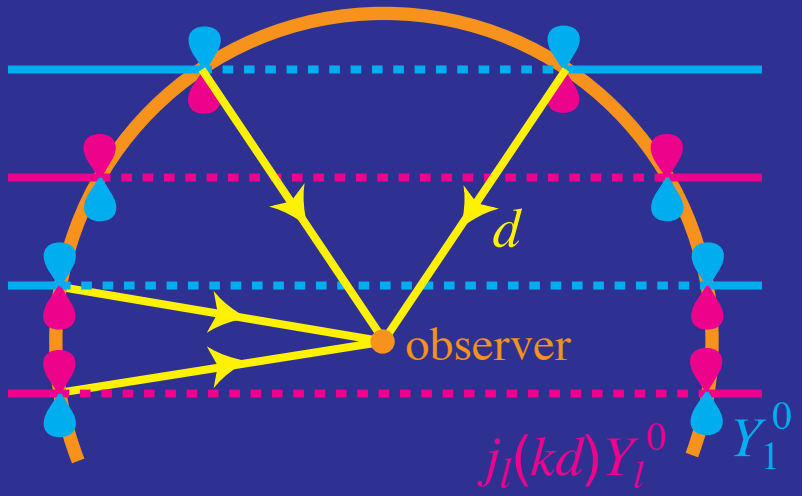

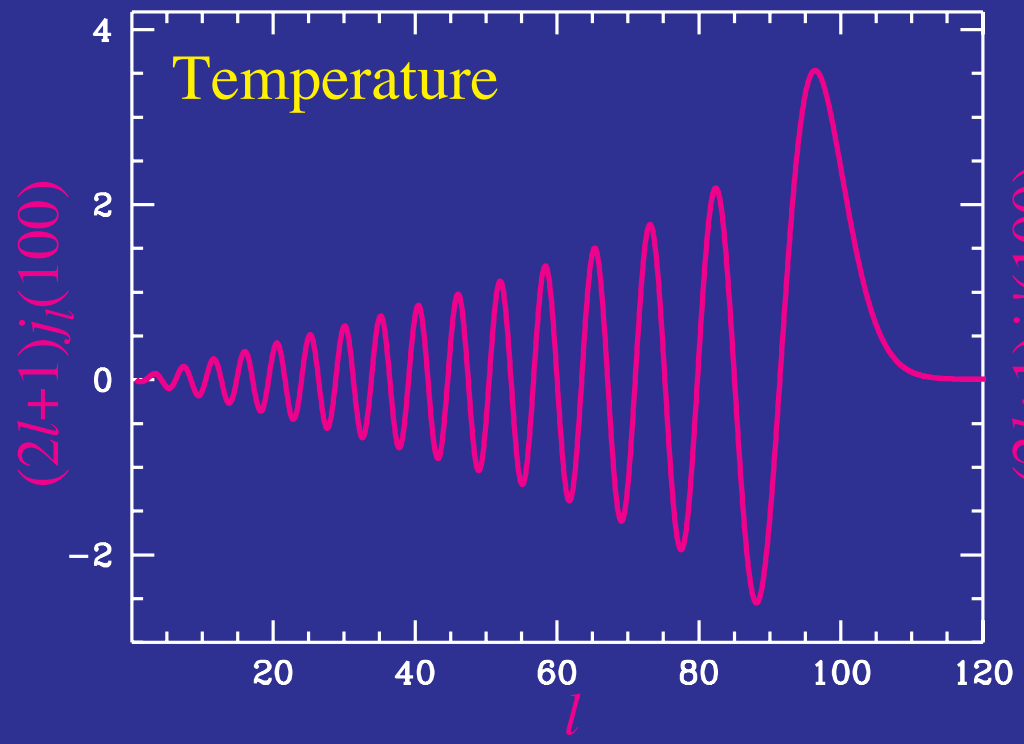

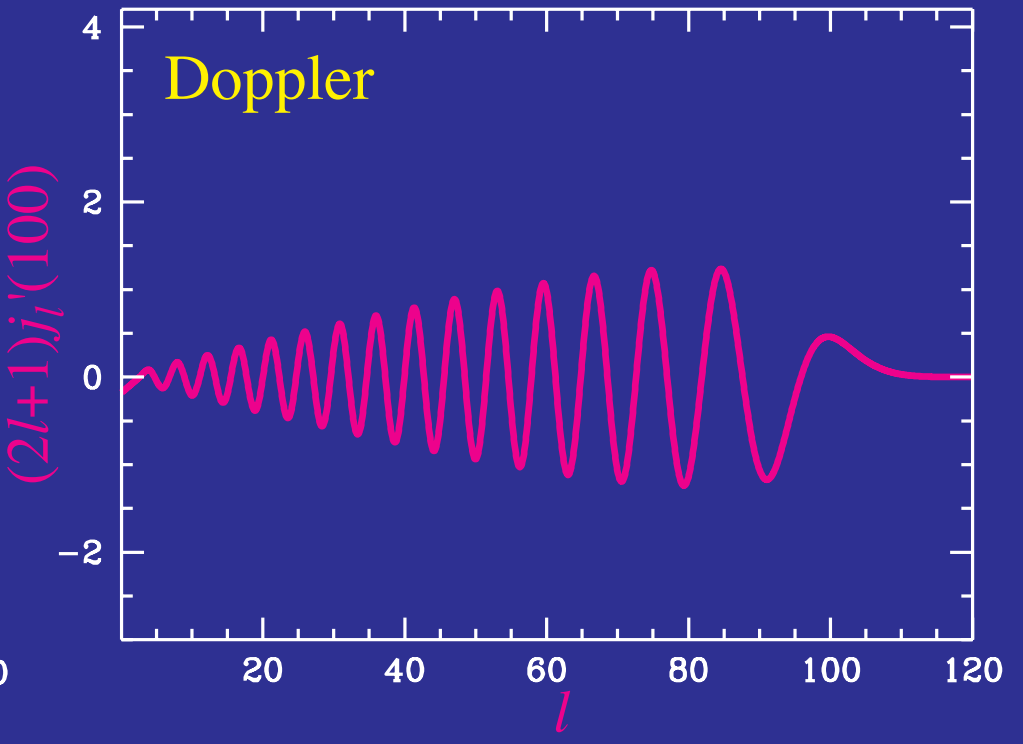

Cancellation of the Linear Effect

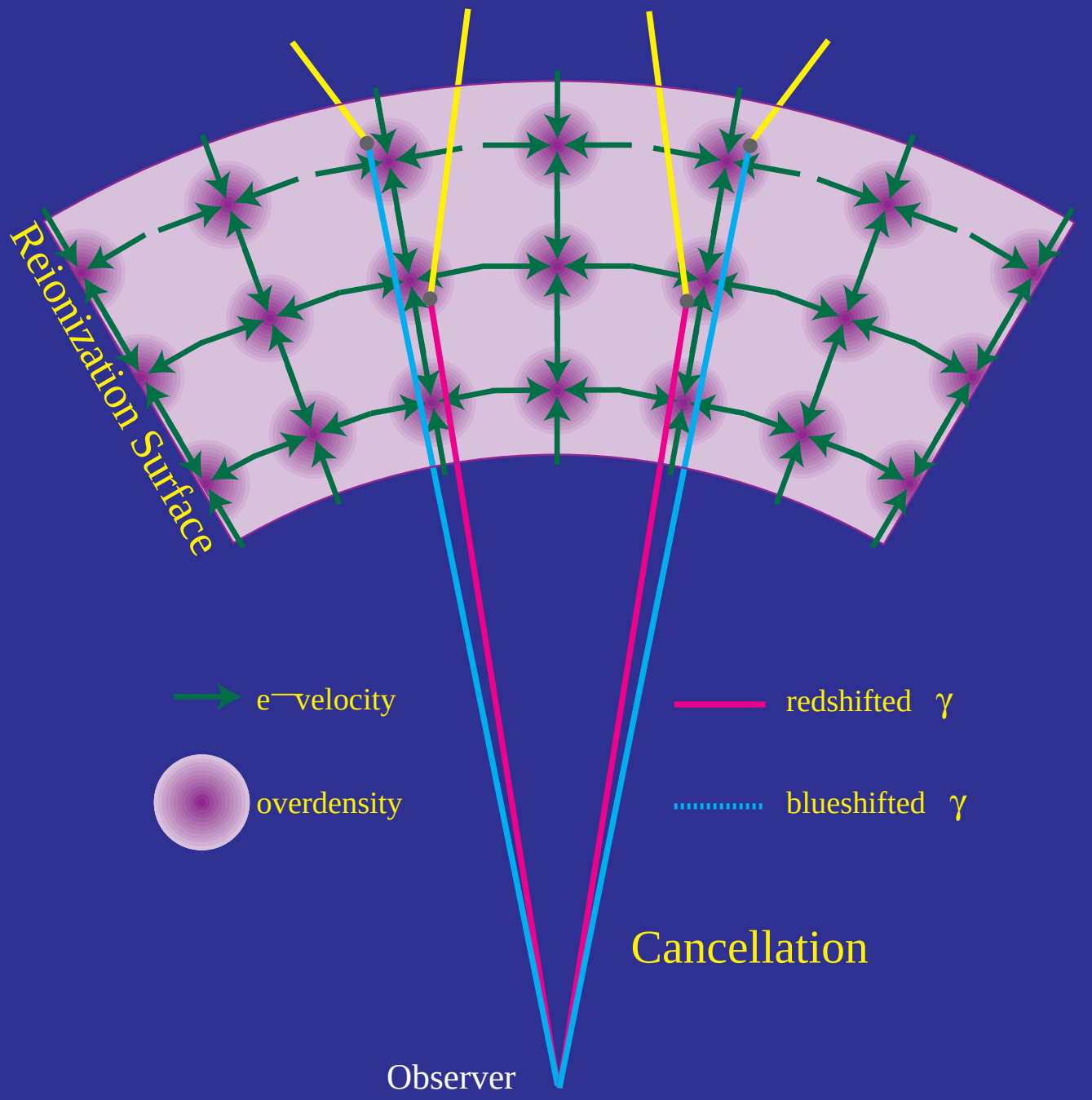

Modulated Doppler Effect

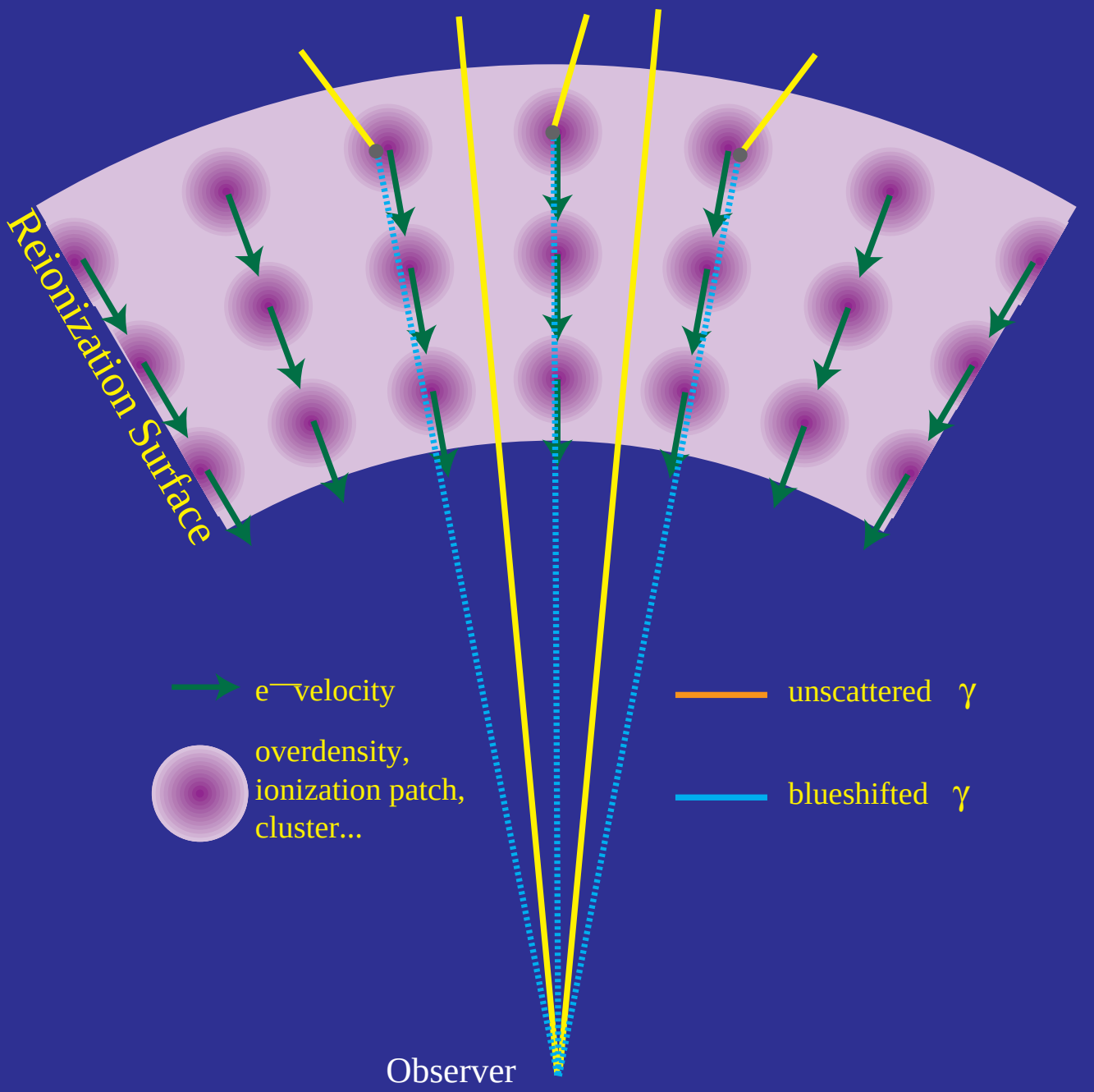

Ostriker–Vishniac Effect

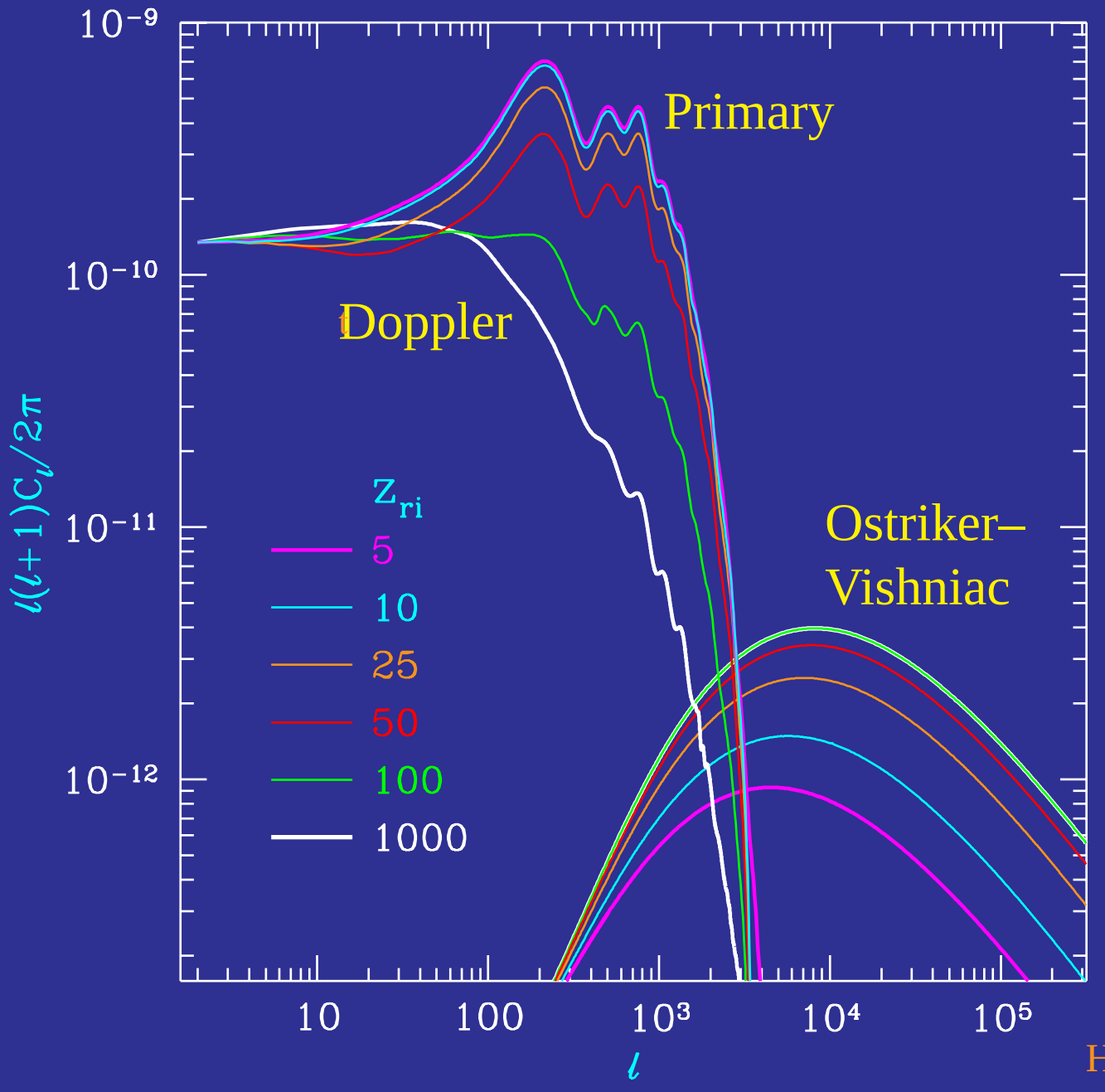

Hu & White (1996)

Inhomogeneous Ionization

- As reionization completes, ionization regions grow and fill the space

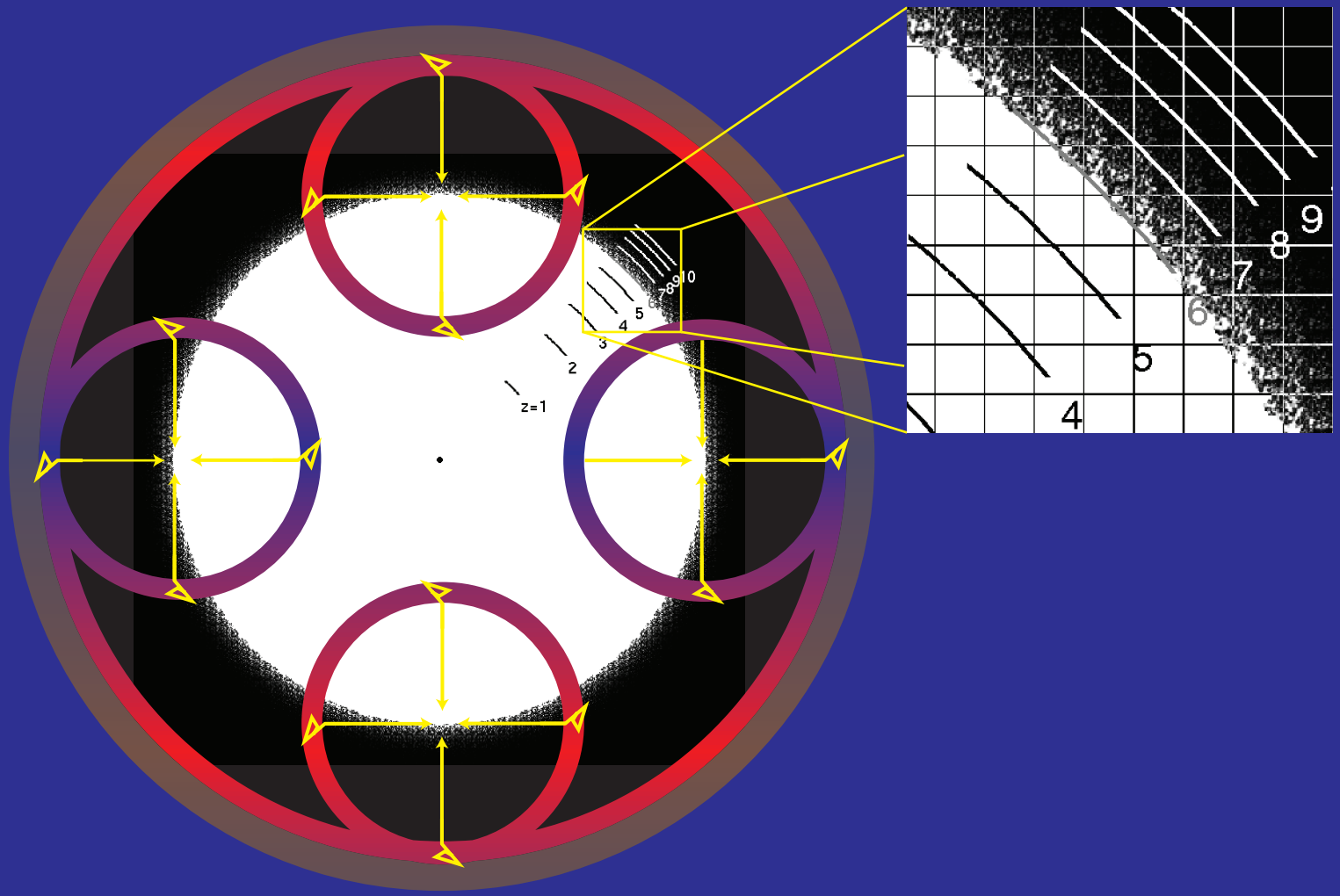

Zahn et al. (2006) [Mortonson et al (2009)]

Inhomogeneous Ionization

- Provides a source for modulated Doppler effect that appears on the scale of the ionization region

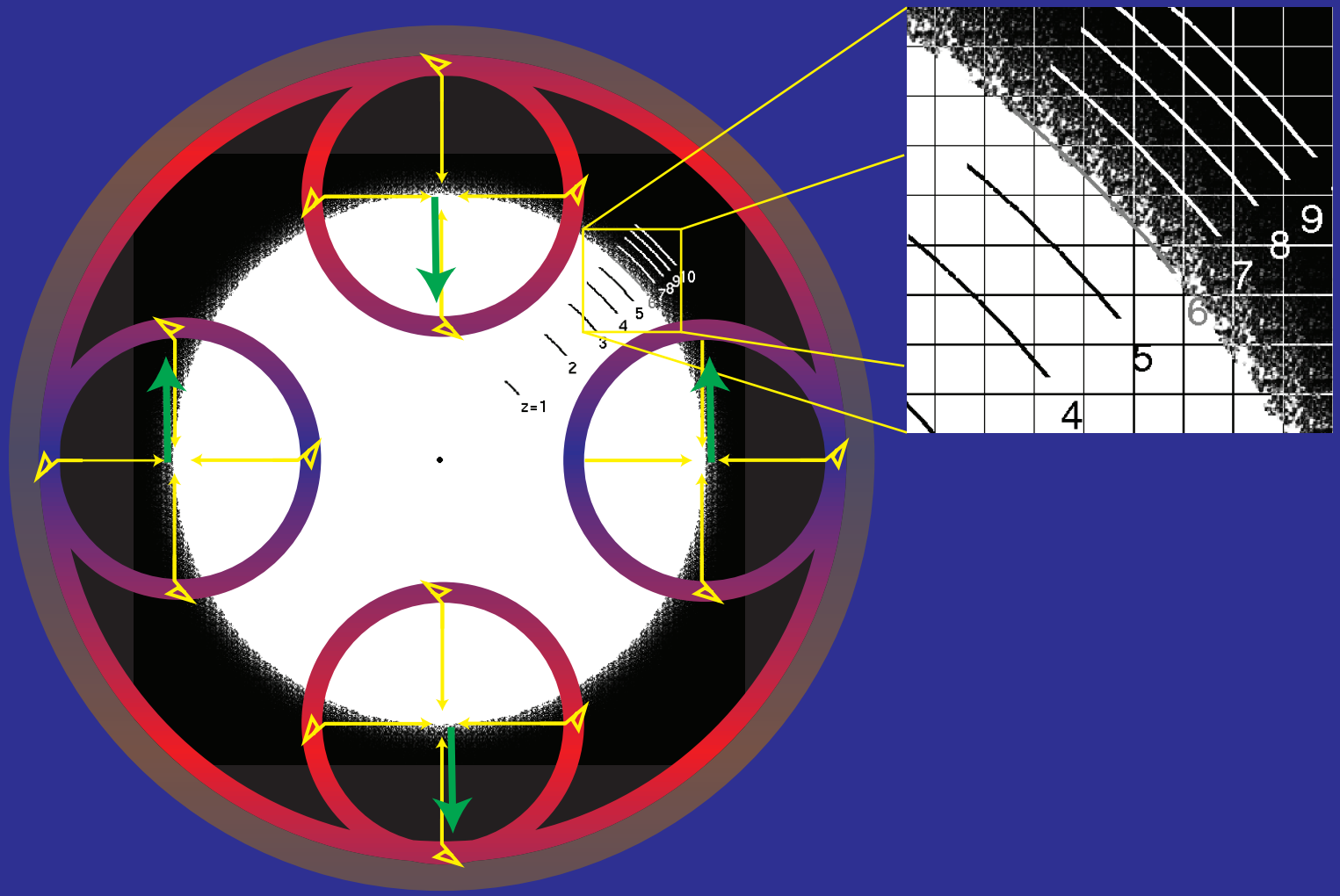

Patchy Reionization

Aghanim et al (1996)

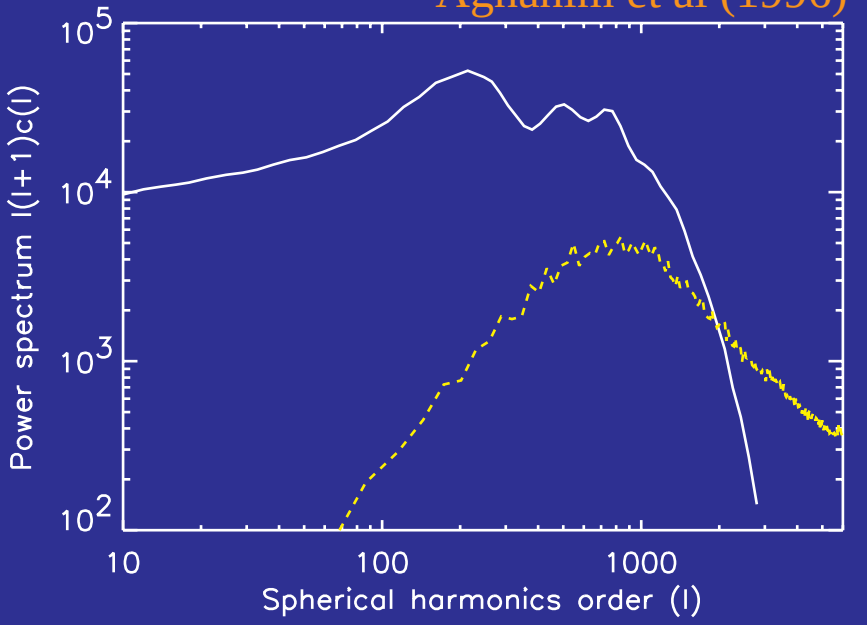

Gruzinov & Hu (1998)

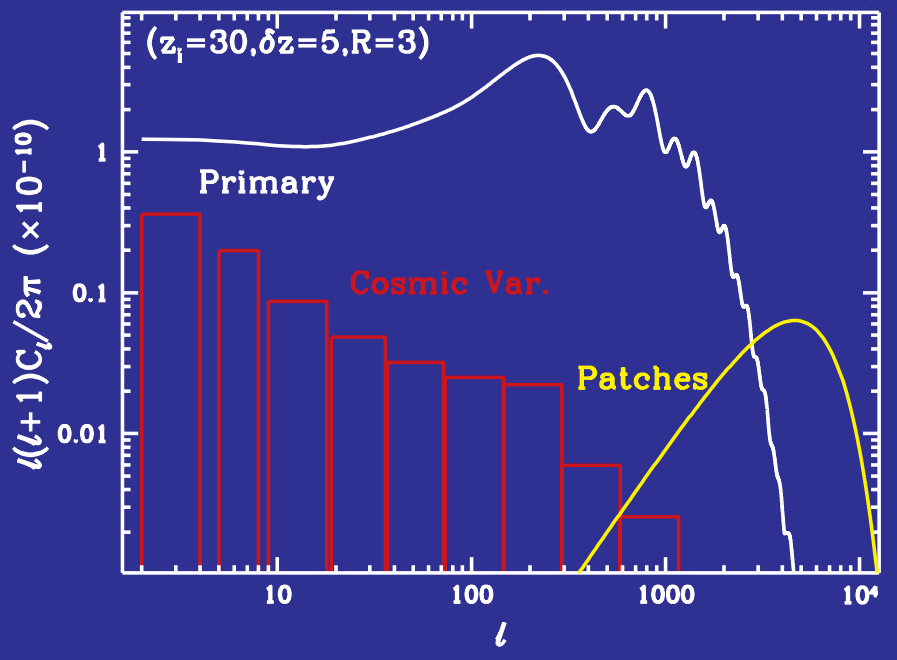

Knox, Scocciomarro & Dodelson (1998)

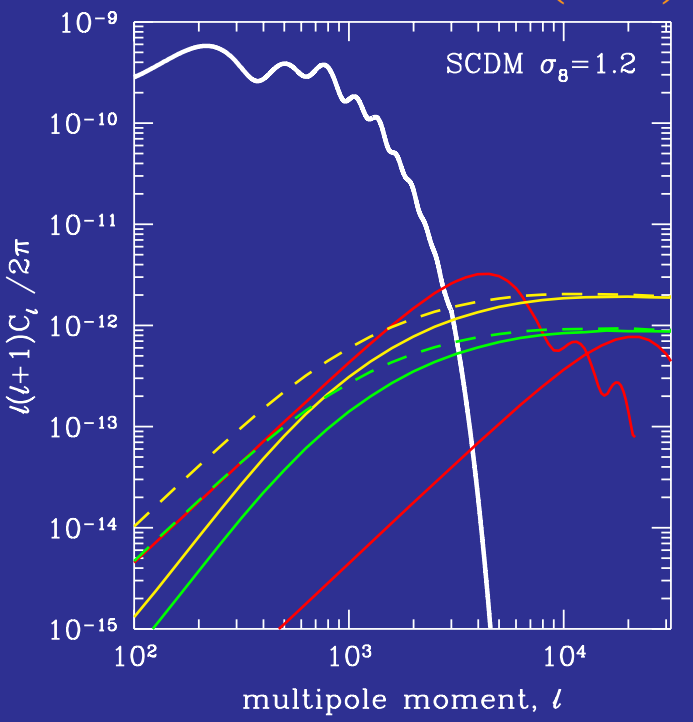

Secondary Polarization

WMAP Correlation

- Reionization polarization first detected in WMAP1 through temperature cross correlation at an anomalously high value

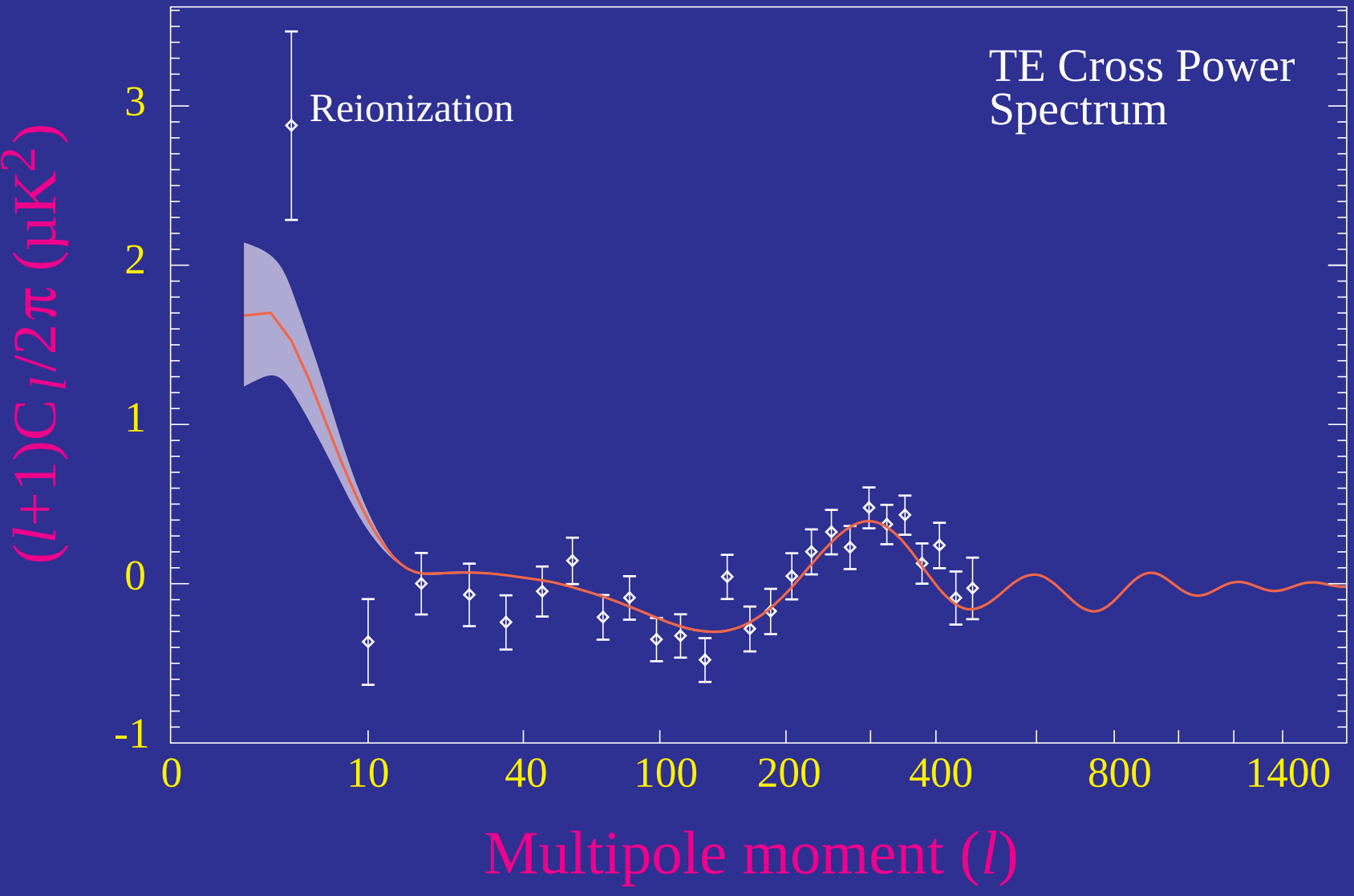

Polarization from Thomson Scattering

- Differential cross section depends on polarization and angle

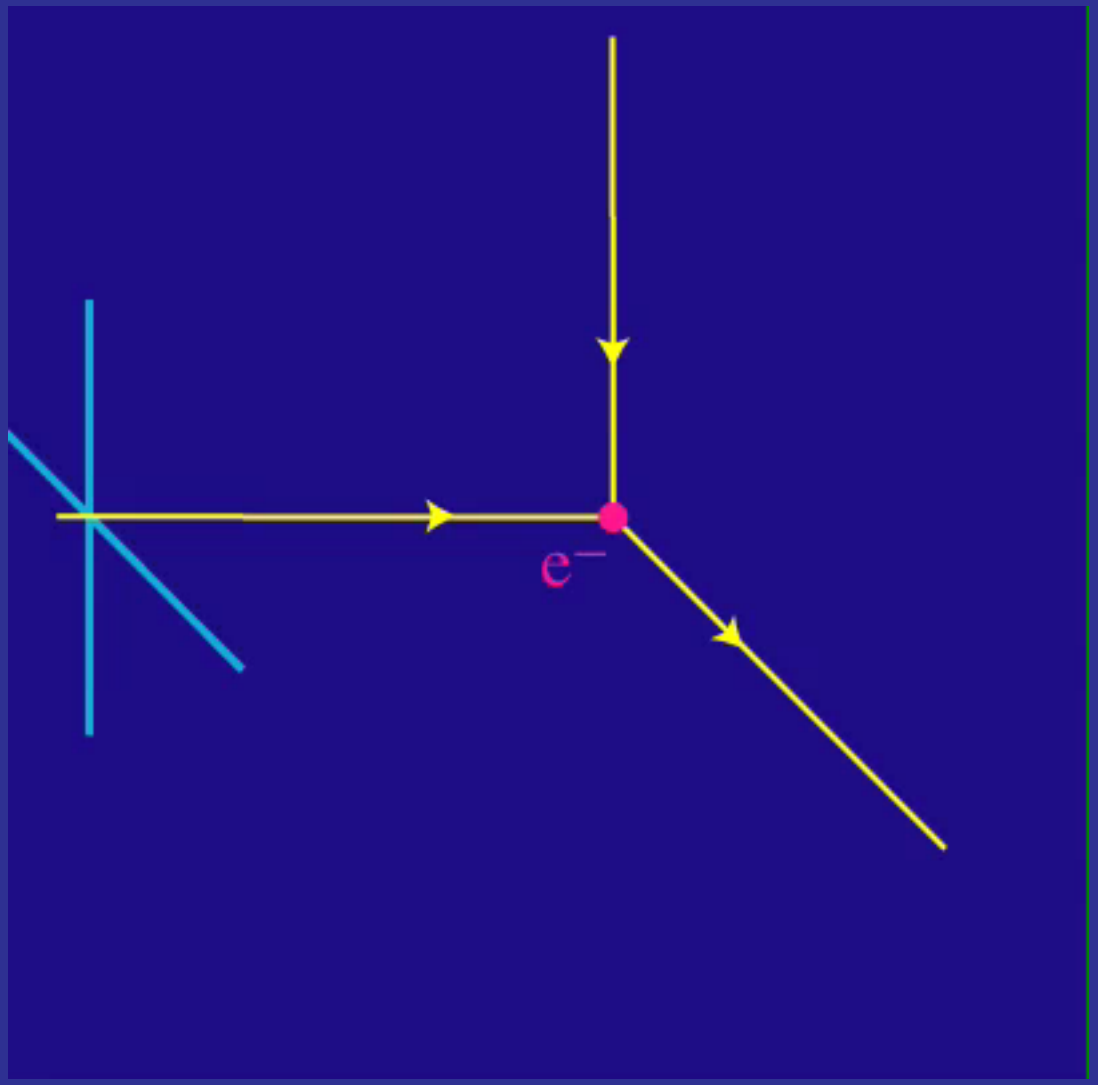

$$\frac{d\sigma}{d\Omega} = \frac{3}{8\pi}|\hat{\varepsilon}' \cdot \hat{\varepsilon}|^2 \sigma_T$$

Polarization from Thomson Scattering

- Isotropic radiation scatters into unpolarized radiation

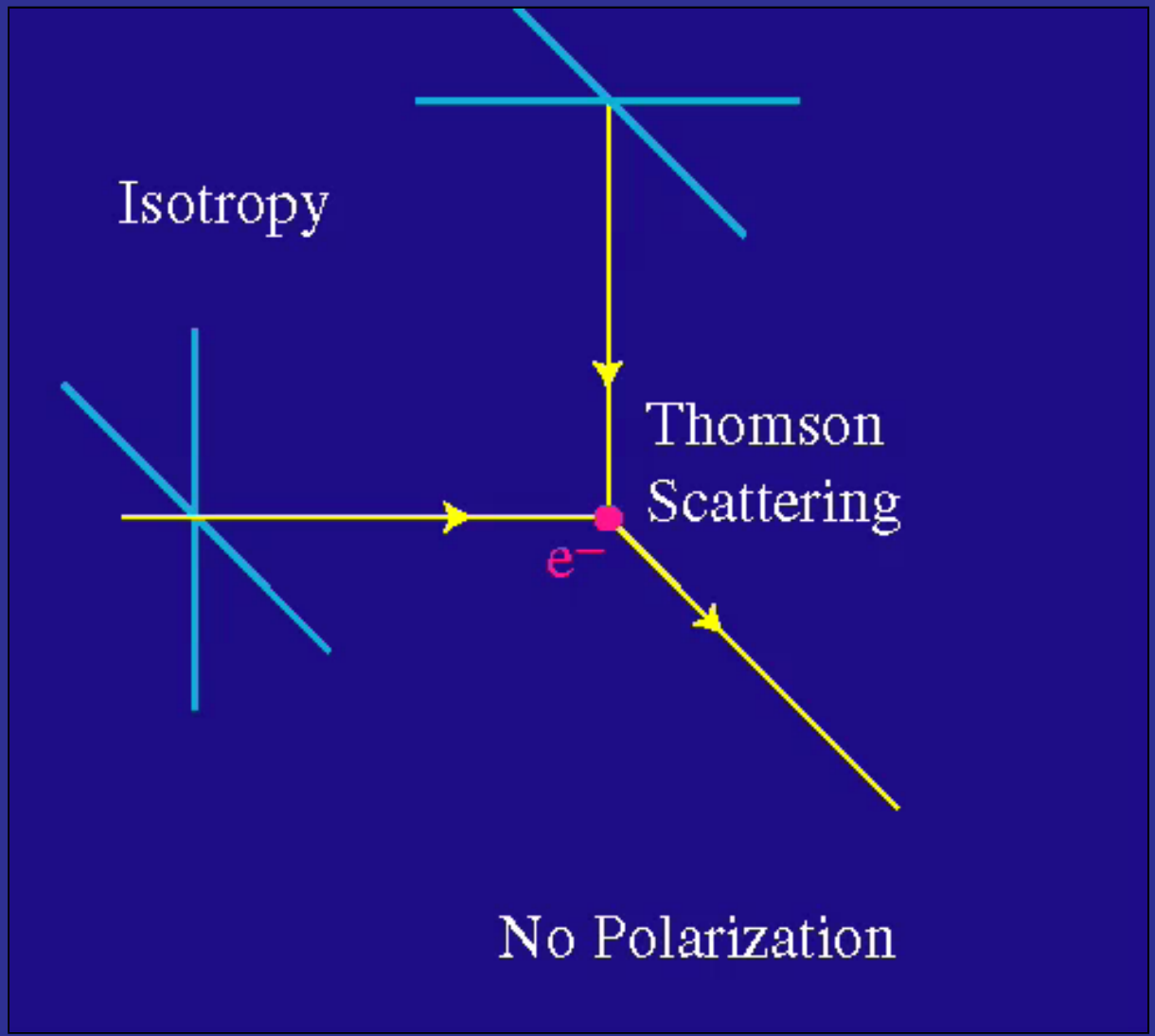

Polarization from Thomson Scattering

- Quadrupole anisotropies scatter into linear polarization

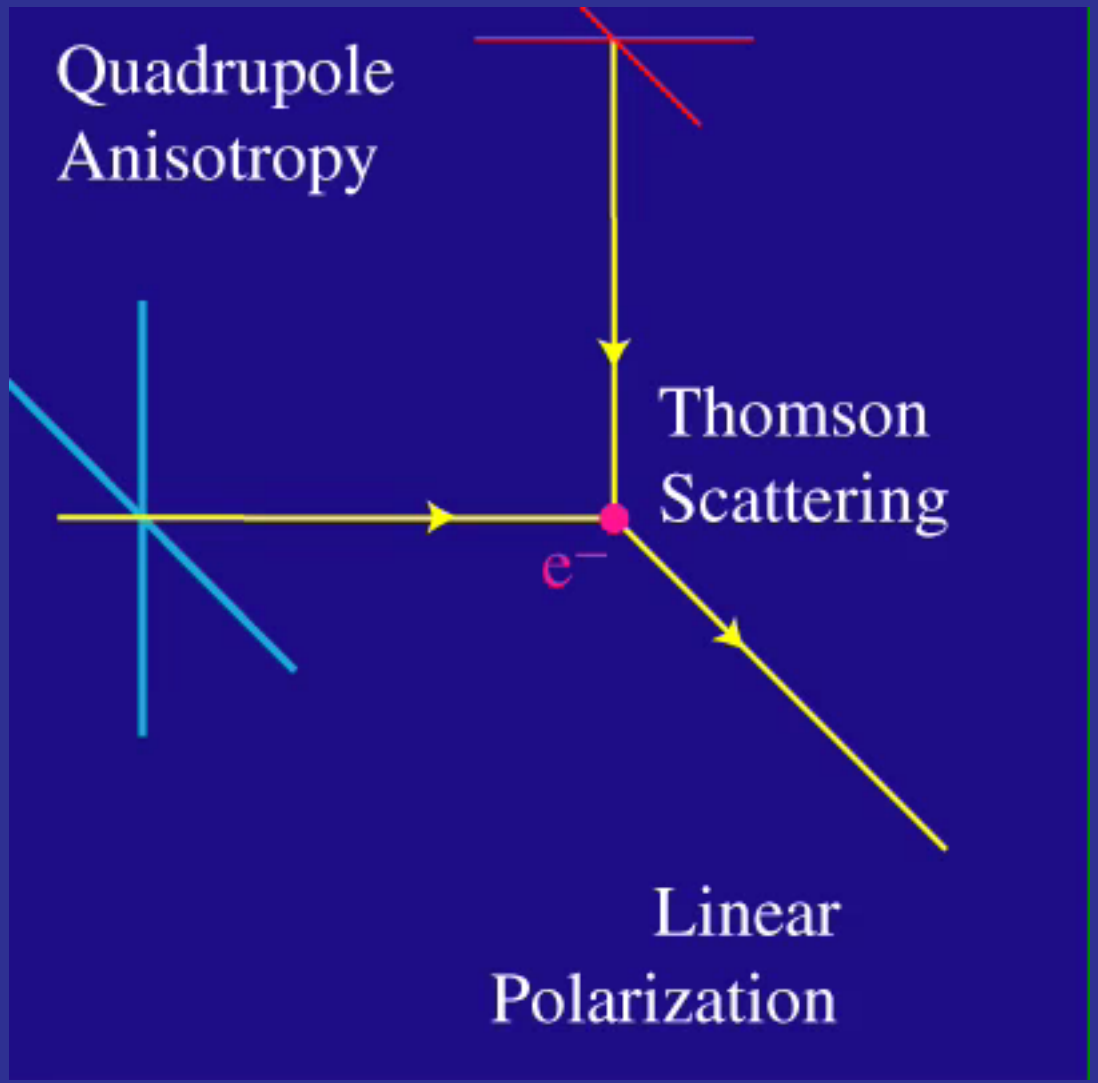

aligned with
cold lobe

Whence Quadrupoles?

- Temperature inhomogeneities in a medium
- Photons arrive from different regions producing an anisotropy

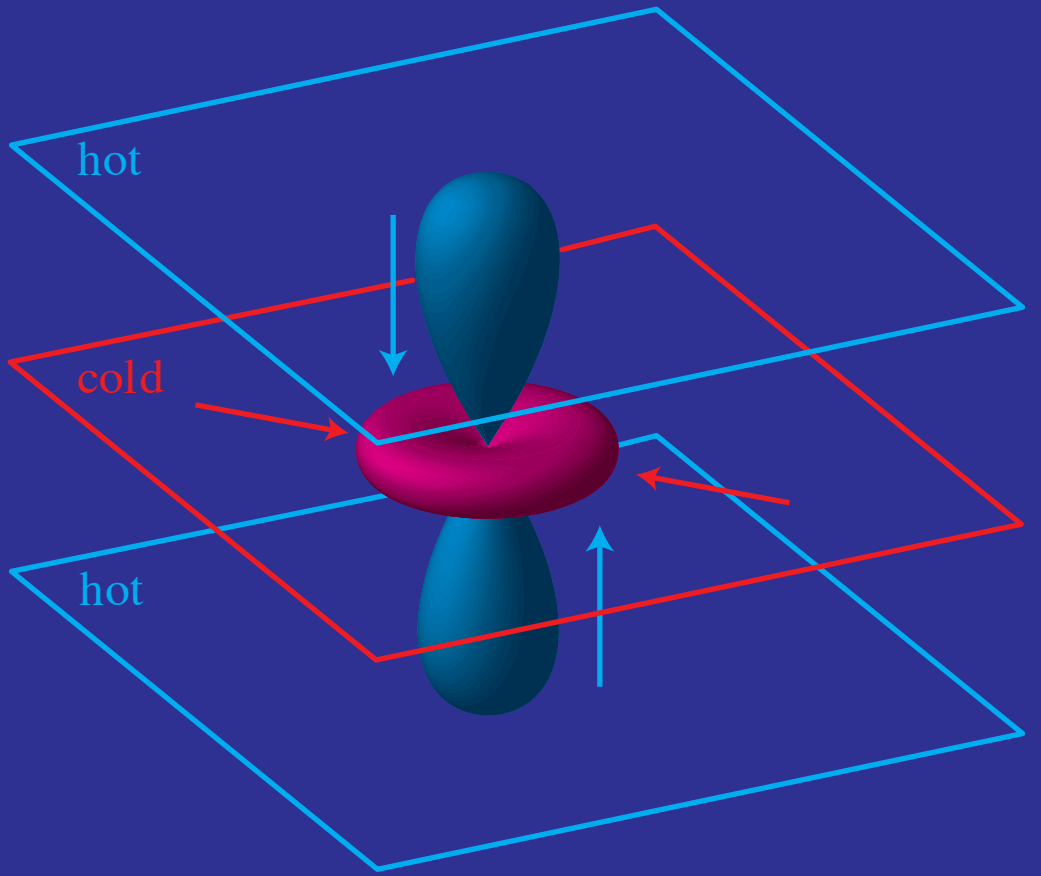

(Scalar) Temperature Inhomogeneity

Hu & White (1997)

CMB Anisotropy

- WMAP map of the CMB temperature anisotropy

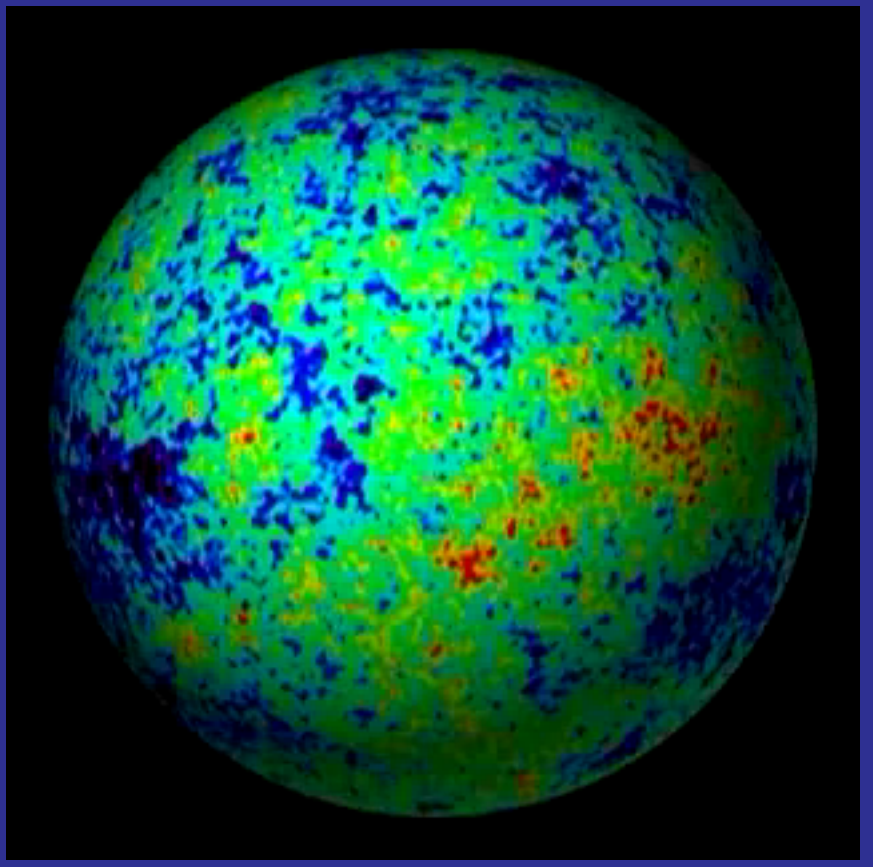

Whence Polarization Anisotropy?

- Observed photons scatter into the line of sight
- Polarization arises from the projection of the quadrupole on the transverse plane

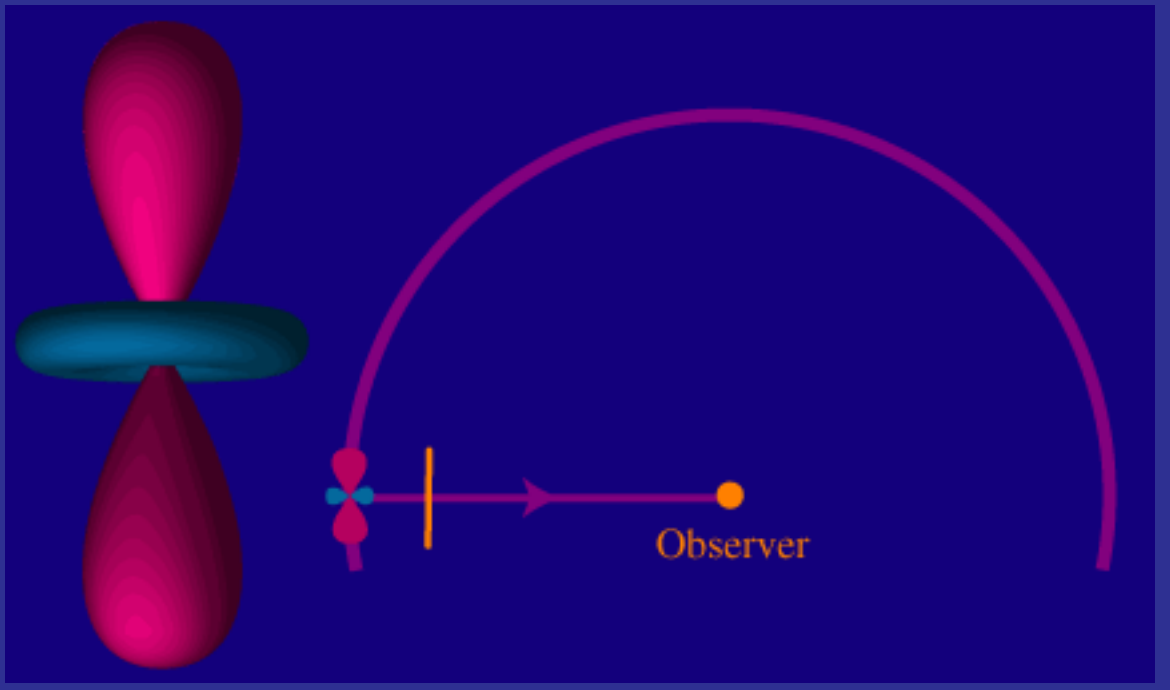

Polarization Multipoles

- Mathematically pattern is described by the tensor (spin-2) spherical harmonics [eigenfunctions of Laplacian on trace-free 2 tensor]
- Correspondence with scalar spherical harmonics established via Clebsch-Gordan coefficients (spin x orbital)
- Amplitude of the coefficients in the spherical harmonic expansion are the multipole moments; averaged square is the power

E-tensor harmonic

$l=2,\ m=0$

Modulation by Plane Wave

- Amplitude modulated by plane wave → higher multipole moments
- Direction detemined by perturbation type → E-modes

Polarization Pattern

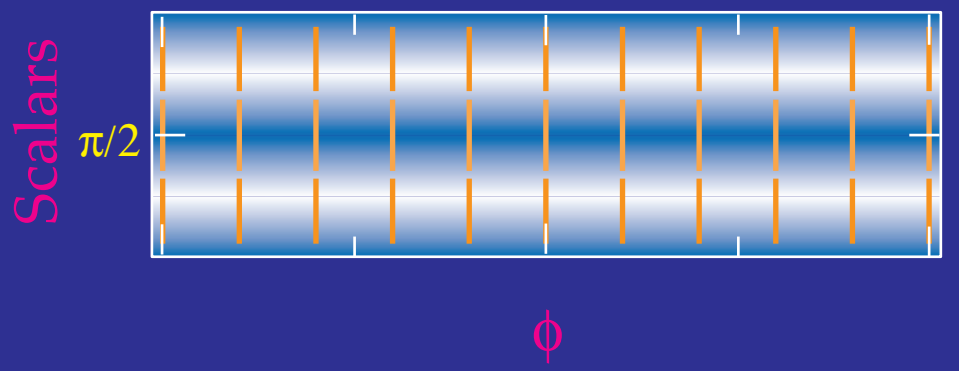

Multipole Power

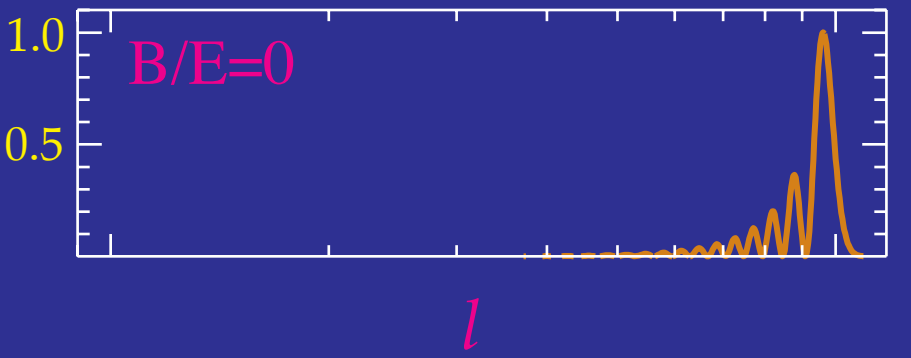

A Catch-22

- Polarization is generated by scattering of anisotropic radiation
- Scattering isotropizes radiation
- Polarization only arises in optically thin conditions: reionization and end of recombination
- Polarization fraction is at best a small fraction of the 10^{-5} anisotropy: $\sim 10^{-6}$ or μK in amplitude

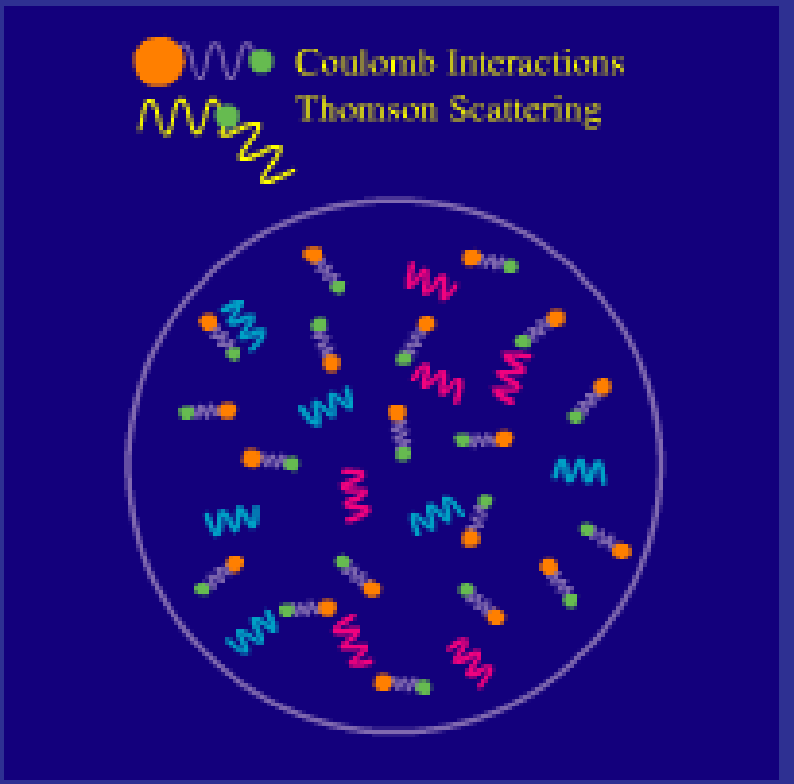

WMAP 3yr Data

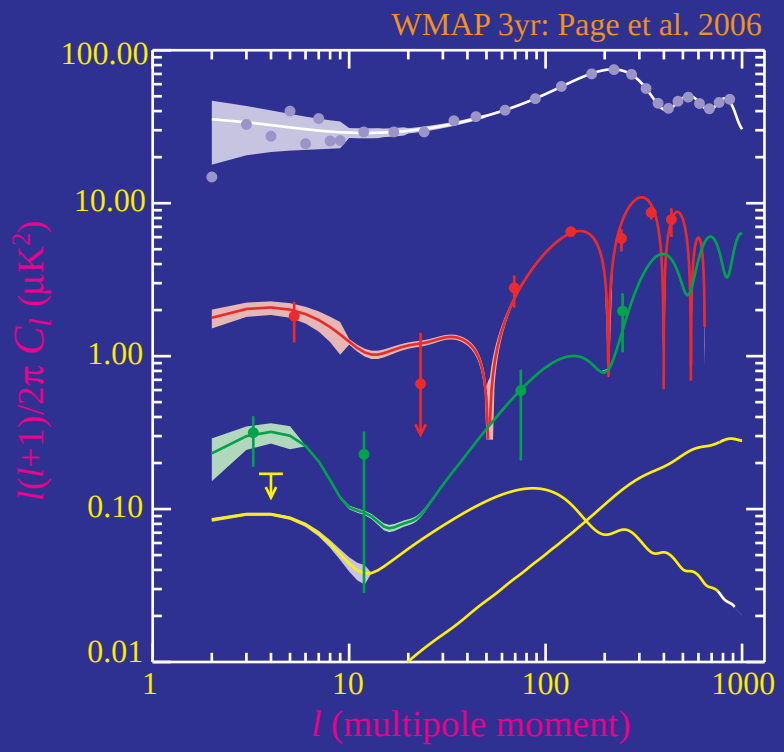

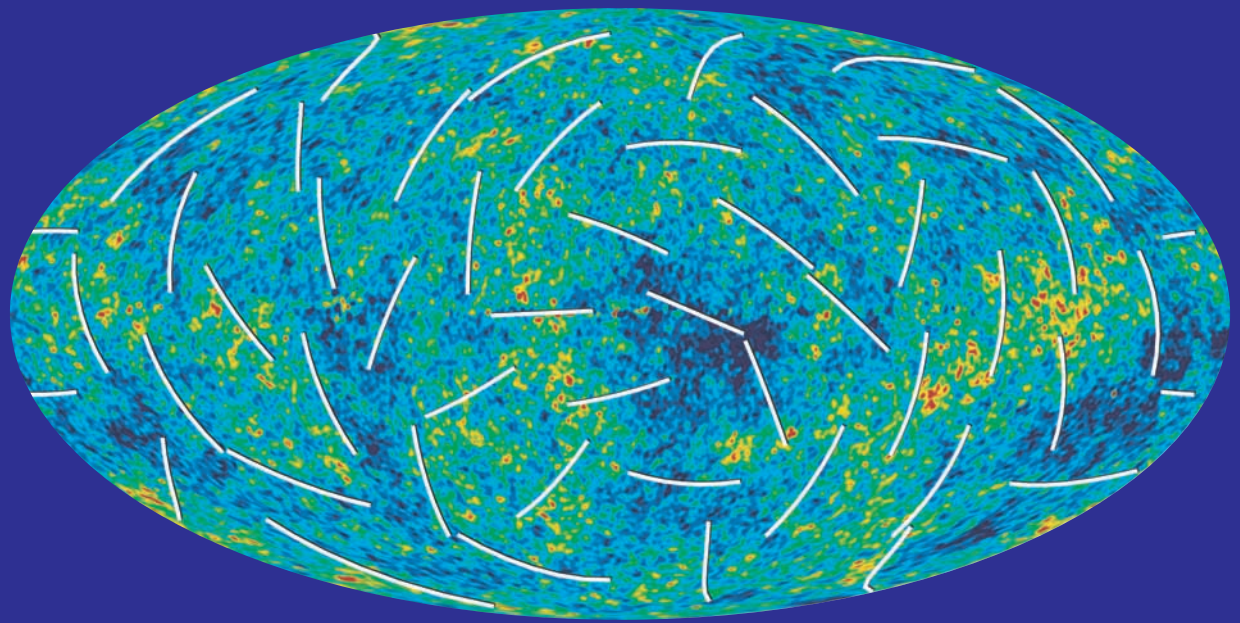

Temperature Inhomogeneity

- Temperature inhomogeneity reflects initial density perturbation on large scales
- Consider a single Fourier moment:

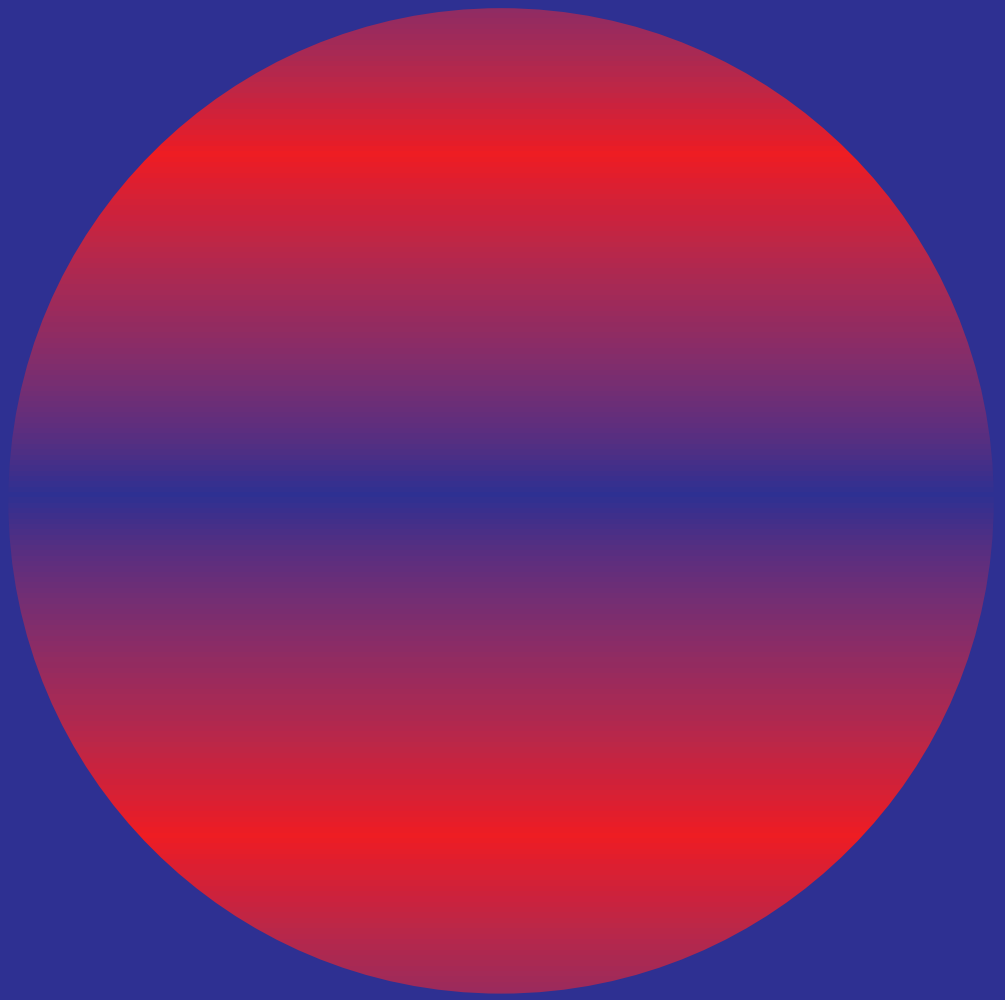

Locally Transparent

- Presently, the matter density is so low that a typical CMB photon will not scatter in a Hubble time (~age of universe)

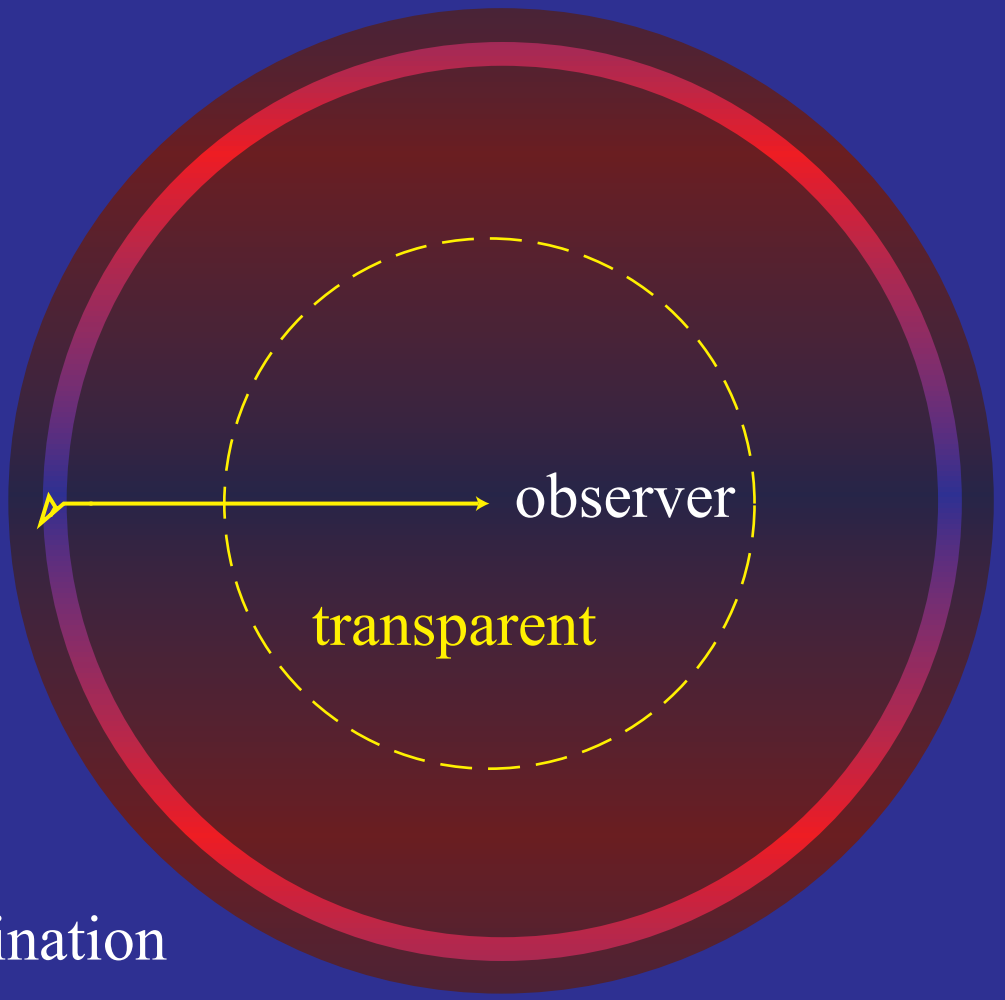

Reversed Expansion

- Free electron density in an ionized medium increases as scale factor a^{-3}; when the universe was a tenth of its current size CMB photons have a finite (~10%) chance to scatter

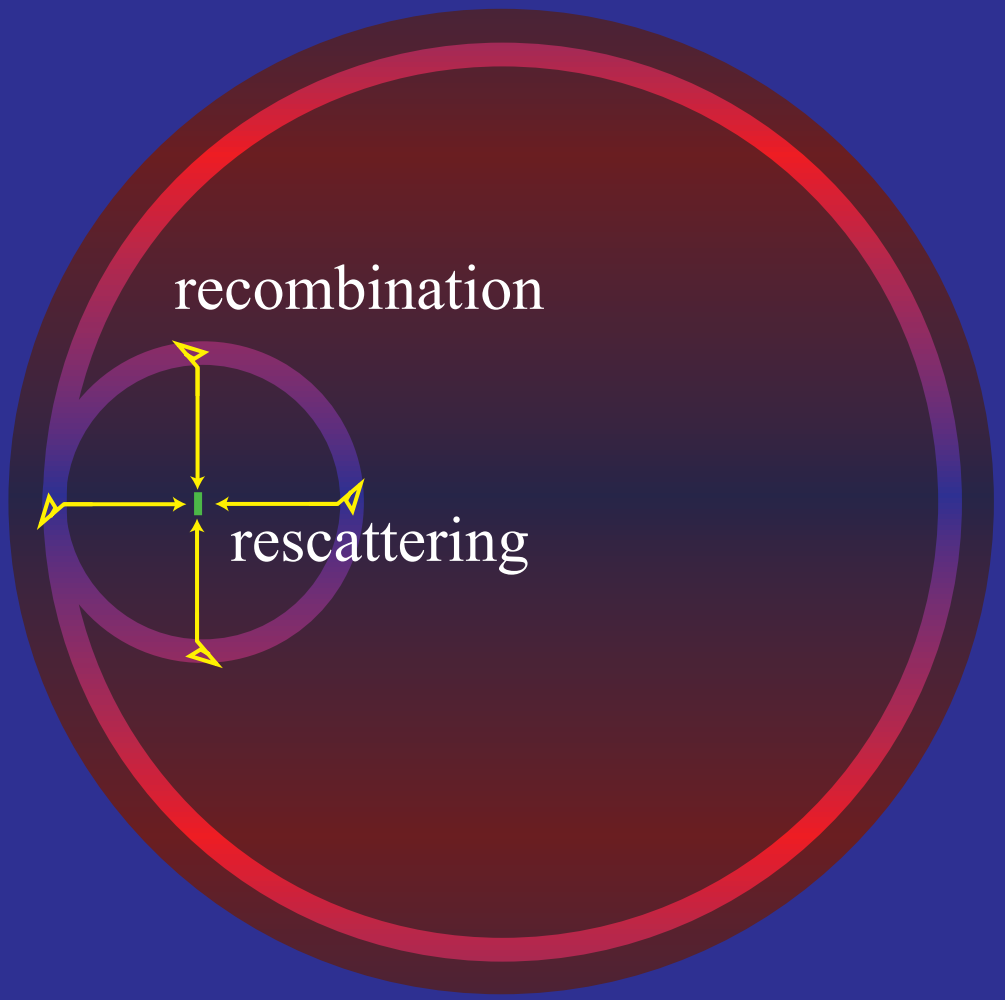

Polarization Anisotropy

- Electron sees the temperature anisotropy on its recombination surface and scatters it into a polarization

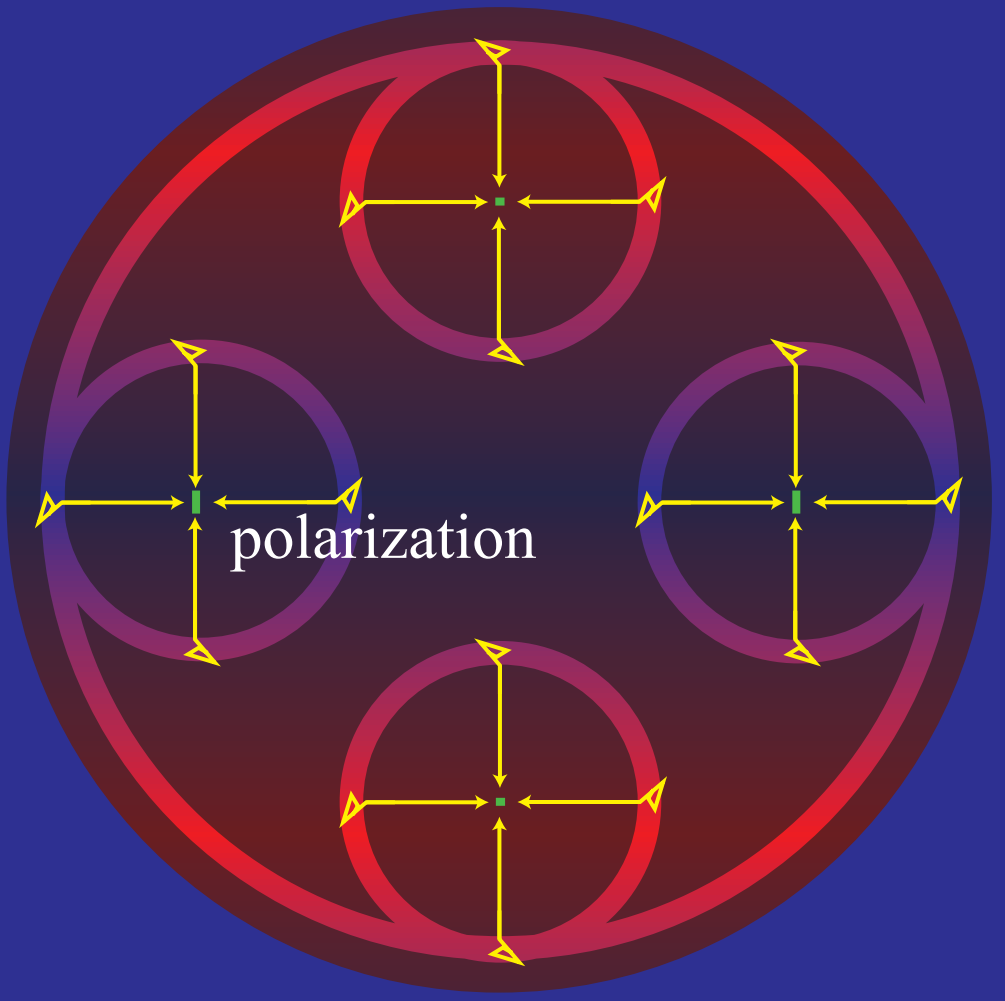

Temperature Correlation

- Pattern correlated with the temperature anisotropy that generates it; here an m=0 quadrupole

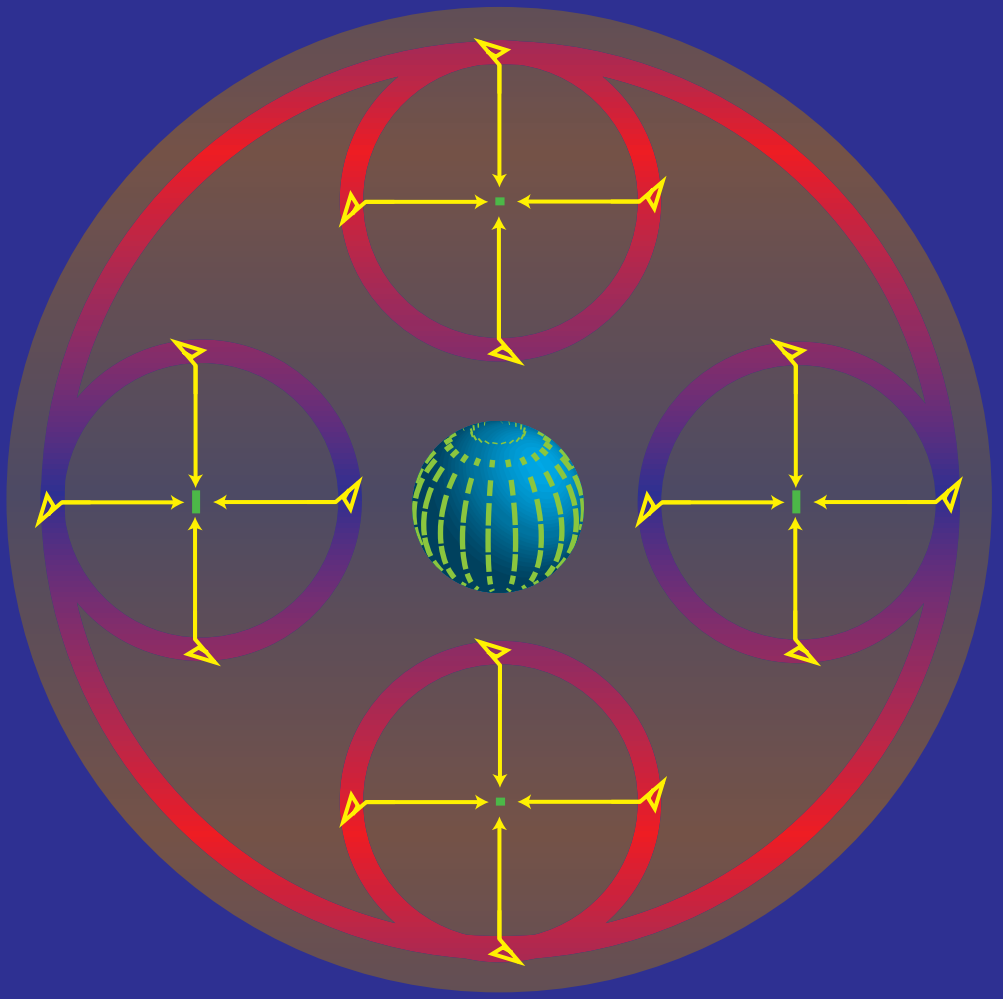

Instantaneous Reionization

- WMAP data constrains optical depth for instantaneous models of $\tau=0.087\pm0.017$
- Upper limit on gravitational waves weaker than from temperature

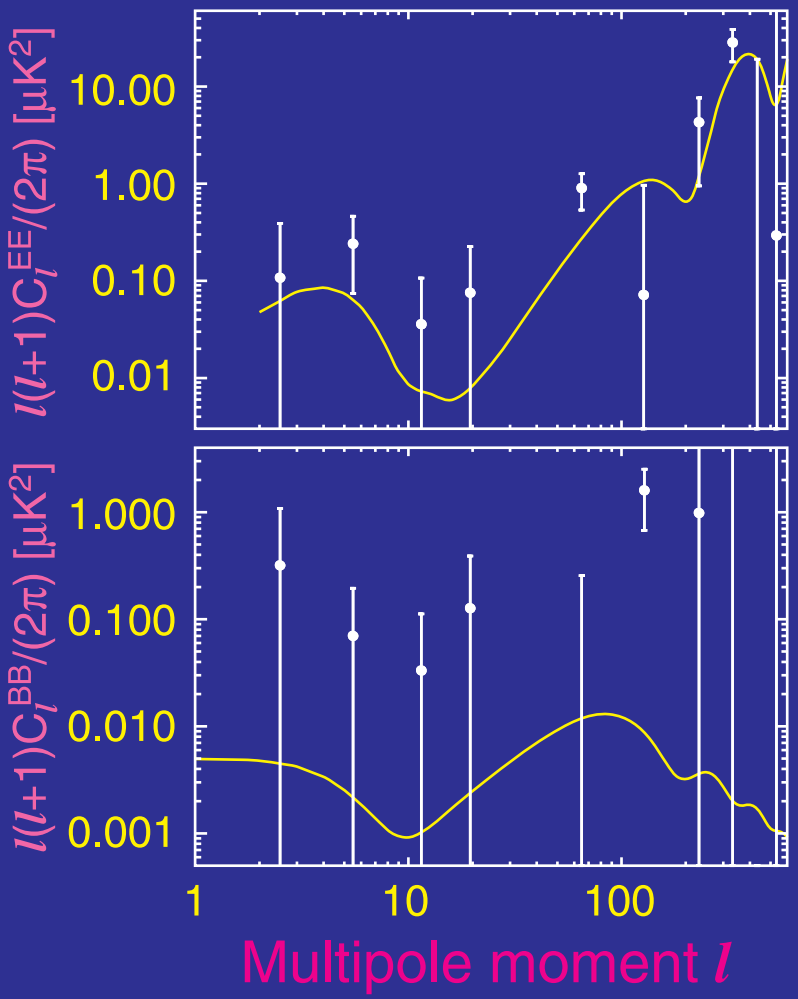

Why Care?

- Early ionization is puzzling if due to ionizing radiation from normal stars; may indicate more exotic physics is involved

- Reionization screens temperature anisotropy on small scales making the true amplitude of initial fluctuations larger by e^{τ}
- Measuring the growth of fluctuations is one of the best ways of determining the neutrino masses and the dark energy

- Offers an opportunity to study the origin of the low multipole statistical anomalies
- Presents a second, and statistically cleaner, window on gravitational waves from the early universe

Distance Predicts Growth

- With smooth dark energy, distance predicts scale-invariant growth to a few percent - a falsifiable prediction

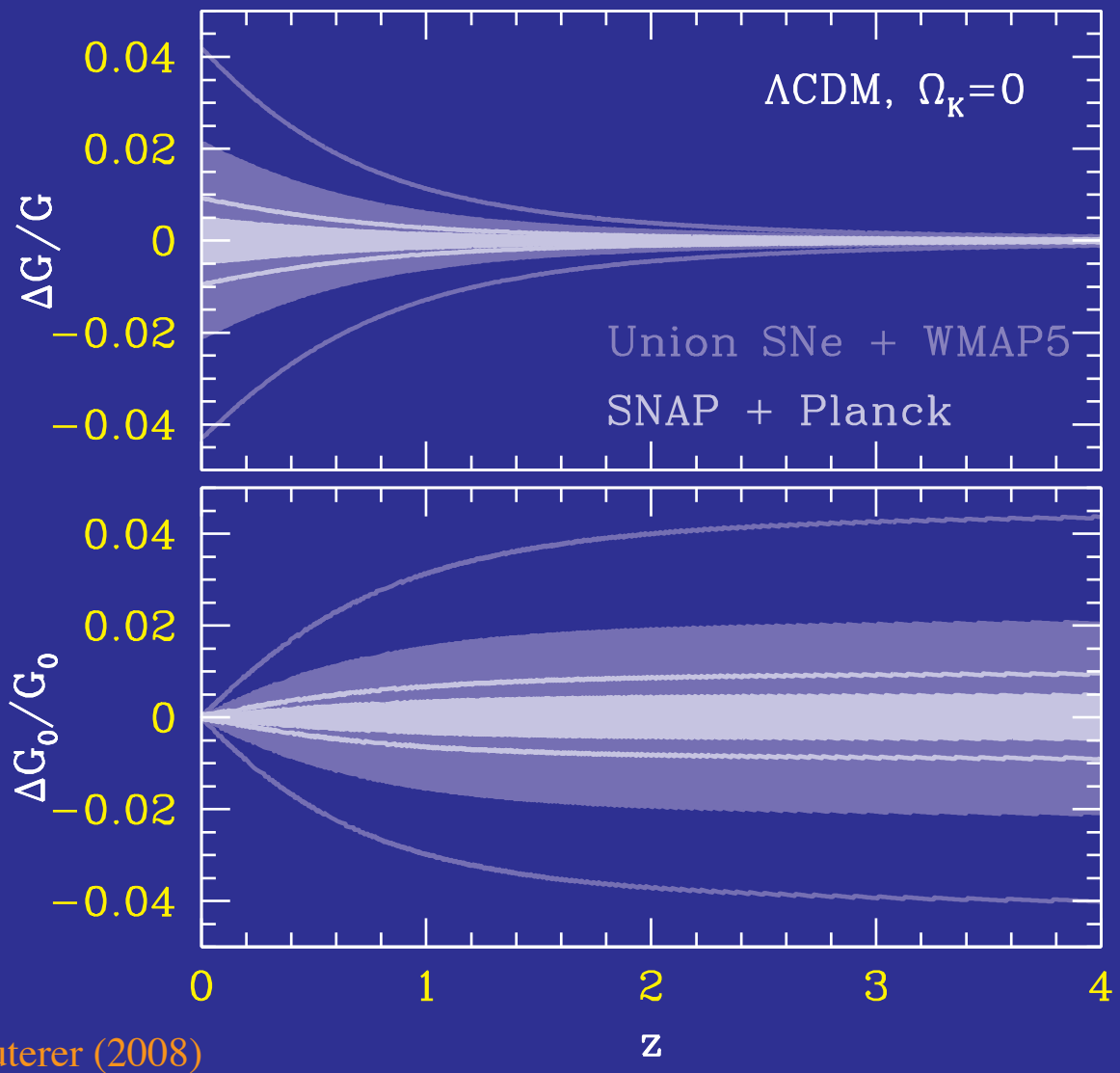

Mortonson, Hu, Huterer (2008)

Ionization History

- Two models with same optical depth τ but different ionization history

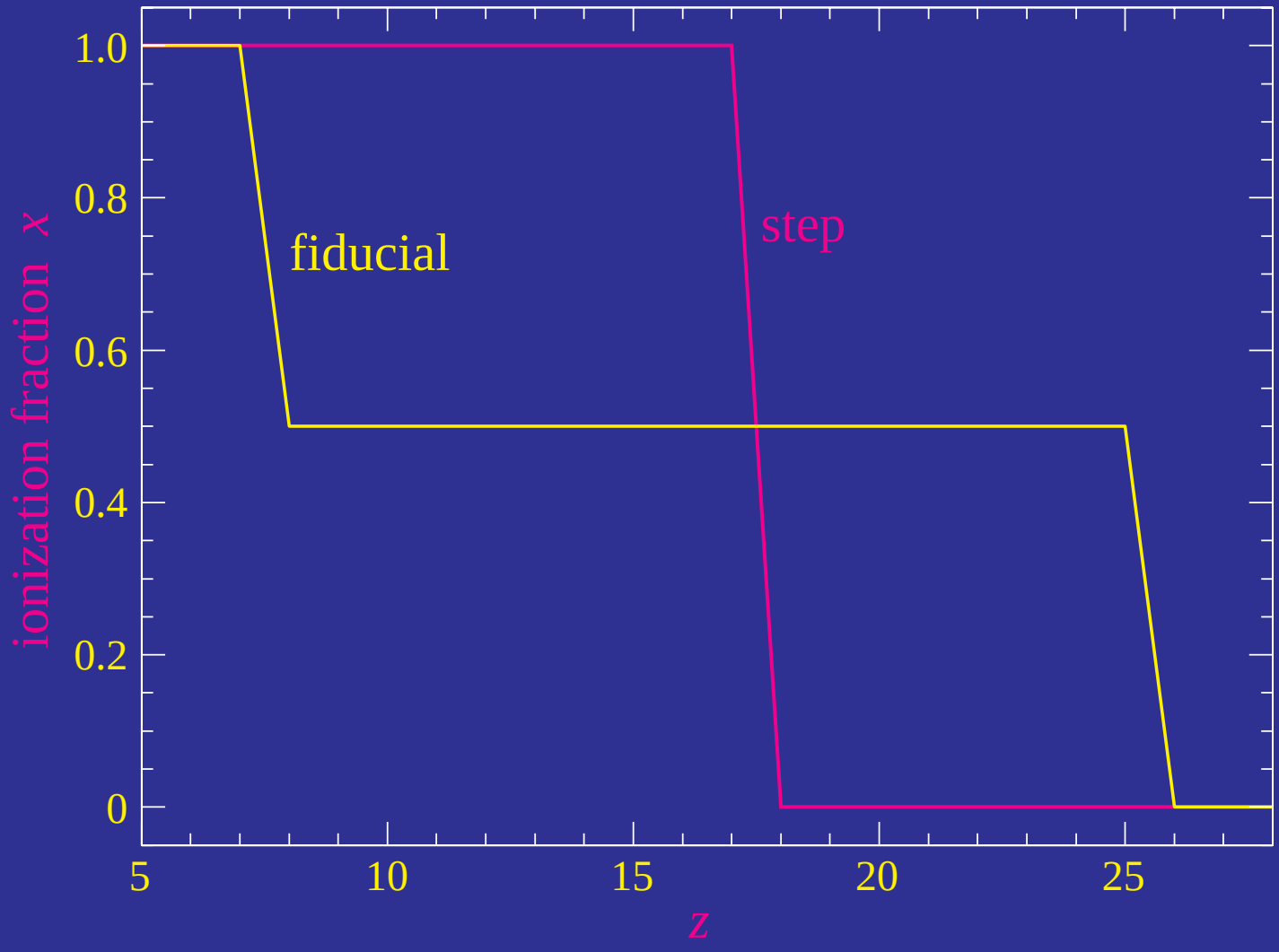

Kaplinghat et al. (2002); Hu & Holder (2003)

Distinguishable History

- Same optical depth, but different coherence - horizon scale during scattering epoch

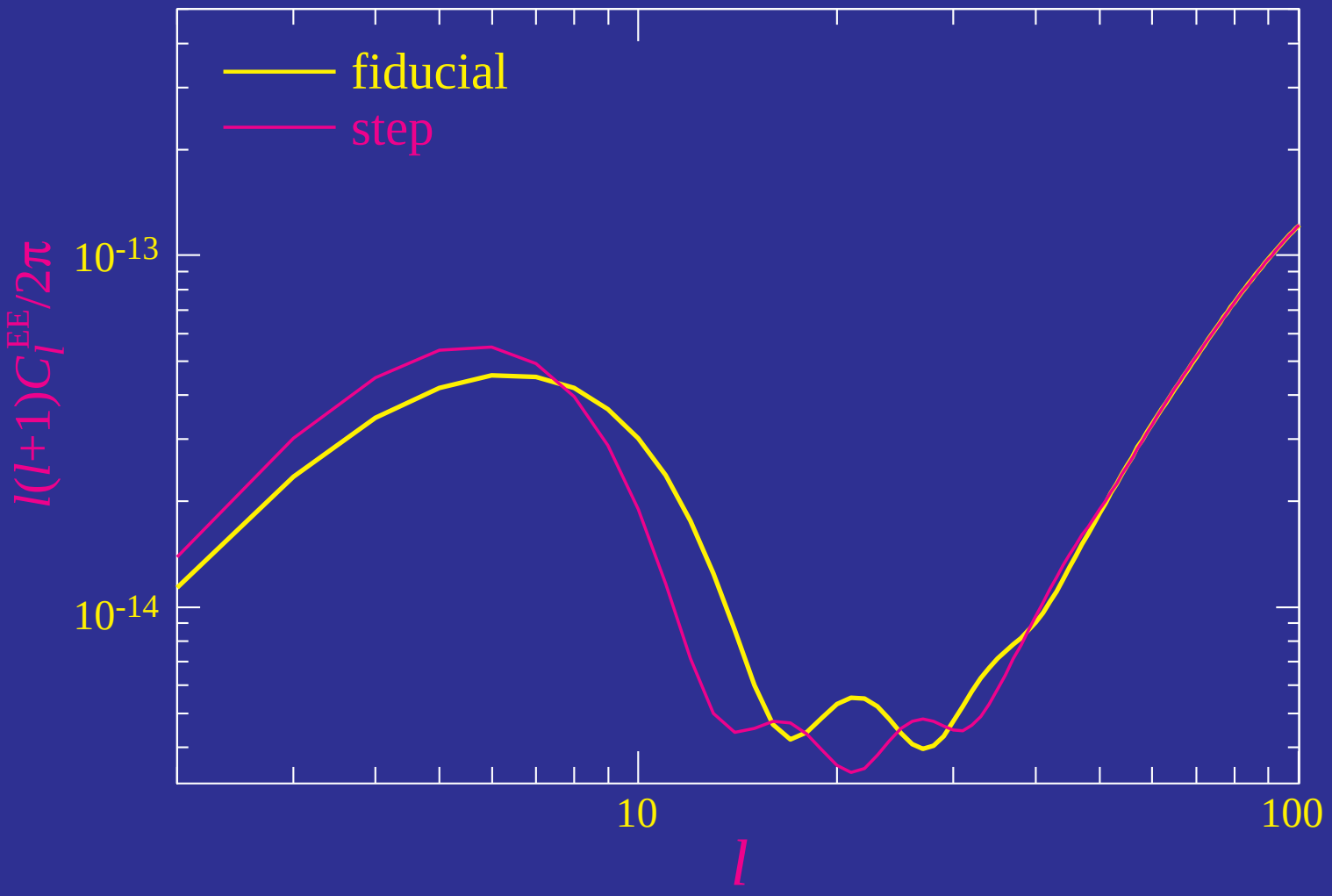

Kaplinghat et al. (2002); Hu & Holder (2003)

Transfer Function

- Linearized response to delta function ionization perturbation

$$T_{\ell i} \equiv \frac{\partial \ln C_\ell^{EE}}{\partial x(z_i)}, \qquad \delta C_\ell^{EE} = C_\ell^{EE} \sum_i T_{\ell i} \delta x(z_i)$$

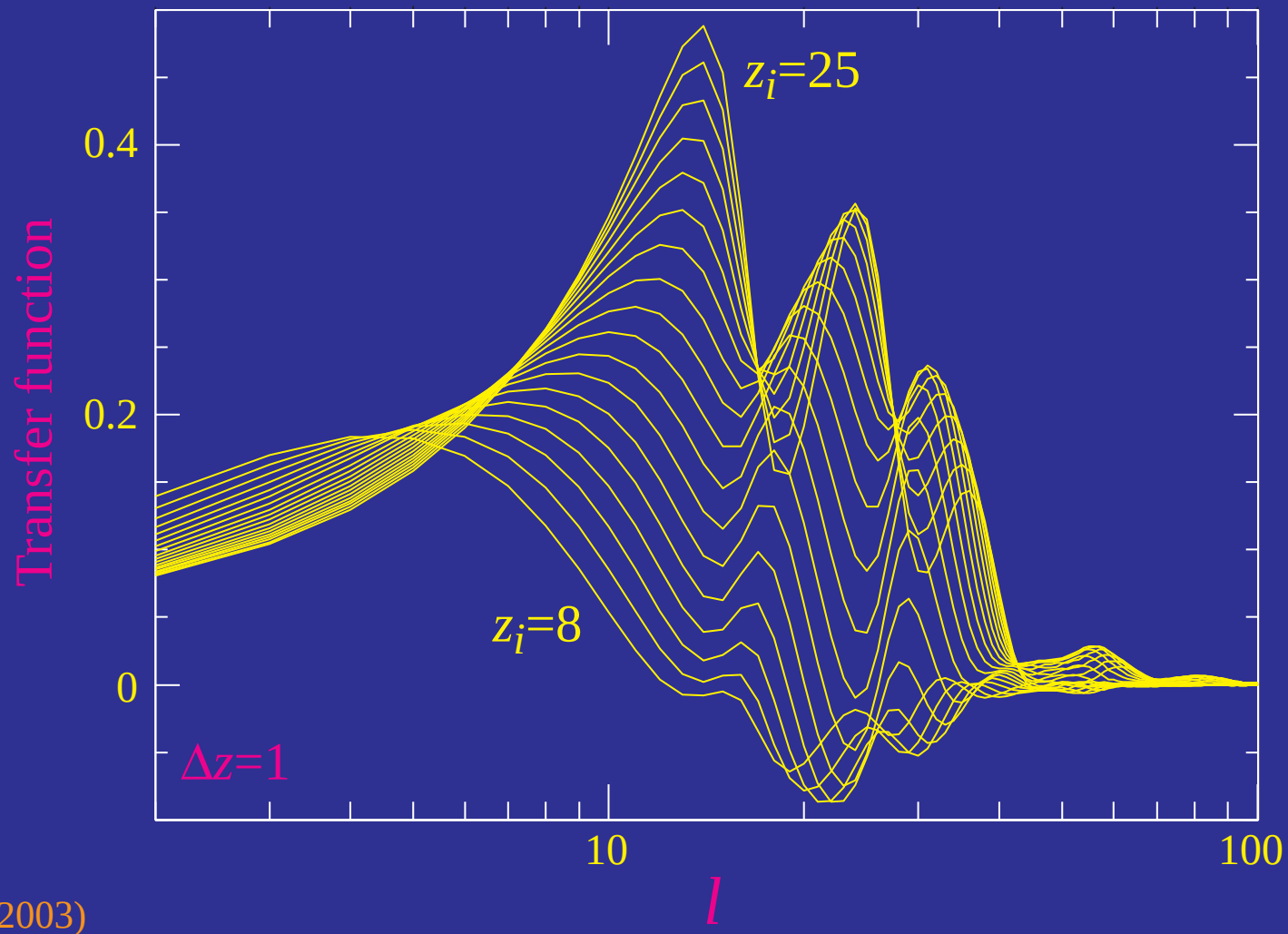

Hu & Holder (2003)

Principal Components

- Eigenvectors of the Fisher Matrix

$$F_{ij} \equiv \sum_{\ell} (\ell + 1/2) T_{\ell i} T_{\ell j} = \sum_{\mu} S_{i\mu} \sigma_{\mu}^{-2} S_{j\mu}$$

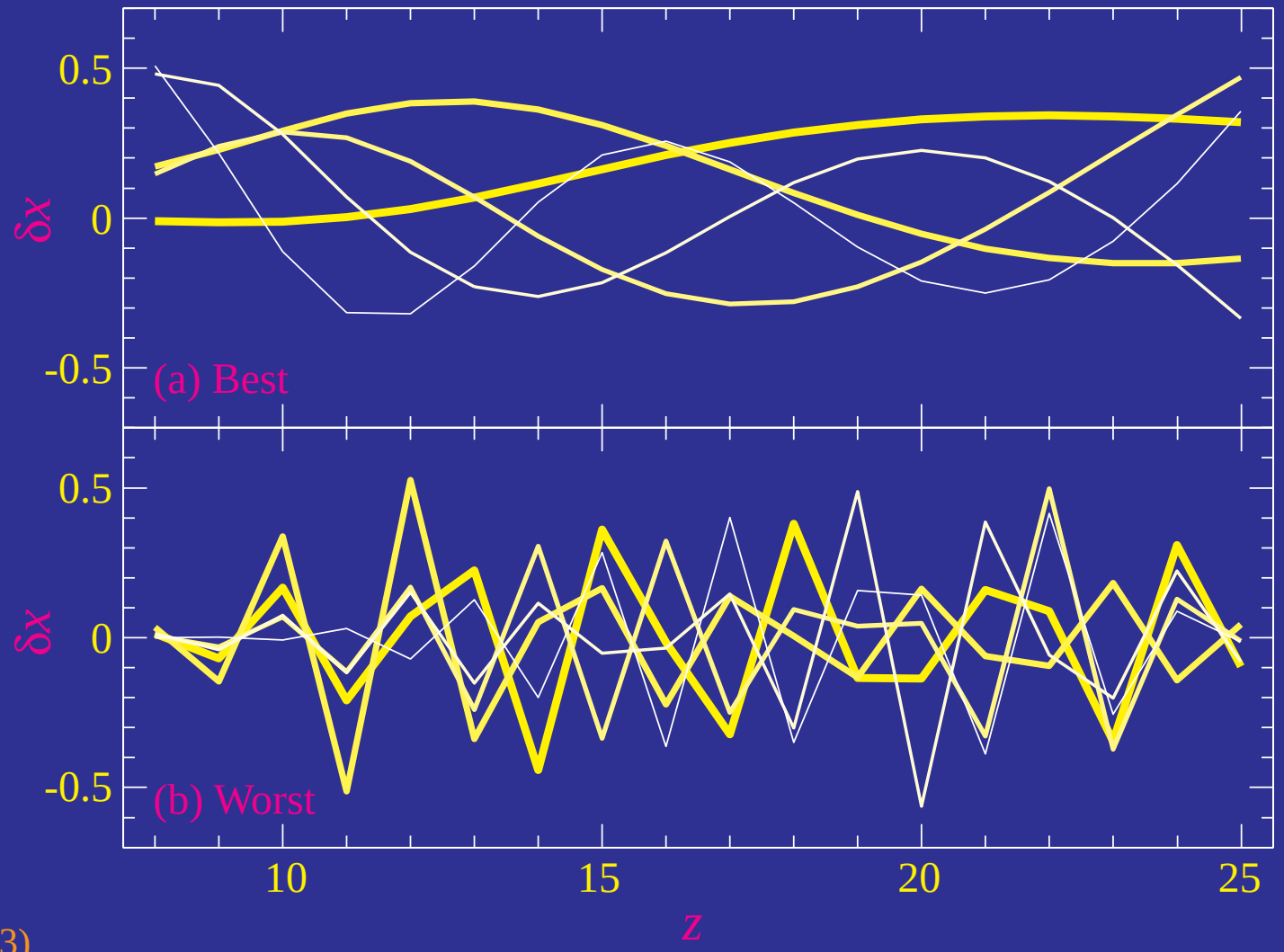

Hu & Holder (2003)

Capturing the Observables

- First 5 modes have the information content and most of optical depth

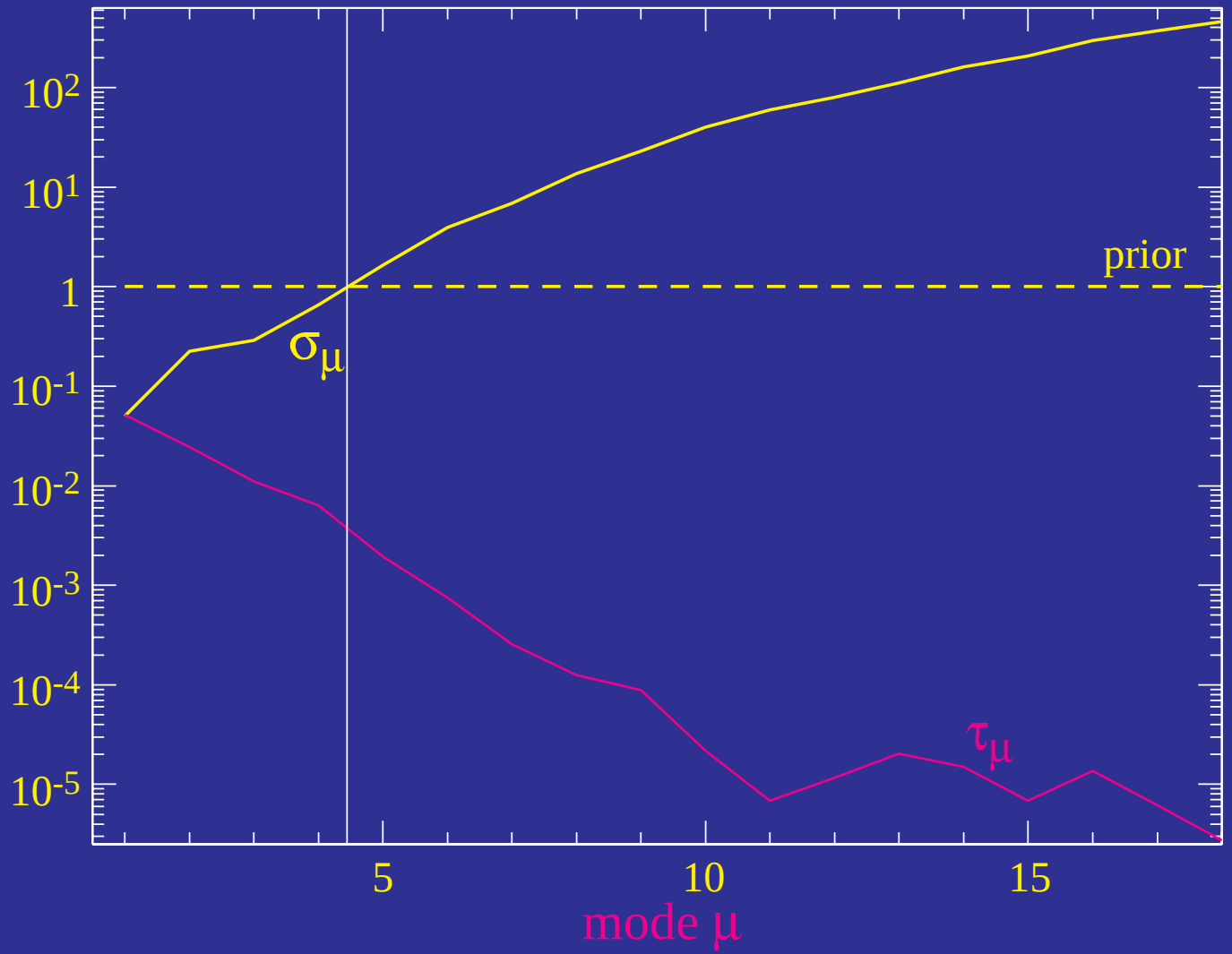

Hu & Holder (2003)

Representation in Modes

- Truncation at 5 modes leaves a low pass filtered of ionization history
- Ionization fraction allowed to go negative (Boltzmann code has negative sources)

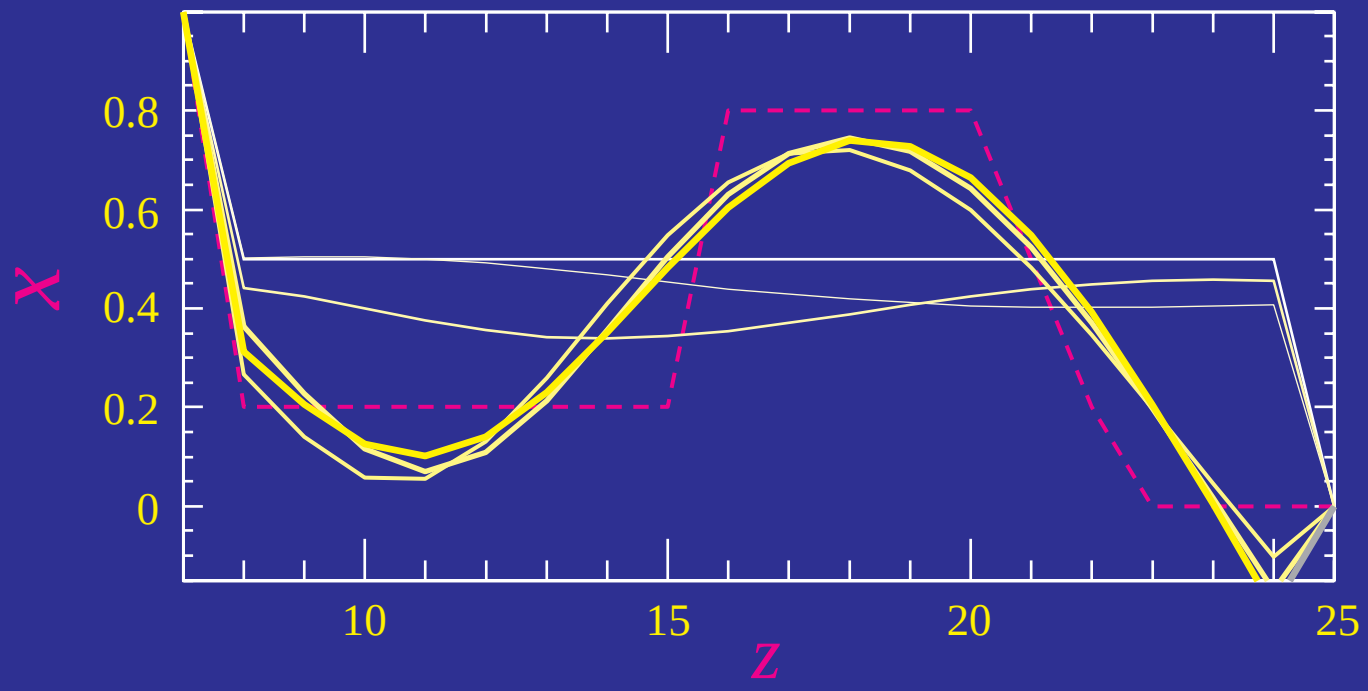

Hu & Holder (2003)

Representation in Modes

- Reproduces the power spectrum with sum over >3 modes
  more generally 5 modes suffices: e.g. total τ=0.1375 vs 0.1377

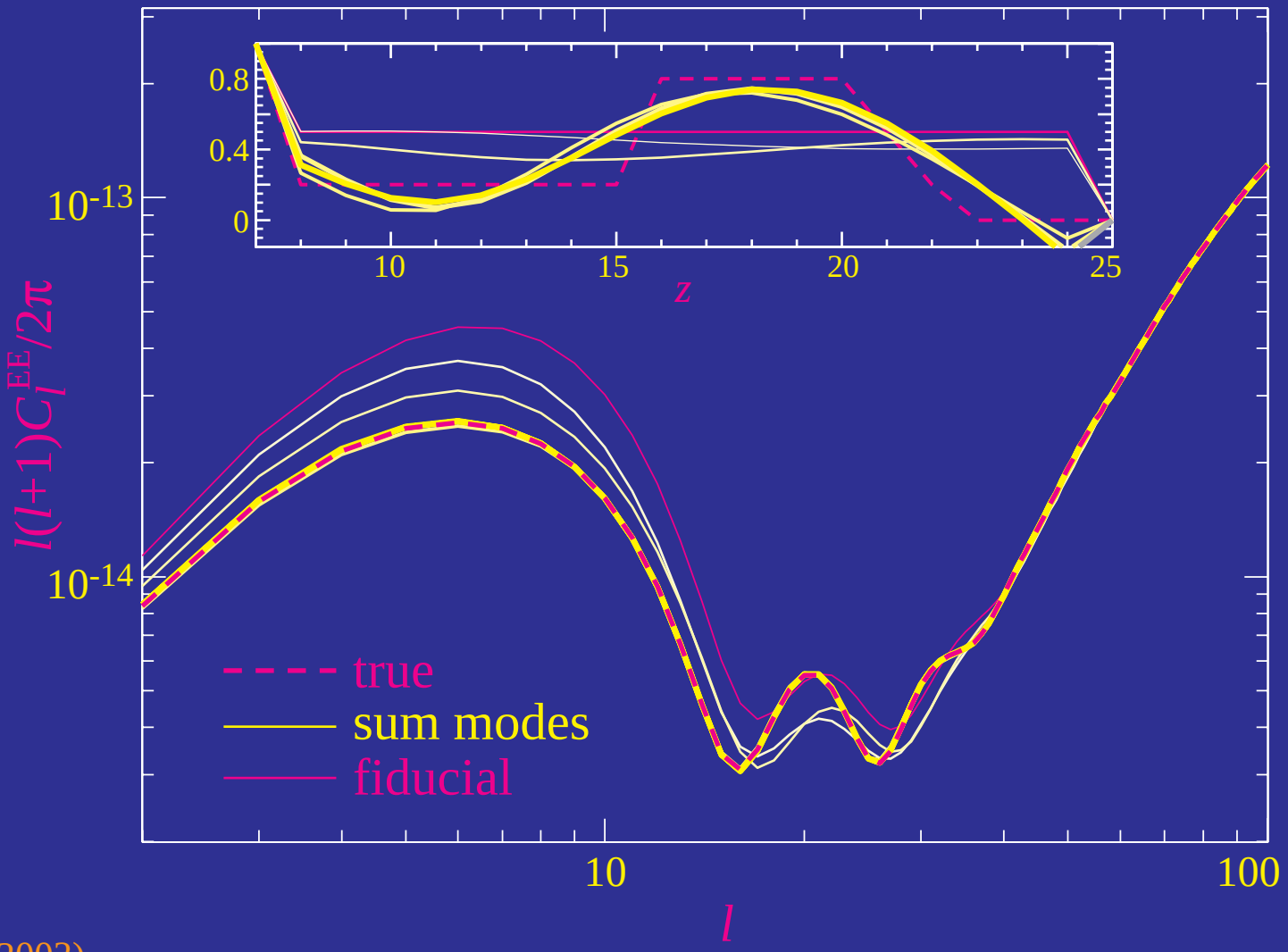

Hu & Holder (2003)

Total Optical Depth

- Optical depth measurement unbiased
- Ultimate errors set by cosmic variance here 0.01
- Equivalently 1% measure of initial amplitude, impt for dark energy

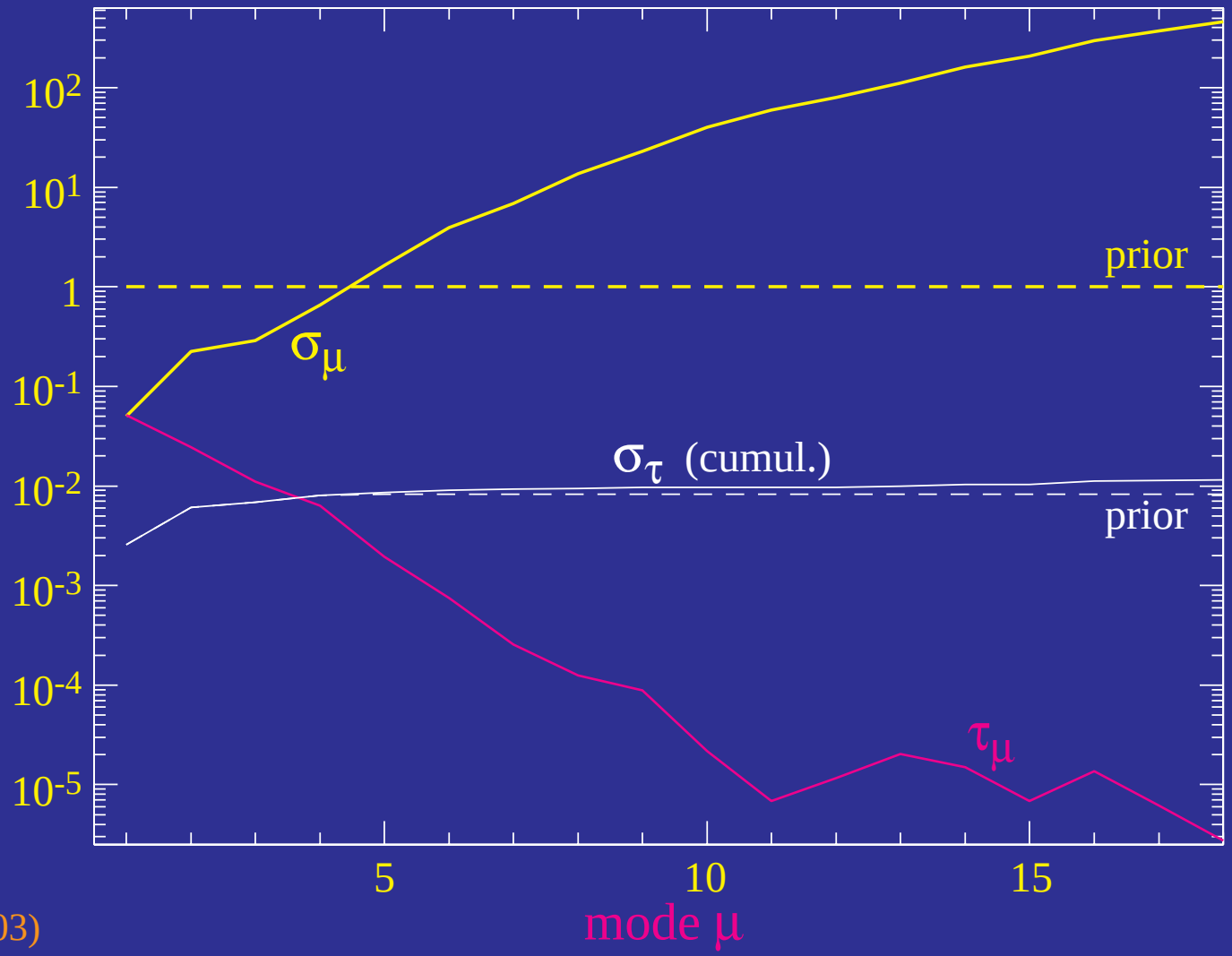

Hu & Holder (2003)

WMAP5 Ionization PCs

- Only first two modes constrained, τ=0.101±0.017

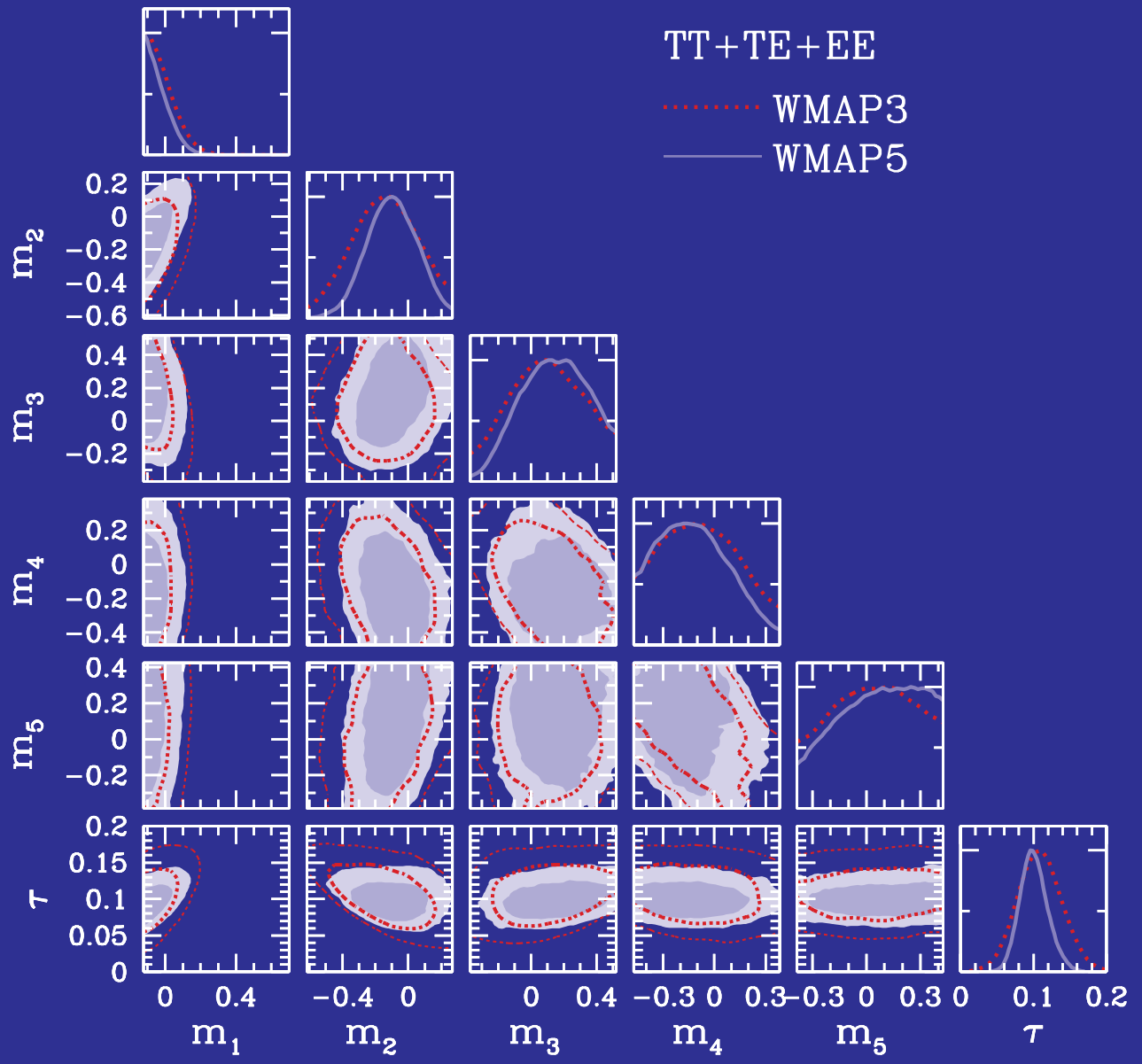

Mortonson & Hu (2008)

Model-Independent Reionization

- All possible ionization histories at $z<30$
- Detections at $20<l<30$ required to further constrain general ionization which widens the τ-n_s degeneracy allowing $n_s=1$
- Quadrupole & octopole predicted to better than cosmic variance test ΛCDM for anomalies

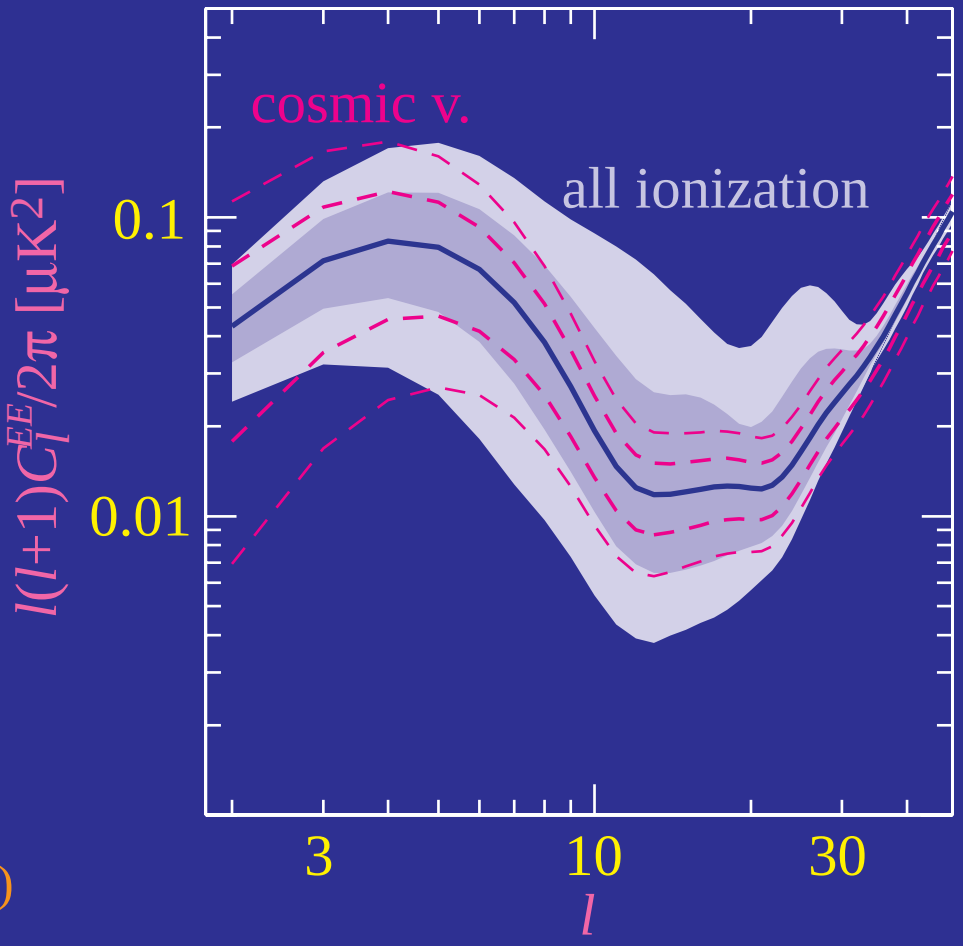

Mortonson & Hu (2008)

Large Scale Anomalies

Large Angle Anomalies

- Low planar quadrupole aligned with planar octopole
- More power in south ecliptic hemisphere
- Non-Gaussian spot

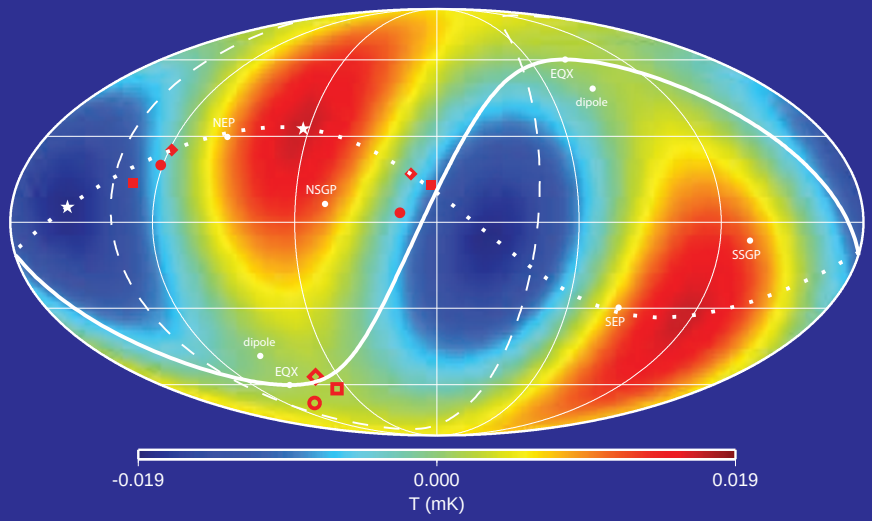

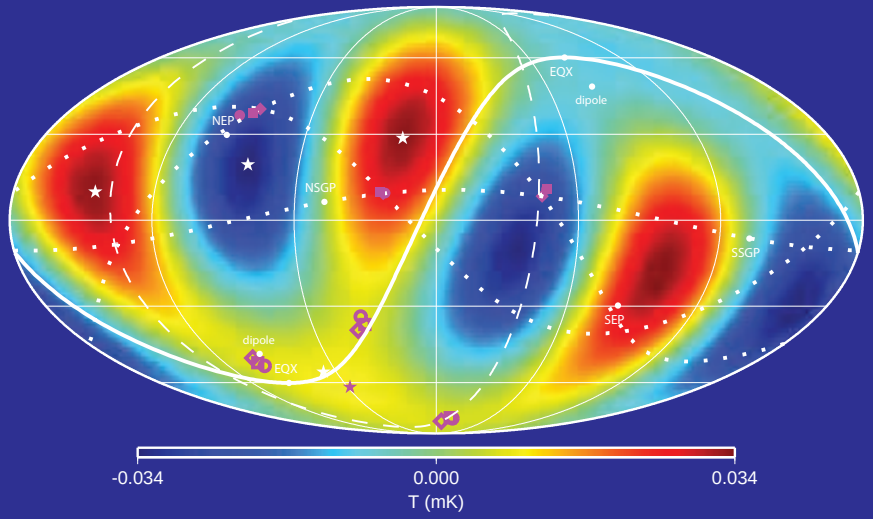

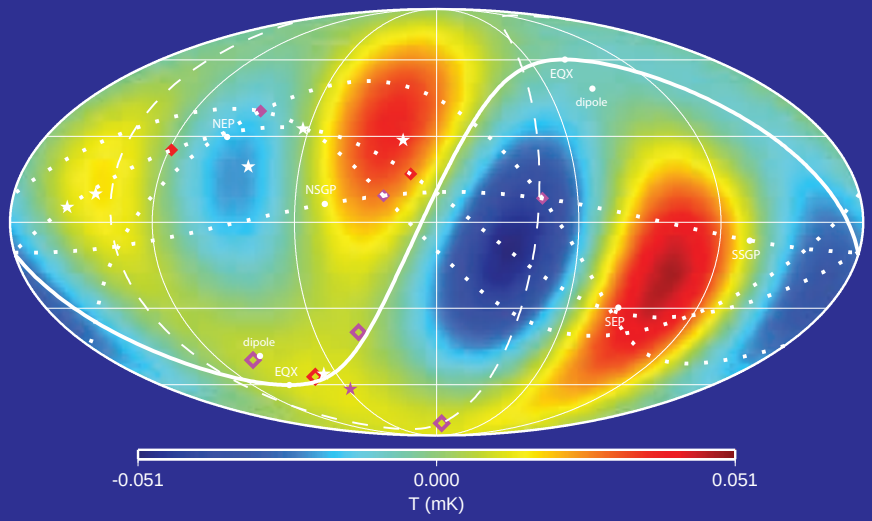

Copi et al (2006)

Polarization Tests

- Matching polarization anomalies if cosmological

Dvorkin, Peiris, Hu (2007)

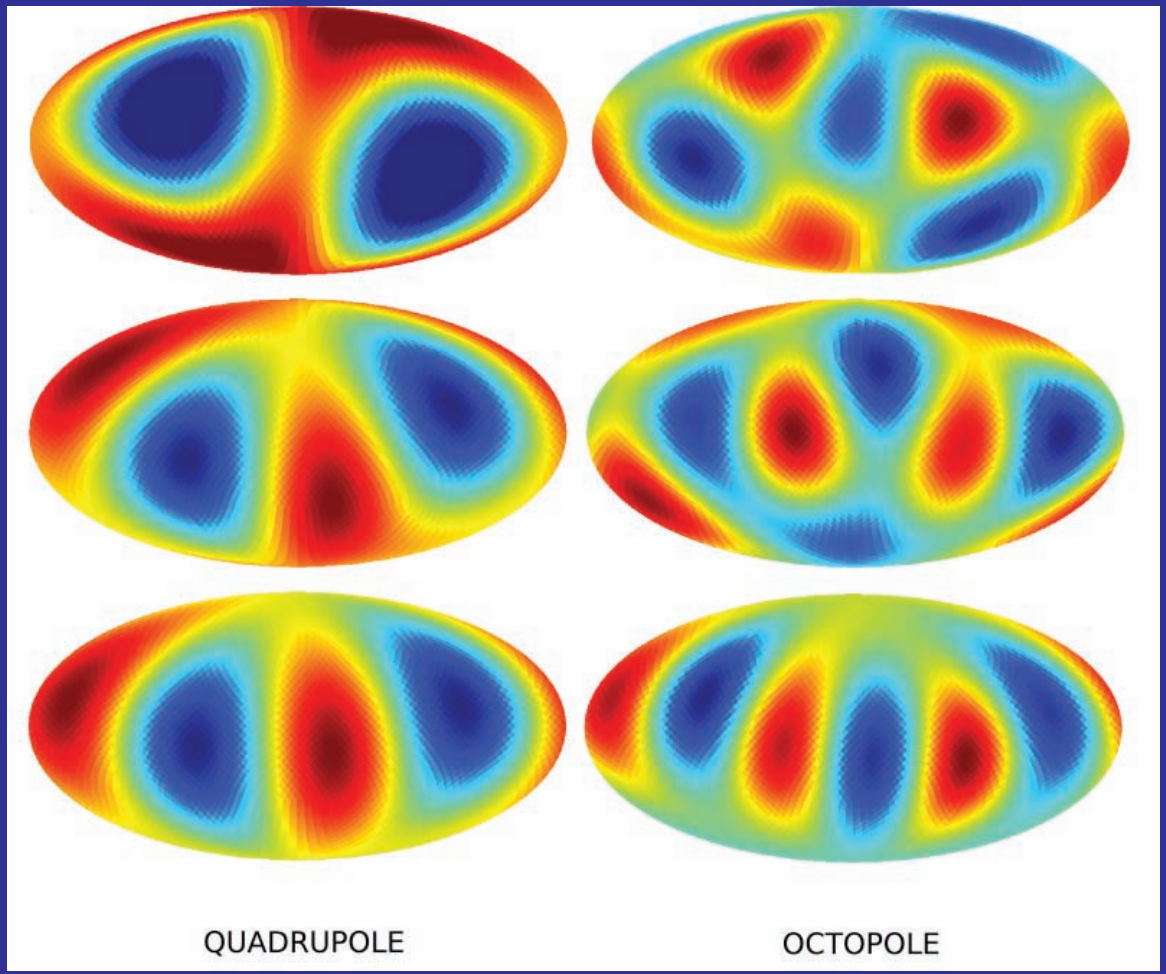

Polarization Bumps

- If features in the temperature spectrum reflect features in the power spectrum (inflationary potential), reflected in polarization with little ambiguity from reionization

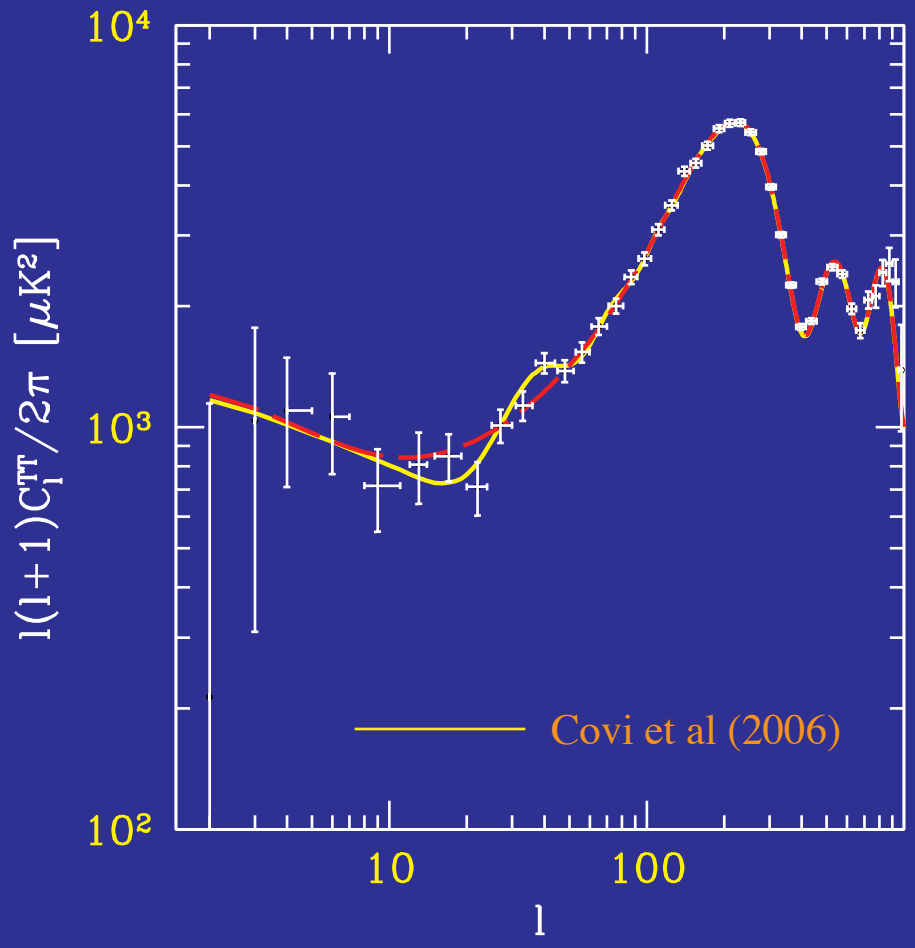

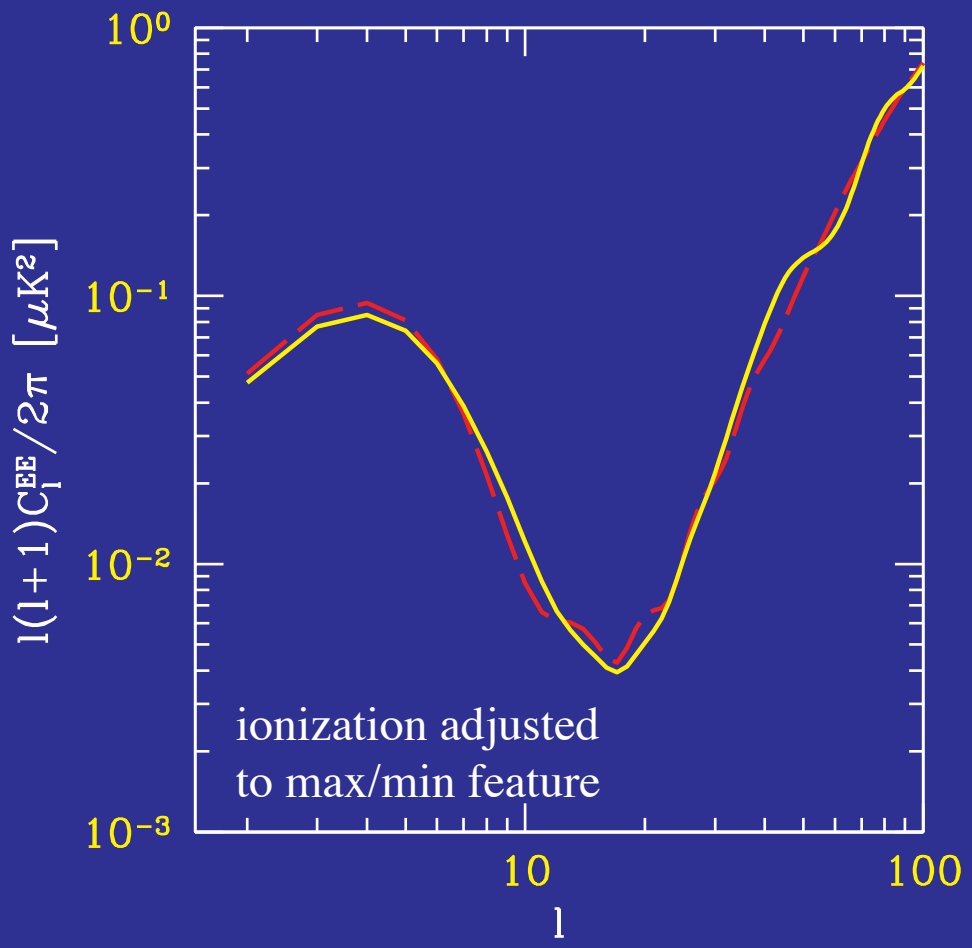

Mortonson et al (2009)

Summary: Lecture I

- Reionization suppresses primary anisotropy as $e^{-\tau}$ so the precision of initial normalization and growth rate measurements depends on τ precision
- In temperature spectrum, suppression acts on small scalesand looks like tilt for WMAP (not Planck)
- Linear Doppler effect highly suppressed on small scales, leading order term is modulated effect: OV, kSZ, patchy reionization
- Rescattering of quadrupole anisotropy leads to linear polarization at large angles
- Shape of polarization spectrum carries sufficient information to measure τ independently of ionization history (through PCs)
- If large angle anomalies are cosmological, they will be reflected in polarization

Physics of Secondary Anisotropies

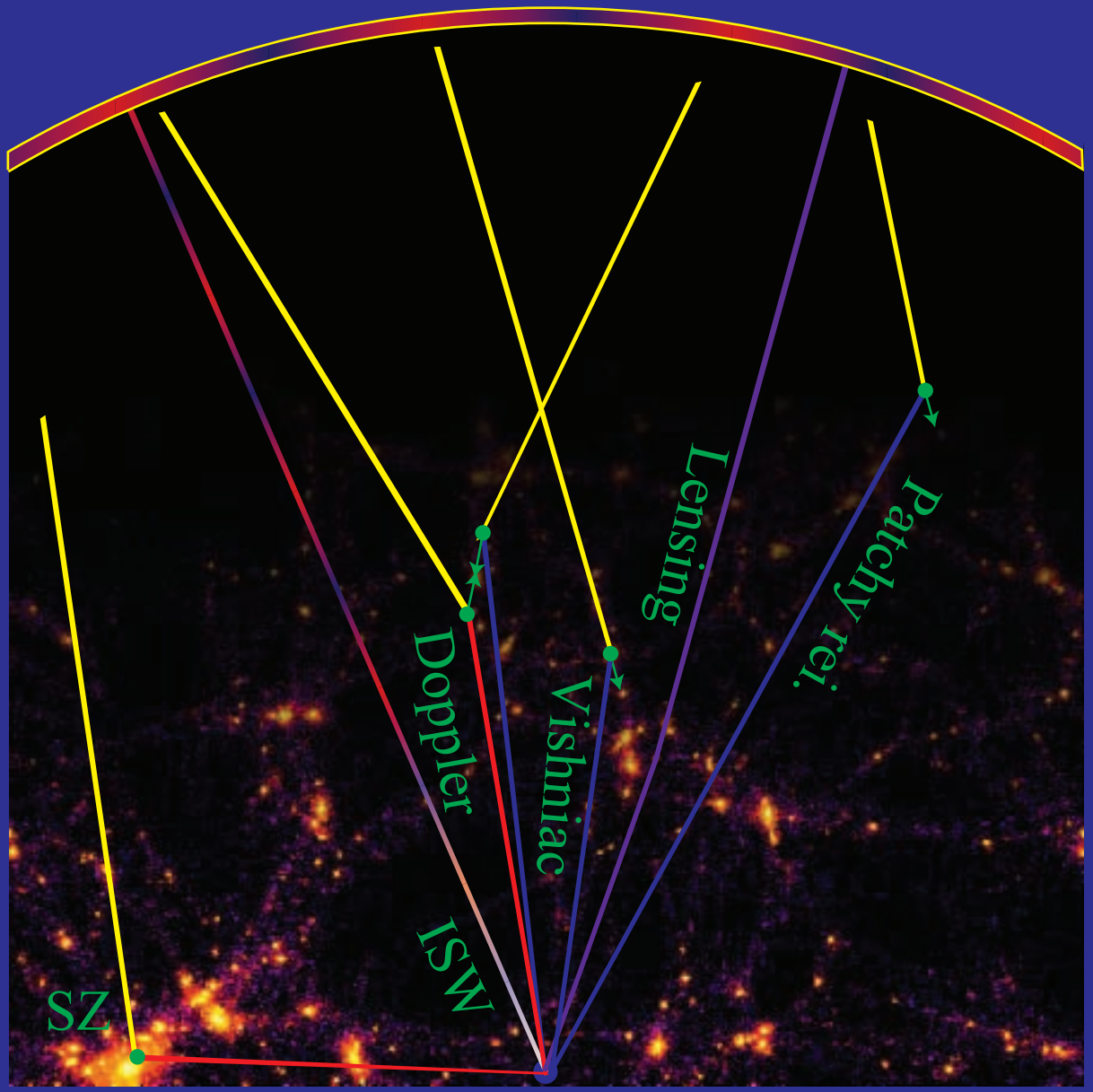

Polarized Landscape

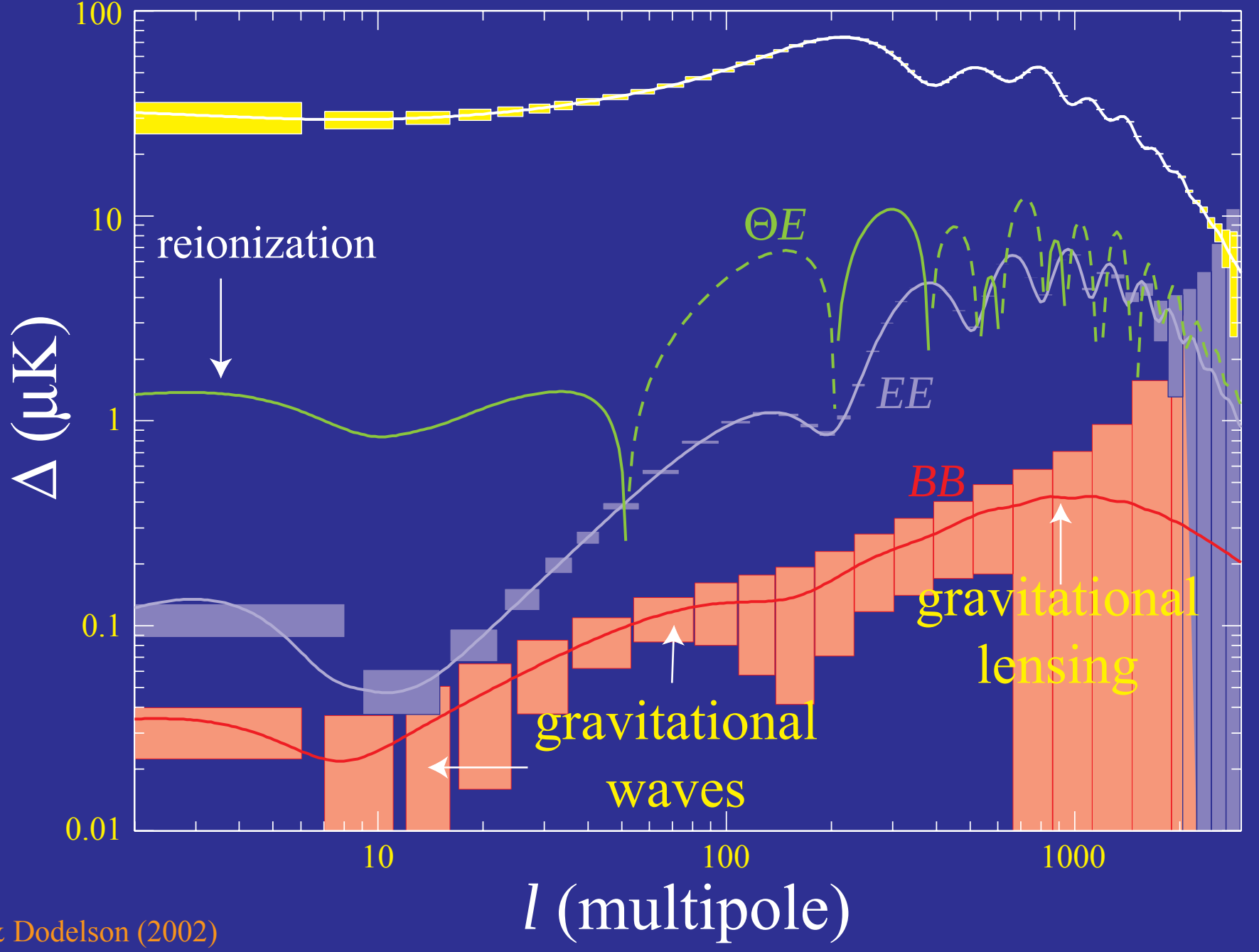

Hu & Dodelson (2002)

B-mode Polarization

Electric & Magnetic Polarization

(a.k.a. gradient & curl)

- Alignment of principal vs polarization axes (curvature matrix vs polarization direction)

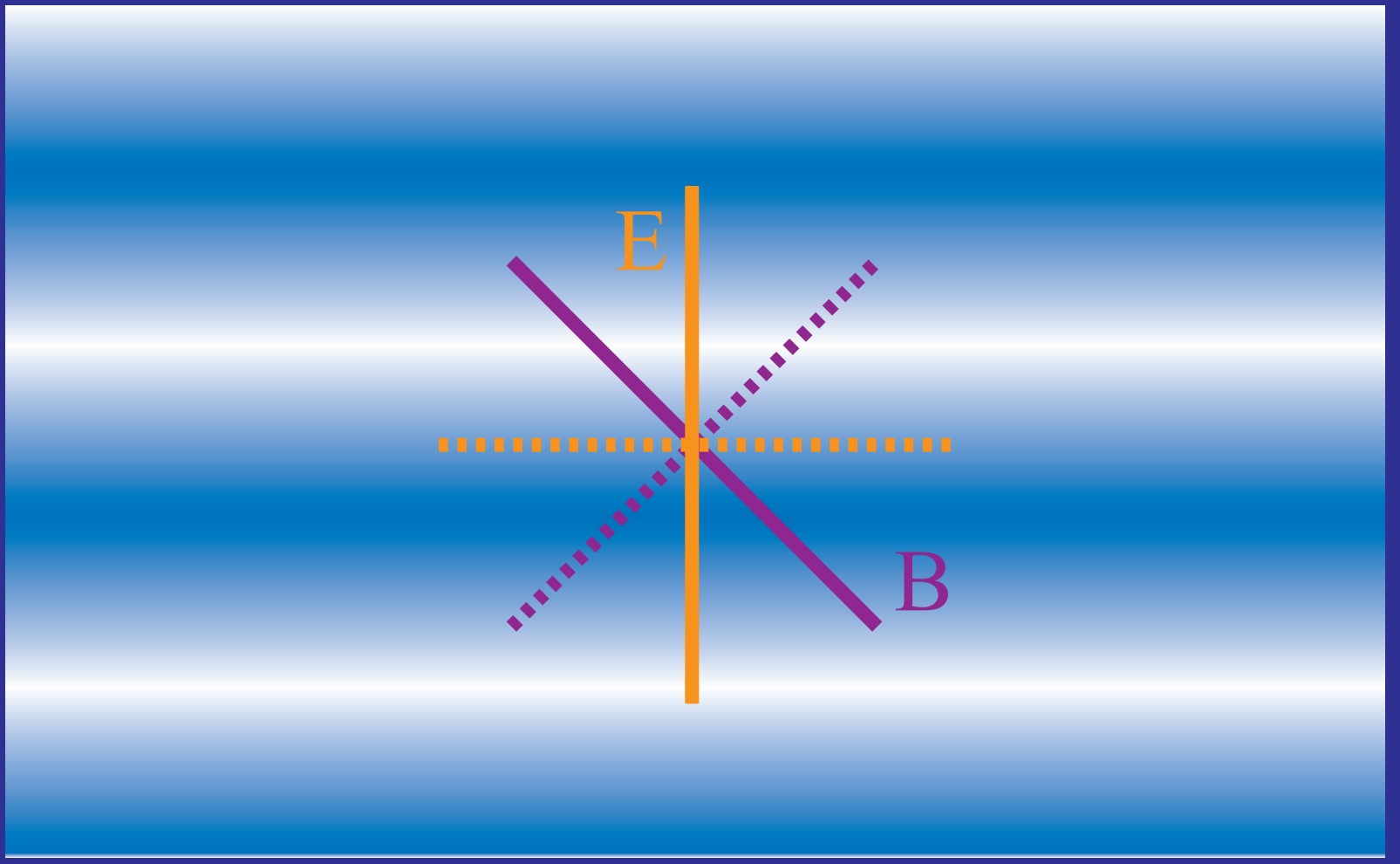

Kamionkowski, Kosowsky, Stebbins (1997)
Zaldarriaga & Seljak (1997)

Gravitational Waves

Quadrupoles from Gravitational Waves

- Transverse-traceless distortion provides temperature quadrupole
- Gravitational wave polarization picks out direction transverse to wavevector

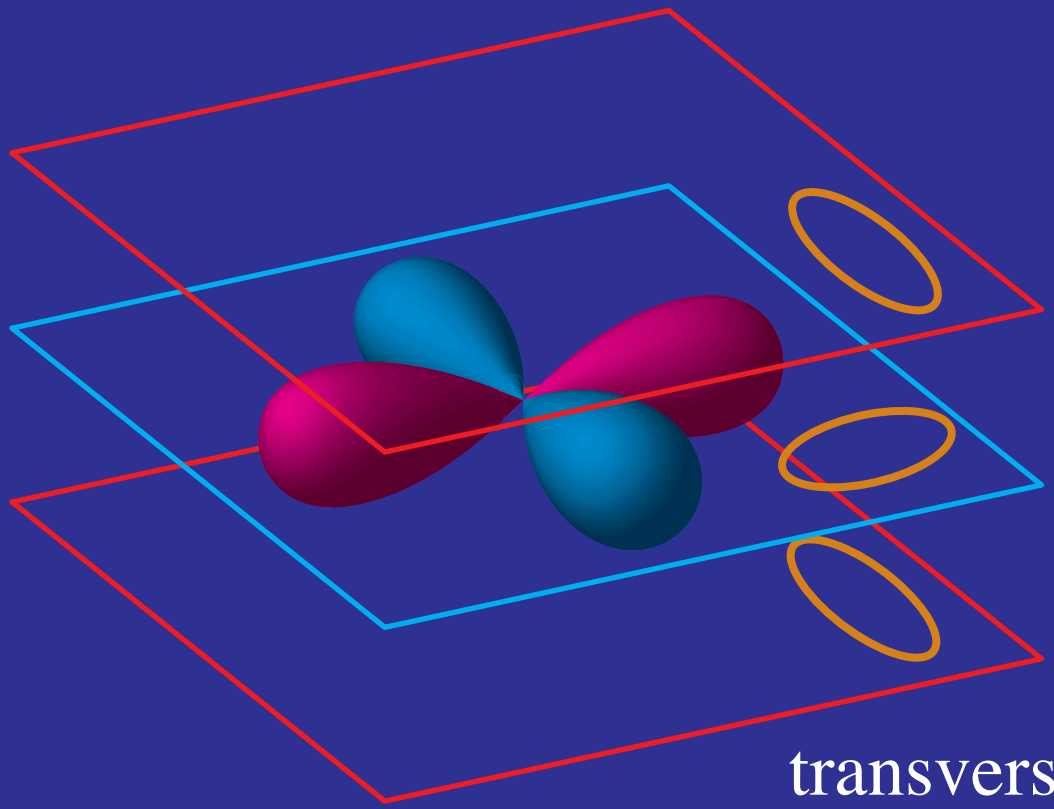

transverse-traceless distortion

Gravitational Wave Pattern

- Projection of the quadrupole anisotropy gives polarization pattern
- Transverse polarization of gravitational waves breaks azimuthal symmetry

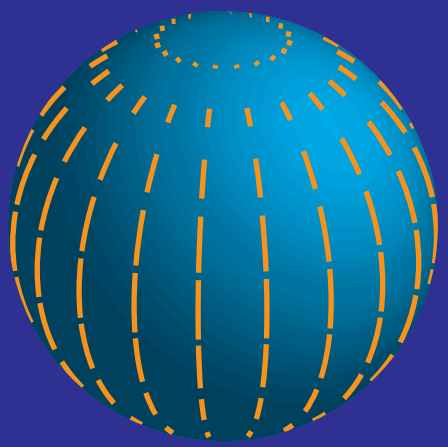

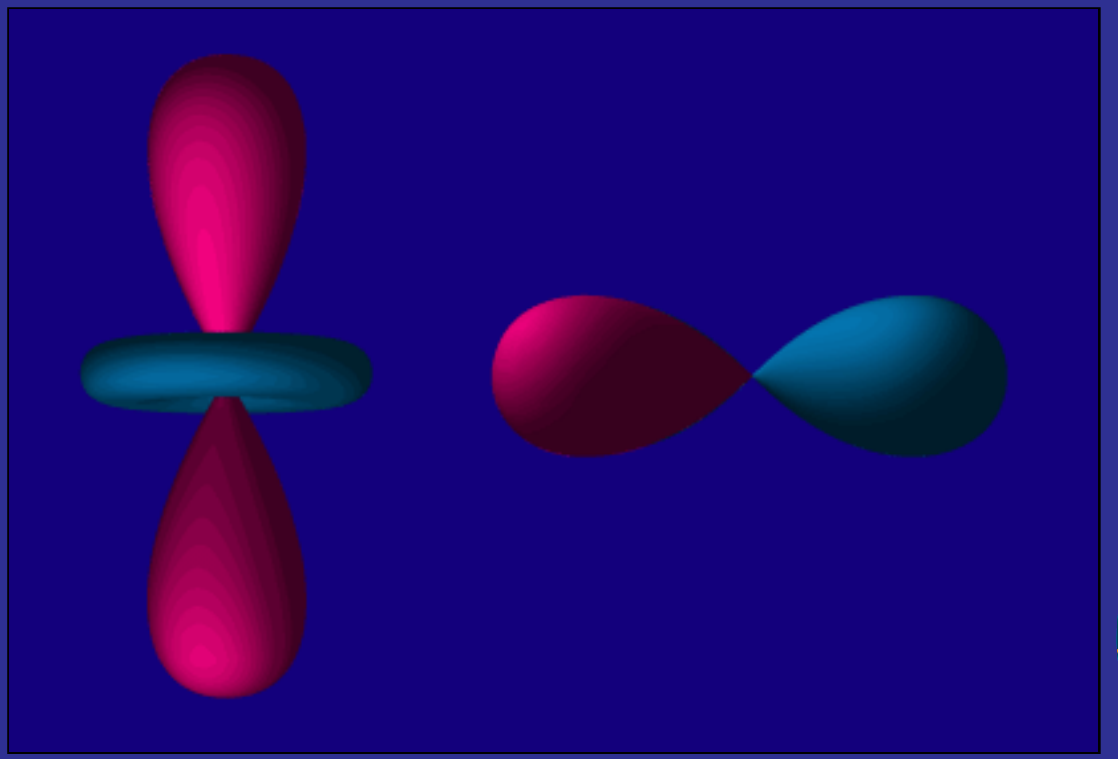

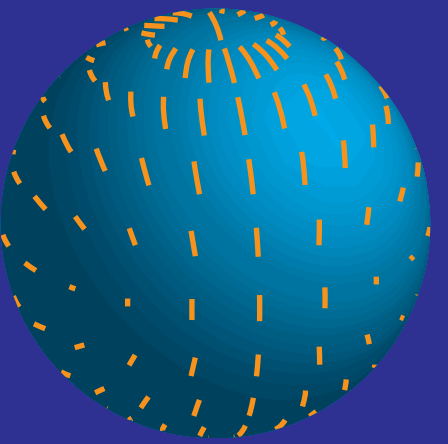

density perturbation

gravitational wave

Energy Scale of Inflation

- Amplitude of B-mode peak scales as square of energy scale (Hubble parameter) during inflation, power as E_i^4
- Good: upper limits are at GUT scale. Bad: secondaries & foregrounds

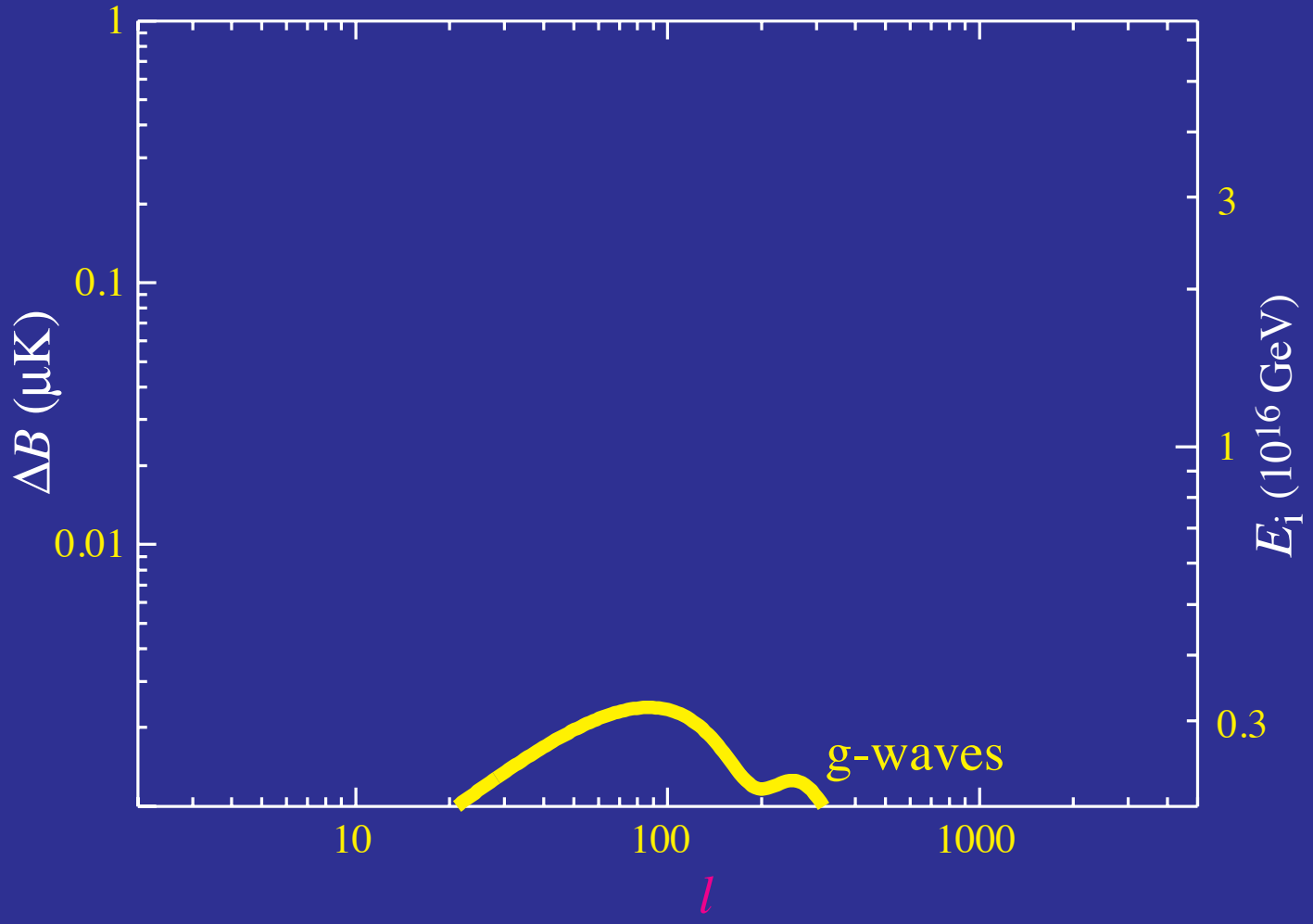

The B-Bump

- Rescattering of gravitational wave anisotropy generates the B-bump
- Potentially the most sensitive probe of inflationary energy scale

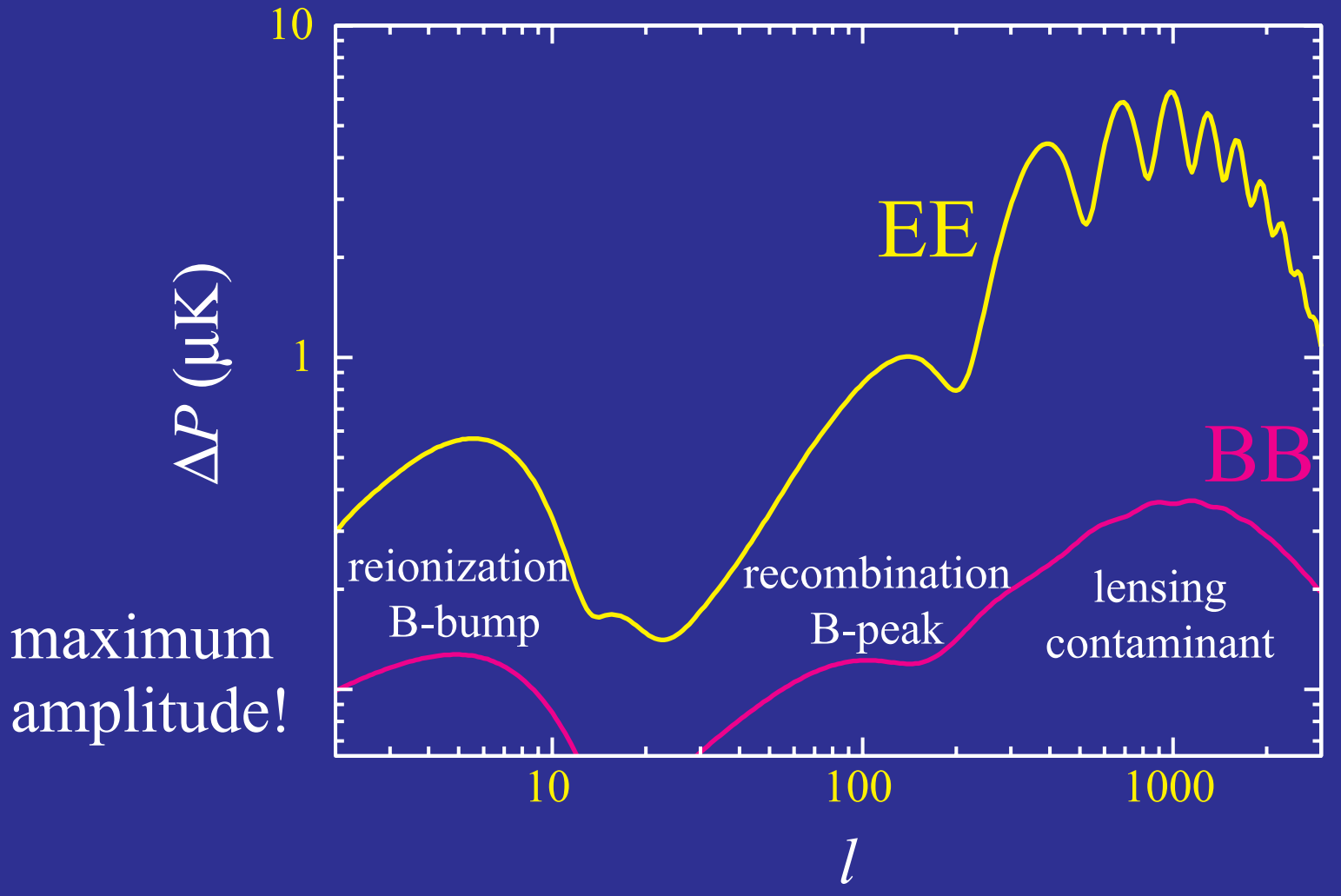

Slow Roll Consistency Relation

- Consistency relation between tensor-scalar ratio and tensor tilt $r = -8n_t$ tested by reionization
- Reionization uncertainties controlled by a complete p.c. analysis

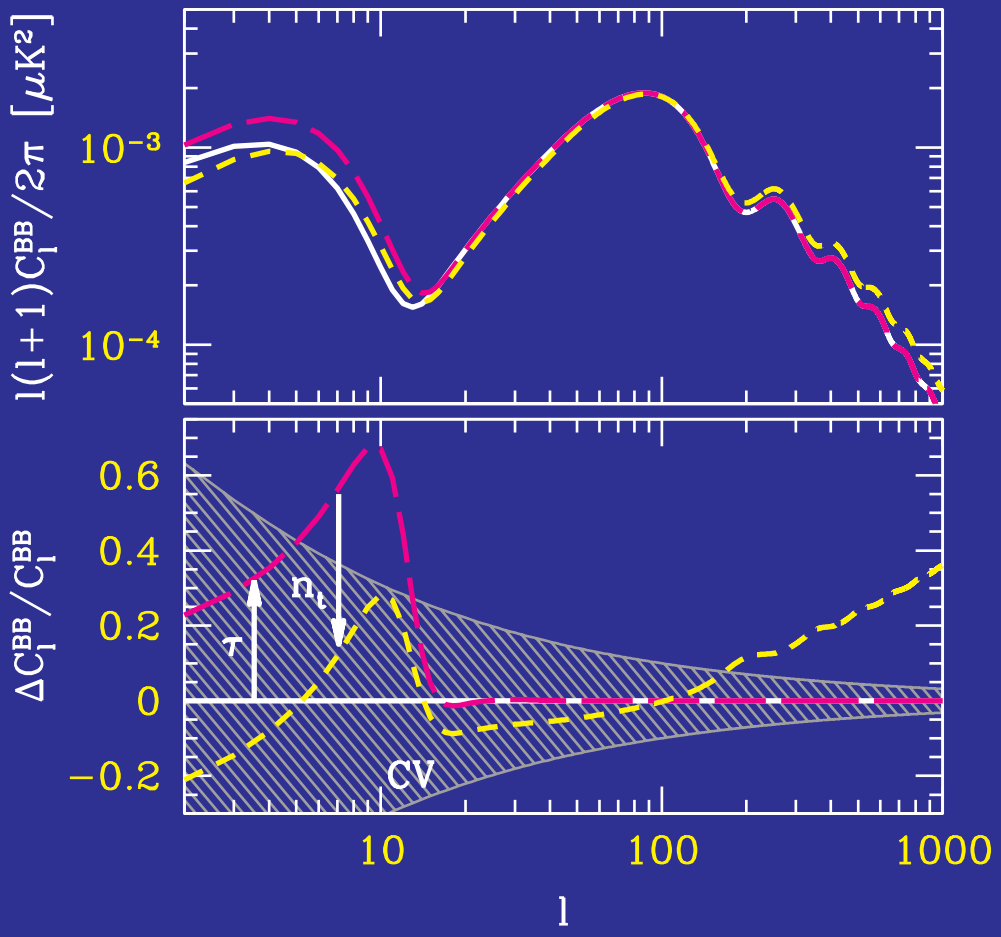

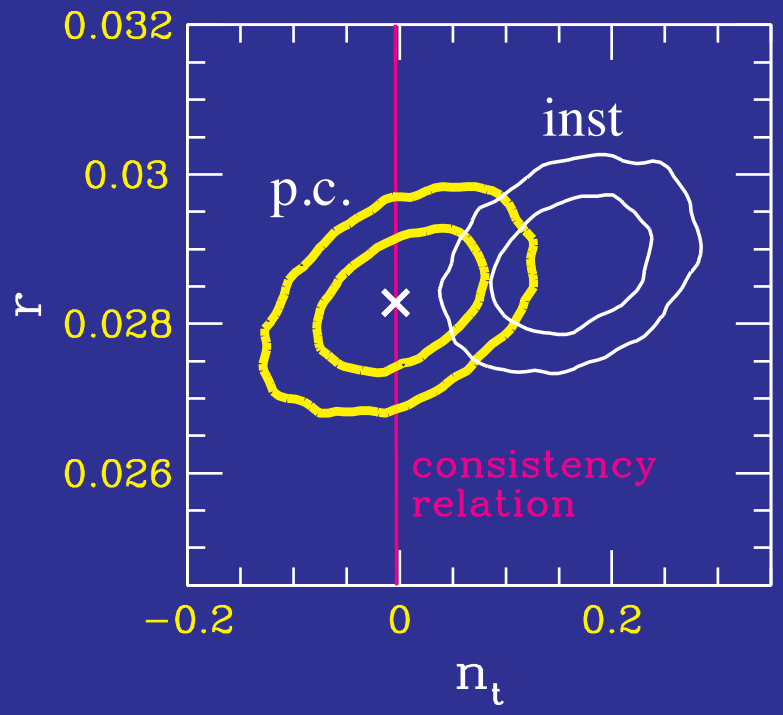

Mortonson & Hu (2007)

Patchy Reionization

Modulated Polarization

- Ionization or density fluctuations modulate large angle E polarization into small angle E and B polarization

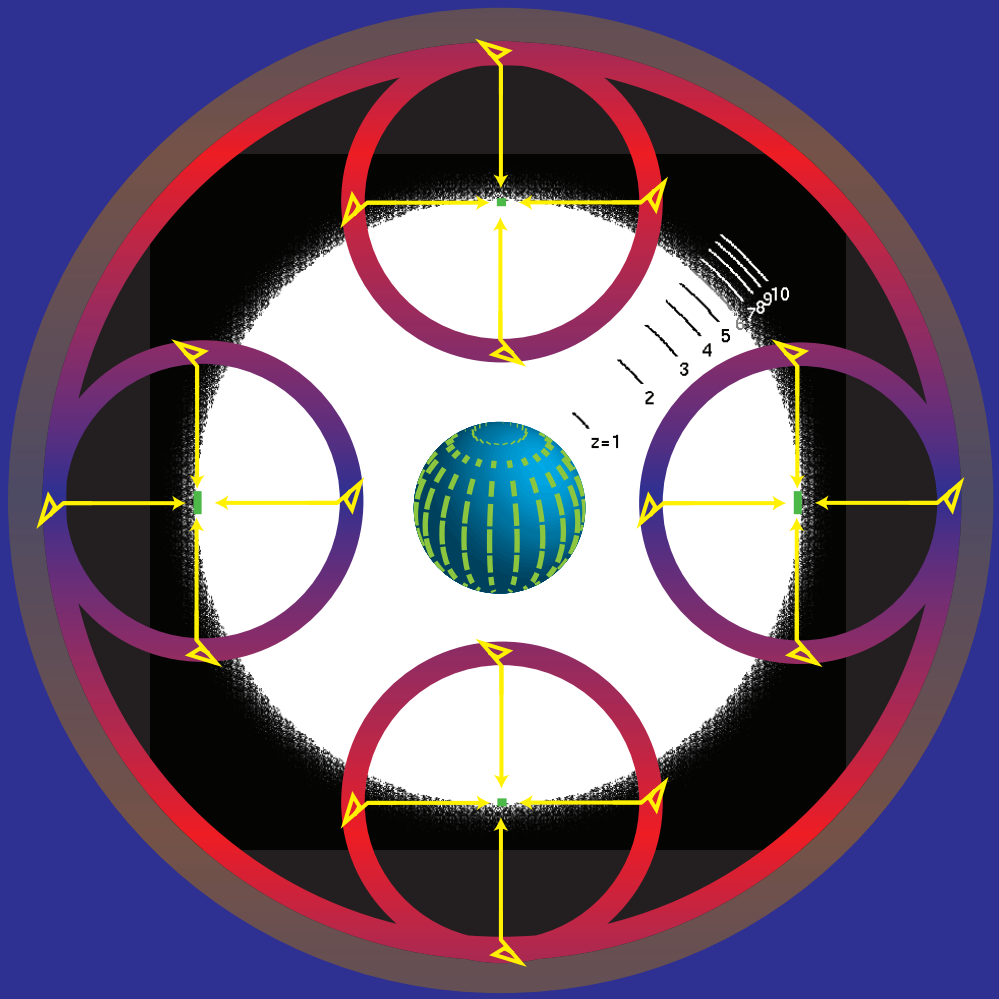

B-mode Contamination from Reionization

- Inhomogeneous reionization modulates polarization into B-modes
  (Hu 2000)
- Large signals if ionization bubbles >100Mpc at z~20-30

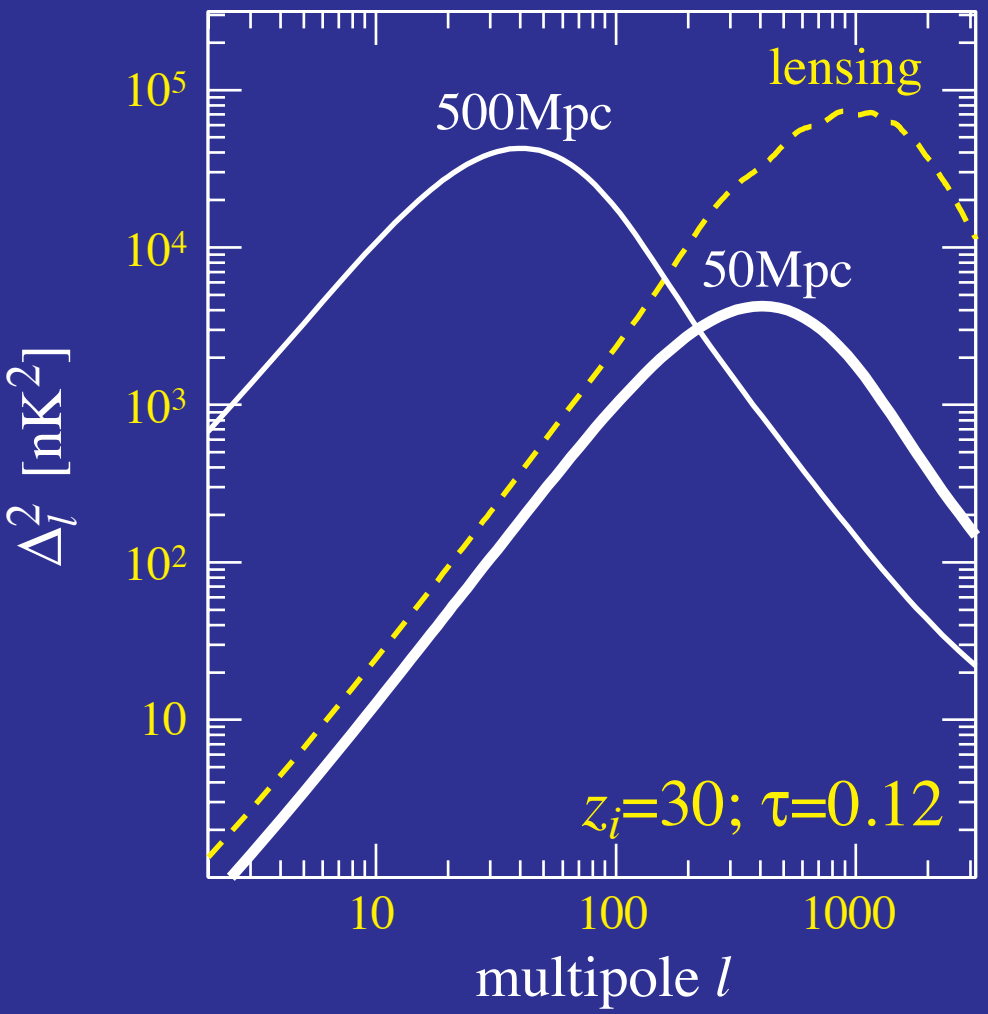

Potentially removeable if large:
Dvorkin & Smith (2008)

Mortonson & Hu (2006)

B-mode Contamination from Reionization

- Inhomogeneous reionization modulates polarization into B-modes
  (Hu 2000)
- Current expectation: grow to 10-100Mpc only at $z<10$
  (Furlanetto et al 2004; Zahn et al 2006)

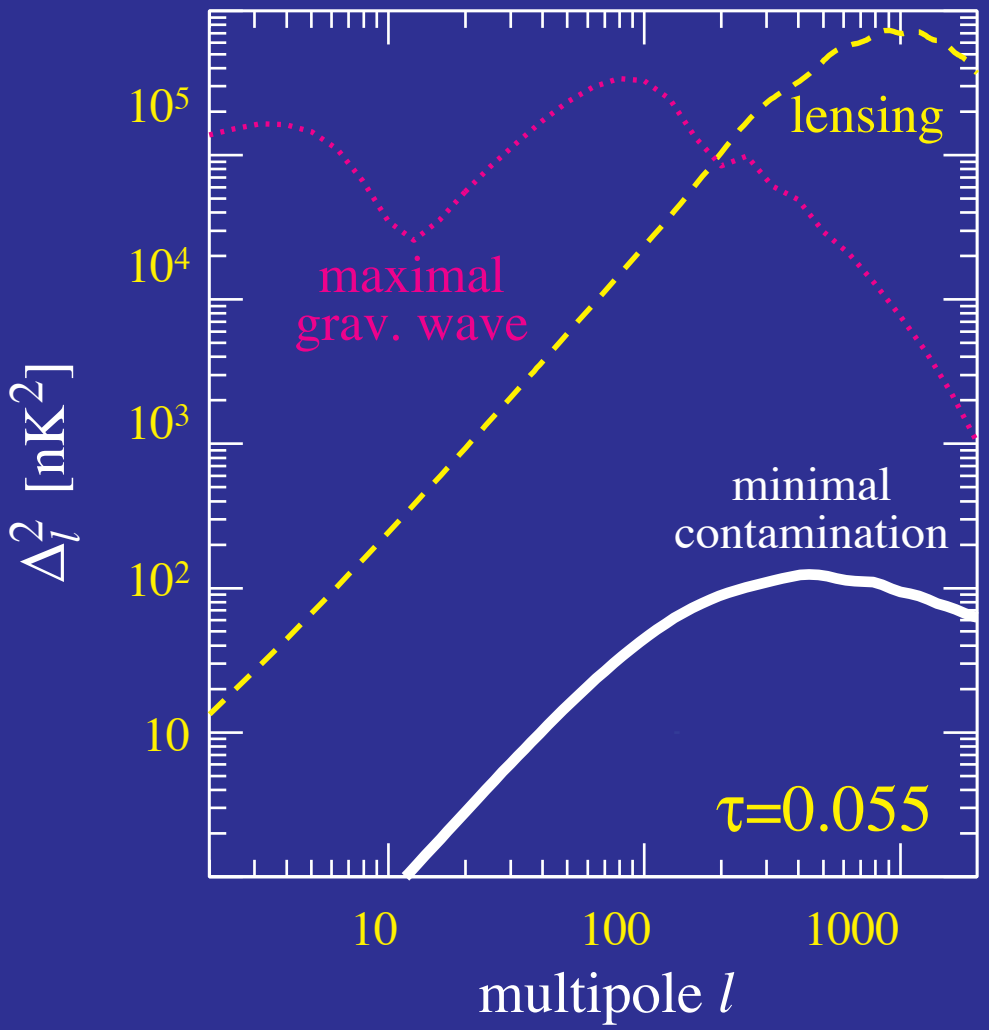

Mortonson & Hu (2006)

Gravitational Lensing

Example of CMB Lensing

- Toy example of lensing of the CMB primary anisotropies
- Shearing of the image

Gravitational Lensing

- Gravitational lensing by large scale structure distorts the observed temperature and polarization fields
- Exaggerated example for the temperature

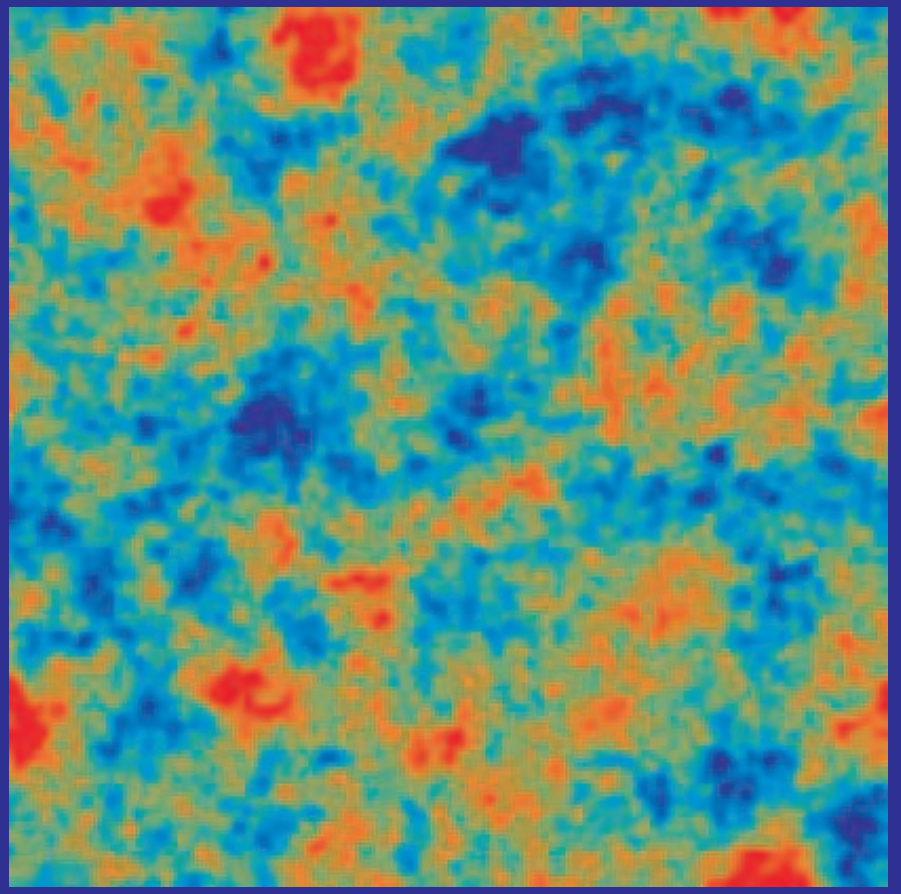

Original

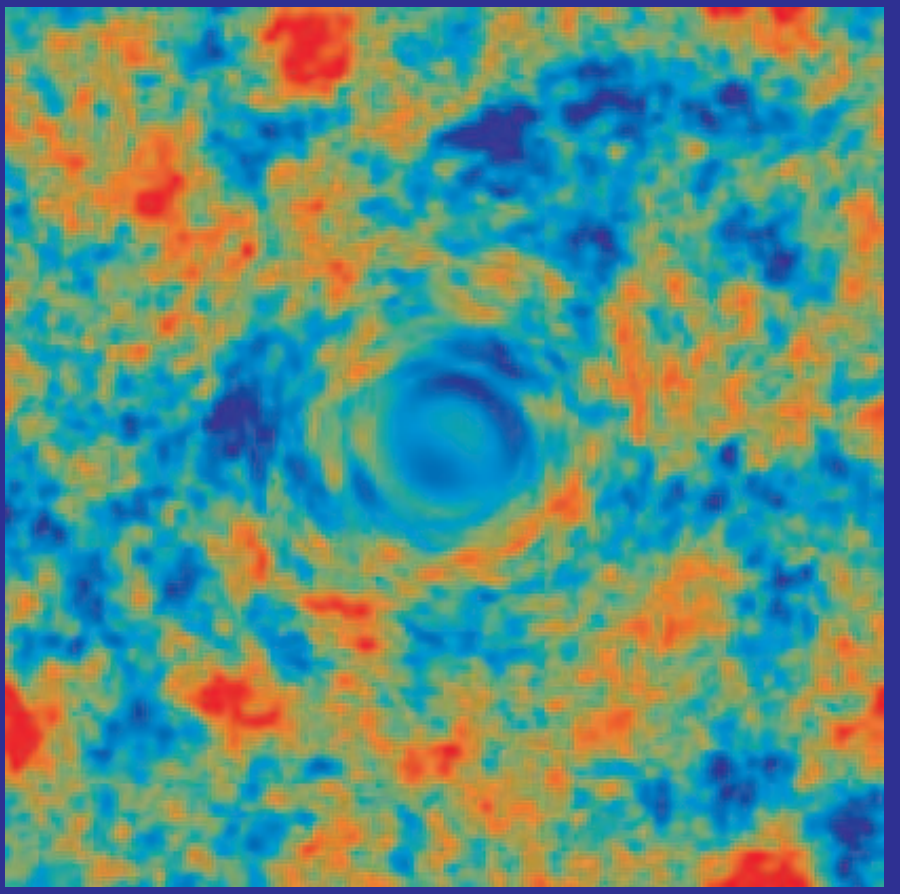

Lensed

Lensing by a Gaussian Random Field

- Mass distribution at large angles and high redshift in in the linear regime
- Projected mass distribution (low pass filtered reflecting deflection angles): 1000 sq. deg

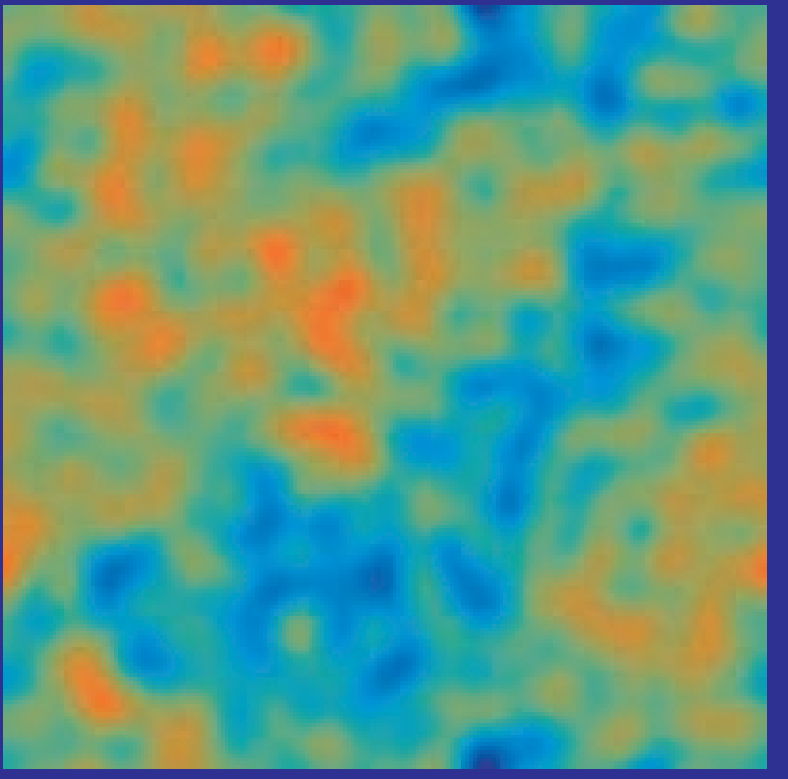

rms deflection
2.6'
deflection coherence
10°

Lensing in the Power Spectrum

- Lensing smooths the power spectrum with a width $\Delta l \sim 60$
- Convolution with specific kernel: higher order correlations between multipole moments – not apparent in power

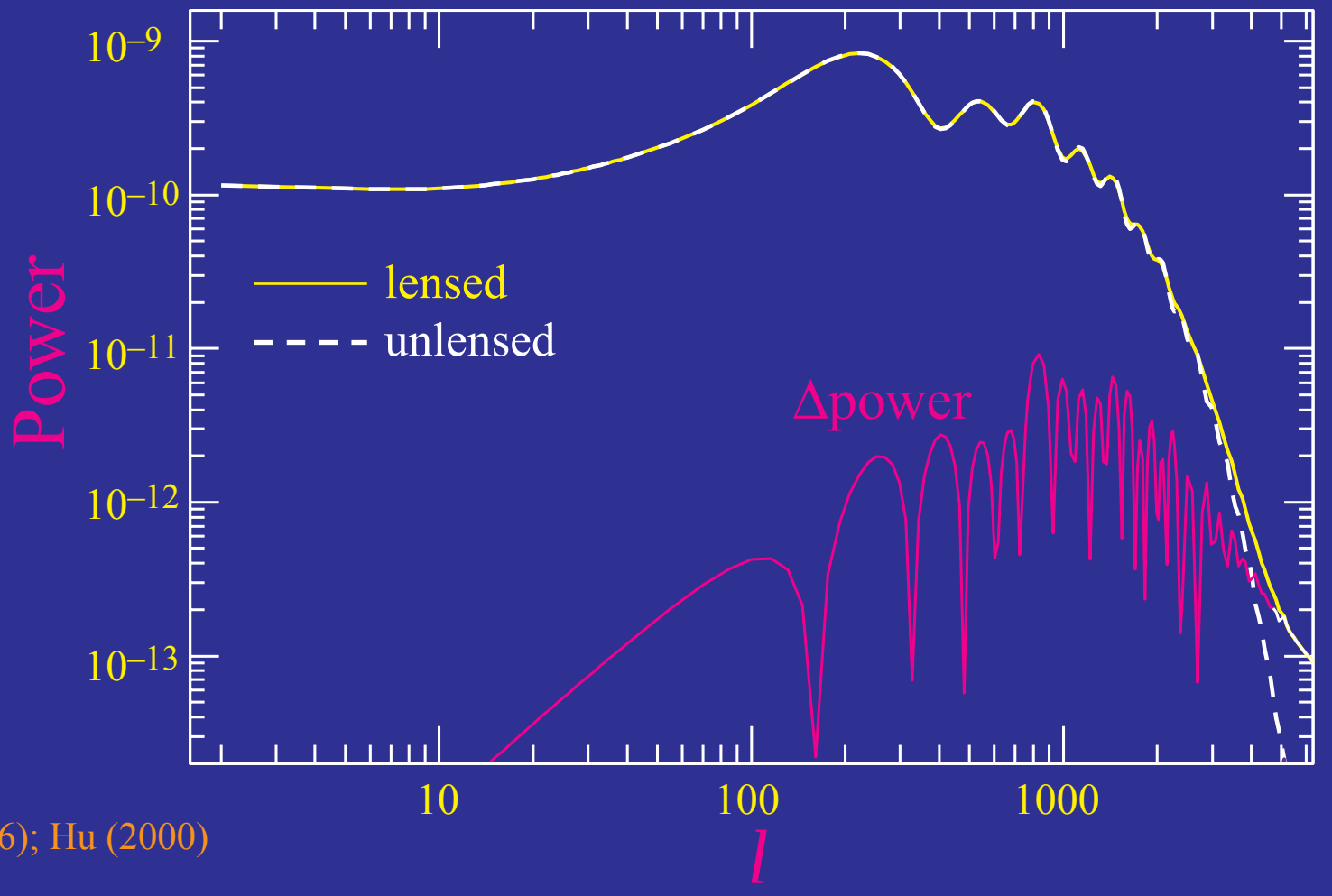

Seljak (1996); Hu (2000)

Gravitational Lensing

- Lensing is a surface brightness conserving remapping of source to image planes by the gradient of the projected potential

$$\phi(\hat{\mathbf{n}}) = 2 \int_{\eta_*}^{\eta_0} d\eta \, \frac{(D_* - D)}{D \, D_*} \Phi(D\hat{\mathbf{n}}, \eta) \, .$$

  such that the fields are remapped as

$$x(\hat{\mathbf{n}}) \rightarrow x(\hat{\mathbf{n}} + \nabla\phi) \, ,$$

  where $x \in \{\Theta, Q, U\}$ temperature and polarization.

- Taylor expansion leads to product of fields and Fourier mode-coupling

Flat-sky Treatment

- Taylor expand

$$\Theta(\hat{\mathbf{n}}) = \tilde{\Theta}(\hat{\mathbf{n}} + \nabla\phi)$$

$$= \tilde{\Theta}(\hat{\mathbf{n}}) + \nabla_i\phi(\hat{\mathbf{n}})\nabla^i\tilde{\Theta}(\hat{\mathbf{n}}) + \frac{1}{2}\nabla_i\phi(\hat{\mathbf{n}})\nabla_j\phi(\hat{\mathbf{n}})\nabla^i\nabla^j\tilde{\Theta}(\hat{\mathbf{n}}) + \ldots$$

- Fourier decomposition

$$\phi(\hat{\mathbf{n}}) = \int \frac{d^2l}{(2\pi)^2}\phi(\mathbf{l})e^{i\mathbf{l}\cdot\hat{\mathbf{n}}}$$

$$\tilde{\Theta}(\hat{\mathbf{n}}) = \int \frac{d^2l}{(2\pi)^2}\tilde{\Theta}(\mathbf{l})e^{i\mathbf{l}\cdot\hat{\mathbf{n}}}$$

Flat-sky Treatment

- Mode coupling of harmonics

$$\Theta(\mathbf{l}) = \int d\hat{\mathbf{n}}\, \Theta(\hat{\mathbf{n}}) e^{-i\mathbf{l}\cdot\hat{\mathbf{n}}}$$
$$= \tilde{\Theta}(\mathbf{l}) - \int \frac{d^2\mathbf{l}_1}{(2\pi)^2} \tilde{\Theta}(\mathbf{l}_1) L(\mathbf{l}, \mathbf{l}_1)\,,$$

where

$$L(\mathbf{l}, \mathbf{l}_1) = \phi(\mathbf{l} - \mathbf{l}_1)\,(\mathbf{l} - \mathbf{l}_1)\cdot\mathbf{l}_1$$
$$+ \frac{1}{2}\int \frac{d^2\mathbf{l}_2}{(2\pi)^2} \phi(\mathbf{l}_2)\phi^*(\mathbf{l}_2 + \mathbf{l}_1 - \mathbf{l})\,(\mathbf{l}_2\cdot\mathbf{l}_1)(\mathbf{l}_2 + \mathbf{l}_1 - \mathbf{l})\cdot\mathbf{l}_1\,.$$

- Represents a coupling of harmonics separated by $L \approx 60$ peak of deflection power

Power Spectrum

- Power spectra

$$\langle \Theta^*(\mathbf{l})\Theta(\mathbf{l}')\rangle = (2\pi)^2\delta(\mathbf{l}-\mathbf{l}')\, C_l^{\Theta\Theta}\,,$$
$$\langle \phi^*(\mathbf{l})\phi(\mathbf{l}')\rangle = (2\pi)^2\delta(\mathbf{l}-\mathbf{l}')\, C_l^{\phi\phi}\,,$$

becomes

$$C_l^{\Theta\Theta} = \left(1 - l^2 R\right)\tilde{C}_l^{\Theta\Theta} + \int \frac{d^2\mathbf{l}_1}{(2\pi)^2}\tilde{C}^{\Theta\Theta}_{|\mathbf{l}-\mathbf{l}_1|}C_{l_1}^{\phi\phi}[(\mathbf{l}-\mathbf{l}_1)\cdot\mathbf{l}_1]^2\,,$$

where

$$R = \frac{1}{4\pi}\int \frac{dl}{l}\, l^4 C_l^{\phi\phi}\,.$$

Smoothing Power Spectrum

- If $\tilde{C}_l^{\Theta\Theta}$ slowly varying then two term cancel

$$\tilde{C}_l^{\Theta\Theta} \int \frac{d^2\mathbf{l}_1}{(2\pi)^2} C_l^{\phi\phi} (\mathbf{l}\cdot\mathbf{l}_1)^2 \approx l^2 R \tilde{C}_l^{\Theta\Theta} \, .$$

- So lensing acts to smooth features in the power spectrum. Smoothing kernel is $\Delta L \sim 60$ the peak of deflection power spectrum
- Because acoustic feature appear on a scale $l_A \sim 300$, smoothing is a subtle effect in the power spectrum.
- Lensing generates power below the damping scale which directly reflect power in deflections on the same scale

Lensing in the Power Spectrum

- Lensing smooths the power spectrum with a width $\Delta l \sim 60$
- Convolution with specific kernel: higher order correlations between multipole moments – not apparent in power

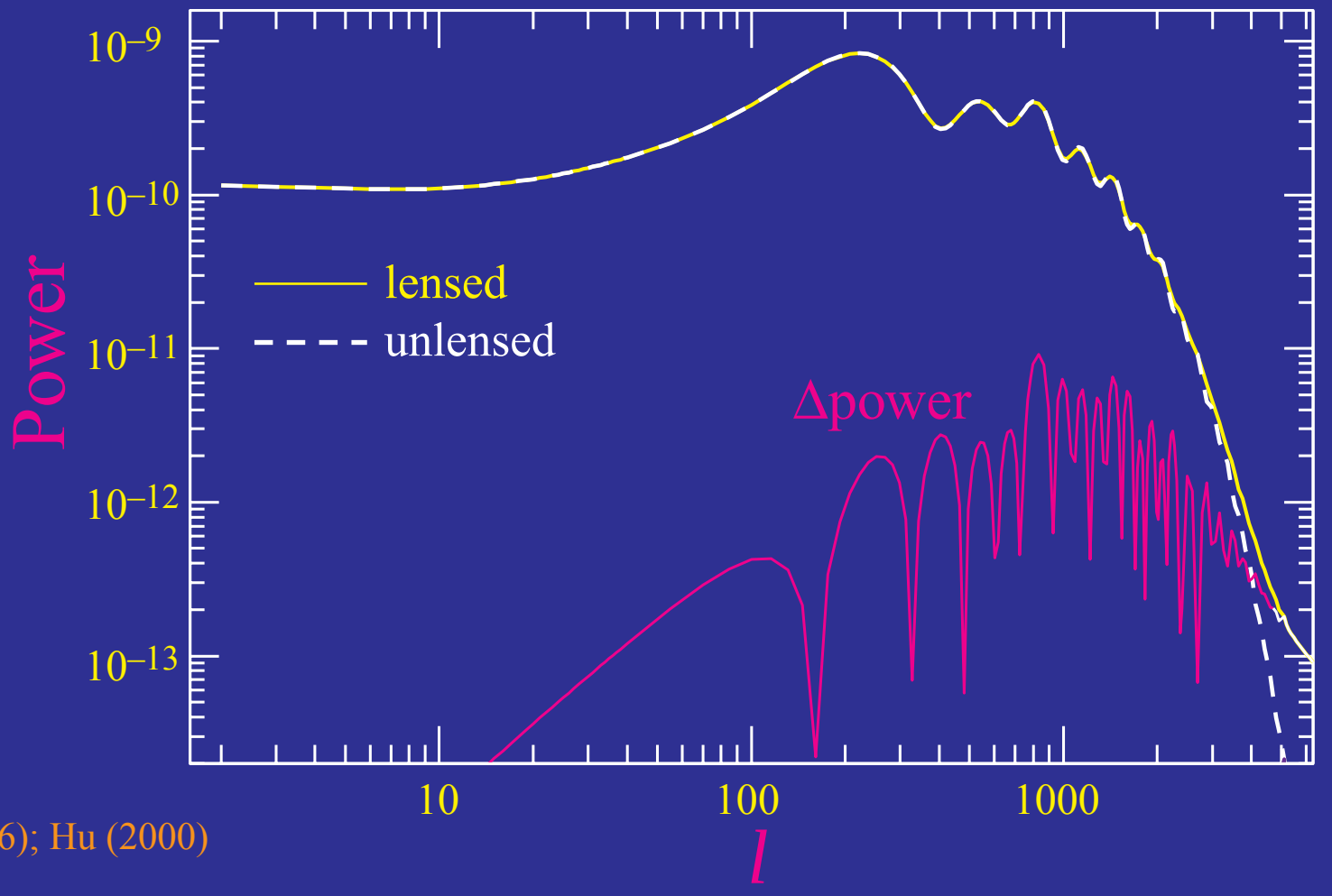

Seljak (1996); Hu (2000)

Generation of Power

- On scales below the damping scale, primary CMB looks like a smooth gradient
- Lensing effects modulate the gradient ($l_1 \ll l$):

$$C_l^{\Theta\Theta} \approx \int \frac{d^2\mathbf{l}_1}{(2\pi)^2} \tilde{C}_{l_1}^{\Theta\Theta} C_{|\mathbf{l}-\mathbf{l}_1|}^{\phi\phi} [(\mathbf{l}-\mathbf{l}_1)\cdot\mathbf{l}_1]^2$$

$$\approx \frac{1}{2} l^2 C_l^{\phi\phi} \int \frac{d^2\mathbf{l}_1}{(2\pi)^2} l_1^2 \tilde{C}_{l_1}^{\Theta\Theta}$$

and produce power on the same scale from power in the primary gradient (Zaldarriaga 2000)

Lensing in the Power Spectrum

- Small scale lenses modulate the large scale temperature field
- Generates power below damping scale from gradient power

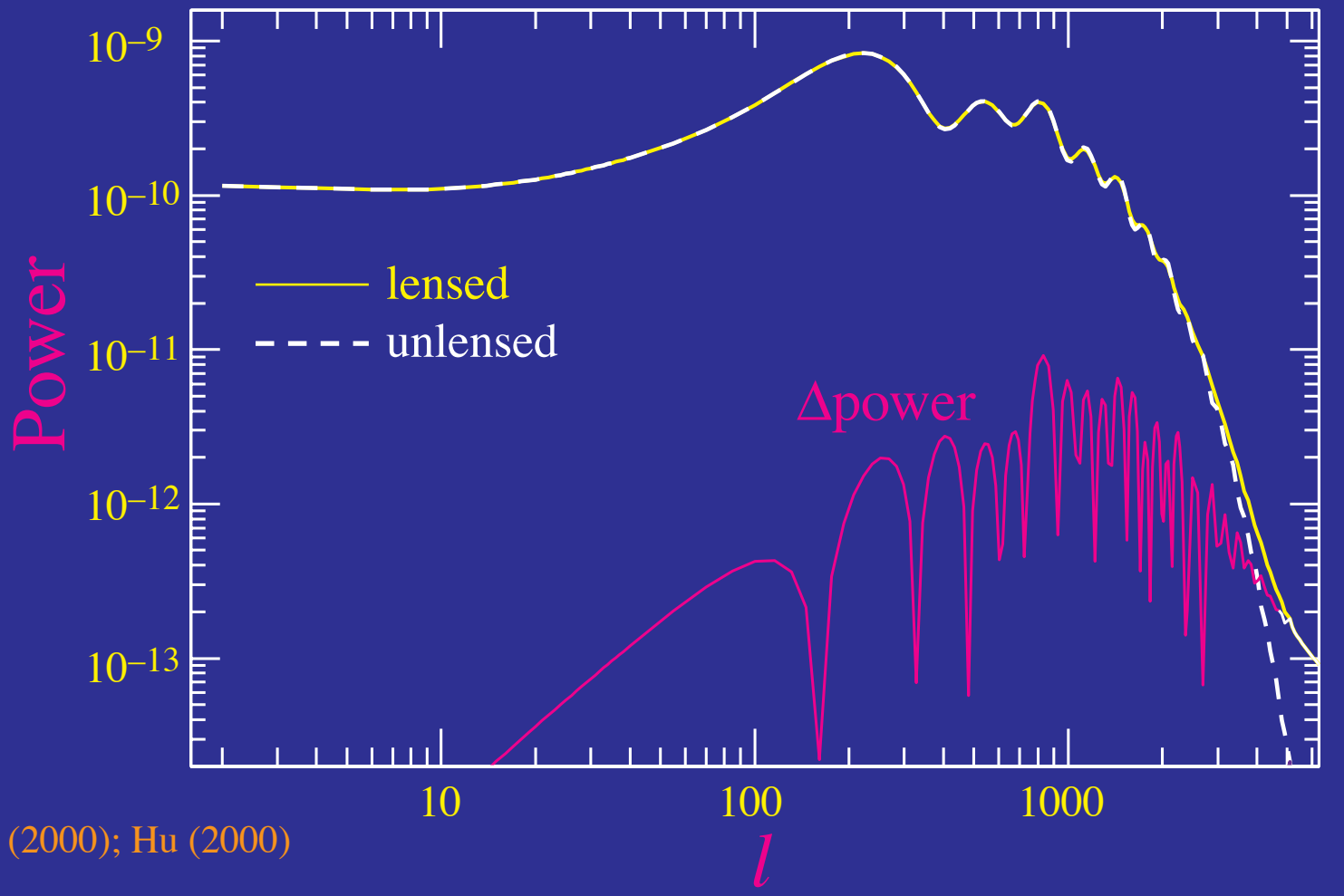

Zaldarriaga (2000); Hu (2000)

Lensing Smoothing

- Lensing smooths acoustic peaks and is favored by ACBAR data (~3σ)

Reichardt et al (2008)

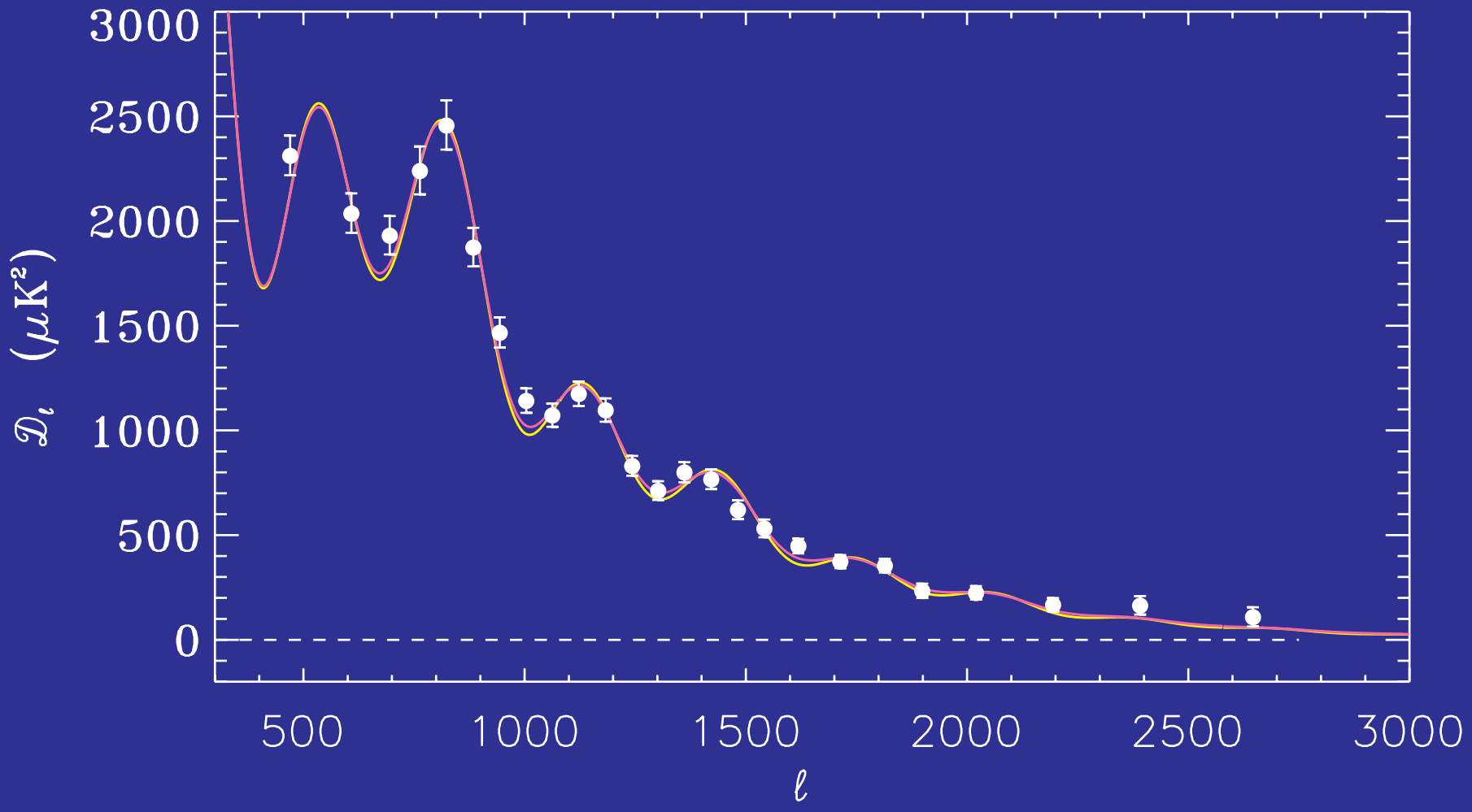

cf. Calabrese et al (2008)

Polarization Lensing

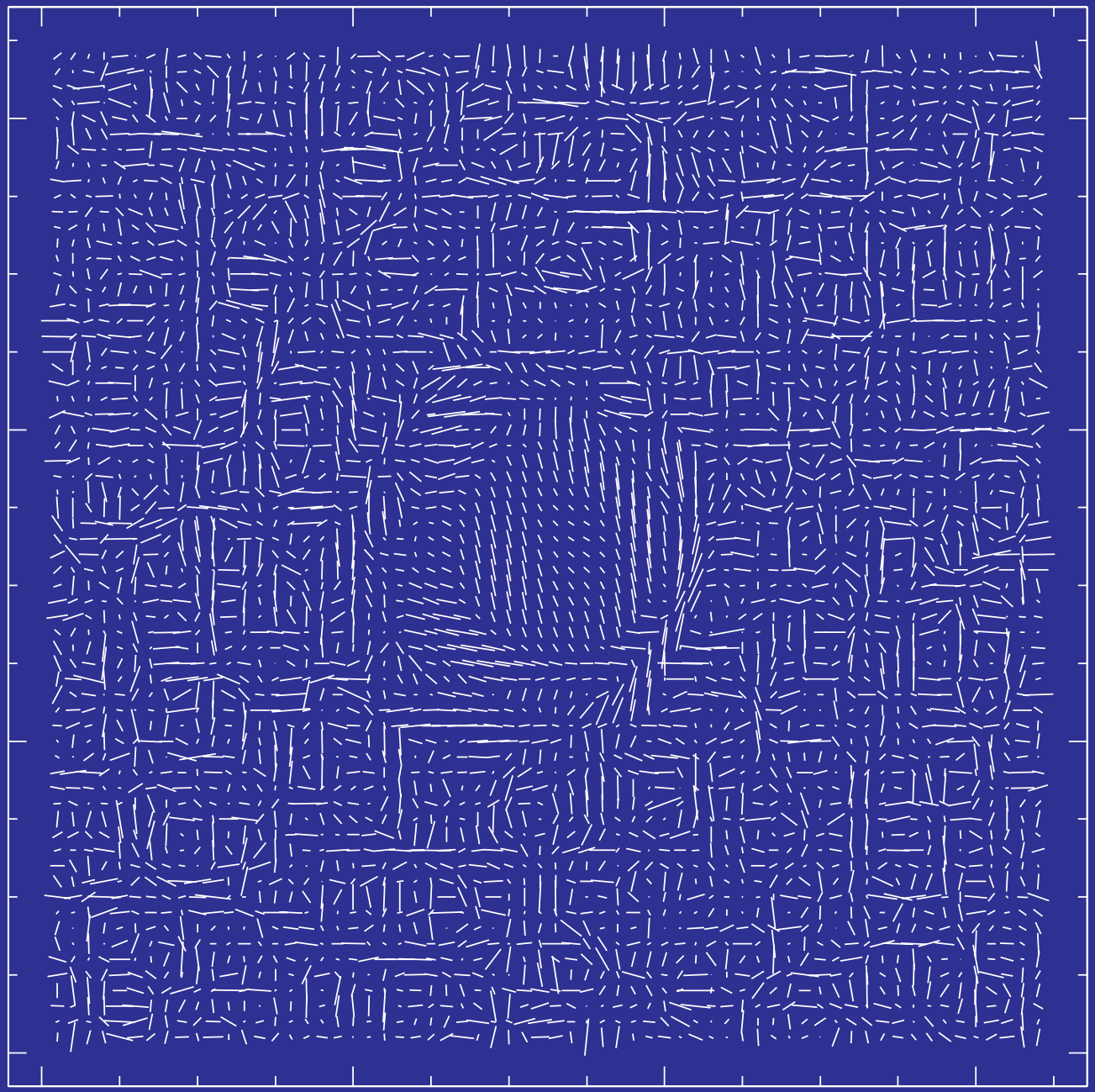

Polarization Lensing

- Since E and B denote the relationship between the polarization amplitude and direction, warping due to lensing creates B-modes

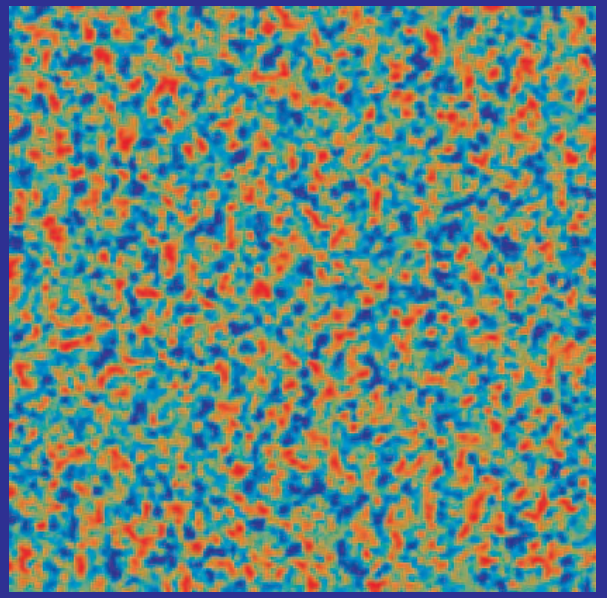

Original

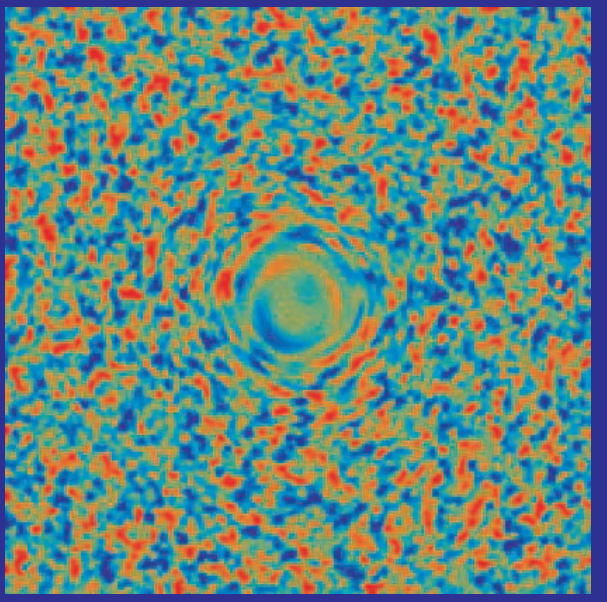

Lensed E

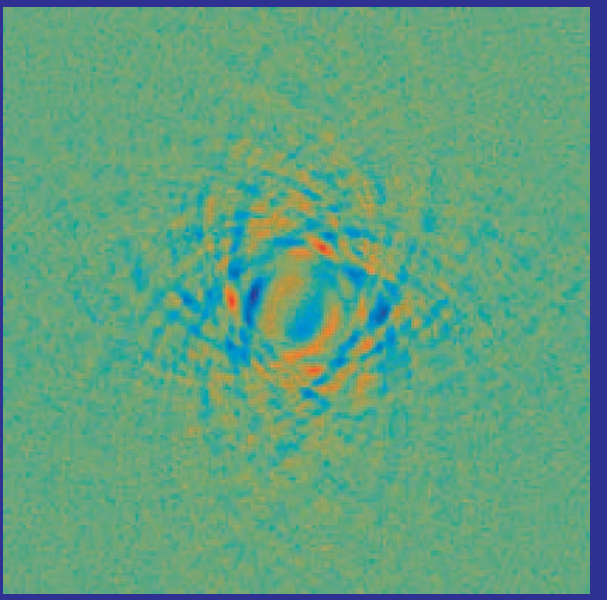

Lensed B

Zaldarriaga & Seljak (1998) [figure: Hu & Okamoto (2001)]

Polarization Lensing

- Polarization field harmonics lensed similarly

$$[Q \pm iU](\hat{\mathbf{n}}) = -\int \frac{d^2 l}{(2\pi)^2}[E \pm iB](\mathbf{l}) e^{\pm 2i\phi_{\mathbf{l}}} e^{\mathbf{l}\cdot\hat{\mathbf{n}}}$$

so that

$$\begin{aligned}[Q \pm iU](\hat{\mathbf{n}}) &= [\tilde{Q} \pm i\tilde{U}](\hat{\mathbf{n}} + \nabla\phi) \\ &\approx [\tilde{Q} \pm i\tilde{U}](\hat{\mathbf{n}}) + \nabla_i\phi(\hat{\mathbf{n}})\nabla^i[\tilde{Q} \pm i\tilde{U}](\hat{\mathbf{n}}) \\ &\quad + \frac{1}{2}\nabla_i\phi(\hat{\mathbf{n}})\nabla_j\phi(\hat{\mathbf{n}})\nabla^i\nabla^j[\tilde{Q} \pm i\tilde{U}](\hat{\mathbf{n}})\end{aligned}$$

Polarization Power Spectra

- Carrying through the algebra to the power spectrum

$$C_l^{EE} = \left(1 - l^2 R\right) \tilde{C}_l^{EE} + \frac{1}{2} \int \frac{d^2\mathbf{l}_1}{(2\pi)^2} [(\mathbf{l} - \mathbf{l}_1) \cdot \mathbf{l}_1]^2 C^{\phi\phi}_{|\mathbf{l}-\mathbf{l}_1|}$$
$$\times \left[(\tilde{C}_{l_1}^{EE} + \tilde{C}_{l_1}^{BB}) + \cos(4\varphi_{l_1}) (\tilde{C}_{l_1}^{EE} - \tilde{C}_{l_1}^{BB}) \right],$$

$$C_l^{BB} = \left(1 - l^2 R\right) \tilde{C}_l^{BB} + \frac{1}{2} \int \frac{d^2\mathbf{l}_1}{(2\pi)^2} [(\mathbf{l} - \mathbf{l}_1) \cdot \mathbf{l}_1]^2 C^{\phi\phi}_{|\mathbf{l}-\mathbf{l}_1|}$$
$$\times \left[(\tilde{C}_{l_1}^{EE} + \tilde{C}_{l_1}^{BB}) - \cos(4\varphi_{l_1}) (\tilde{C}_{l_1}^{EE} - \tilde{C}_{l_1}^{BB}) \right],$$

$$C_l^{\Theta E} = \left(1 - l^2 R\right) \tilde{C}_l^{\Theta E} + \int \frac{d^2\mathbf{l}_1}{(2\pi)^2} [(\mathbf{l} - \mathbf{l}_1) \cdot \mathbf{l}_1]^2 C^{\phi\phi}_{|\mathbf{l}-\mathbf{l}_1|}$$
$$\times \tilde{C}_{l_1}^{\Theta E} \cos(2\varphi_{l_1}),$$

- Lensing generates B-modes out of the acoustic polaraization E-modes contaminates gravitational wave signature if $E_i < 10^{16}$GeV.

Polarized Landscape

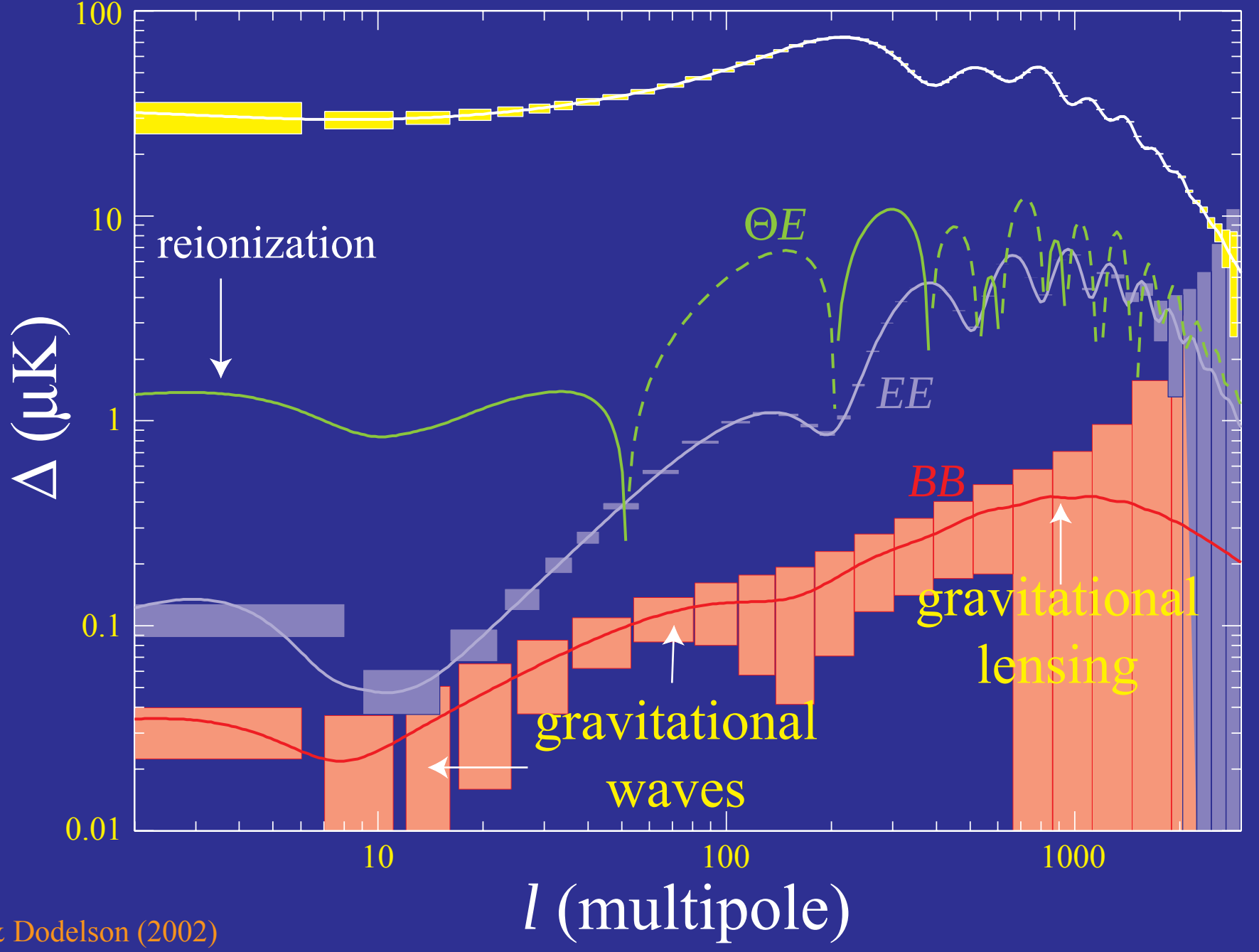

Hu & Dodelson (2002)

Power Spectrum Measurements

- Lensed field is non-Gaussian in that a single degree scale lens controls the polarization at arcminutes
- Increased variance and covariance implies that 10x as much sky needed compared with Gaussian fields

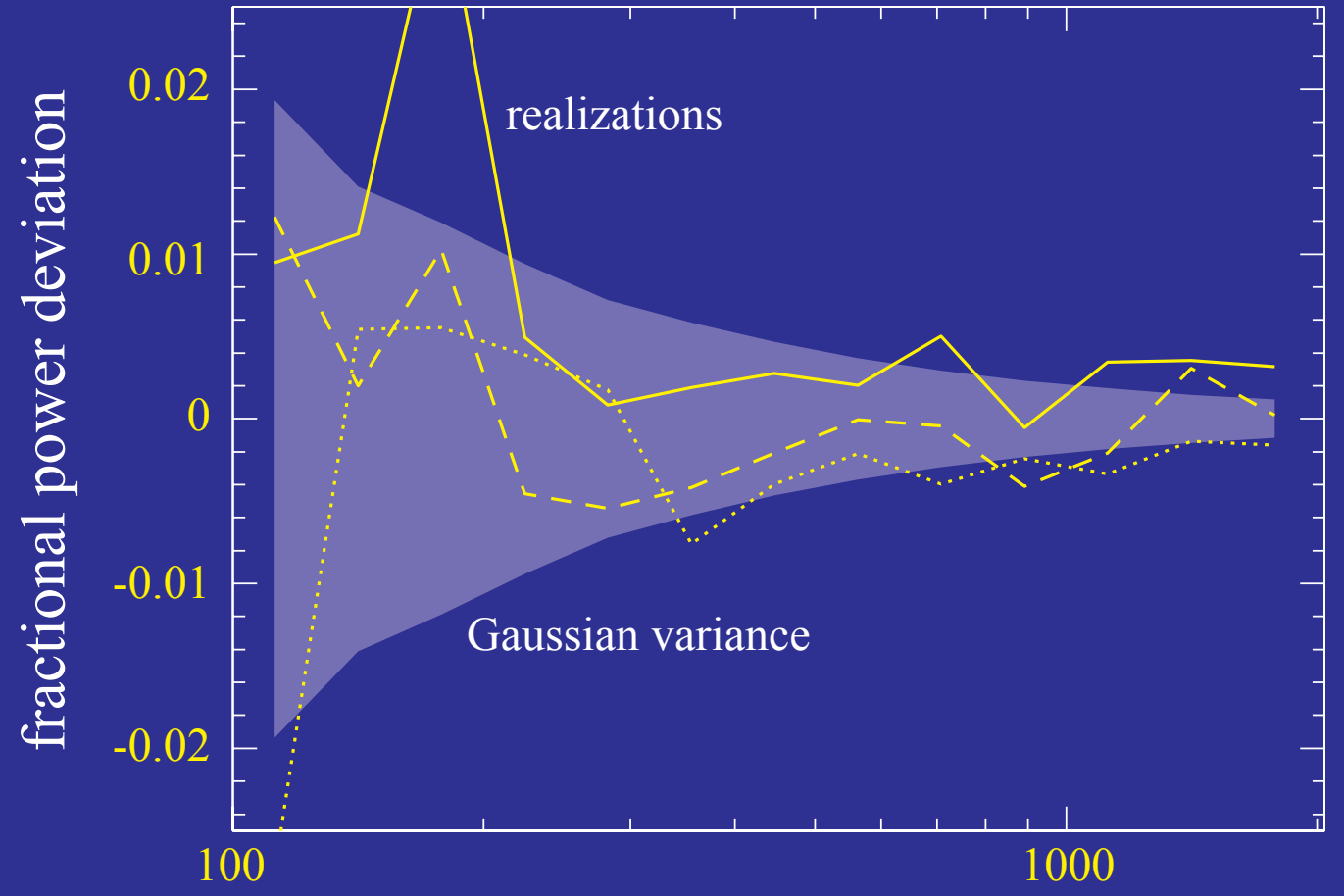

Smith, Hu & Kaplinghat (2004)

Lensed Power Spectrum Observables

- Principal components show two observables in lensed power spectra
- Temperature and E-polarization: deflection power at l~100
  B-polarization: deflection power at l~500
- Normalized so that observables error = fractional lens power error

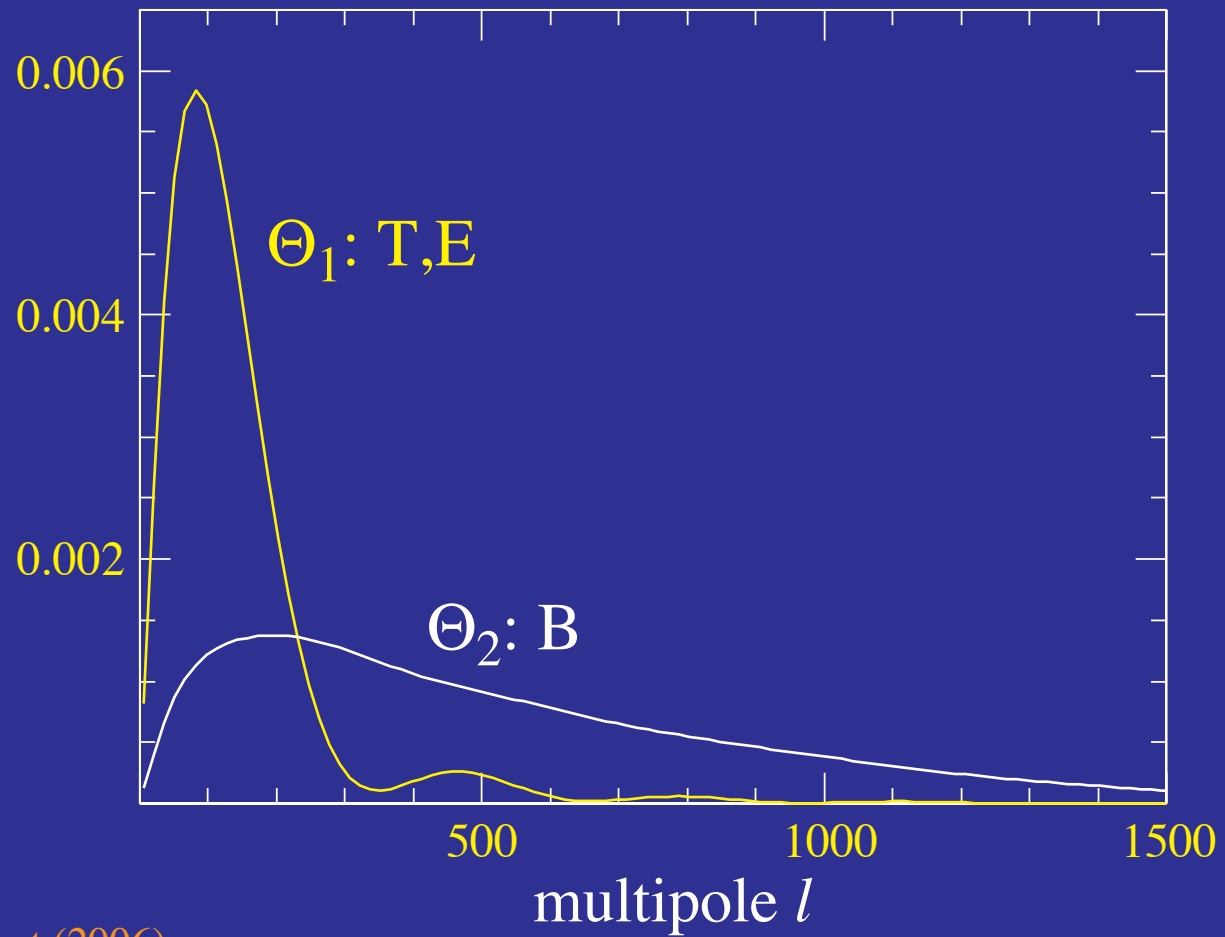

Smith, Hu & Kaplinghat (2006)

Redshift Sensitivity

- Lensing observables probe distance and structure at high redshift $\frac{\delta\Theta_i}{\Theta_i} = \left[\left(3 - \frac{d\ln\Delta_m^2}{d\ln k}\right)\frac{\delta D_A}{D_A} - \frac{\delta H}{H} + 2\frac{\delta G}{G} + 2\frac{\delta D_A(D_s - D)}{D_A(D_s - D)}\right]$

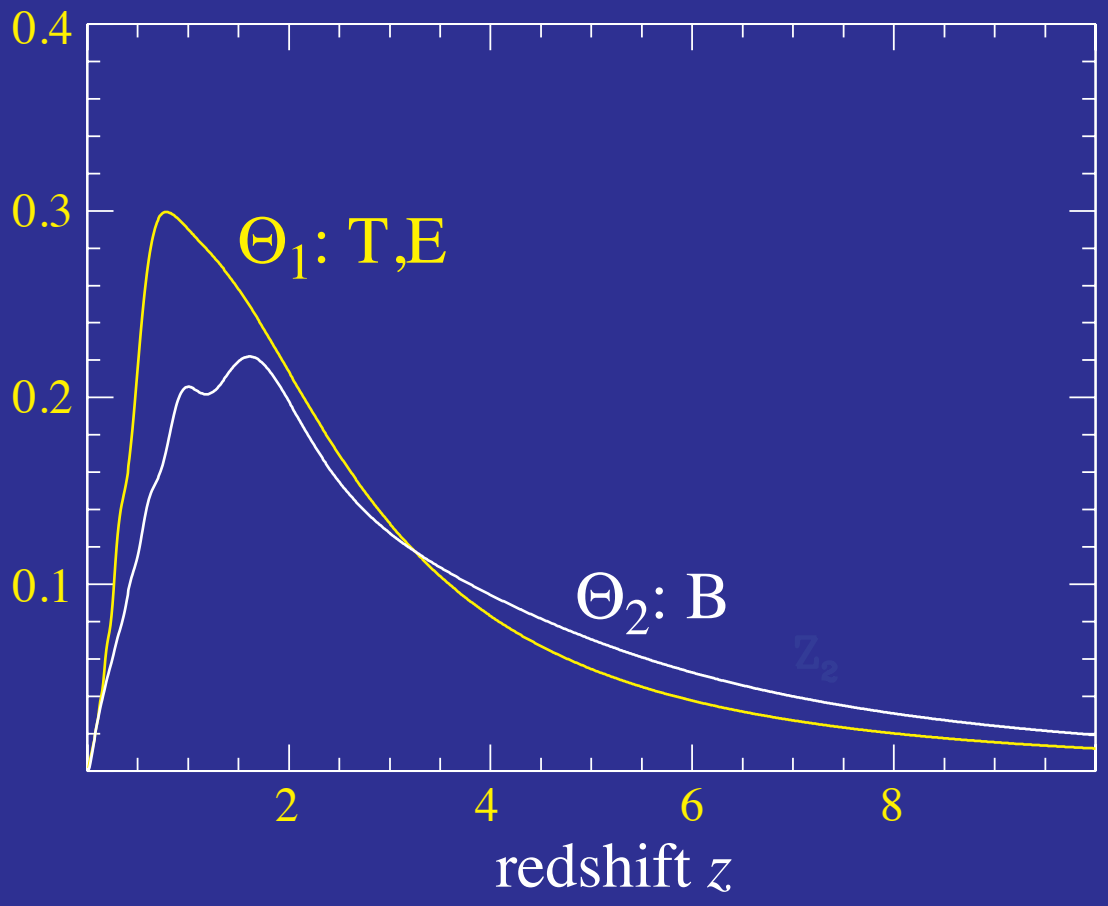

Smith, Hu & Kaplinghat (2006)

Constraints on Lensing Observables

- Lensing observables in T,E are limited by CMB sample variance
- Lensing observables in B are limited by lens sample variance
- B-modes require 10x as much sky at high signal-to-noise or 3x as much sky at the optimal signal-to-noise with Δ_P=4.7uK'

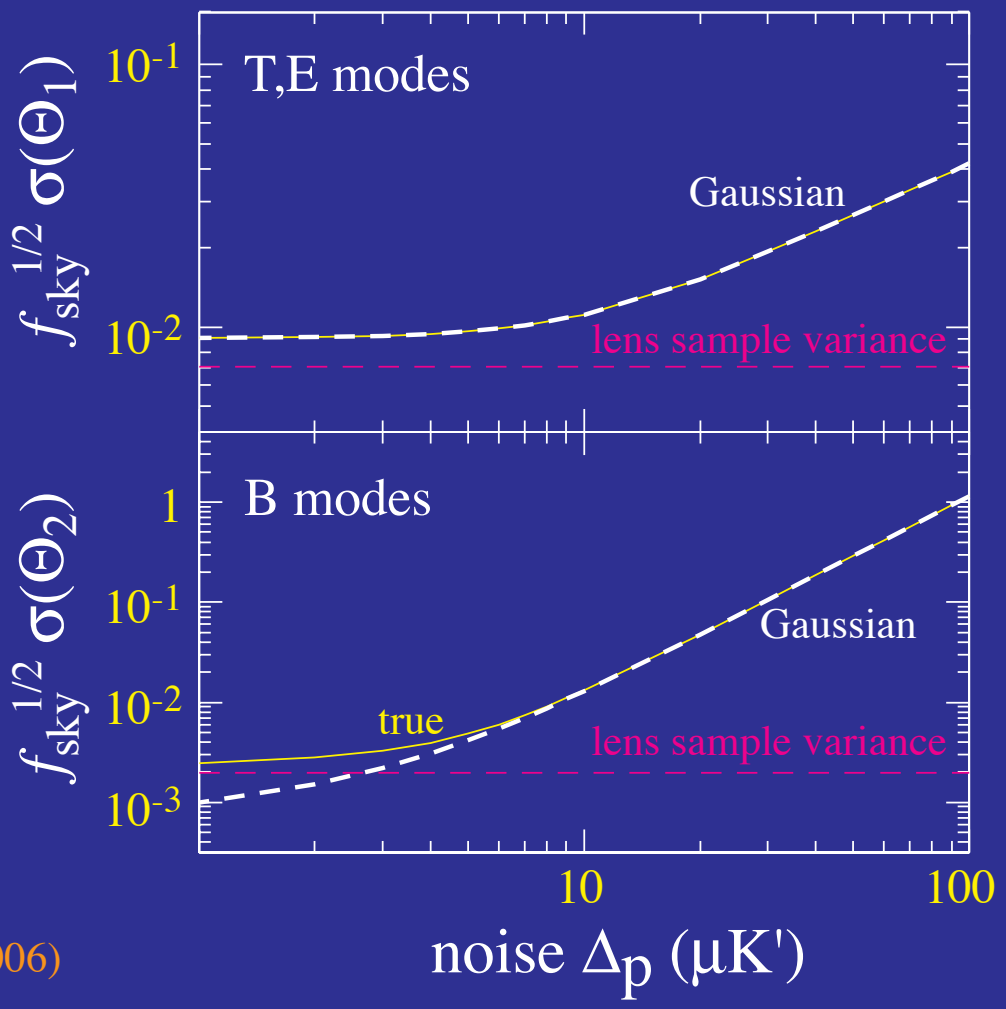

Smith, Hu & Kaplinghat (2006)

Lensing Observables

- Lensing observables provide a simple way of accounting for non-Gaussianity and parameter degeneracies
- Direct forecasts for Planck + 10% sky with noise Δ_P=1.4uK'

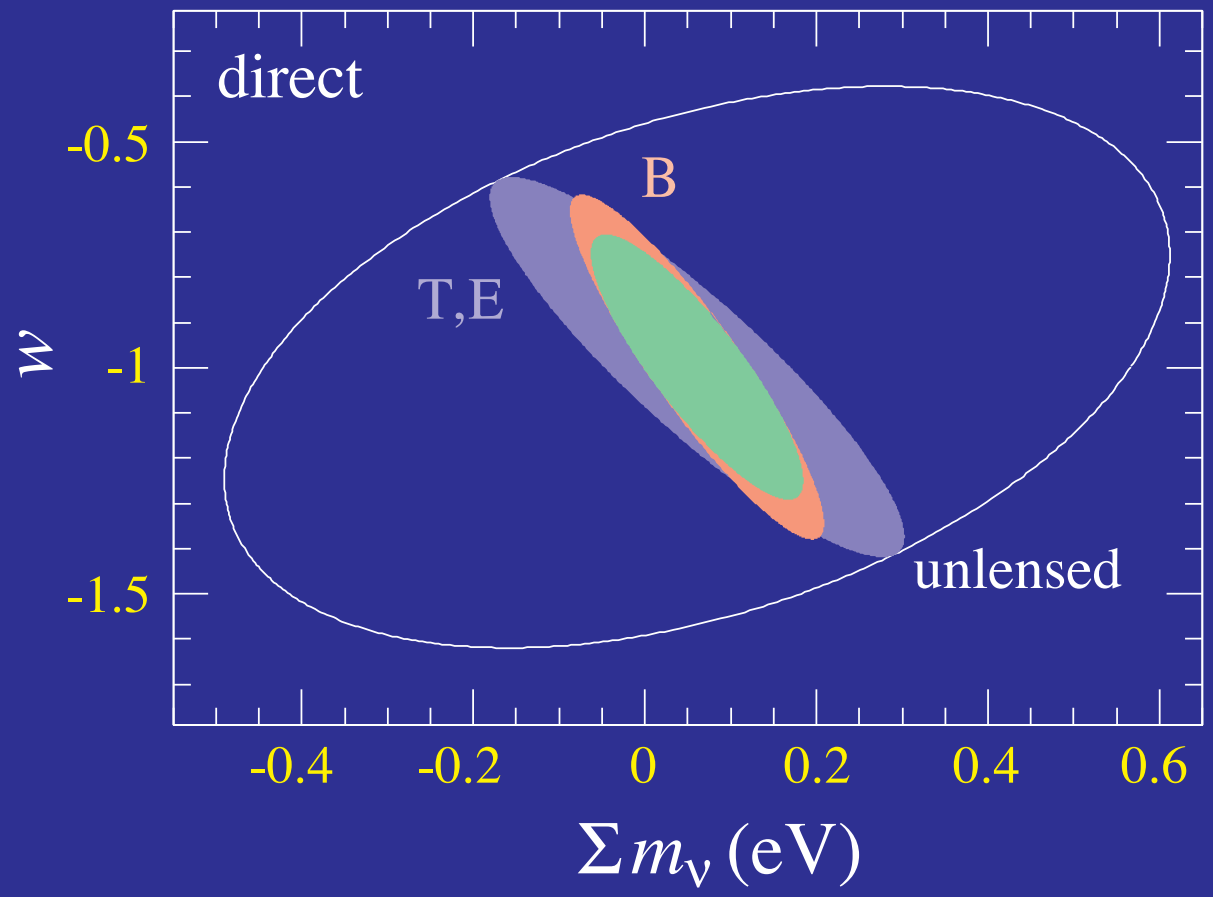

Smith, Hu, Kaplinghat (2006) [see also: Kaplinghat et. al 2003, Acquaviva & Baccigalupi 2005, Smith et al 2005, Li et al 2006]

Lensing Observables

- Lensing observables provide a simple way of accounting for non-Gaussianity and parameter degeneracies
- Observables forecasts for Planck + 10% sky with noise Δ_P=1.4uK'

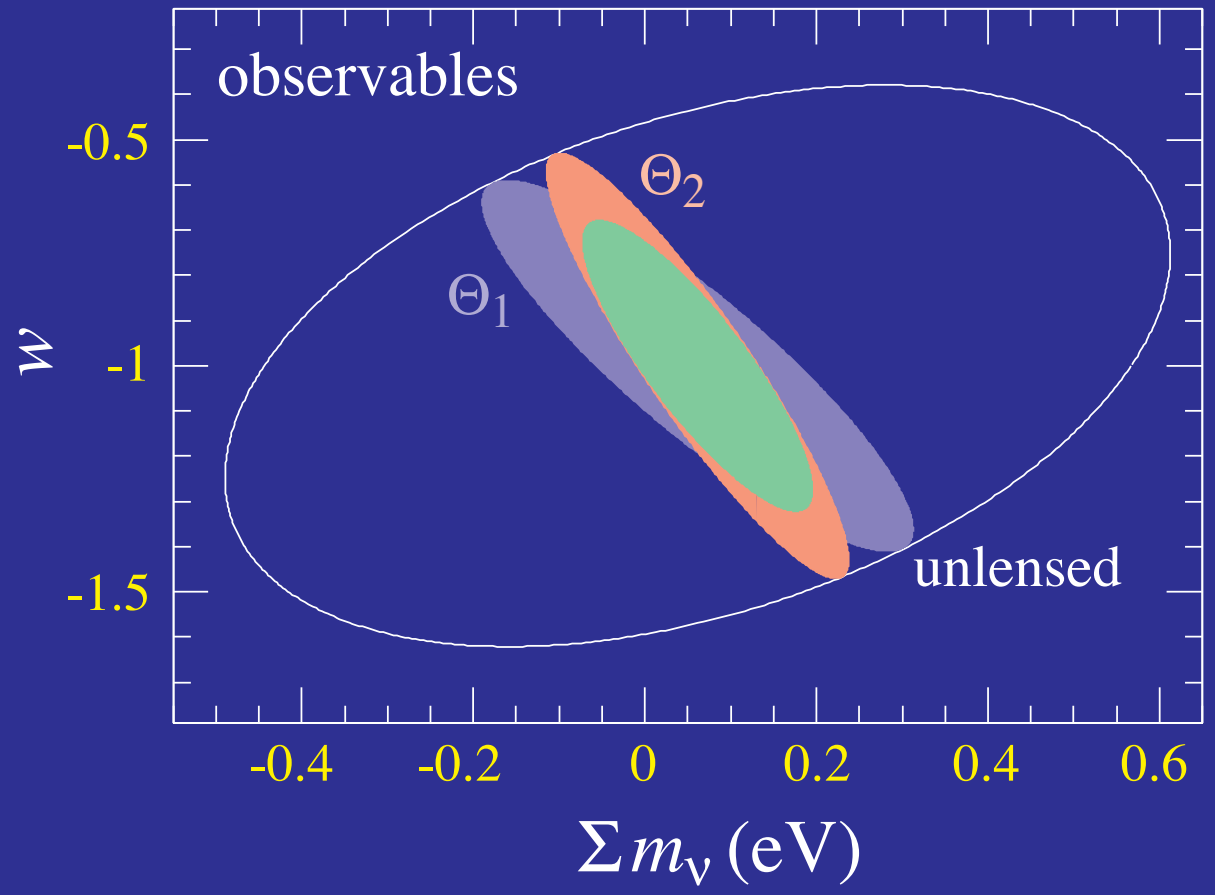

Smith, Hu, Kaplinghat (2006)

Lensing Reconstruction

Quadratic Estimator

- Taylor expand mapping

$$\Theta(\hat{\mathbf{n}}) = \tilde{\Theta}(\hat{\mathbf{n}} + \nabla\phi)$$
$$= \tilde{\Theta}(\hat{\mathbf{n}}) + \nabla_i\phi(\hat{\mathbf{n}})\nabla^i\tilde{\Theta}(\hat{\mathbf{n}}) + \ldots$$

- Fourier decomposition $\rightarrow$ mode coupling of harmonics

$$\Theta(\mathbf{l}) = \int d\hat{\mathbf{n}}\,\Theta(\hat{\mathbf{n}})e^{-i\mathbf{l}\cdot\hat{\mathbf{n}}}$$
$$= \tilde{\Theta}(\mathbf{l}) - \int \frac{d^2\mathbf{l}_1}{(2\pi)^2}\,(\mathbf{l}-\mathbf{l}_1)\cdot\mathbf{l}_1\,\tilde{\Theta}(\mathbf{l}_1)\phi(\mathbf{l}-\mathbf{l}_1)$$

- Consider fixed lens and Gaussian random CMB realizations: each pair is an estimator of the lens at $\mathbf{L} = \mathbf{l}_1 + \mathbf{l}_2$ (Hu 2001):

$$\langle\Theta(\mathbf{l})\Theta'(\mathbf{l}')\rangle_{\rm CMB} \approx \left[\tilde{C}_{l_1}^{\Theta\Theta}(\mathbf{L}\cdot\mathbf{l}_1) + \tilde{C}_{l_2}^{\Theta\Theta}(\mathbf{L}\cdot\mathbf{l}_2)\right]\phi(\mathbf{L}) \quad (\mathbf{l} \neq -\mathbf{l}')$$

Quadratic Reconstruction

- Matched filter (minimum variance) averaging over pairs of multipole moments
- Real space: divergence of a temperature-weighted gradient

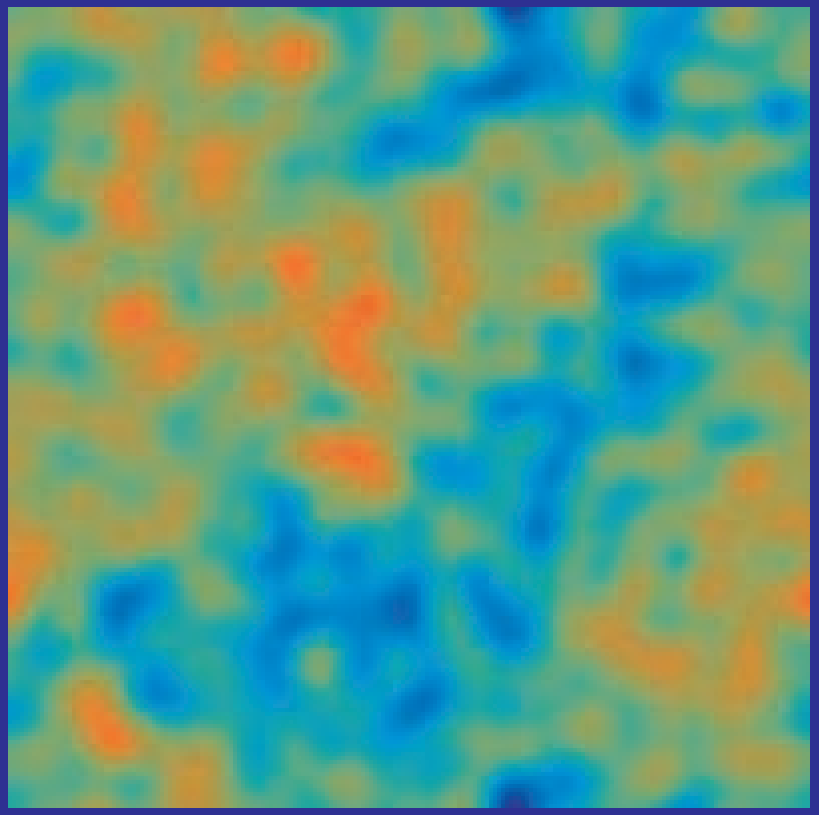

original

potential map (1000sq. deg)

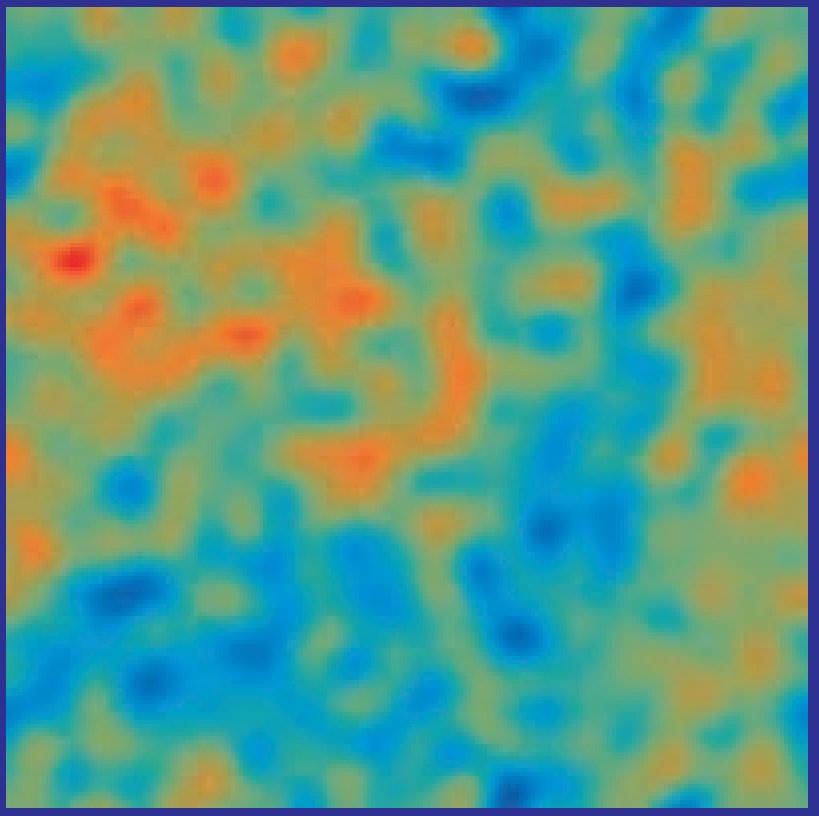

reconstructed

1.5' beam; 27μK-arcmin noise

Hu (2001)

Reconstruction from the CMB

- Generalize to polarization: each quadratic pair of fields estimates the lensing potential (Hu & Okamoto 2002)

$$\langle x(\mathbf{l})x'(\mathbf{l}')\rangle_{\rm CMB} = f_\alpha(\mathbf{l},\mathbf{l}')\phi(\mathbf{l}+\mathbf{l}')\,,$$

  where $x \in$ temperature, polarization fields and f_α is a fixed weight that reflects geometry

- Each pair forms a noisy estimate of the potential or projected mass - just like a pair of galaxy shears
- Minimum variance weight all pairs to form an estimator of the lensing mass
- Generalize to inhomogeneous noise, cut sky and maximum likelihood by iterating the quadratic estimator (Seljak & Hirata 2002)

High Signal-to-Noise B-modes

- Cosmic variance of CMB fields sets ultimate limit for *T*,*E*
- *B*-polarization allows mapping to finer scales and in principle is not limited by cosmic variance of *E* (Hirata & Seljak 2003)

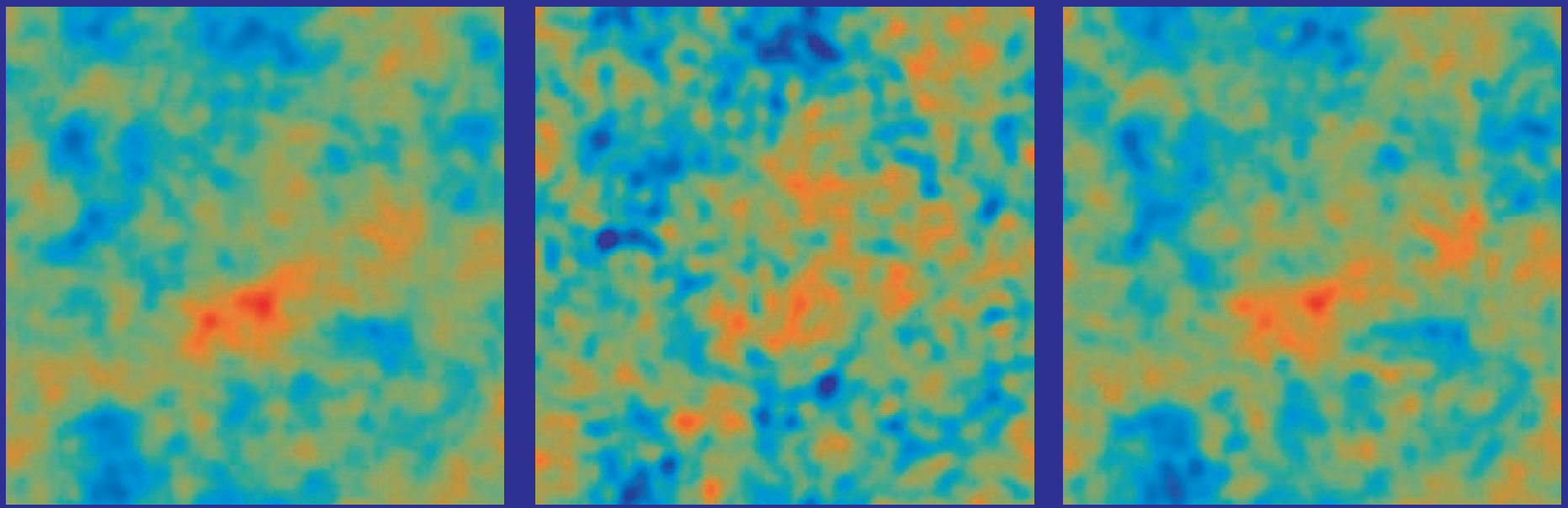

mass | temp. reconstruction | EB pol. reconstruction

100 sq. deg; 4' beam; 1μK-arcmin

Hu & Okamoto (2001)

Lensing-Galaxy Correlation

- ~3σ+ joint detection of WMAP lensing reconstruction with large scale structure (galaxies)
- Consistent with ΛCDM

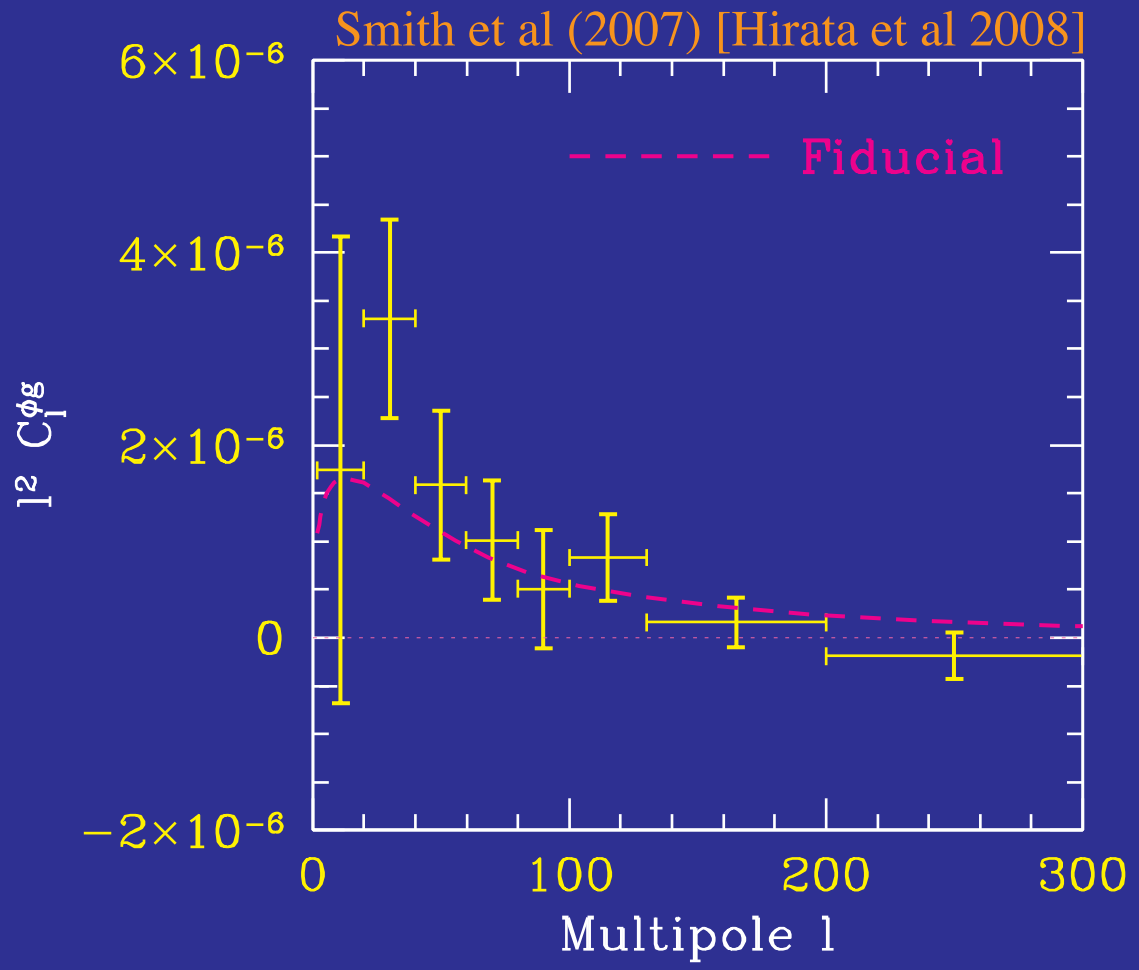

Matter Power Spectrum

- Measuring projected matter power spectrum to cosmic variance limit across whole linear regime $0.002 < k < 0.2\ h/\mathrm{Mpc}$

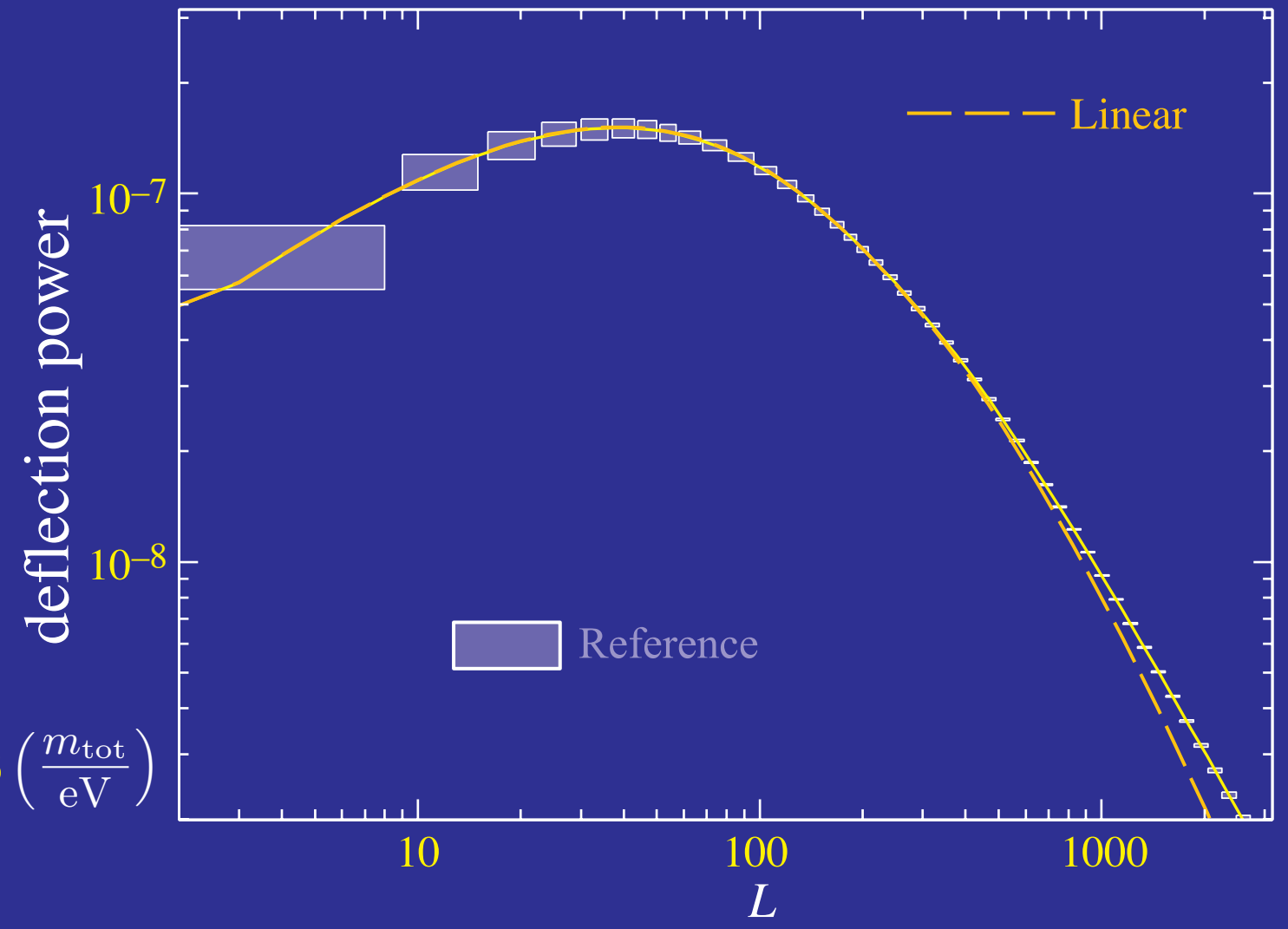

$$\frac{\Delta P}{P} \approx -0.6 \left(\frac{m_{\rm tot}}{\rm eV}\right)$$

Hu & Okamoto (2001)

Matter Power Spectrum

- Measuring projected matter power spectrum to cosmic variance limit across whole linear regime $0.002 < k < 0.2\ h/\mathrm{Mpc}$

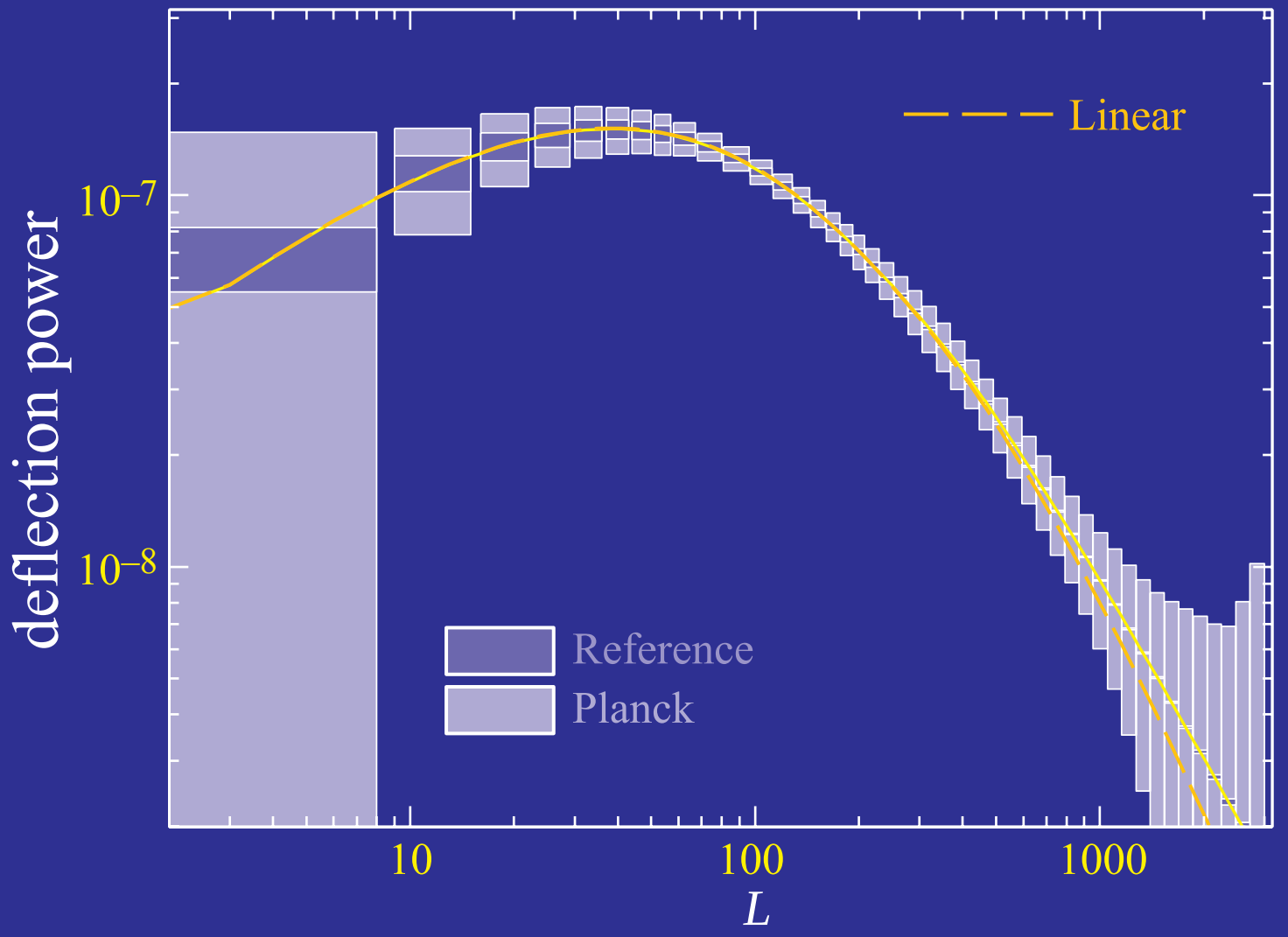

Hu & Okamoto (2001)

Tomography & Growth Rate

- Cross correlation with cosmic shear – mass tomography anchor in the decelerating regime

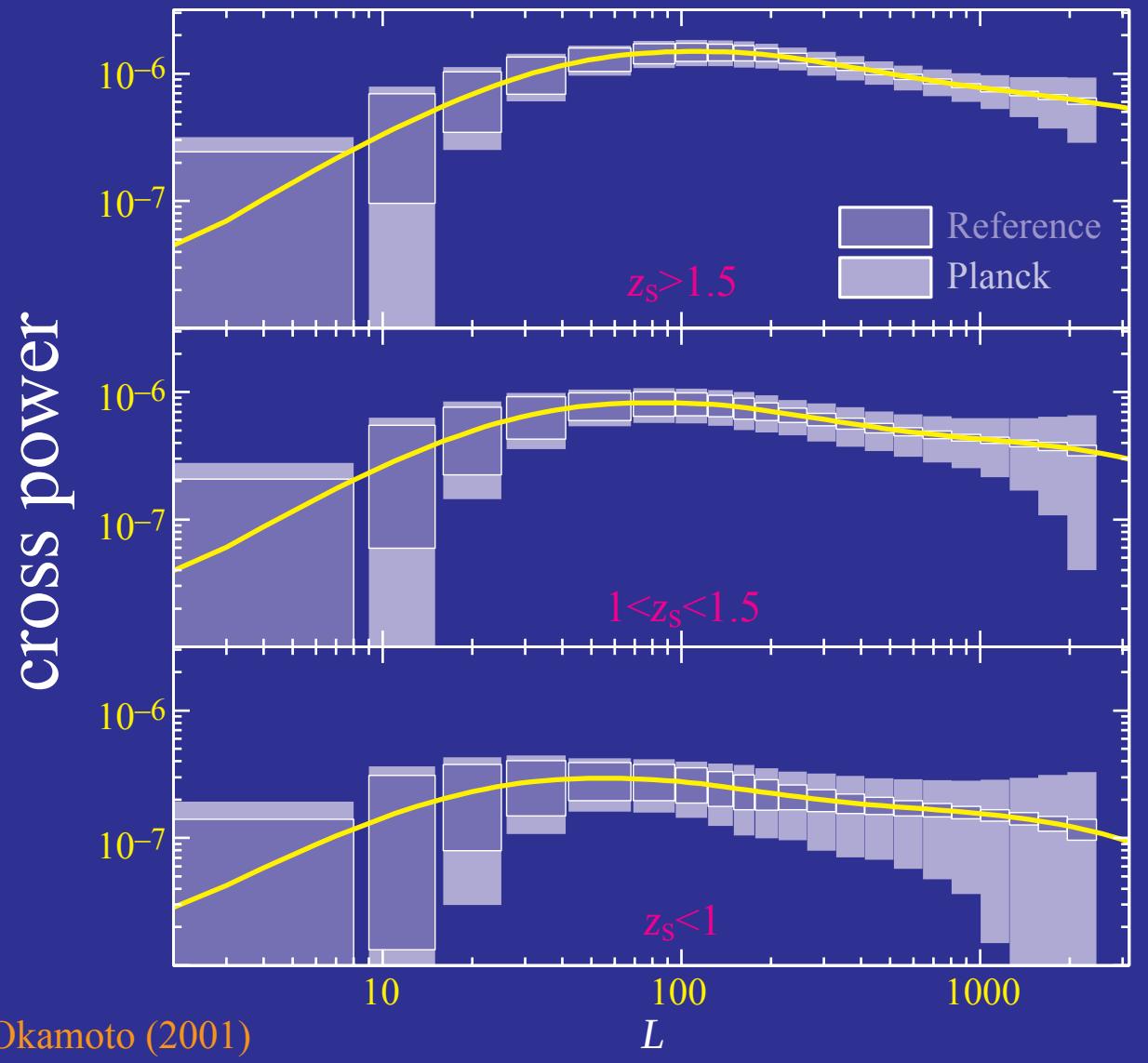

1000 sq. deg.

Hu (2001); Hu & Okamoto (2001)

Cross Correlation with Temperature

- Any correlation is a direct detection of a smooth energy density component through the ISW effect
- 5 nearly independent measures in temperature & polarization

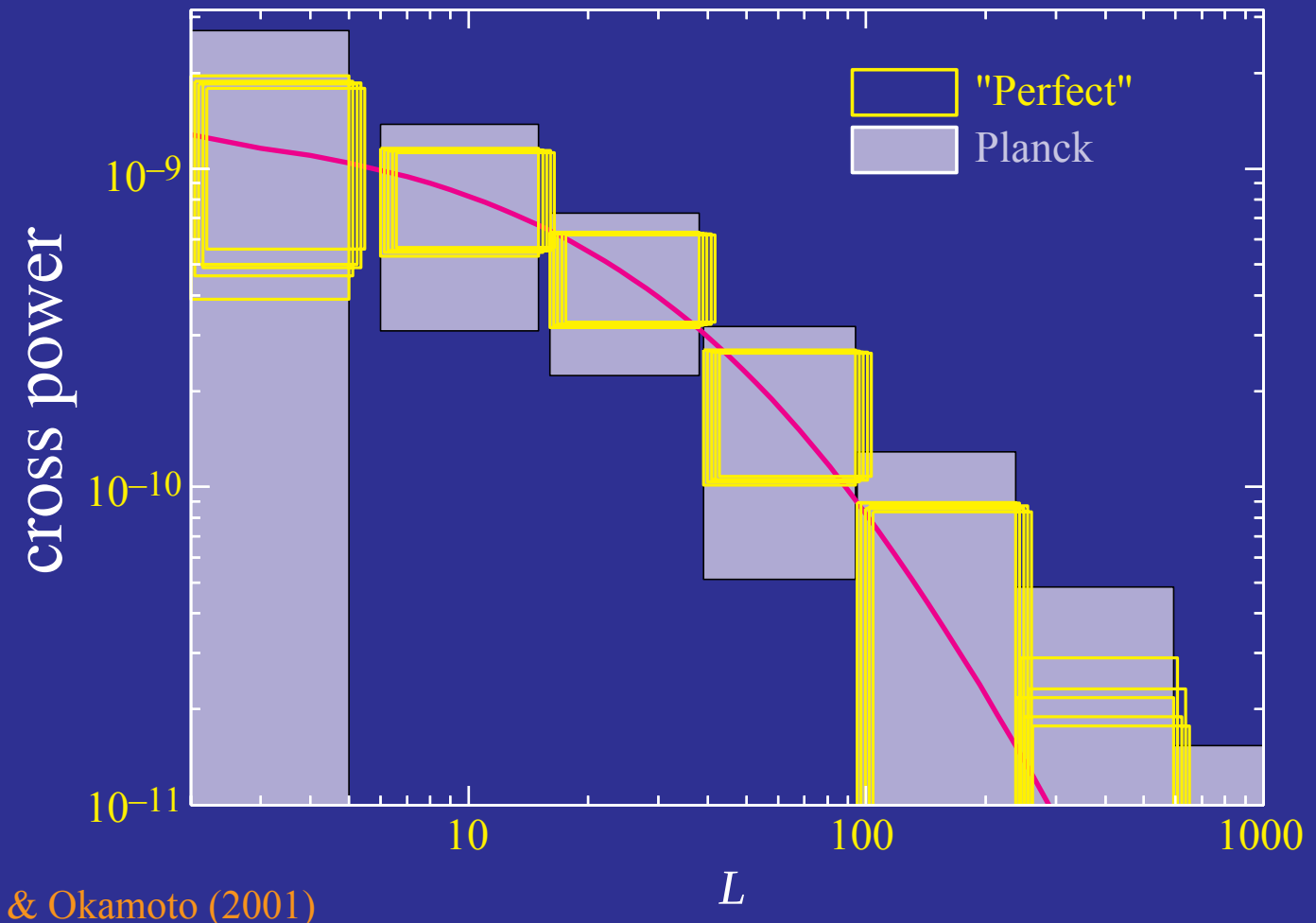

Hu (2001); Hu & Okamoto (2001)

Cross Correlation with Temperature

- Any correlation is a direct detection of a smooth energy density component through the ISW effect
- Show dark energy smooth >5-6 Gpc scale, test quintesence

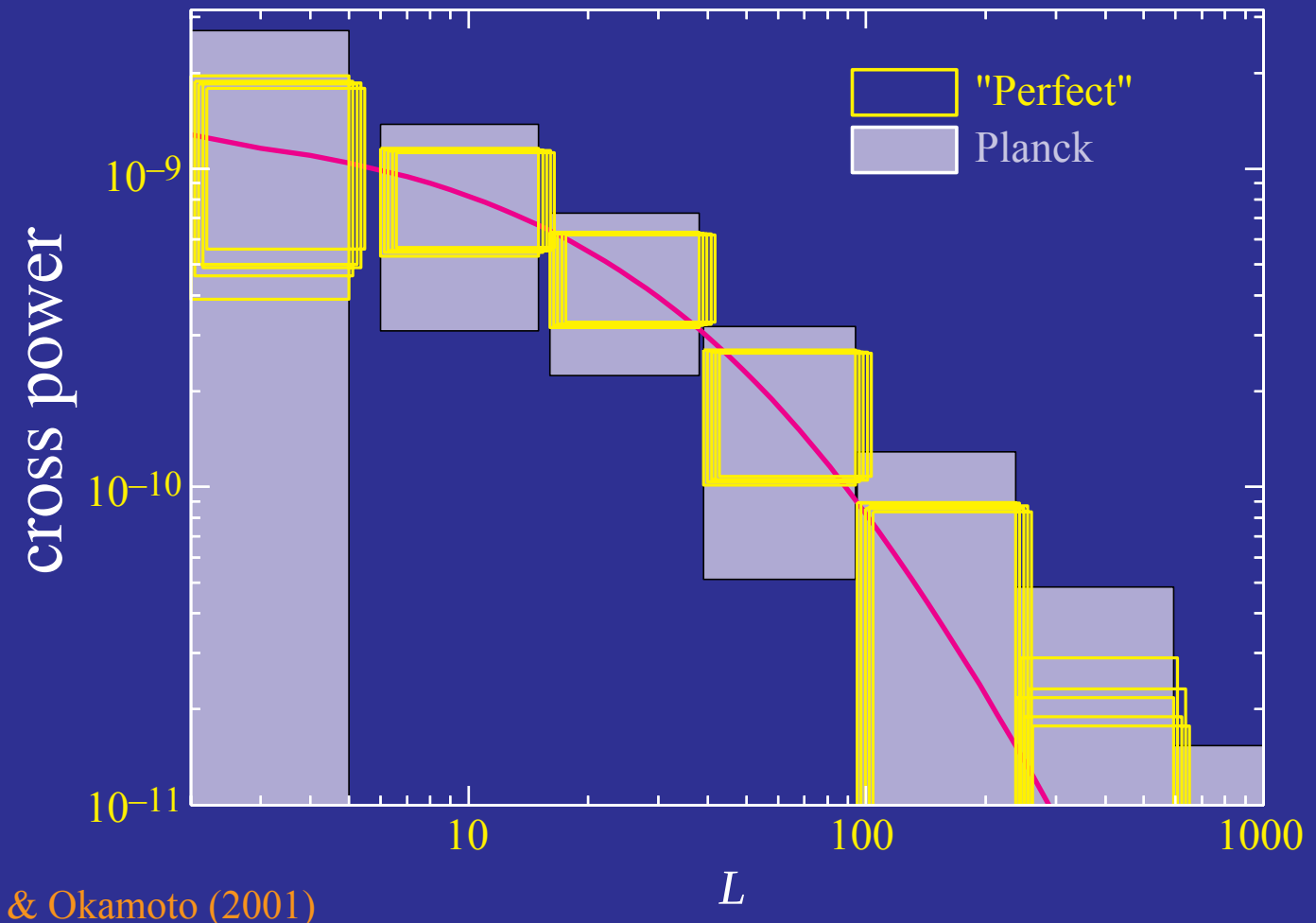

Hu (2001); Hu & Okamoto (2001)

De-Lensing the Polarization

- Gravitational lensing contamination of B-modes from gravitational waves cleaned to $E_I \sim 0.3 \times 10^{16}$ GeV
  Hu & Okamoto (2002); Knox & Song (2002); Cooray, Kedsen, Kamionkowski (2002)
- Potentially further with maximum likelihood Hirata & Seljak (2004)

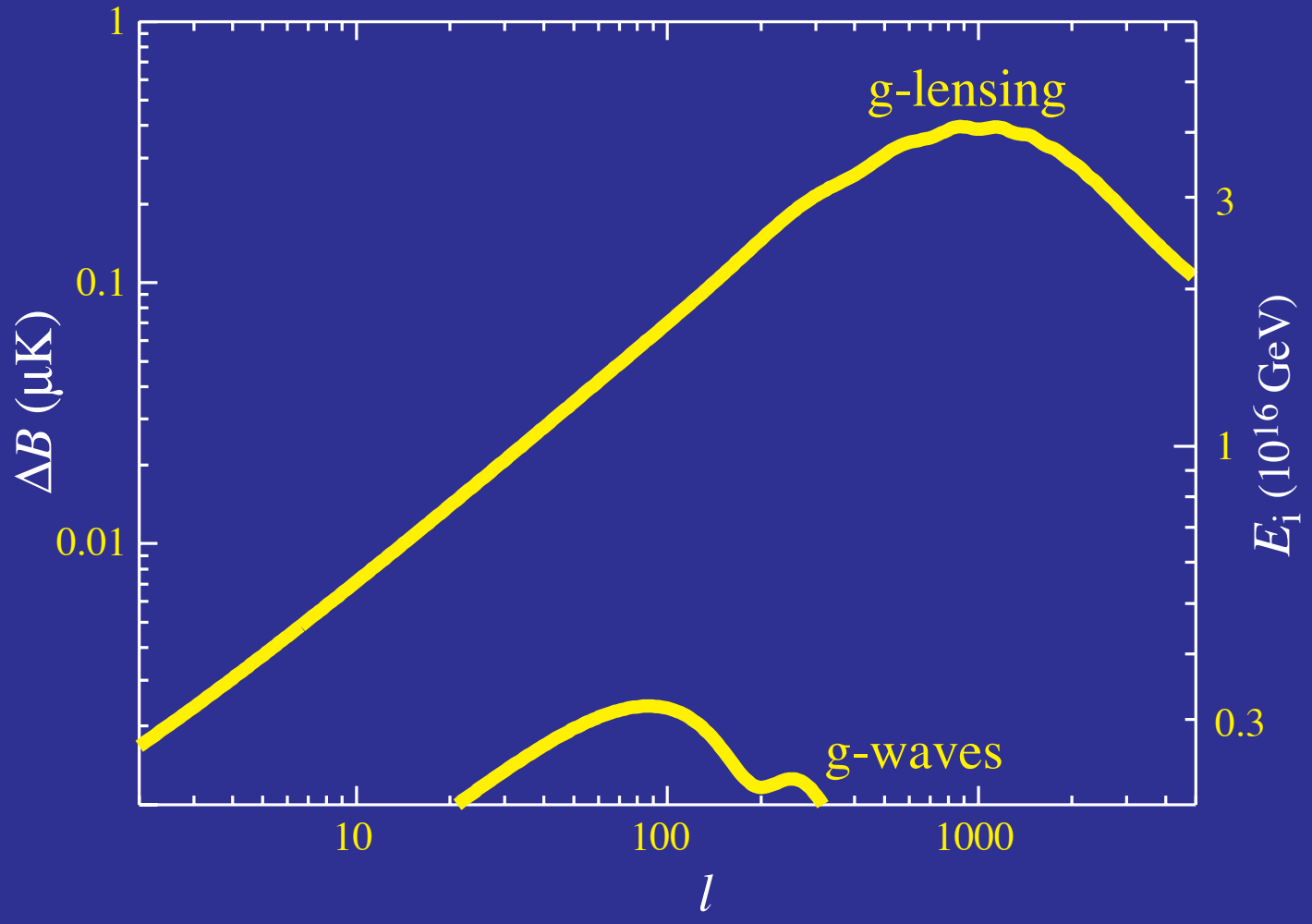

Reconstruction in the Halo Regime

- Reconstruction techniques noisy but nearly unbiased *if* gradients from lensed image and other contaminates filtered out

(Hu, DeDeo, Vale 2007)

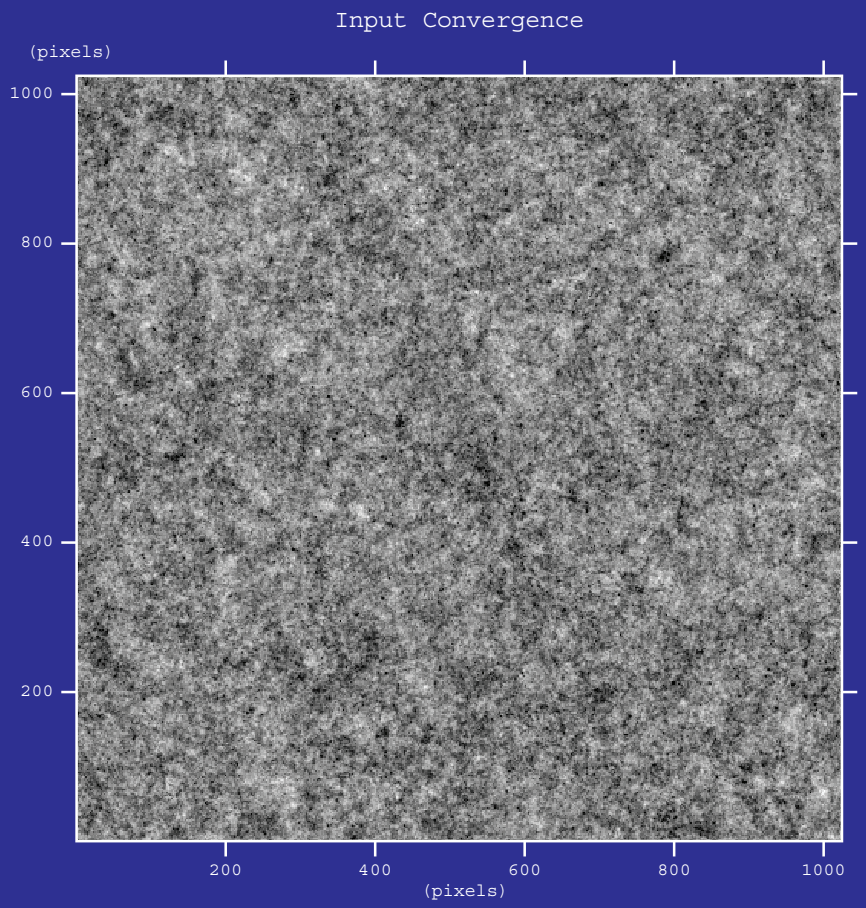

Input κ

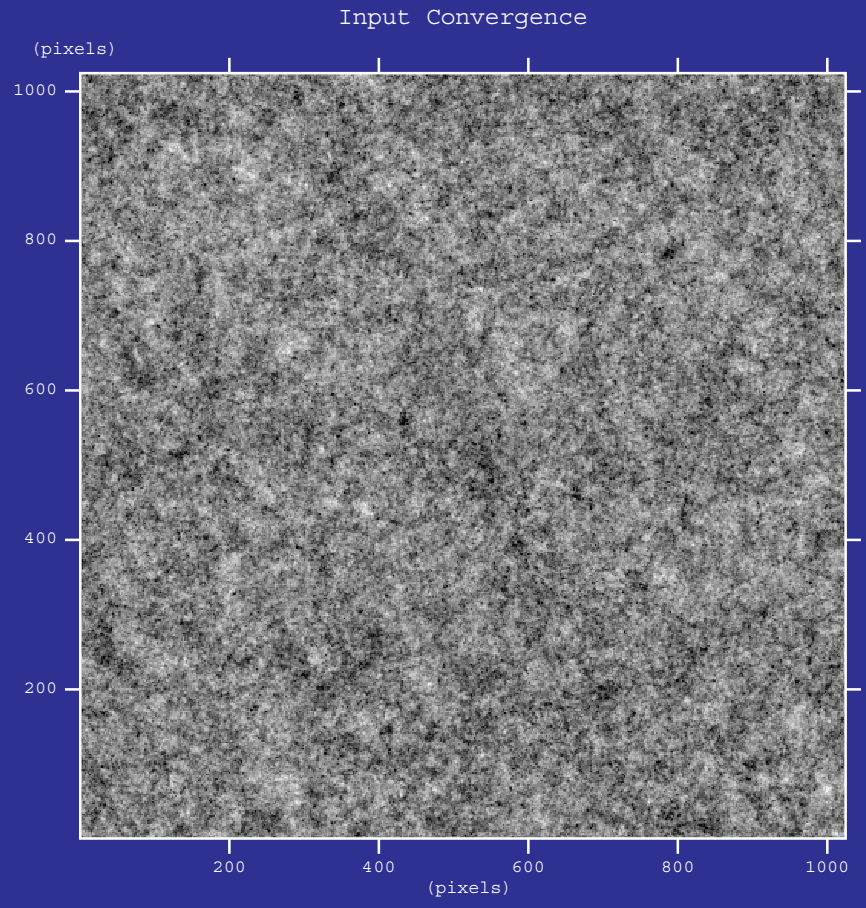

Vale (2007, unpublished); Zahn (in prep)

Reconstruction in the Halo Regime

- Reconstruction techniques noisy but nearly unbiased *if* gradients from lensed image and other contaminates filtered out

(Hu, DeDeo, Vale 2007)

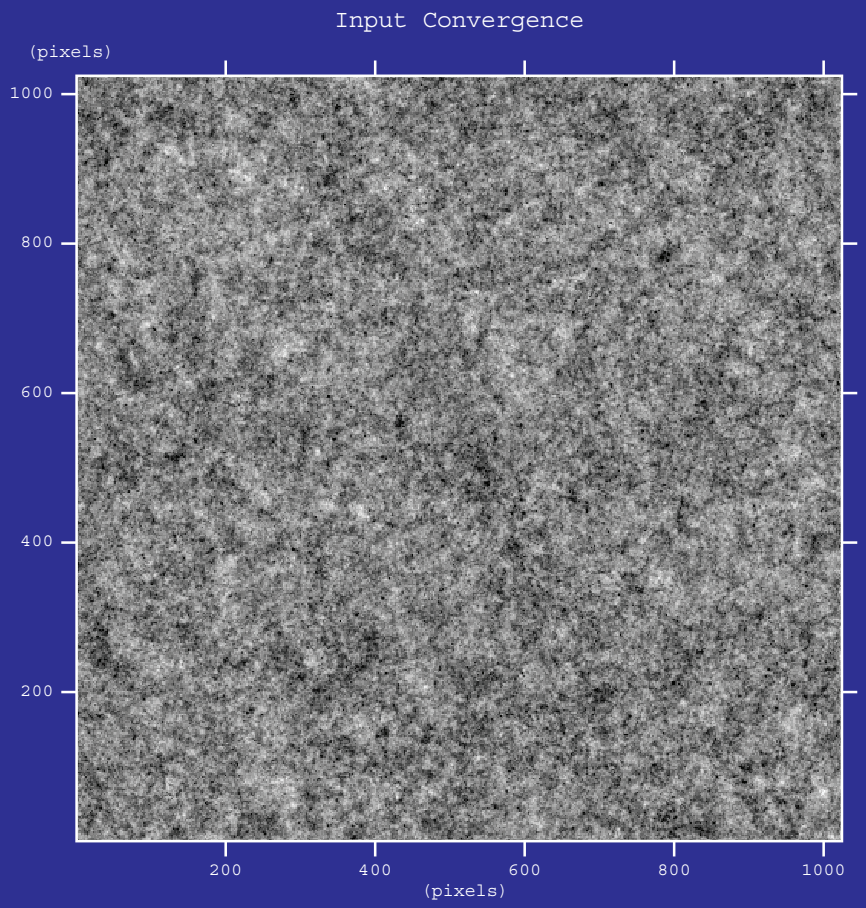

Input κ

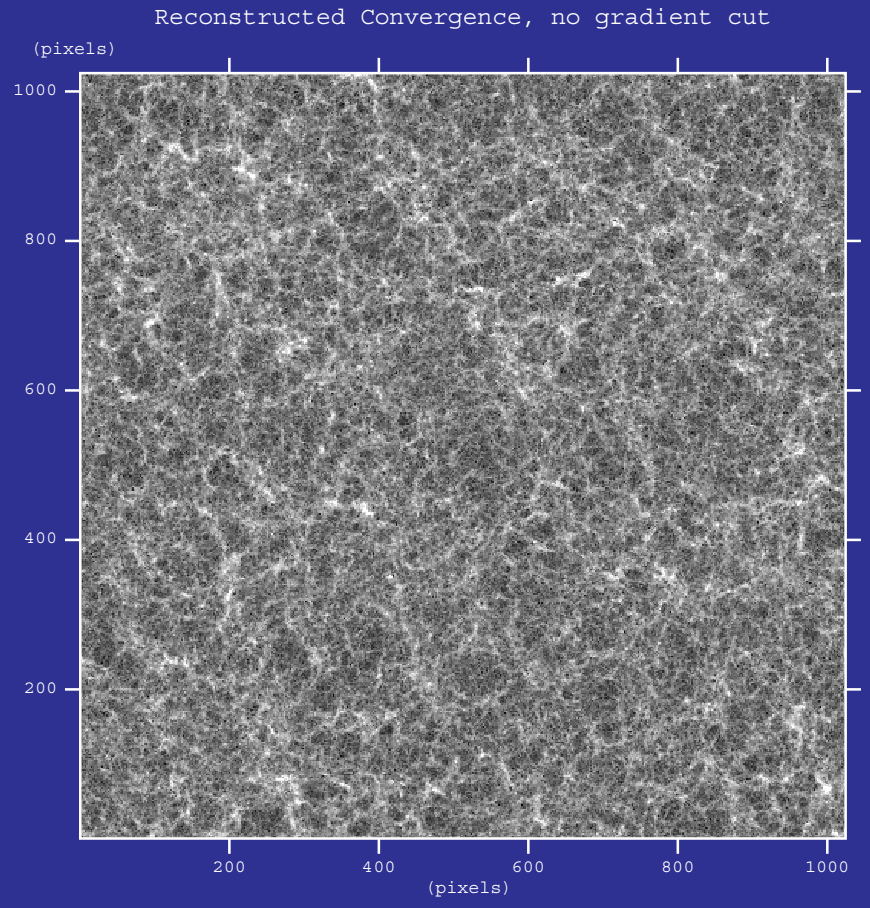

Vale (2007, unpublished); Zahn (in prep)

Reconstruction in the Halo Regime

- Reconstruction techniques noisy but nearly unbiased *if* gradients from lensed image and other contaminates filtered out

(Hu, DeDeo, Vale 2007)

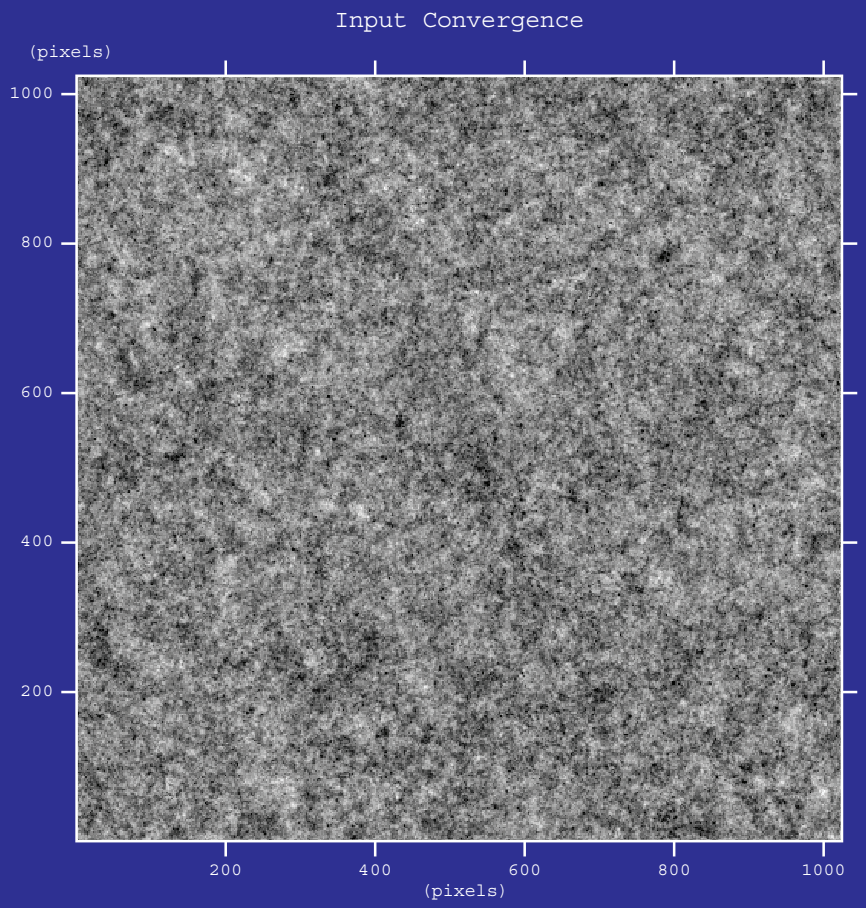

Input κ

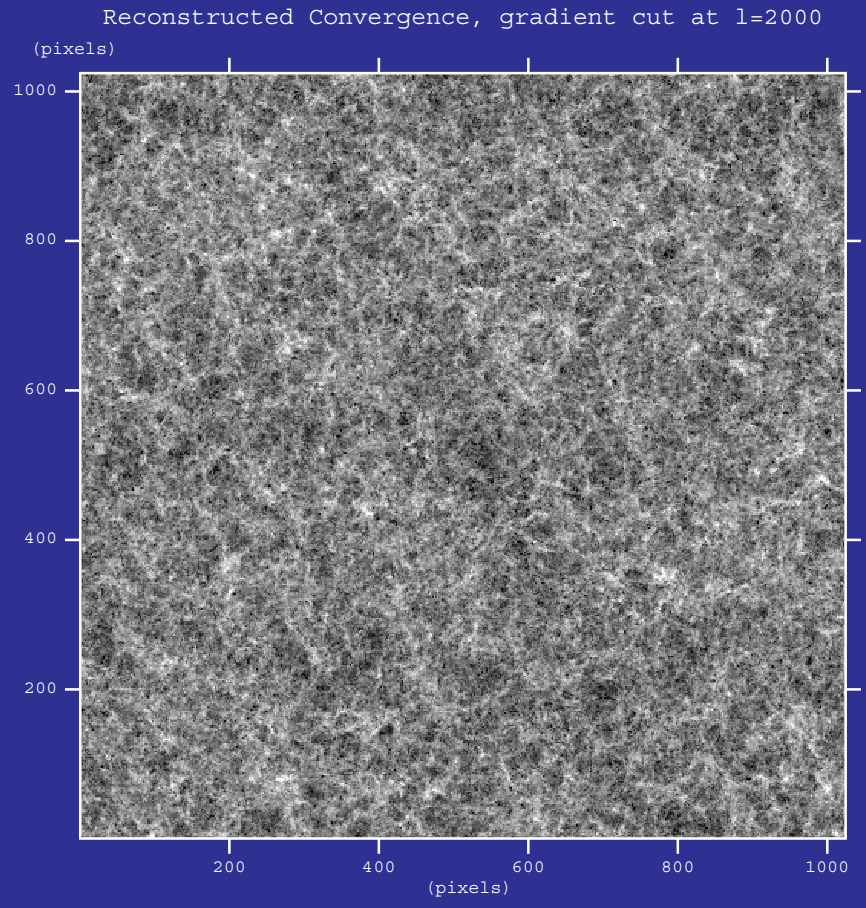

Vale (2007, unpublished); Zahn (in prep)

Cluster Lensing

- CMB lensing reconstruction measures cluster lensing statistically through average profiles or the cluster-mass correlation function

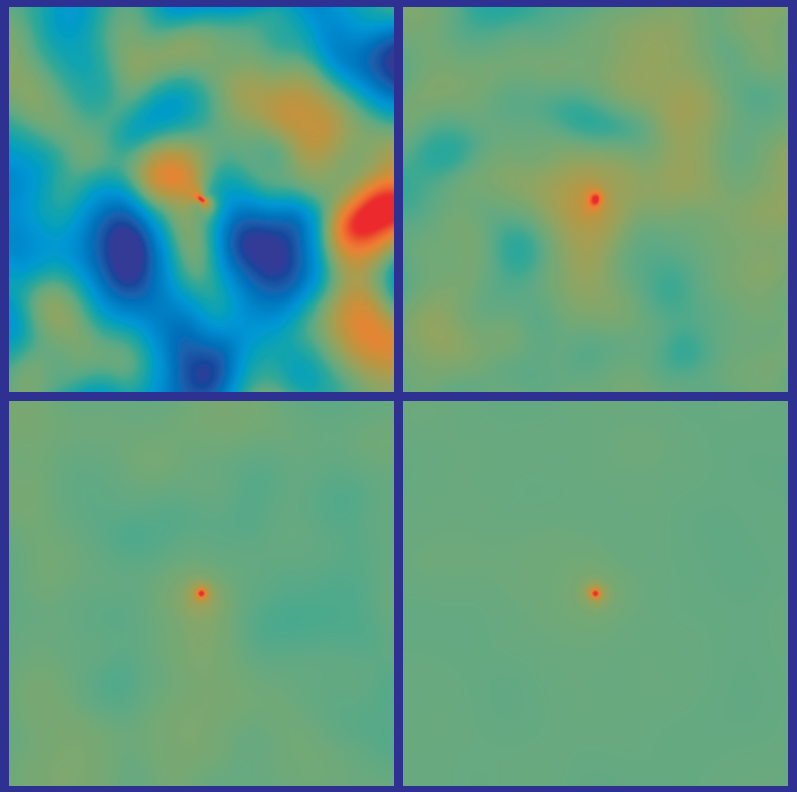

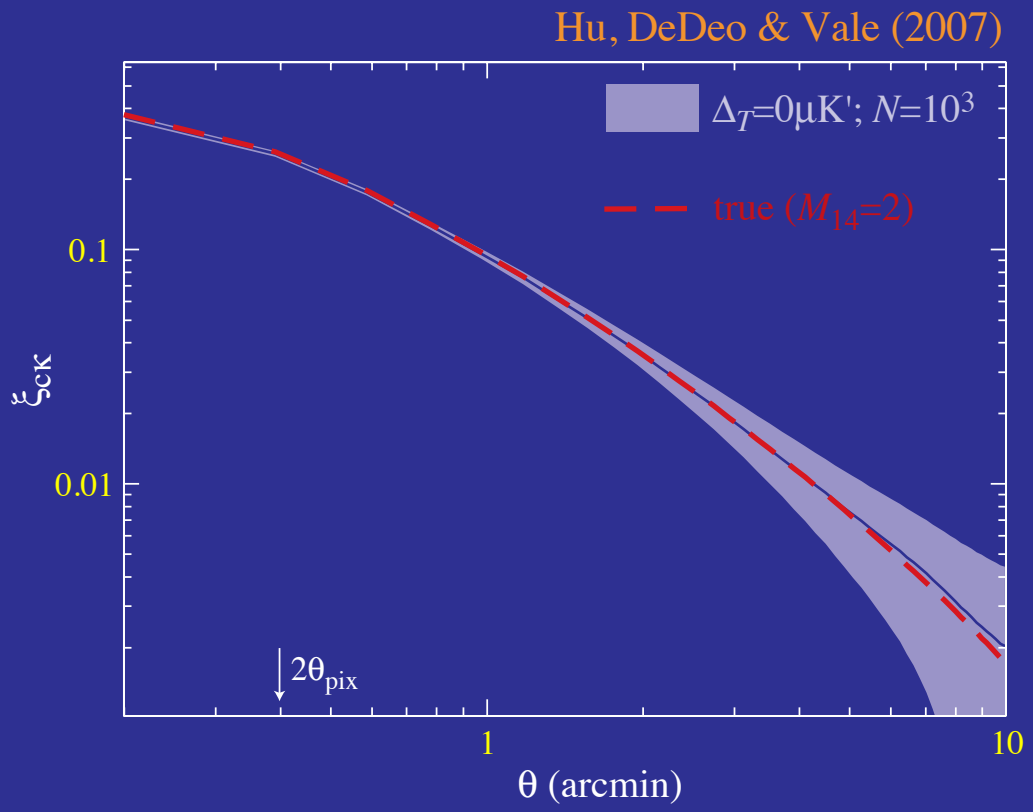

Cluster Lensing

- In combination with optical lensing, can measure distance ratios for (early) dark energy, curvature etc.

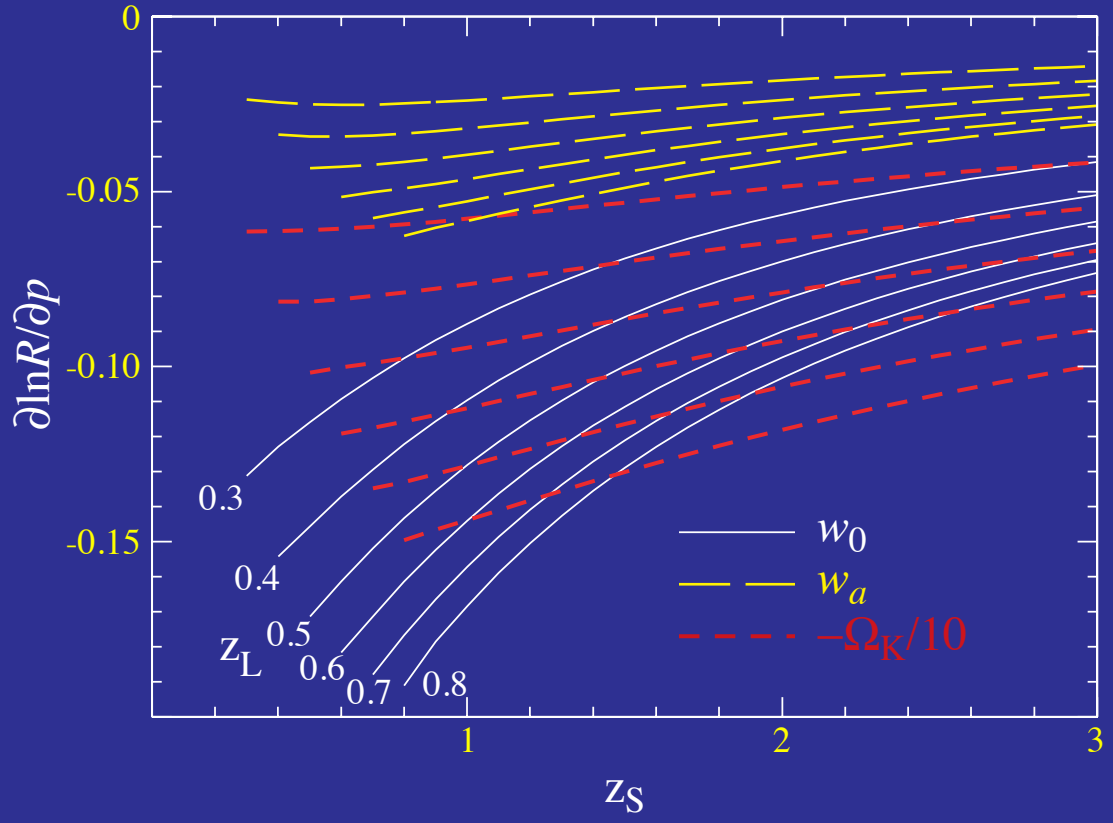

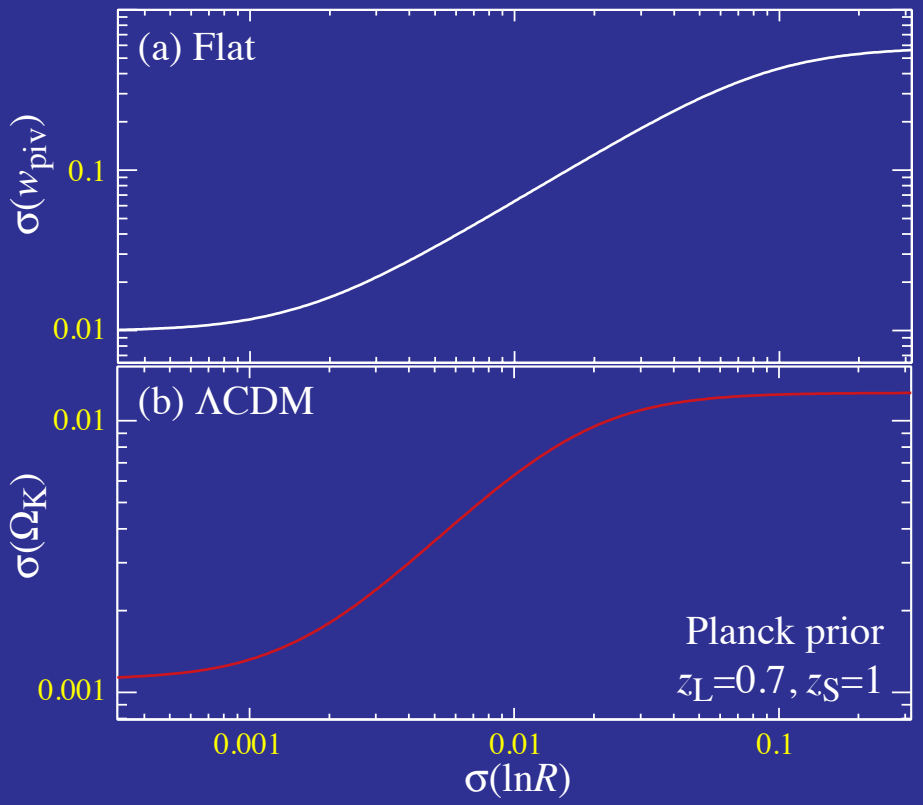

Hu, Holz & Vale (2007); Das & Spergel (2008)

Summary: Lecture II

- Polarization carries information in its direction and amplitude: E and B modes
- Secondary polarization from reionization provides a window on inflation through gravitational wave B modes and allows consistency test of slow roll
- Ionization and density modulation produces B modes on the scale of inhomogeneity (typically $< 10'$)
- Large-scale structure lenses the CMB causing smoothing of temperature power spectrum and creation of B modes
- Information on cosmic acceleration, neutrinos encapsulated in PCs
- Quadratic estimators reconstructs lenses associated with large scale structure, halos in principle allowing precision tests

Physics of Secondary Anisotropies

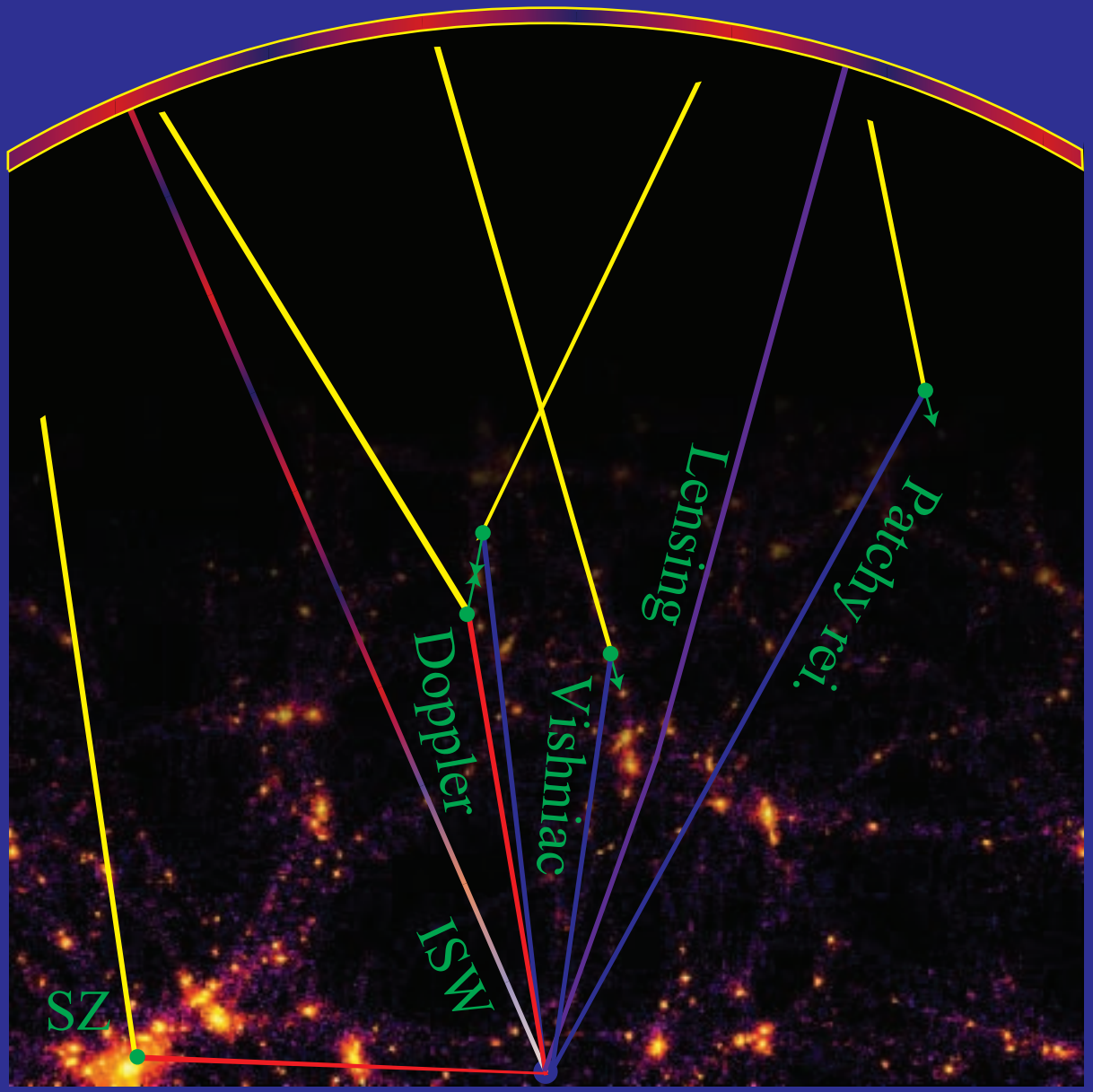

Scattering Secondaries

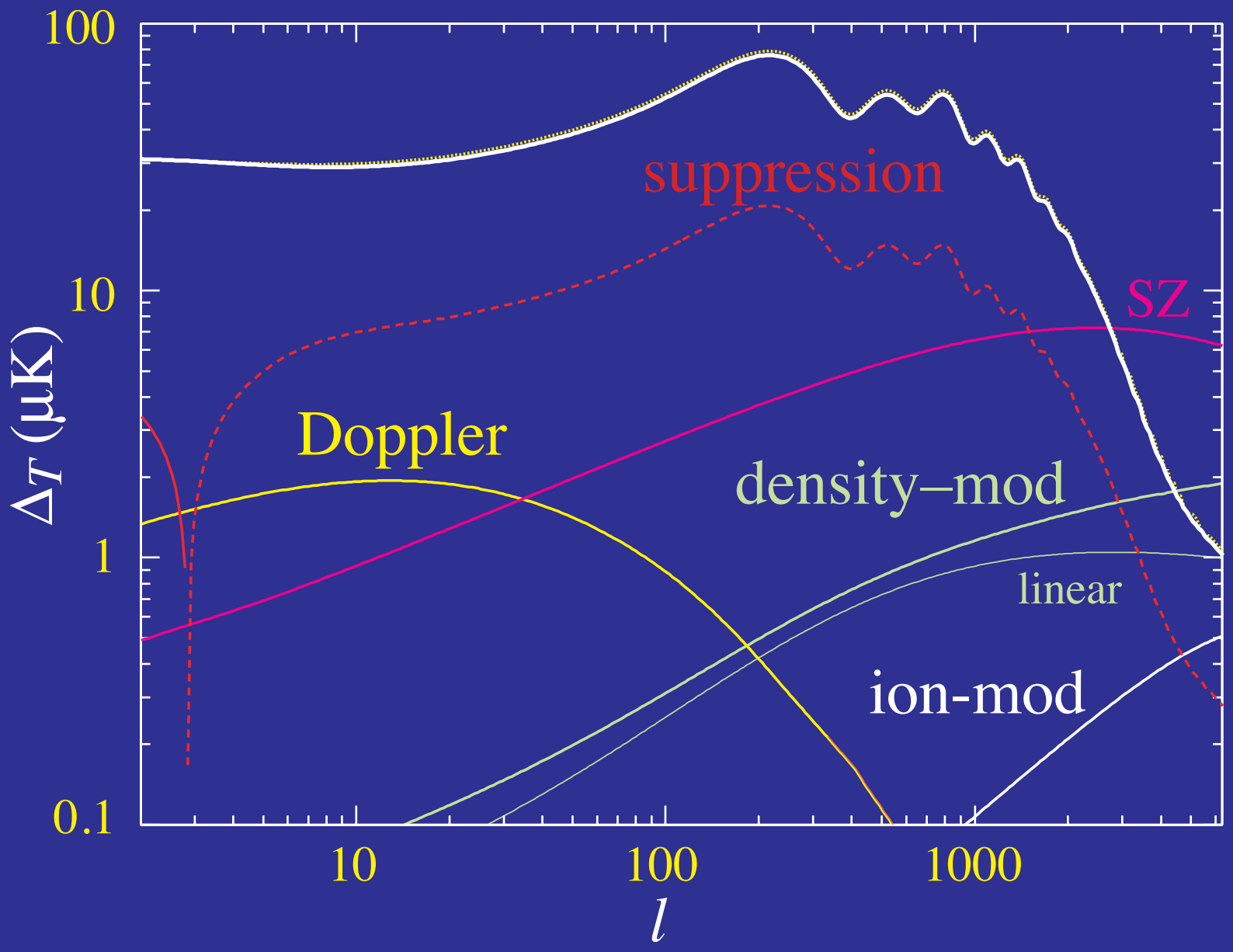

Gravitational Secondaries

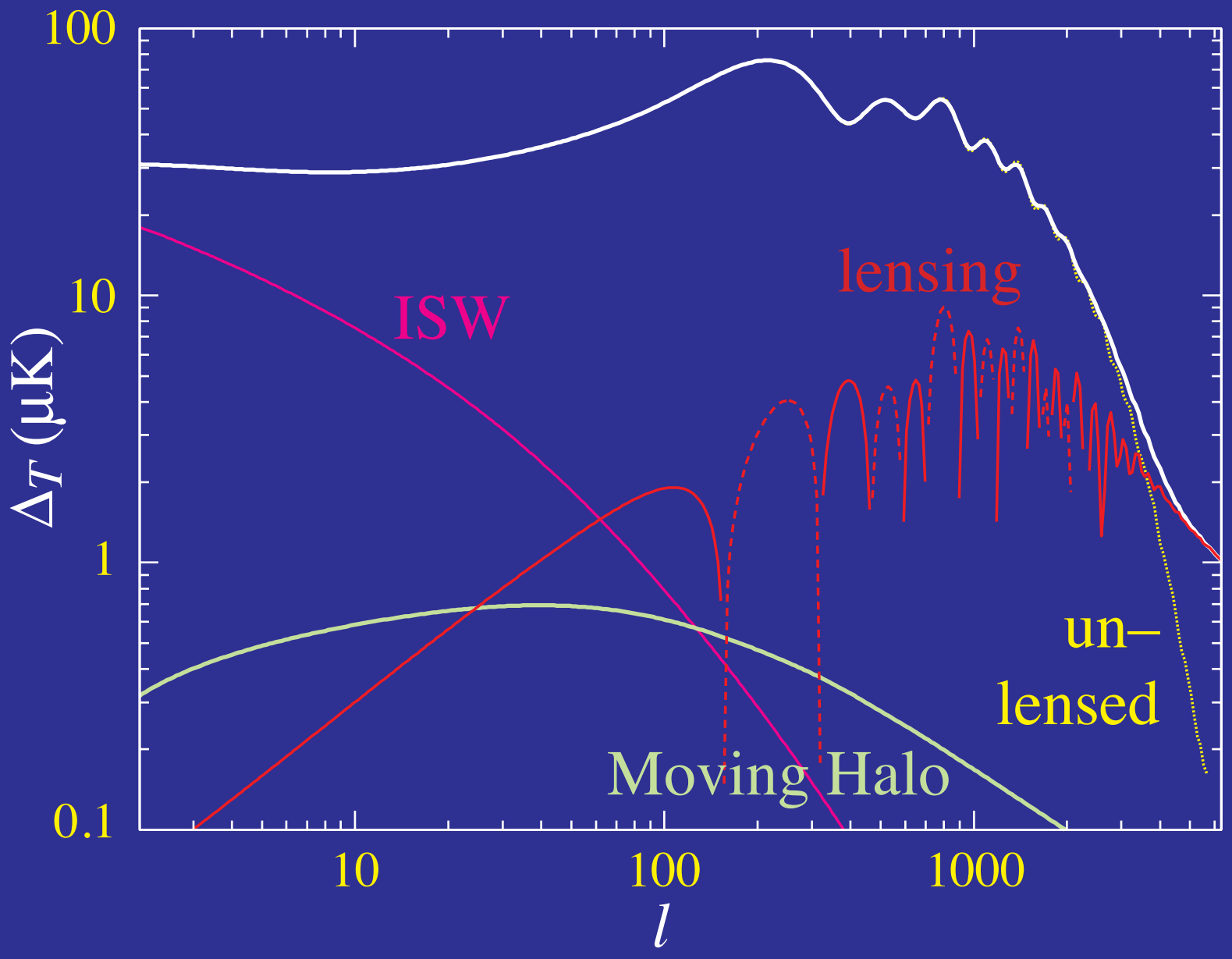

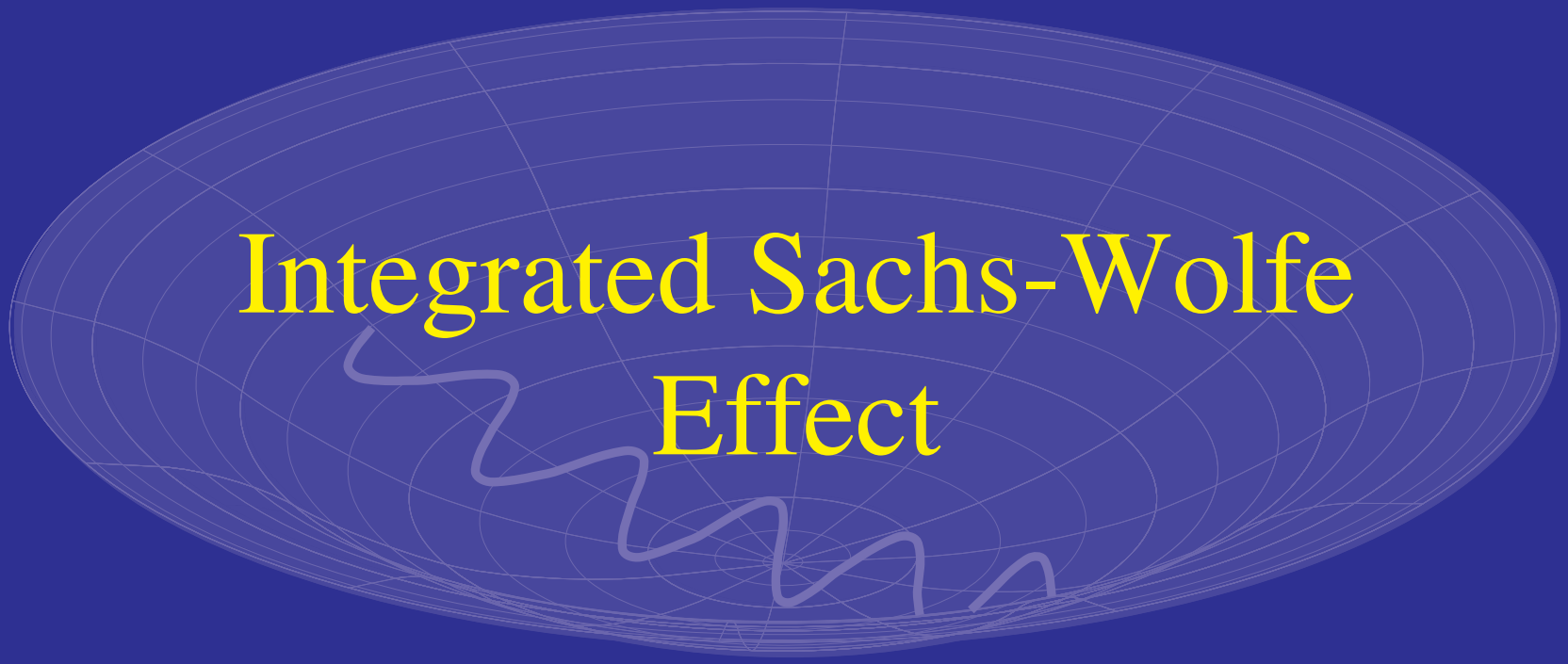

Integrated Sachs-Wolfe Effect

ISW Effect

- Gravitational blueshift on infall does not cancel redshift on climbing out
- Contraction of spatial metric doubles the effect: $\Delta T/T = 2\Delta\Phi$
- Effect from potential hills and wells cancel on small scales

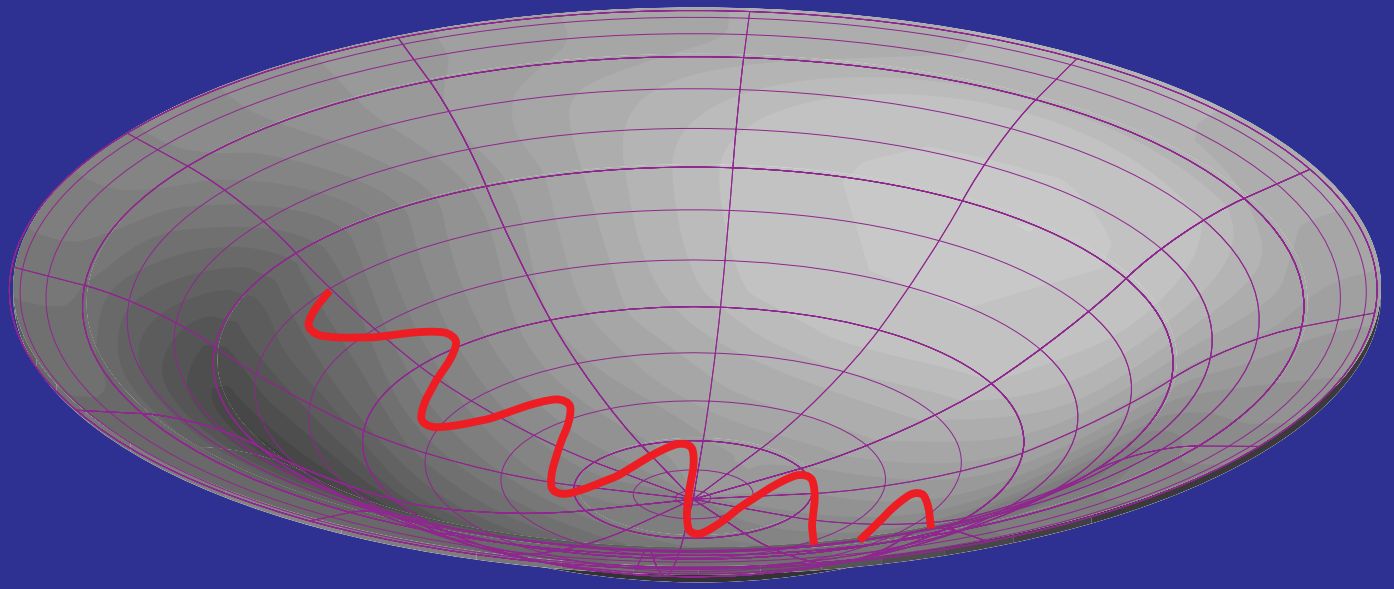

ISW Effect

- Gravitational blueshift on infall does not cancel redshift on climbing out
- Contraction of spatial metric doubles the effect: $\Delta T/T = 2\Delta\Phi$
- Effect from potential hills and wells cancel on small scales

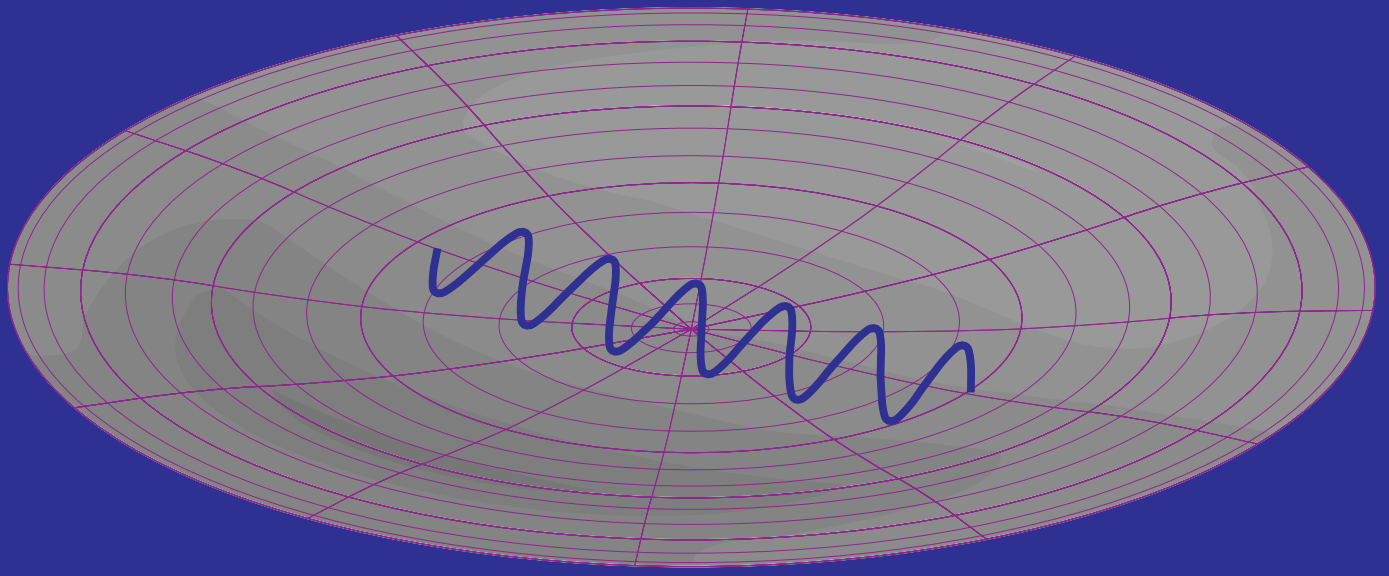

Smooth Energy Density & Potential Decay

- Regardless of the equation of state an energy component that clusters preserves an approximately constant gravitational potential (formally Bardeen curvature ζ)

Smooth Energy Density & Potential Decay

- Regardless of the equation of state an energy component that clusters preserves an approximately constant gravitational potential (formally Bardeen curvature ζ)
- A smooth component contributes
  density ρ to the expansion
  but not
  density fluctuation $\delta\rho$ to the Poisson equation
- Imbalance causes potential to decay once smooth component dominates the expansion

ISW Spatial Modes

- ISW effect comes from nearby acceleration regime
- Shorter wavelengths project onto same angle
- Broad source kernel: Limber cancellation out to quadrupole

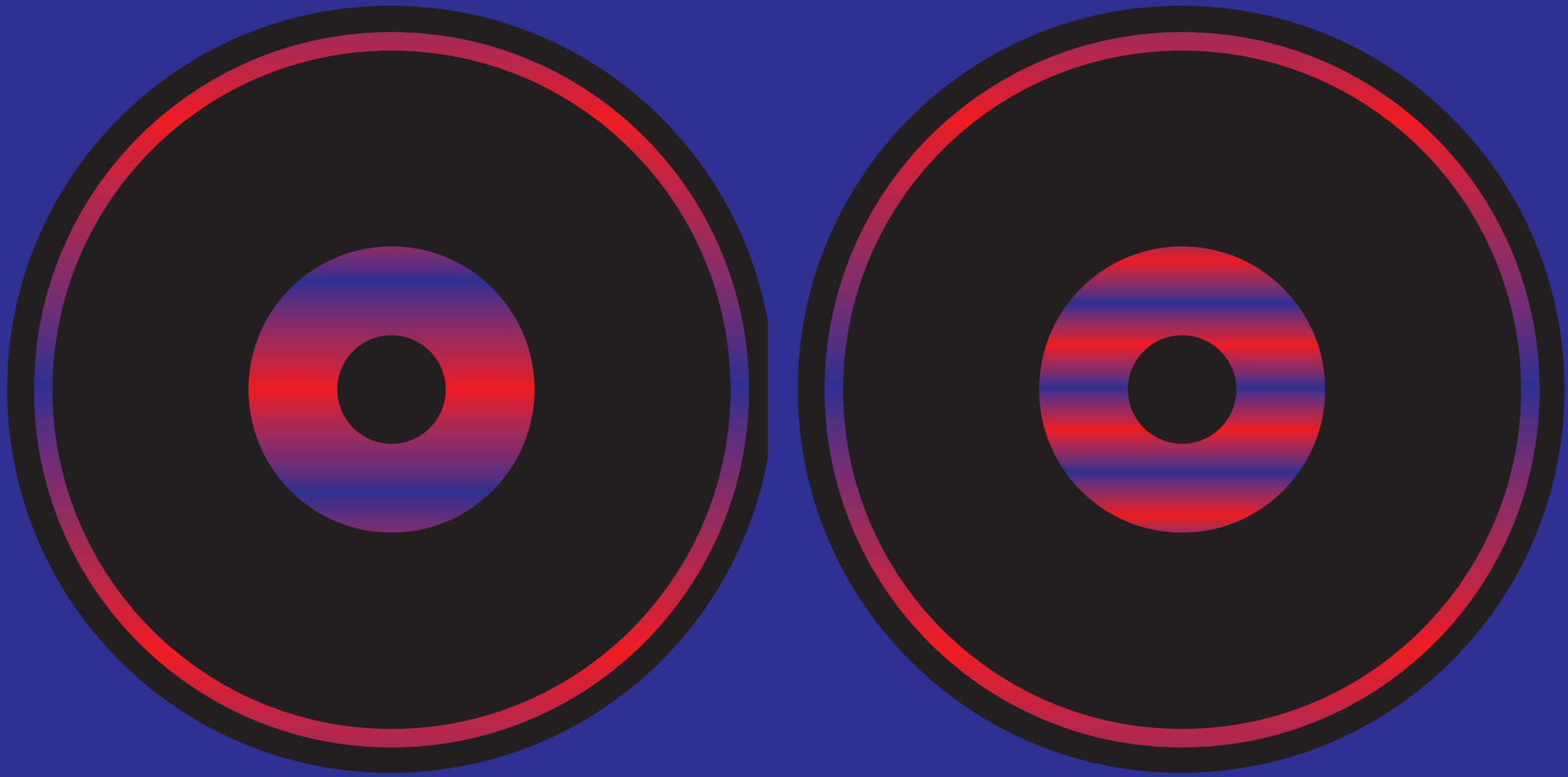

Quadrupole Origins

- Transfer function for the quadrupole

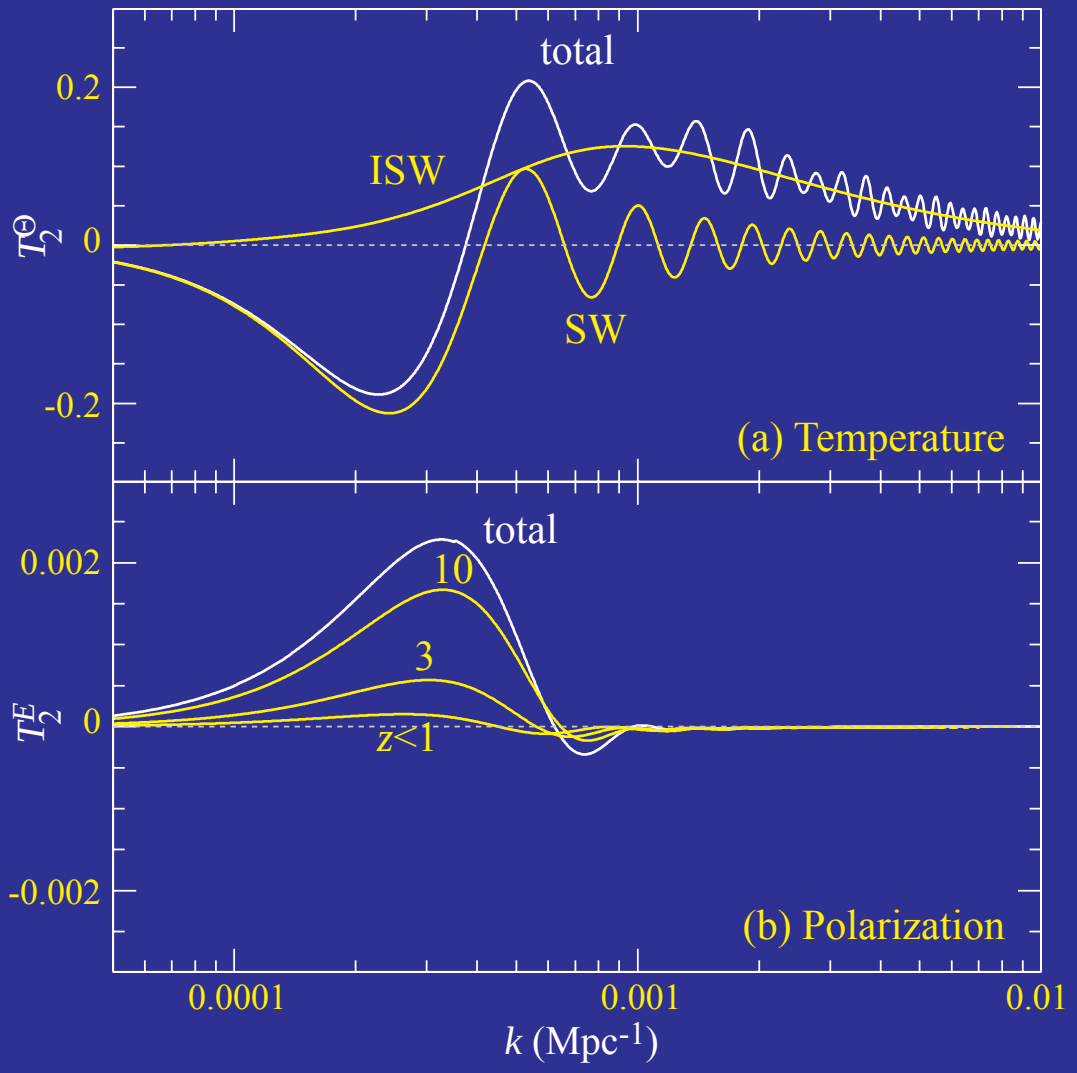

Gordon & Hu (2004)

Smooth Energy Density & Potential Decay

- Regardless of the equation of state an energy component that clusters preserves an approximately constant gravitational potential (formally Bardeen curvature ζ)
- A smooth component contributes
  density ρ to the expansion
  but not
  density fluctuation $\delta\rho$ to the Poisson equation
- Imbalance causes potential to decay once smooth component dominates the expansion
- Scalar field dark energy (quintessence) is smooth out to the horizon scale (sound speed c_s=1)
- Potential decay measures the clustering properties and hence the particle properties of the dark energy

ISW & Dark Energy

Dark Energy

- Peaks measure distance to recombination
- ISW effect constrains dynamics of acceleration

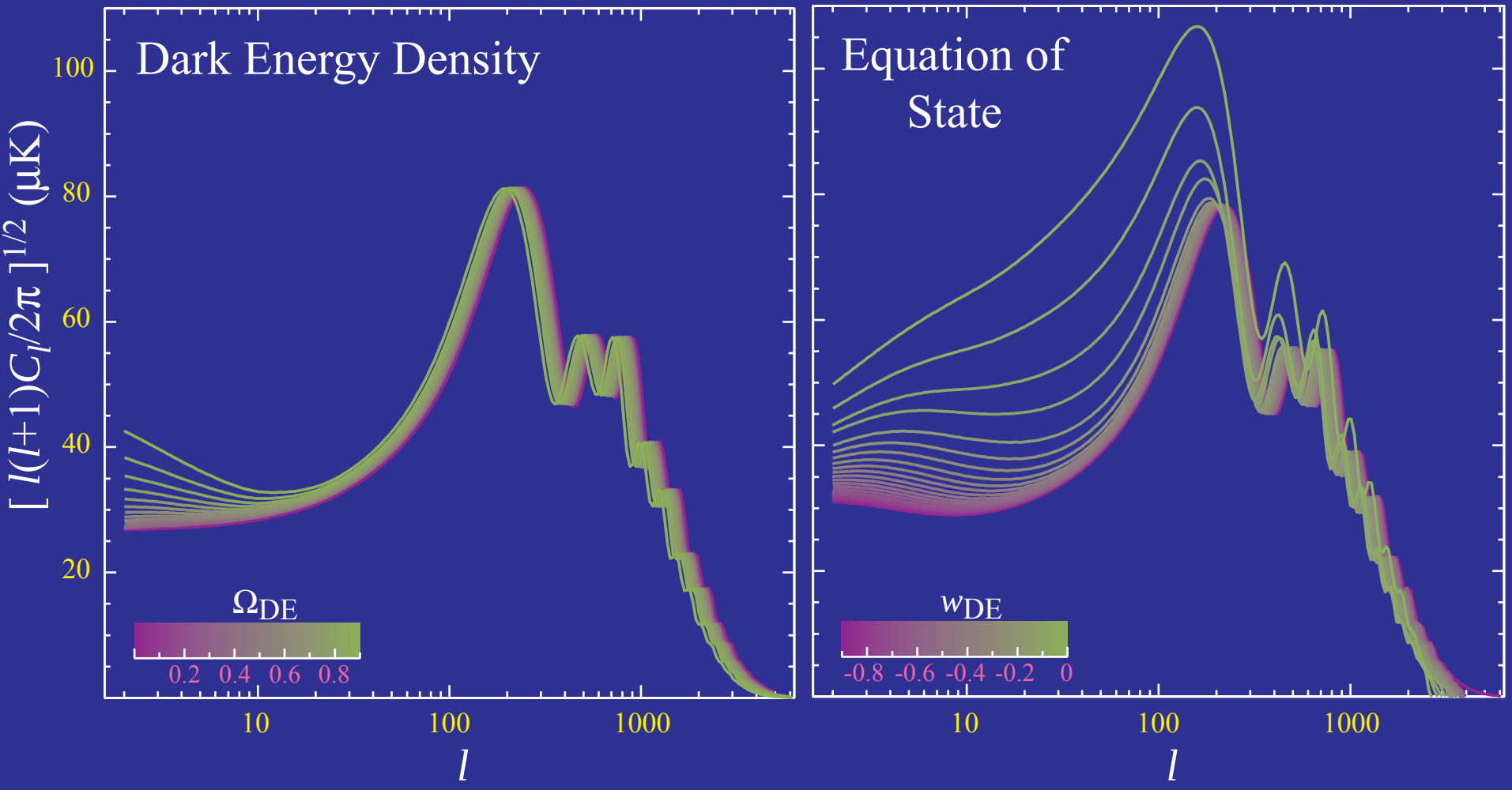

Dark Energy Sound Speed

- Smooth and clustered regimes separated by sound horizon
- Covariant definition: $c_e^2=\delta p/\delta\rho$ where momentum flux vanishes
- For scalar field dark energy uniquely defined by kinetic term

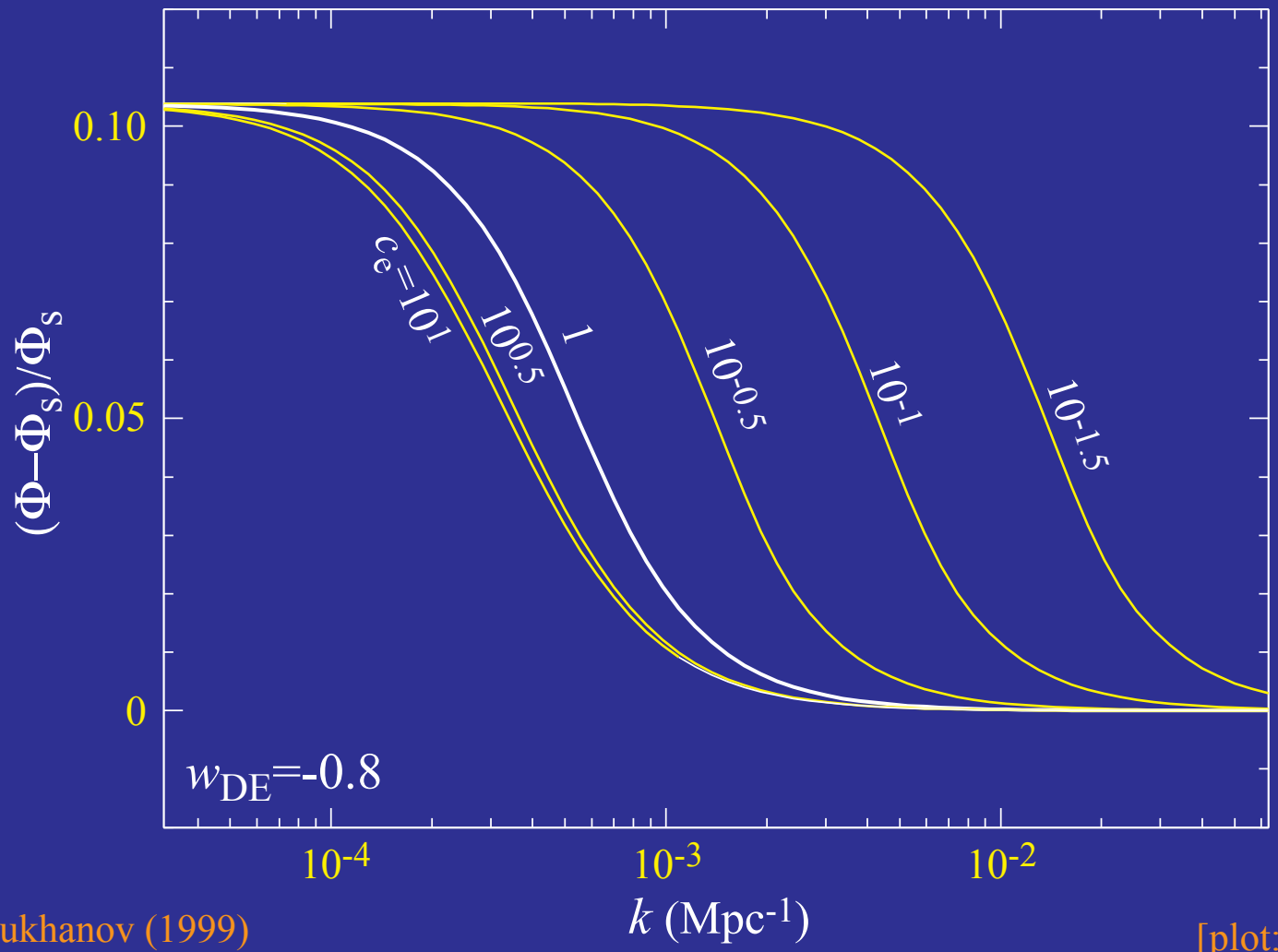

Hu (1998)
Garriga & Mukhanov (1999)

[plot: Hu & Scranton (2004)]

Dark Energy Clustering

- ISW effect intrinsically sensitive to dark energy smoothness
- Large angle contributions reduced if clustered

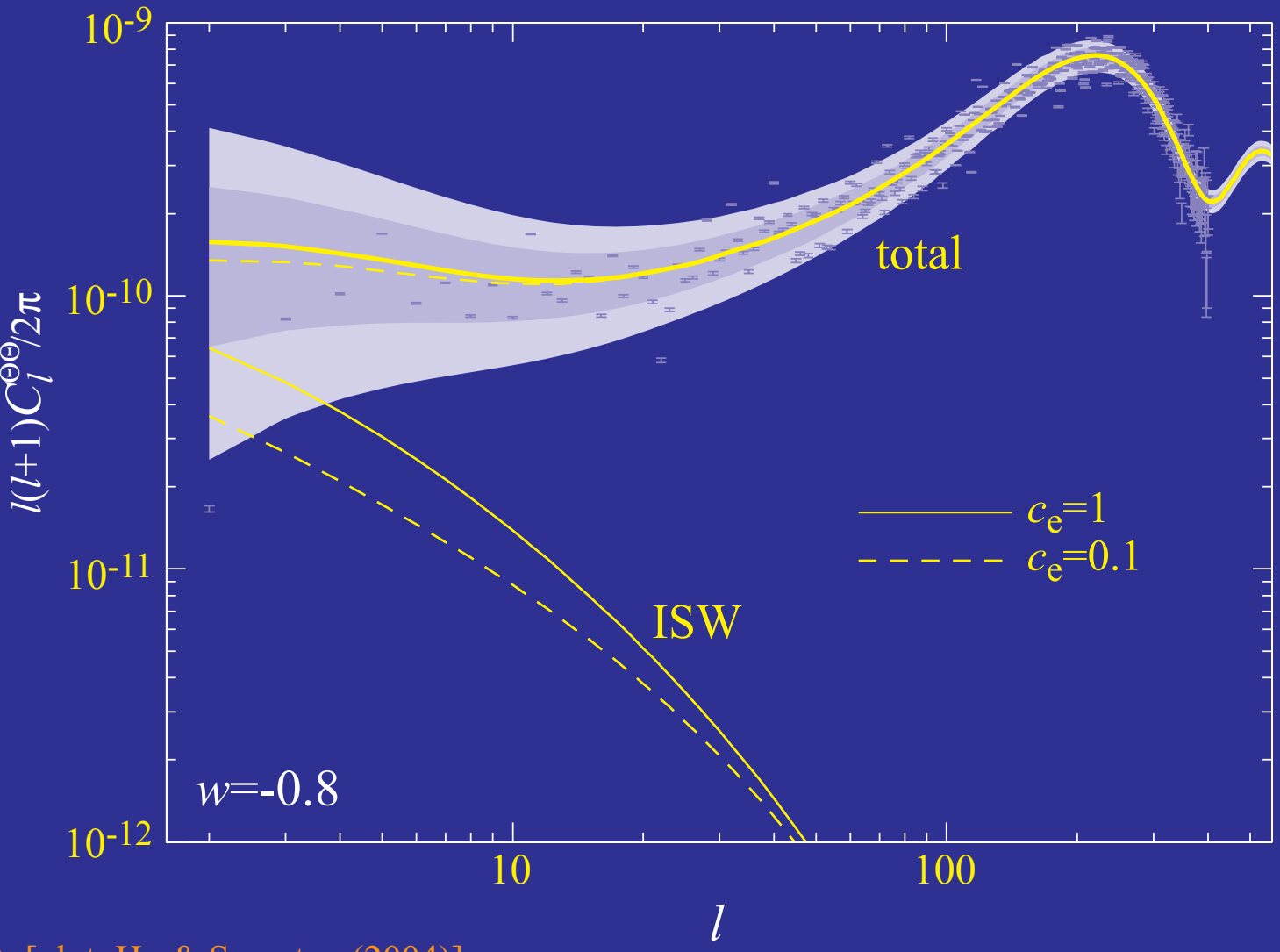

Hu (1998); [plot: Hu & Scranton (2004)]

ISW-Galaxy Correlation

- Decaying potential: galaxy positions correlated with CMB
- Growing potential: galaxy positions anticorrelated with CMB
- Observations indicate correlation

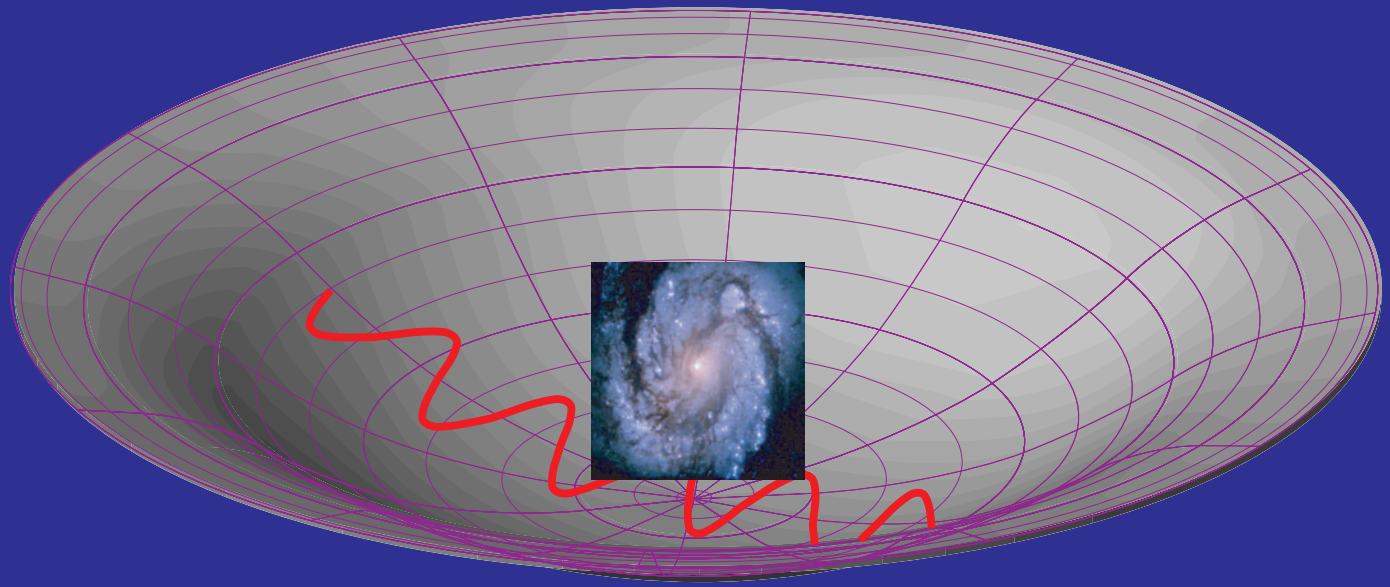

ISW-Galaxy Correlation

- ~4σ joint detection of ISW correlation with large scale structure (galaxies)
- ~2σ high compared with ΛCDM

Ho et al (2007) [Giannantonio et al 2008]

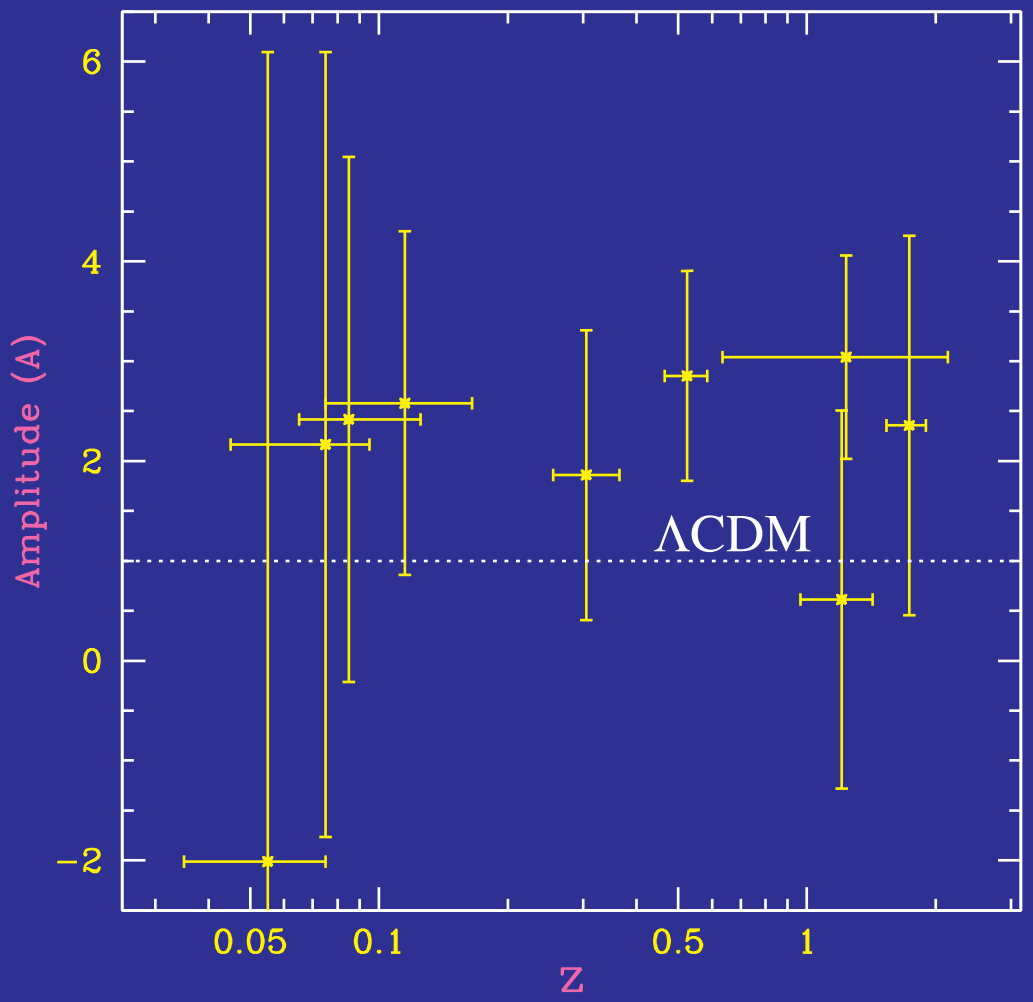

Ultra-Deep Wide Survey

- Ultimate limit: deep wide-field survey with photometric redshift errors of $\sigma(z)=0.03(1+z)$, median redshift $z=1.5$, 70 gal/arcmin^2

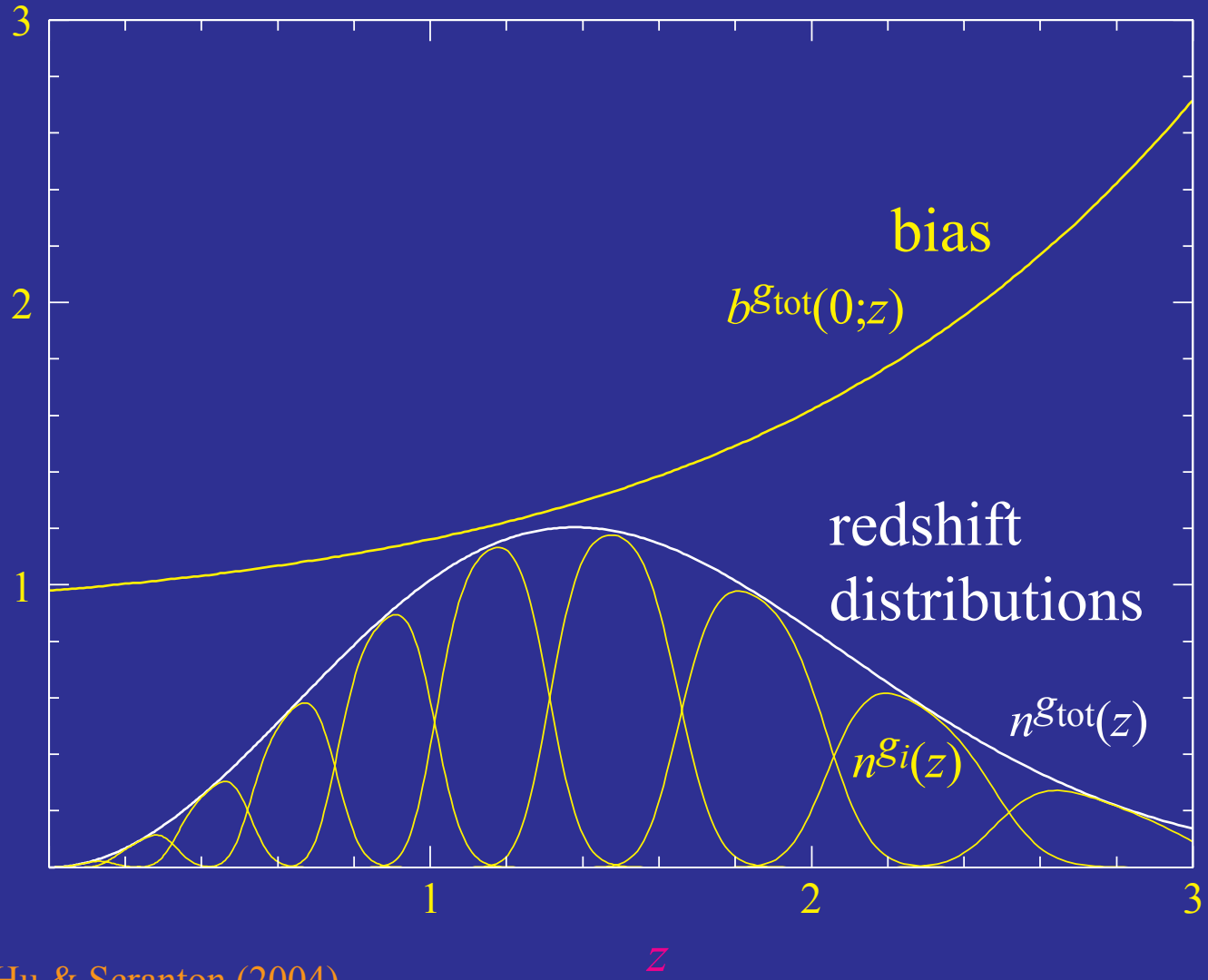

Afshordi (2004); Hu & Scranton (2004)

Galaxy Cross Correlation

- Cross correlation highly sensitive to the dark energy smoothness (parameterized by sound speed)

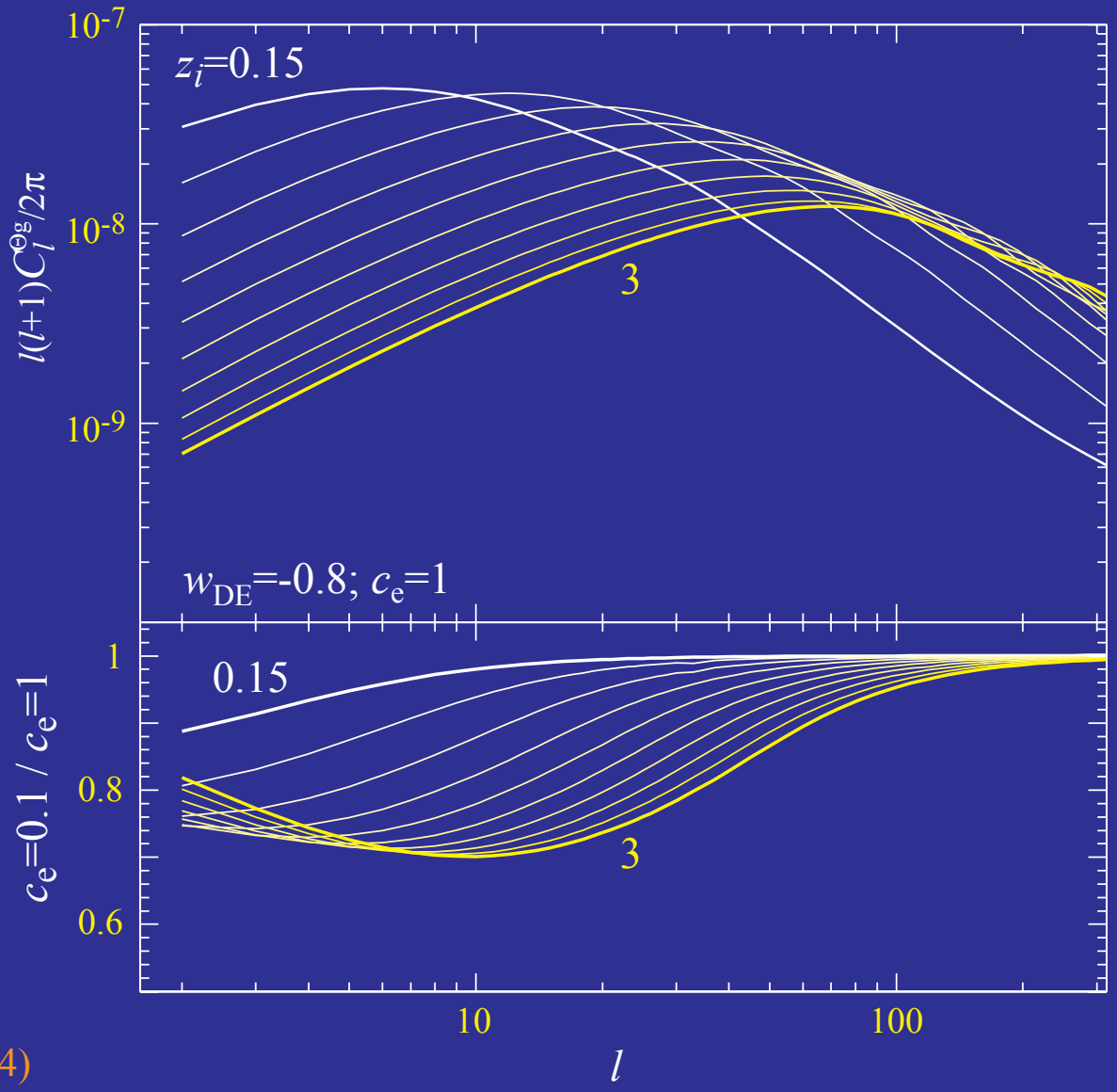

Hu & Scranton (2004)

Galaxy Cross Correlation

- Significance of the separation between quintessence and a more clustered dark energy with sound speed c_e

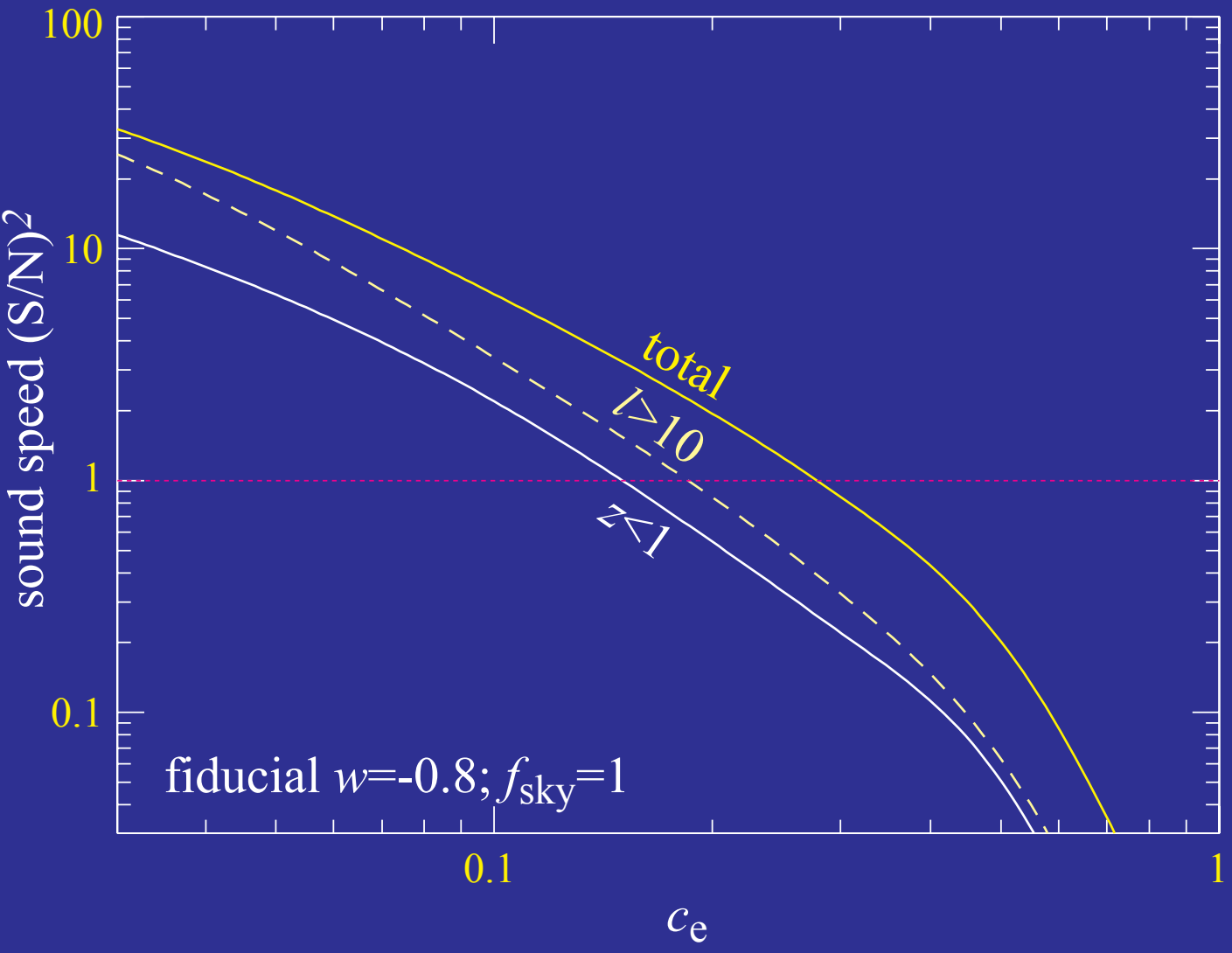

Hu & Scranton (2004)

Dark Energy Smoothness

- More robust way of quoting constraints: how smooth is the dark energy out to a given physical scale:

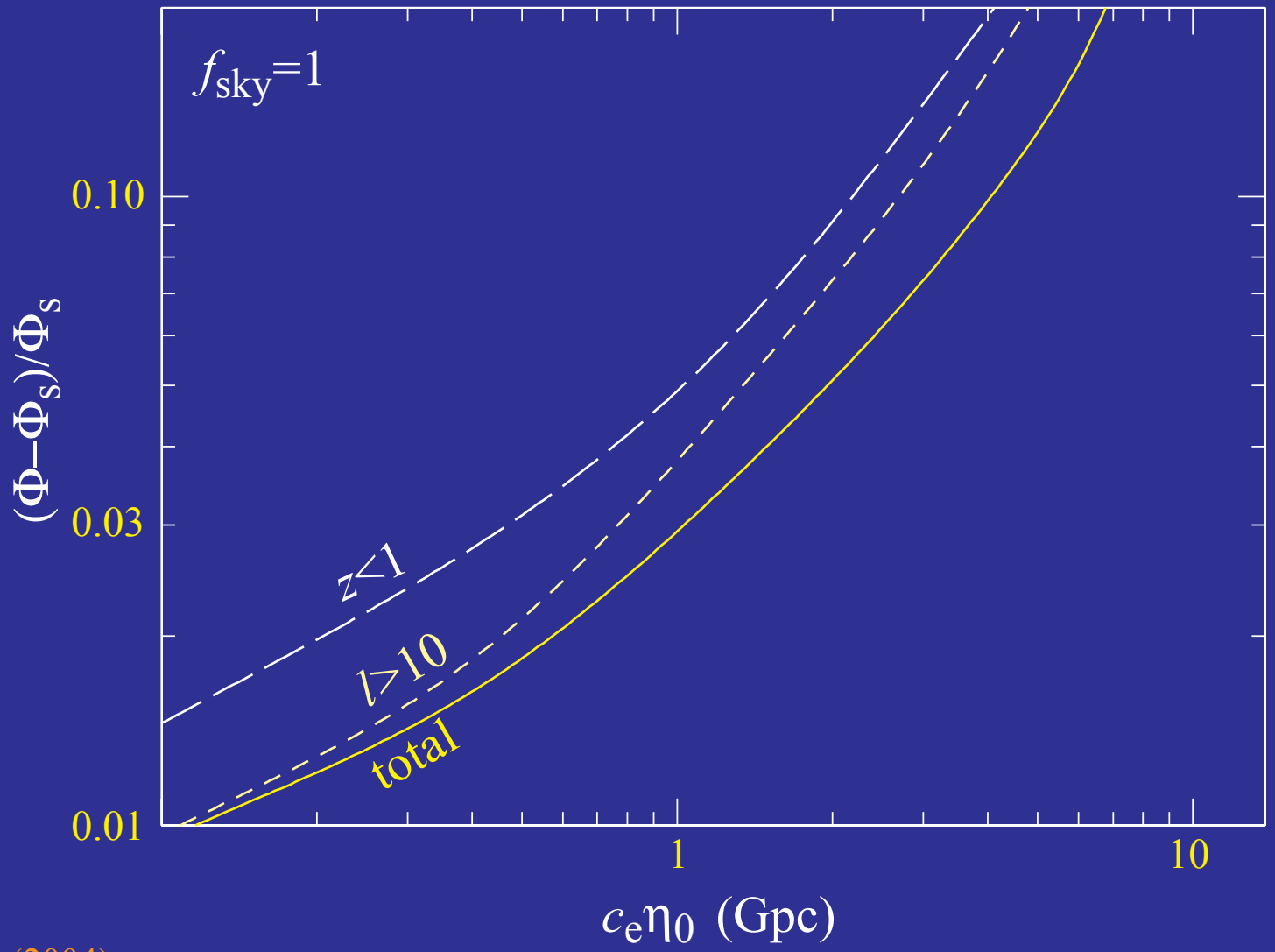

Hu & Scranton (2004)

Isocurvature DE Perturbations

- Anti-correlated DE perturbations: ISW cancel SW effect

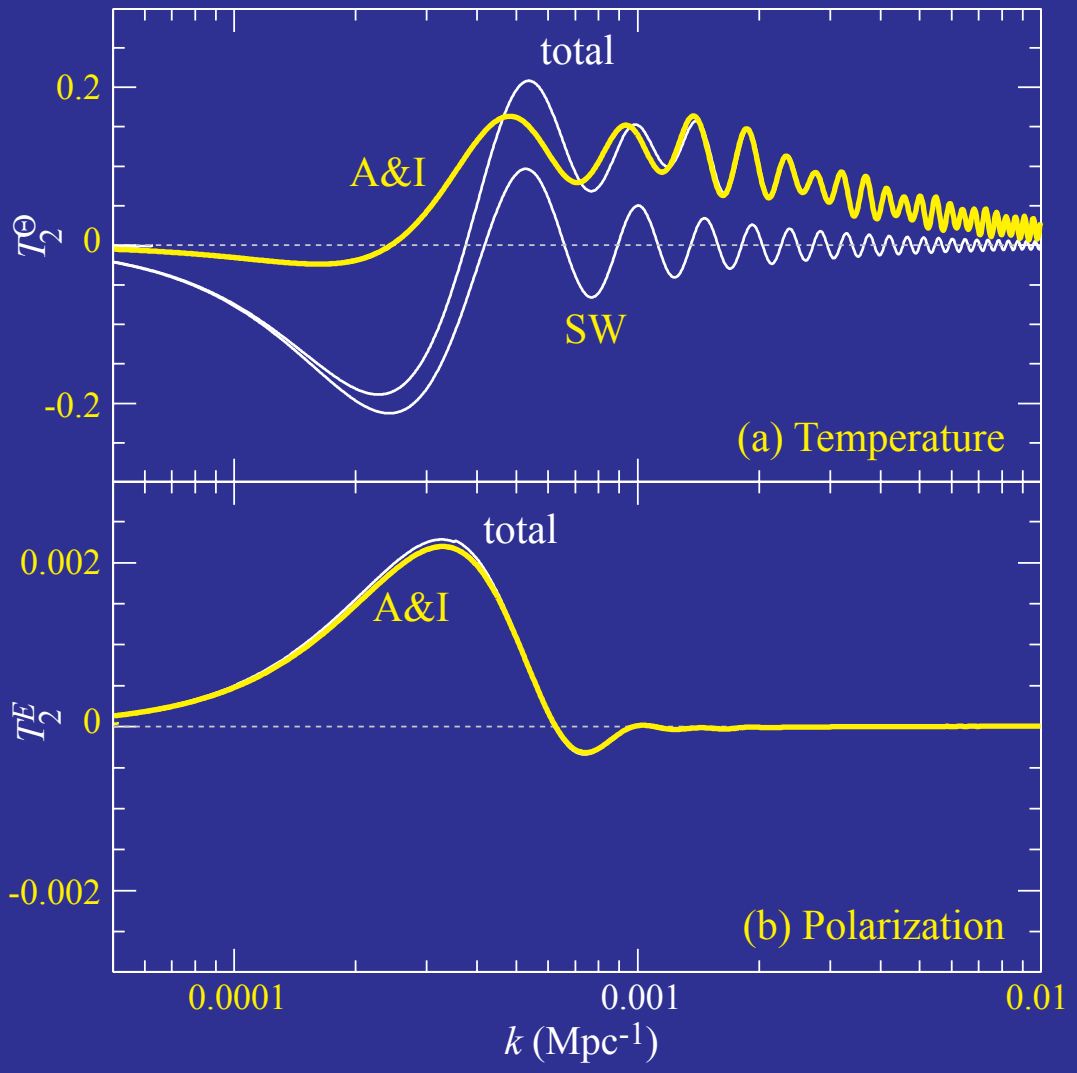

Moroi & Takahashi (2004); Gordon & Hu (2004)

Low Quadrupole Models

- Required isocurvature perturbation can be generated by variable decay reheating mechanism but overpredicts grav w.

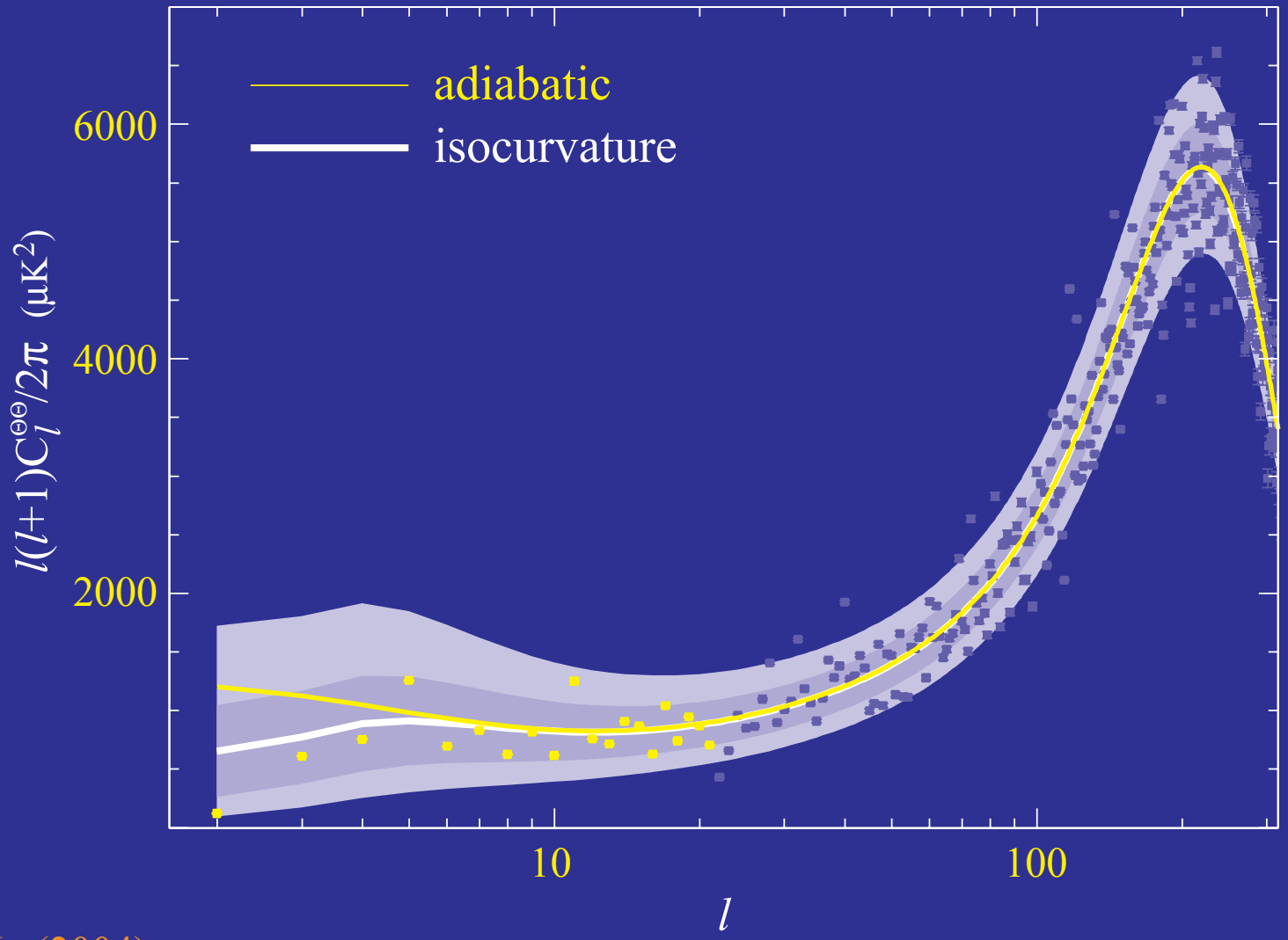

Gordon & Hu (2004) [Dvali, Gruzinov, Zaldarriaga (2004) reheating]

Polarization Rejects ISW

- Polarization unchanged; cross correlation lowered

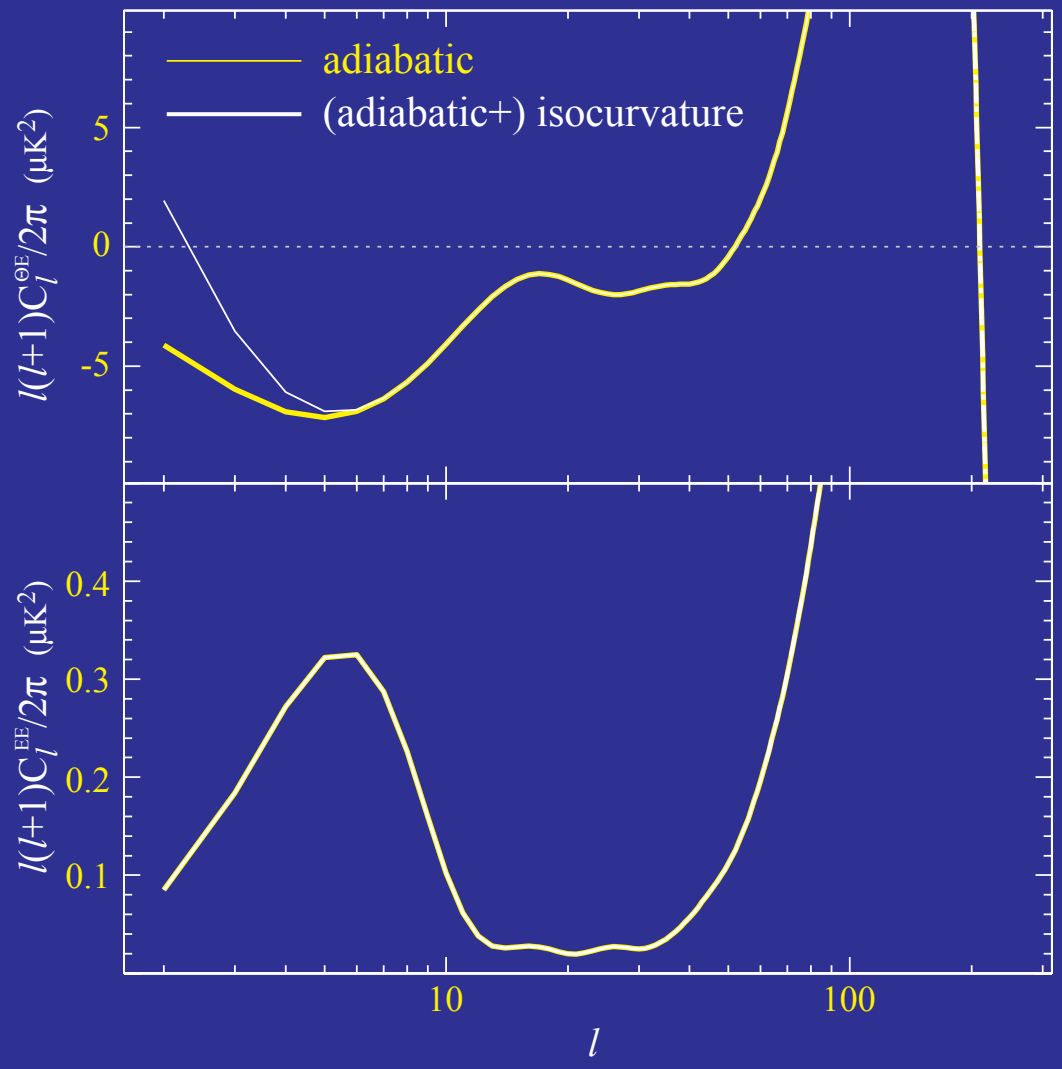

Gordon & Hu (2004)

ISW & Modified Gravity

Parameterizing Acceleration

- Cosmic acceleration, like the cosmological constant, can either be viewed as arising from

  Missing, or dark energy, with $w \equiv \bar{p}/\bar{\rho} < -1/3$

  Modification of gravity on large scales

$$\begin{aligned} G_{\mu\nu} &= 8\pi G \left(T^{\rm M}_{\mu\nu} + T^{\rm DE}_{\mu\nu}\right) \\ F(g_{\mu\nu}) + G_{\mu\nu} &= 8\pi G T^{\rm M}_{\mu\nu} \end{aligned}$$

- Proof of principle models for both exist: quintessence, k-essence; DGP braneworld acceleration, $f(R)$ modified action
- Compelling models for either explanation lacking
- Study models as illustrative toy models whose features can be generalized

DGP Braneworld Acceleration

- Braneworld acceleration (Dvali, Gabadadze & Porrati 2000)

$$S = \int d^5x \sqrt{-g} \left[\frac{{}^{(5)}R}{2\kappa^2} + \delta(\chi) \left(\frac{{}^{(4)}R}{2\mu^2} + \mathcal{L}_m \right) \right]$$

  with crossover scale $r_c = \kappa^2/2\mu^2$

- Influence of bulk through Weyl tensor anisotropy - solve master equation in bulk (Deffayet 2001)
- Matter still minimally coupled and conserved
- Exhibits the 3 regimes of modified gravity
- Weyl tensor anisotropy dominated conserved curvature regime $r > r_c$ (Sawicki, Song, Hu 2006; Cardoso et al 2007)
- Brane bending scalar tensor regime $r_* < r < r_c$ (Lue, Soccimarro, Starkman 2004; Koyama & Maartens 2006)
- Strong coupling General Relativistic regime $r < r_* = (r_c^2 r_g)^{1/3}$ where $r_g = 2GM$ (Dvali 2006)

DGP Horizon Scales

- Metric and matter evolution well-matched by PPF description
- Standard GR tools apply (CAMB), self-consistent, gauge invar.

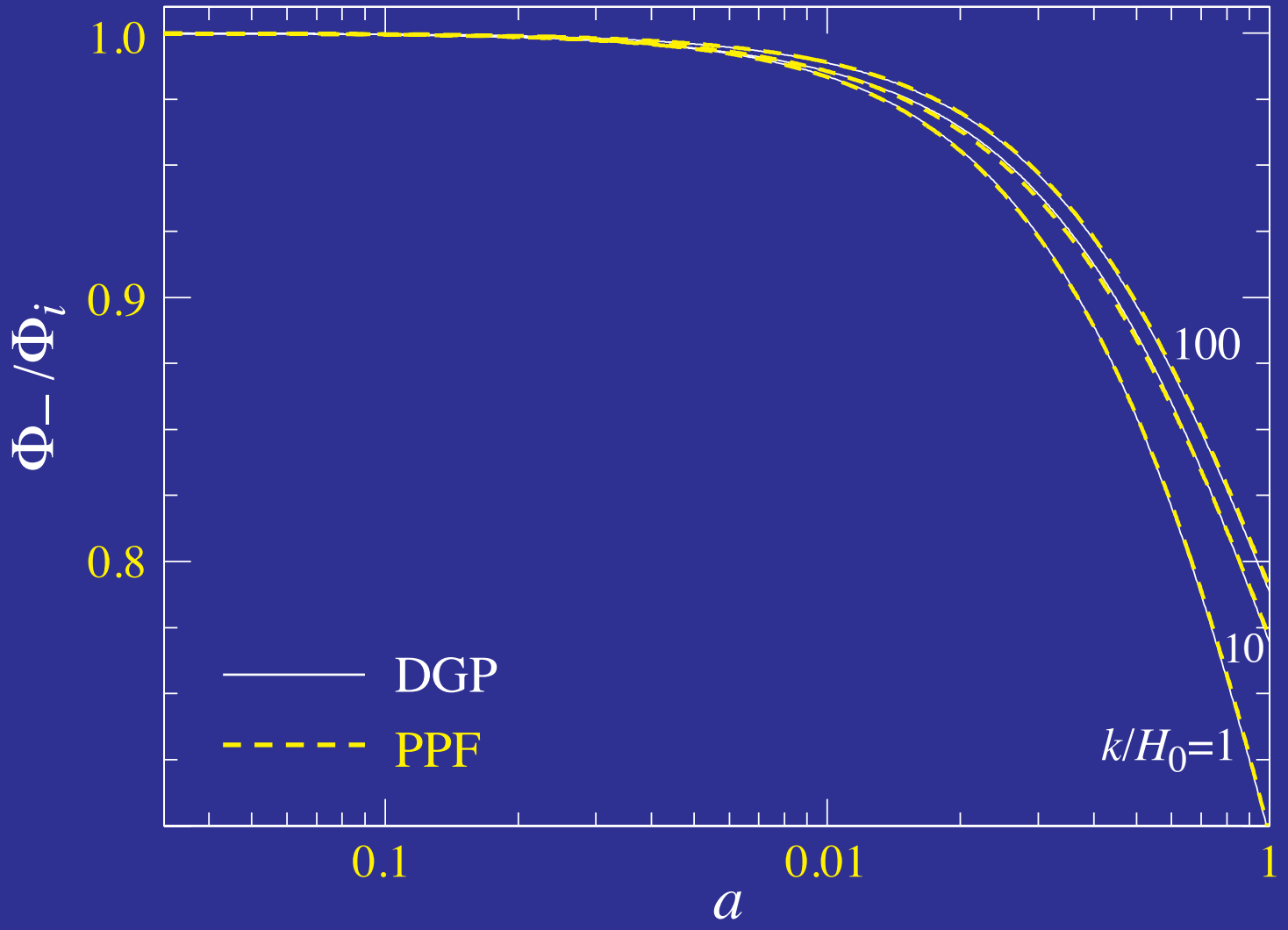

Hu & Sawicki (2007); Hu (2008)

DGP CMB Large-Angle Excess

- Extra dimension modify gravity on large scales
- 4D universe bending into extra dimension alters gravitational redshifts in cosmic microwave background

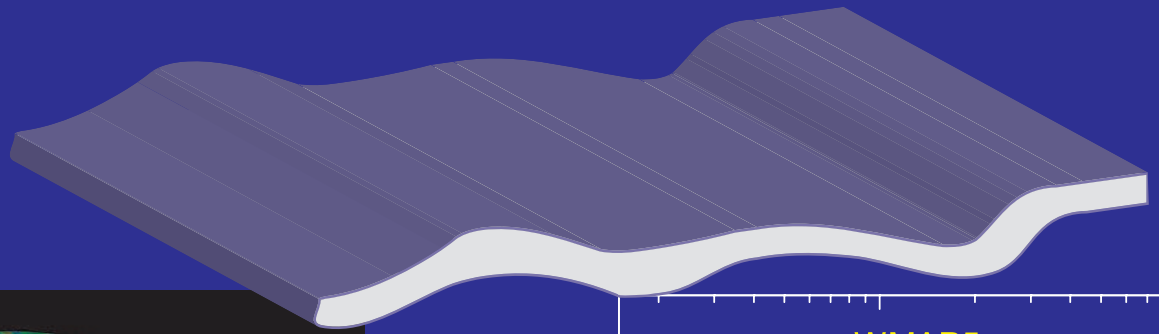

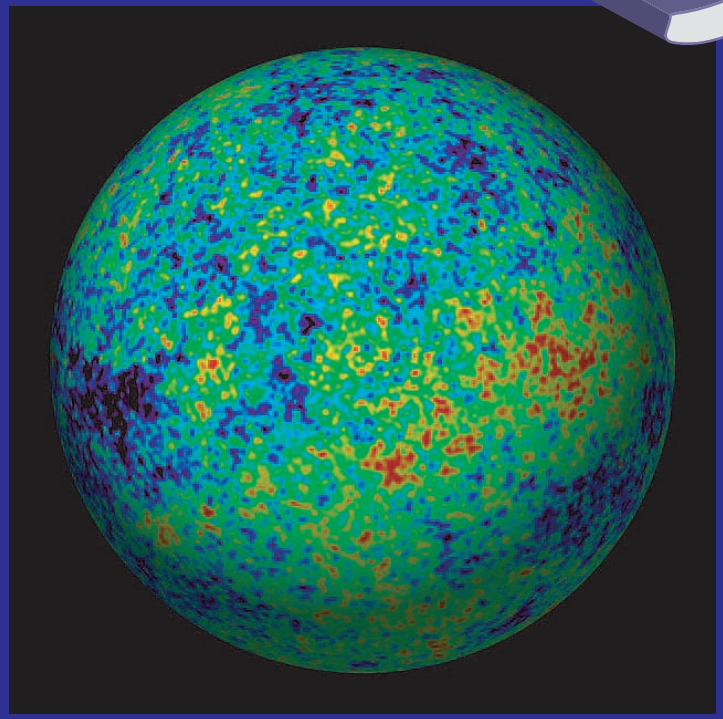

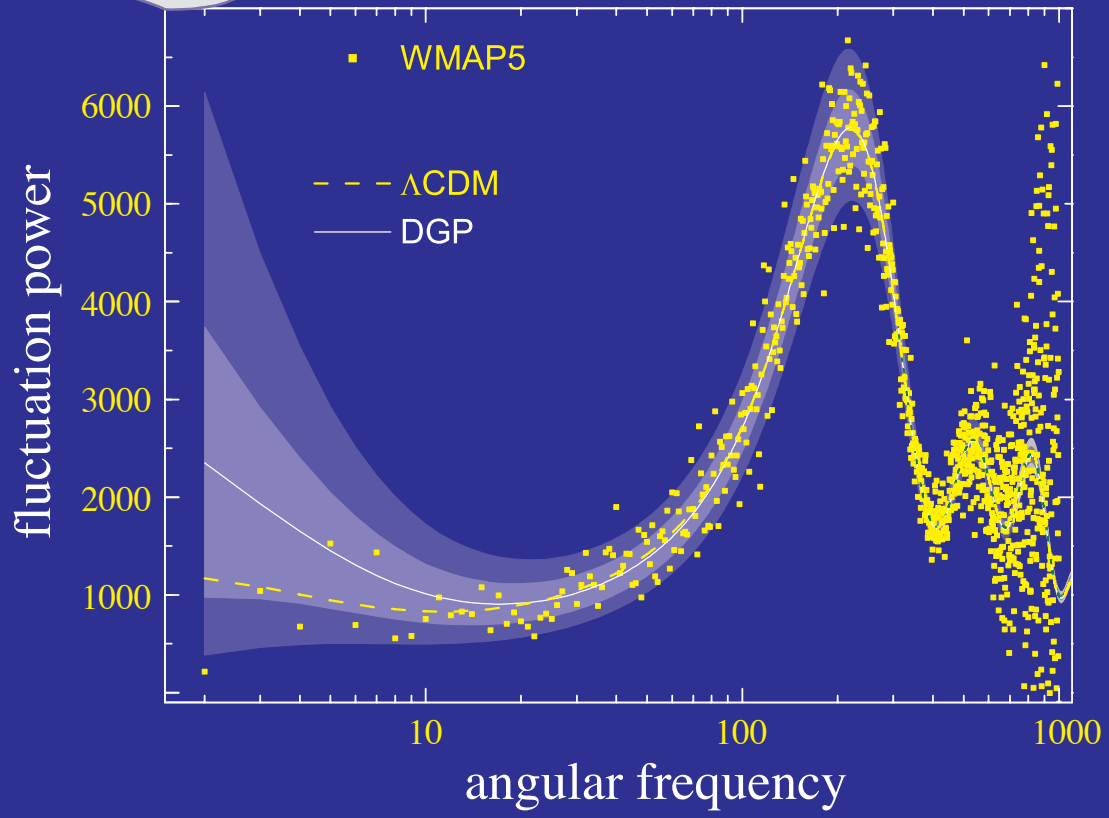

CMB in DGP

- Adding cut off as an epicycle can fix distances, ISW problem
- Suppresses polarization in violation of EE data - cannot save DGP!

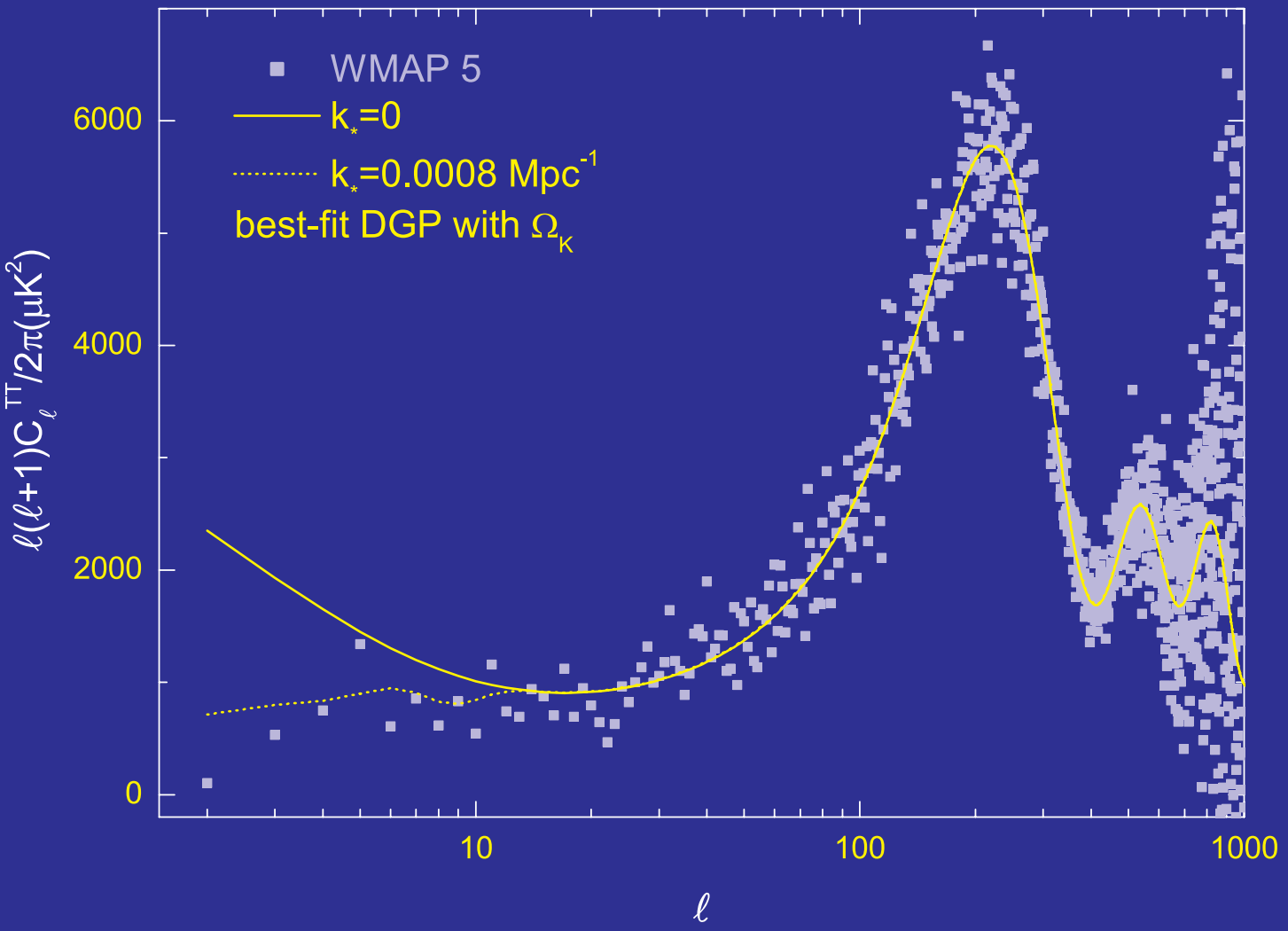

Fang et al (2008)

CMB in DGP

- Adding cut off as an epicycle can fix distances, ISW problem
- Suppresses polarization in violation of EE data - cannot save DGP!

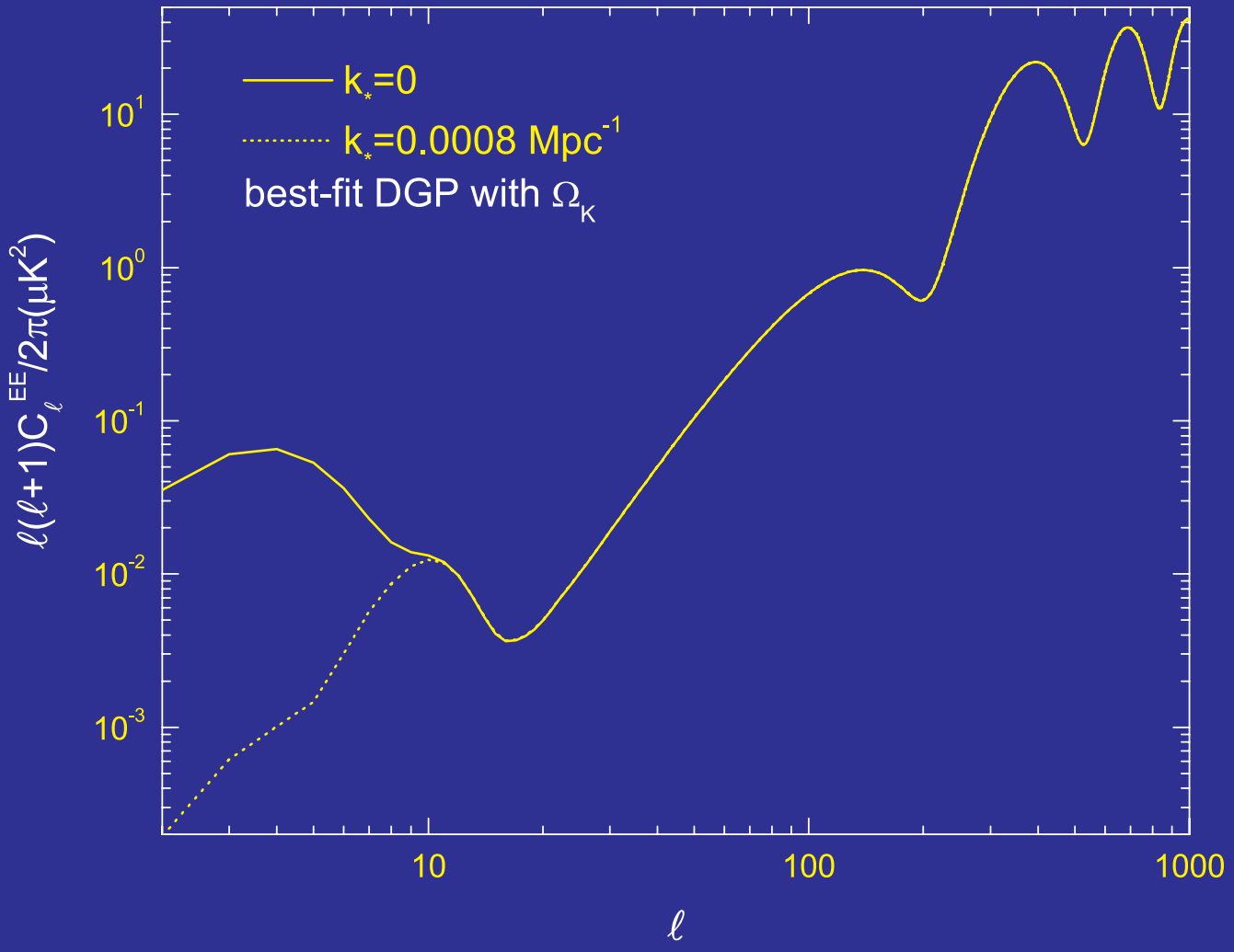

Fang et al (2008)

Modified Action $f(R)$ Model

- R: Ricci scalar or "curvature"
- $f(R)$: modified action (Starobinsky 1980; Carroll et al 2004)

$$S = \int d^4x\sqrt{-g}\left[\frac{R + f(R)}{16\pi G} + \mathcal{L}_{\rm m}\right]$$

- $f_R \equiv df/dR$: additional propagating scalar degree of freedom (metric variation)
- $f_{RR} \equiv d^2 f/dR^2$: Compton wavelength of f_R squared, inverse mass squared
- B: Compton wavelength of f_R squared in units of the Hubble length

$$B \equiv \frac{f_{RR}}{1 + f_R} R' \frac{H}{H'}$$

see Tristan Smith's talk

- $' \equiv d/d\ln a$: scale factor as time coordinate

PPF $f(R)$ Description

- Metric and matter evolution well-matched by PPF description
- Standard GR tools apply (CAMB), self-consistent, gauge invar.

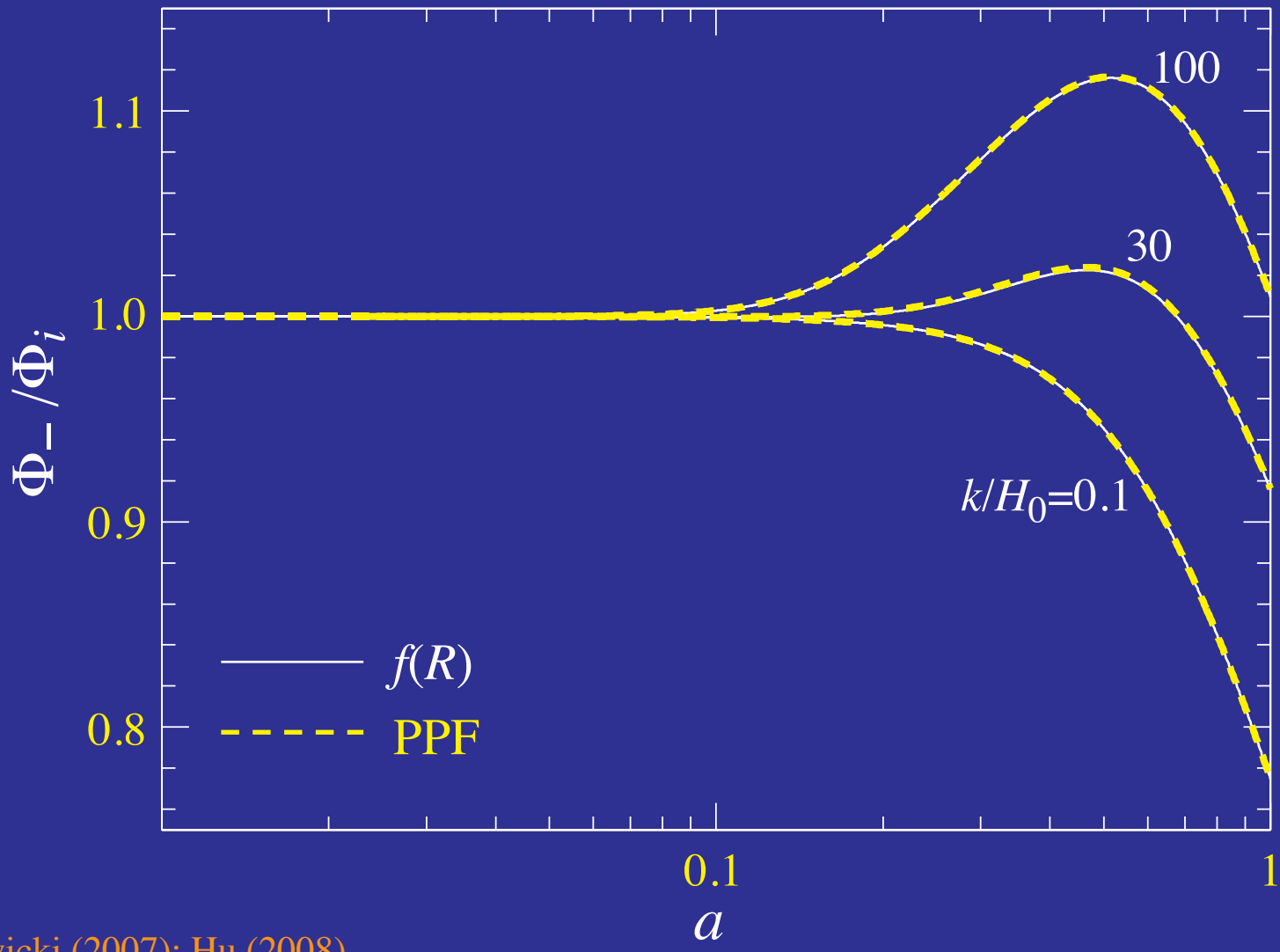

Hu & Sawicki (2007); Hu (2008)

ISW Quadrupole

- Reduction of large angle anisotropy for $B_0 \sim 1$ for same expansion history and distances as ΛCDM
- Well-tested small scale anisotropy unchanged

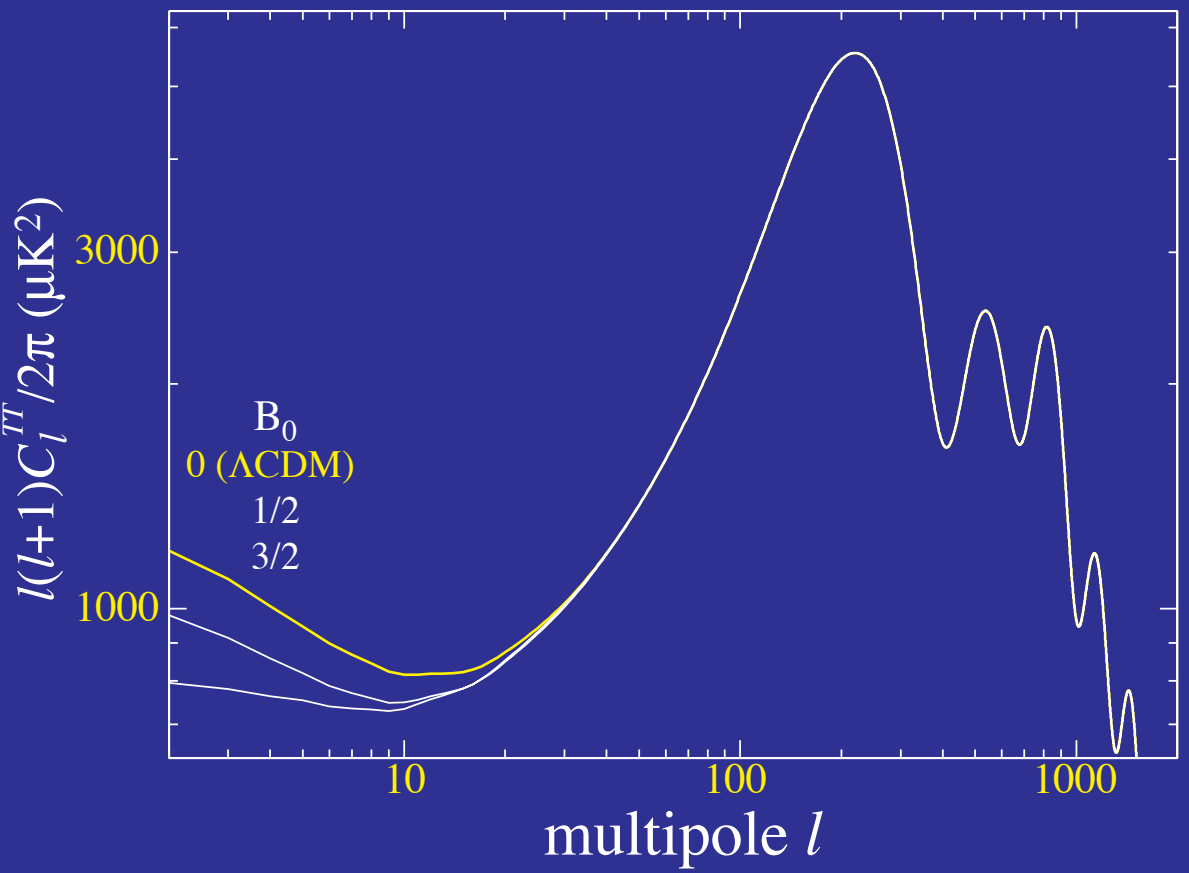

Song, Hu & Sawicki (2006)

PPF $f(R)$ Description

- Metric and matter evolution well-matched by PPF description
- Standard GR tools apply (CAMB), self-consistent, gauge invar.

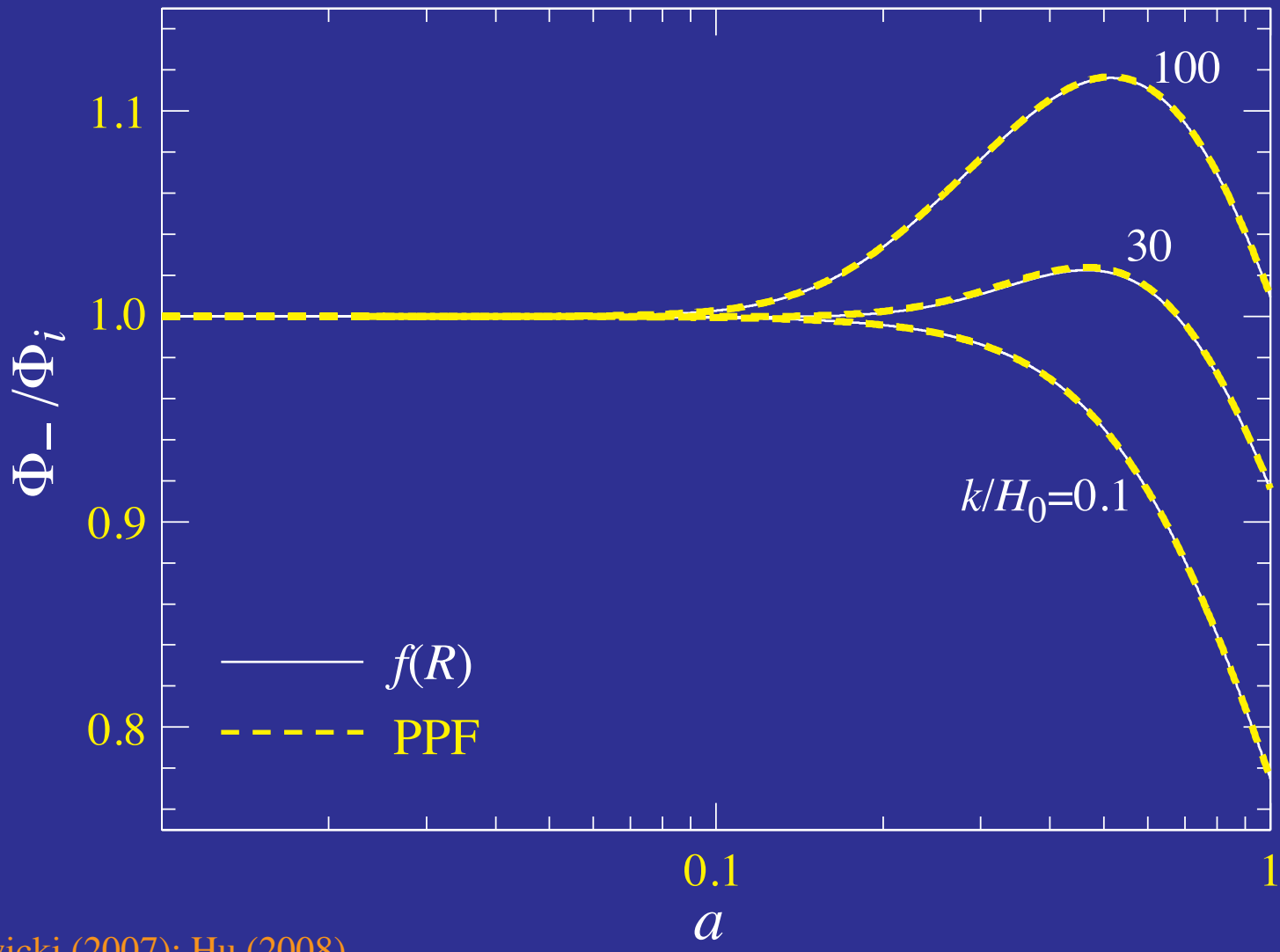

Hu & Sawicki (2007); Hu (2008)

Galaxy-ISW Anti-Correlation

- Large Compton wavelength $B^{1/2}$ creates potential growth which can anti-correlate galaxies and the CMB
- In tension with detections of positive correlations across a range of redshifts

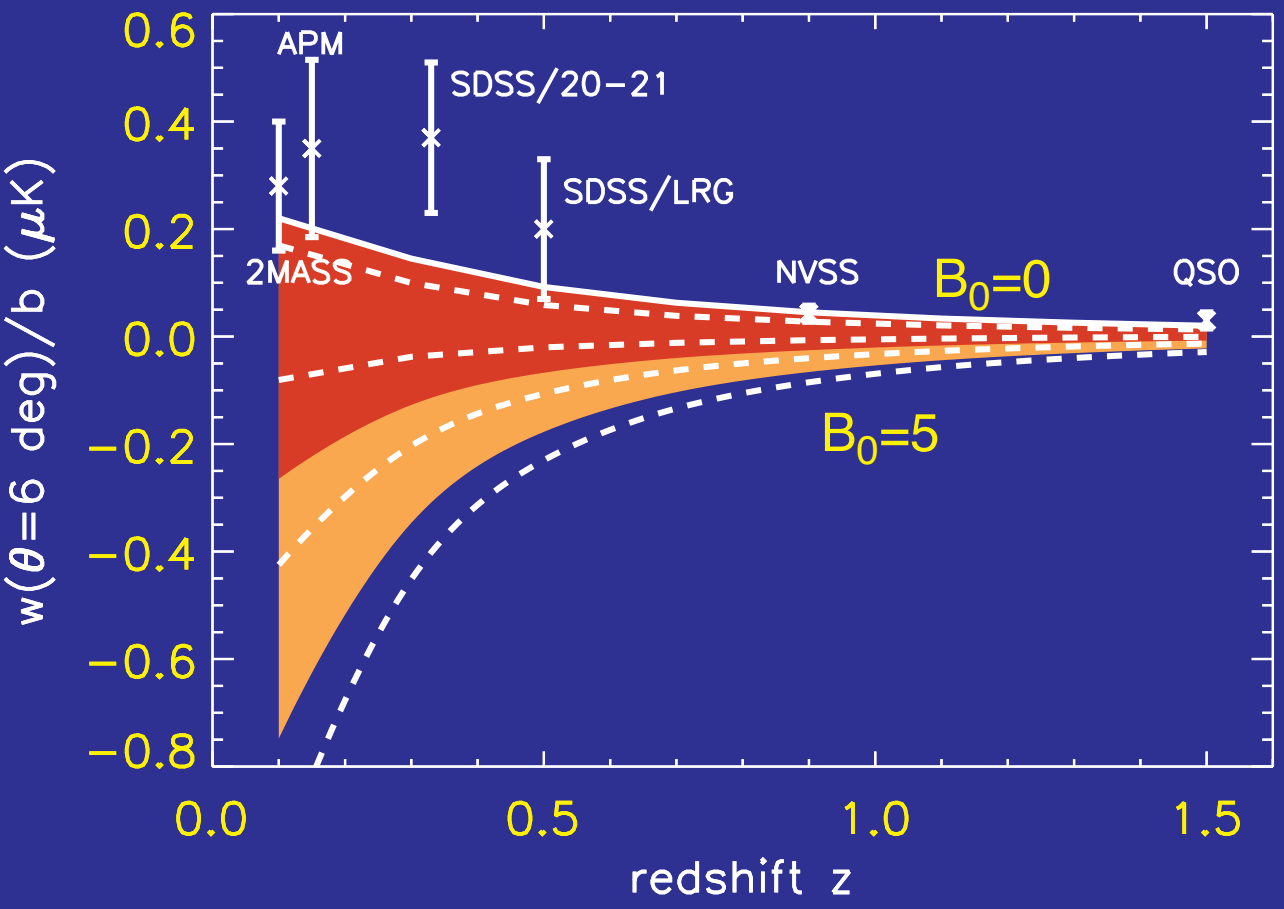

Song, Peiris & Hu (2007)

Parameterized Post-Friedmann

- Parameterizing the degrees of freedom associated with metric modification of gravity that explain cosmic acceleration
- Simple models that add in only one extra scale to explain acceleration tend to predict substantial changes near horizon and hence ISW

Hu (2008)

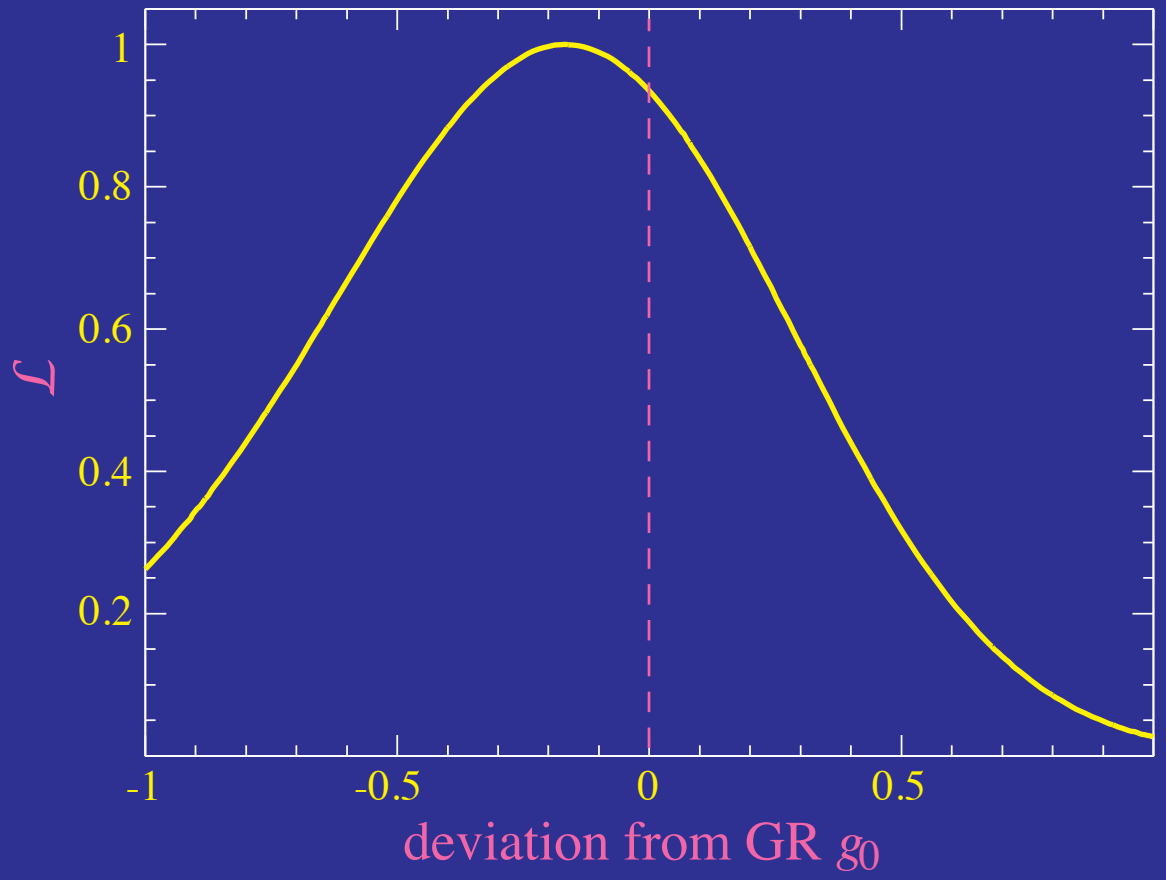

Non-linear ISW Effect

Moving Halo Effect

Moving Halo Effect

- Change in potential due to halo moving across the line of sight

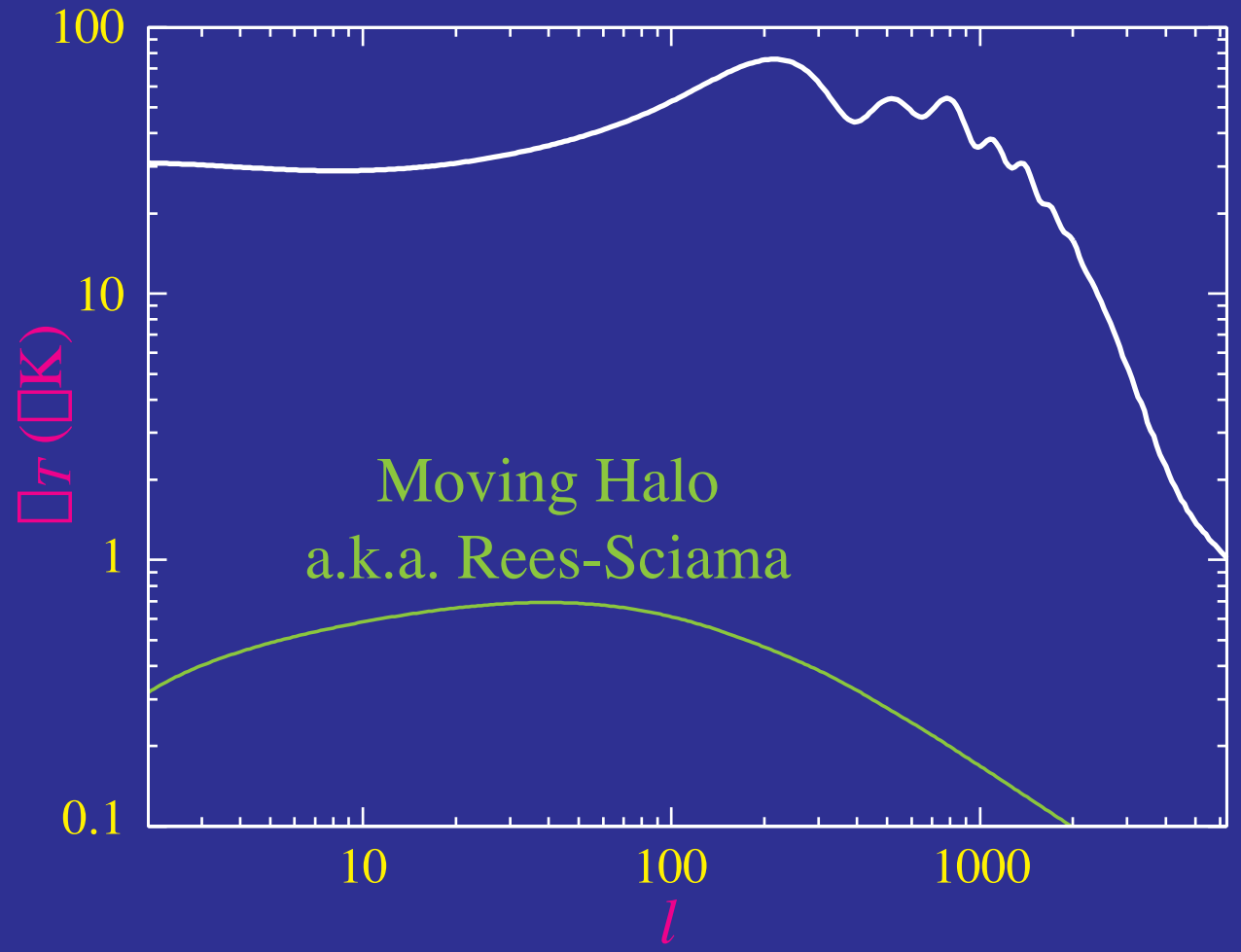

SZ Effect

Modulated Doppler Effect

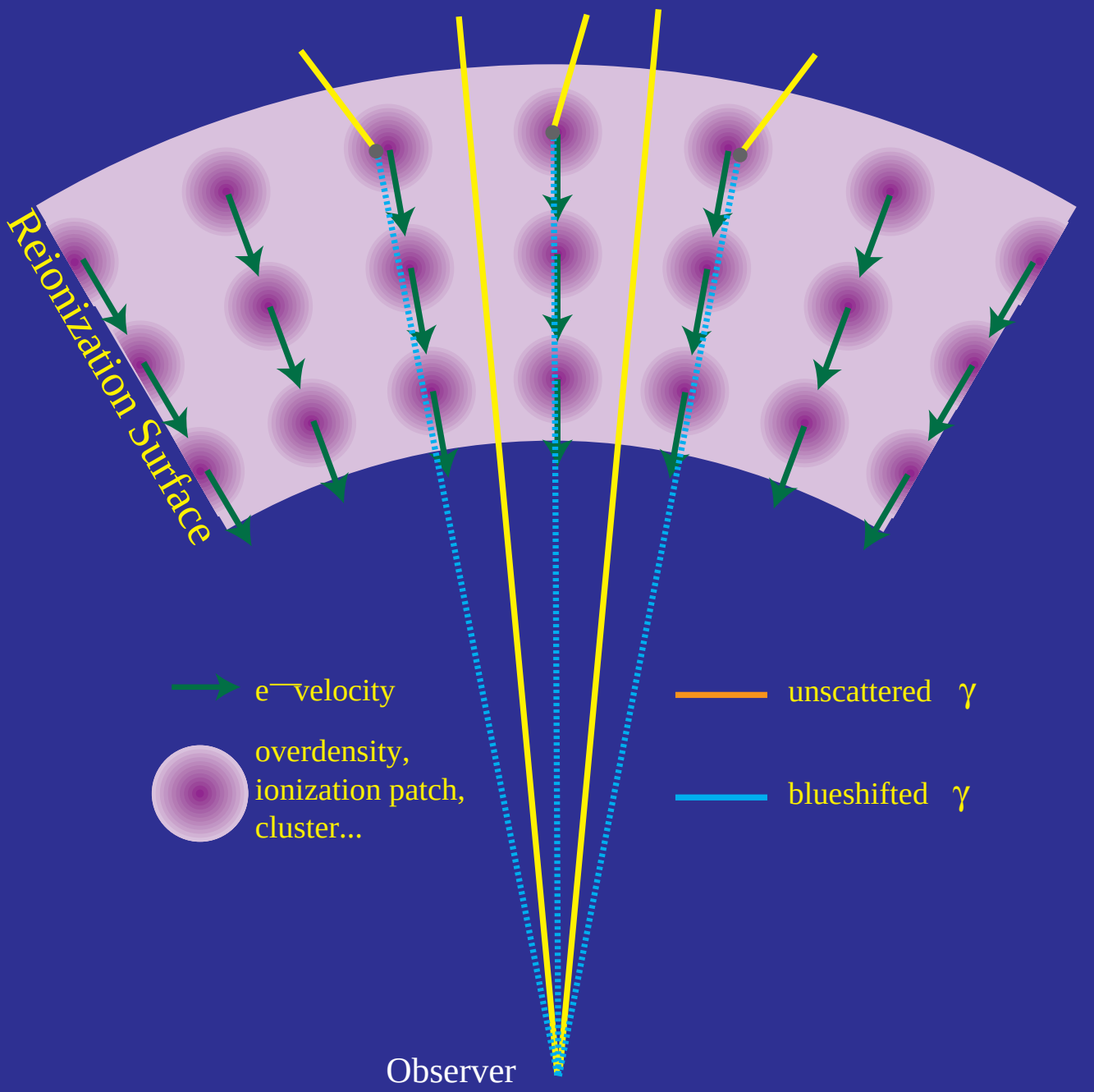

Thermal SZ Effect

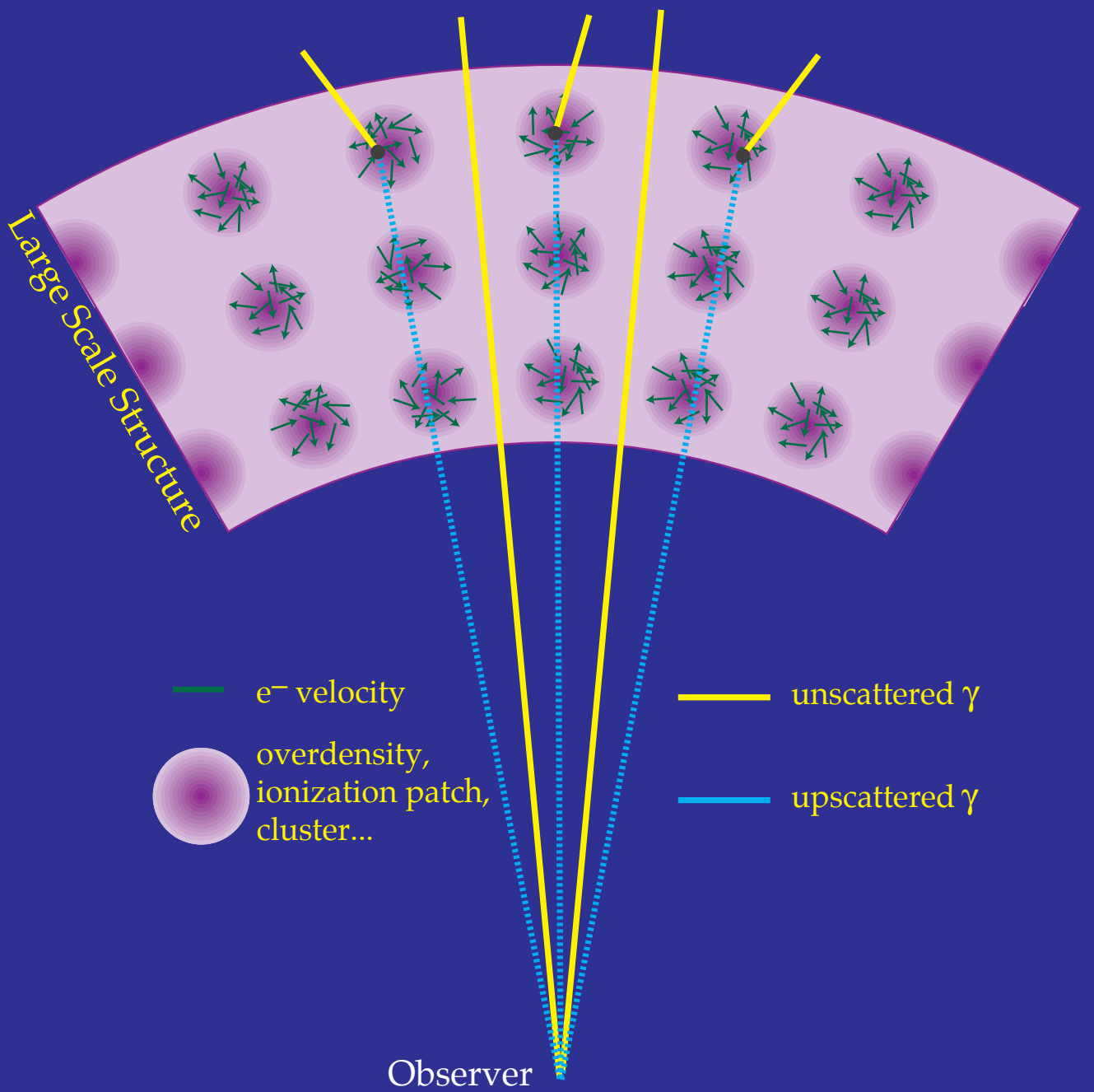

Scattering Secondaries

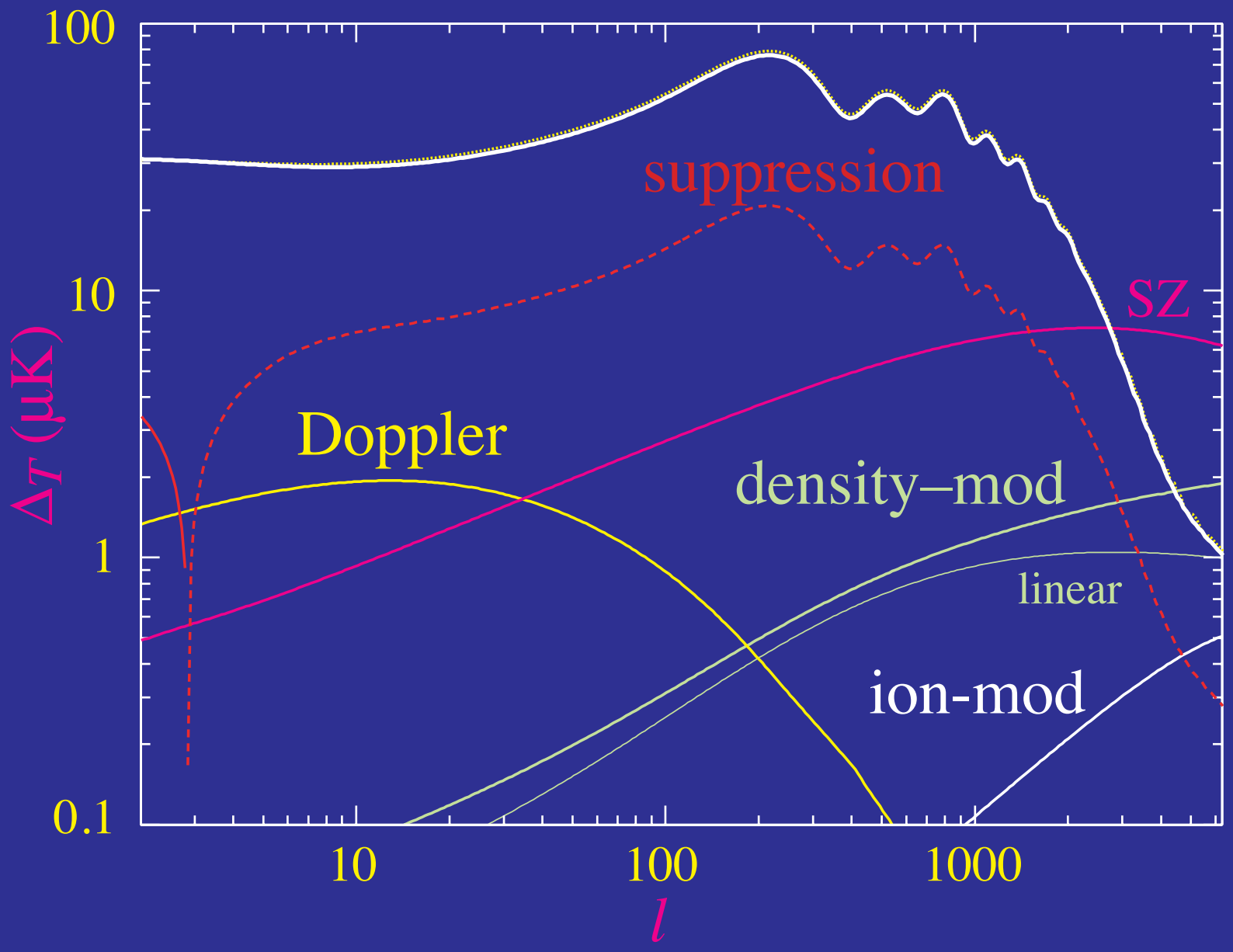

Beyond Thomson Limit

- Thomson scattering $e_i + \gamma_i \rightarrow e_f + \gamma_f$ in rest frame where the frequencies $\omega_i = \omega_f$ (elastic scattering) cannot strictly be true
- Photons carry off E/c momentum and so to conserve momentum the electron must recoil
- Doppler shift from transformation from rest frame contains second order terms
- General case (arbitrary electron velocity)

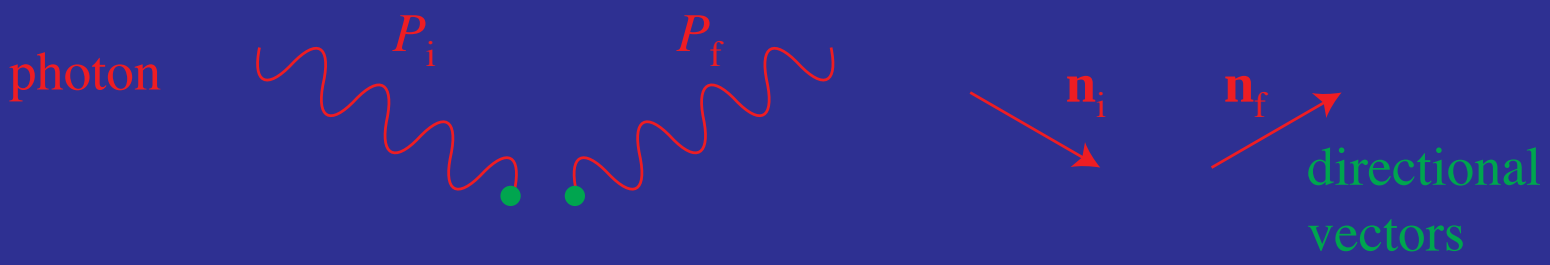

Energy-Momentum Conservation

- From energy-momentum conservation, the energy change is

$$\frac{E_f}{E_i} = \frac{1 - \beta_i \cos\alpha_i}{1 - \beta_i \cos\alpha_f + \frac{E_i}{\gamma m c^2}(1 - \cos\theta)}$$

  where $\hat{\mathbf{n}}_f \cdot \mathbf{v}_i = v_i \cos\alpha_f$ and $\hat{\mathbf{n}}_i \cdot \mathbf{v}_i = v_i \cos\alpha_i$

- Two ways of changing the energy: Doppler boost β_i from incoming electron velocity and E_i non-negligible compared to $\gamma m c^2$

- Isolate recoil in incoming electron rest frame $\beta_i = 0$ and $\gamma = 1$

$$\left.\frac{E_f}{E_i}\right|_{\text{rest}} = \frac{1}{1 + \frac{E_i}{mc^2}(1 - \cos\theta)}$$

Recoil Effect

- Since $-1 \leq \cos\theta \leq 1$, $E_f \leq E_i$, energy is lost from the recoil except for purely forward scattering
- The backwards scattering limit is easy to see

$$|\mathbf{q}_f| = m|\mathbf{v}_f| = 2\frac{E_i}{c}\,,$$

$$\Delta E = \frac{1}{2}mv_f^2 = \frac{1}{2}m\left(\frac{2E_i}{mc}\right)^2 = 2\frac{E_i}{mc^2}E_i$$

$$E_f = E_i - \Delta E = (1 - 2\frac{E_i}{mc^2})E_i \approx \frac{E_i}{1 + 2\frac{E_i}{mc^2}}$$

Second Order Doppler Shift

- Doppler effect: consider the limit of $\beta_i \ll 1$ then expand to first order

$$\frac{E_f}{E_i} = 1 - \beta_i \cos\alpha_i + \beta_i \cos\alpha_f - \frac{E_i}{mc^2}(1 - \cos\theta)$$

however averaging over angles the Doppler shifts don't change the energies

- To second order in the velocities, the Doppler shift transfers energy from the electron to the photon in opposition to the recoil

$$\frac{E_f}{E_i} = 1 - \beta_i \cos\alpha_i + \beta_i \cos\alpha_f + \beta_i^2 \cos^2\alpha_f - \frac{E_i}{mc^2}$$

$$\langle\frac{E_f}{E_i}\rangle \approx 1 + \frac{1}{3}\beta_i^2 - \frac{E_i}{mc^2}$$

Thermalization

- For a thermal distribution of velocities

$$\frac{1}{2}m\langle v^2\rangle = \frac{3kT}{2} \qquad \beta_i^2 \approx \frac{3kT}{mc^2} \rightarrow \langle \frac{E_f}{E_i} - 1\rangle \sim \frac{kT - E_i}{mc^2}$$

  so that if $E_i \ll kT$ the photon gains energy and $E_i \gg kT$ it loses energy $\rightarrow$ this is a thermalization process

Kompaneets Equation

- Radiative transfer or Boltzmann equation

$$\frac{\partial f}{\partial t} = \frac{1}{2E(p_f)} \int \frac{d^3 p_i}{(2\pi)^3} \frac{1}{2E(p_i)} \int \frac{d^3 q_f}{(2\pi)^3} \frac{1}{2E(q_f)} \int \frac{d^3 q_i}{(2\pi)^3} \frac{1}{2E(q_i)}$$
$$\times (2\pi)^4 \delta(p_f + q_f - p_i - q_i) |M|^2$$
$$\times \{ f_e(q_i) f(p_i)[1 + f(p_f)] - f_e(q_f) f(p_f)[1 + f(p_i)] \}$$

- Matrix element is calculated in field theory and is Lorentz invariant. In terms of the rest frame $\alpha = e^2/\hbar c$ (Klein Nishina Cross Section)

$$|M|^2 = 2(4\pi)^2 \alpha^2 \left[\frac{E(p_i)}{E(p_f)} + \frac{E(p_f)}{E(p_i)} - \sin^2 \beta \right]$$

with β as the rest frame scattering angle

Kompaneets Equation

- The Kompaneets equation ($\hbar = c = 1$)

$$\frac{\partial f}{\partial t} = n_e \sigma_T c \left(\frac{kT_e}{mc^2}\right) \frac{1}{x^2} \frac{\partial}{\partial x} \left[x^4 \left(\frac{\partial f}{\partial x} + f(1+f) \right) \right] \qquad x = \hbar\omega / kT_e$$

takes electrons as thermal

$$f_e = e^{-(m-\mu)/T_e} e^{-q^2/2mT_e} \qquad \left[n_e = e^{-(m-\mu)/T_e} \left(\frac{mT_e}{2\pi}\right)^{3/2} \right]$$

$$= \left(\frac{2\pi}{mT_e}\right)^{3/2} n_e e^{-q^2/2mT_e}$$

and assumes that the energy transfer is small (non-relativistic electrons, $E_i \ll m$

$$\frac{E_f - E_i}{E_i} \ll 1 \qquad [\mathcal{O}(T_e/m, E_i/m)]$$

Kompaneets Equation

- Equilibrium solution must be a Bose-Einstein distribution since Compton scattering does not change photon number
- Rate of energy exchange obtained from integrating the energy $\times$ Kompeneets equation over momentum states

$$\frac{\partial u}{\partial t} = 4 n_e \sigma_T c \frac{k T_e}{m c^2} \left[1 - \frac{T_\gamma}{T_e} \right] u$$

$$\frac{1}{u} \frac{\partial u}{\partial t} = 4 n_e \sigma_T c \frac{k (T_e - T_\gamma)}{m c^2}$$

- The analogue to the optical depth for energy transfer is the Compton y parameter

$$d\tau = n_e \sigma_T ds = n_e \sigma_t c dt$$

$$dy = \frac{k (T_e - T_\gamma)}{m c^2} d\tau$$

Spectral Distortion

- Compton upscattering: *y*–distortion
- Redistribution: μ-distortion

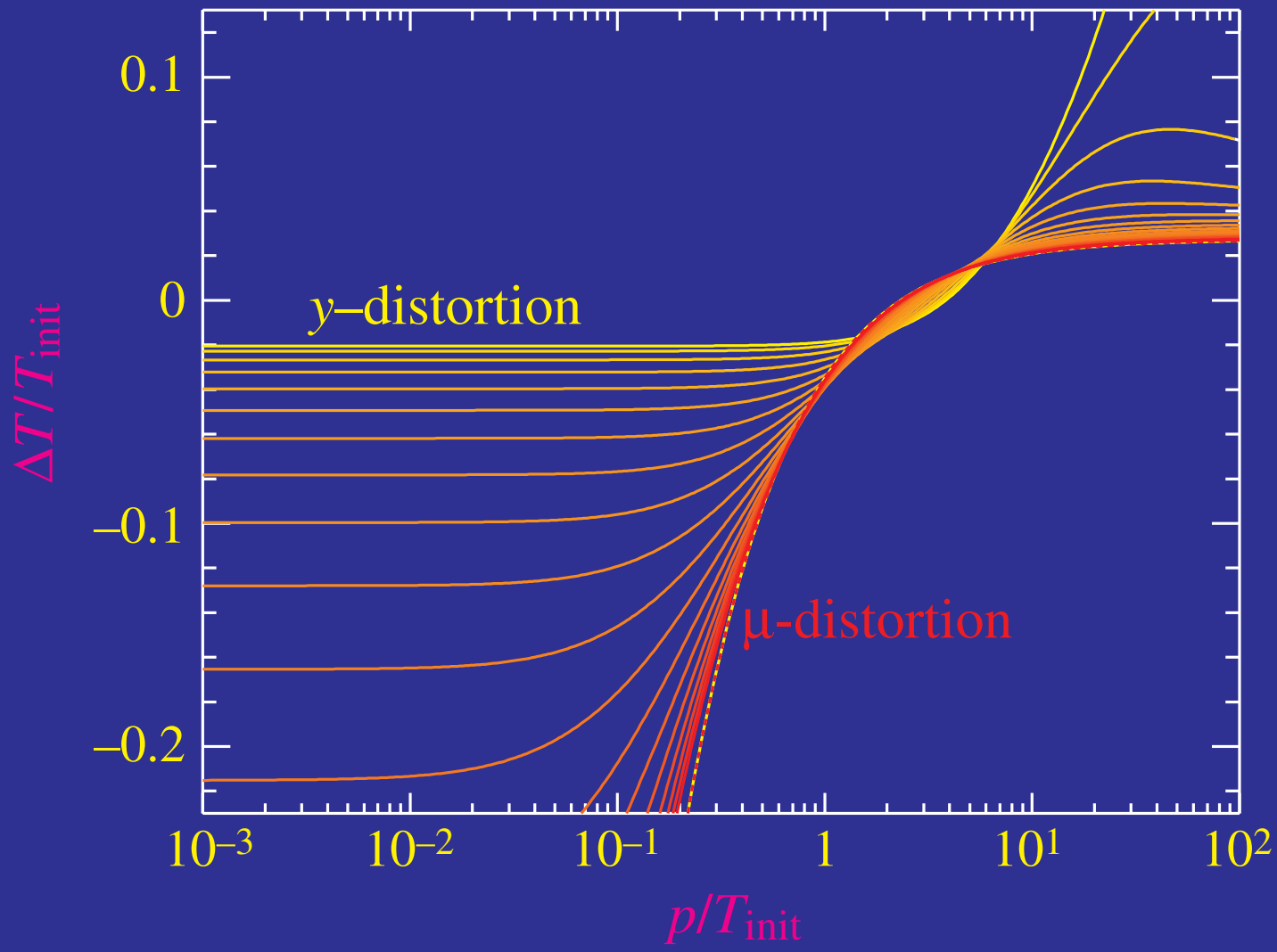

Thermal SZ Effect

- Second order Doppler effect escapes cancellation
- Velocities: thermal velocities in a hot cluster (1-10keV)
- Dominant source of arcminute anisotropies – turns over as clusters are resolved

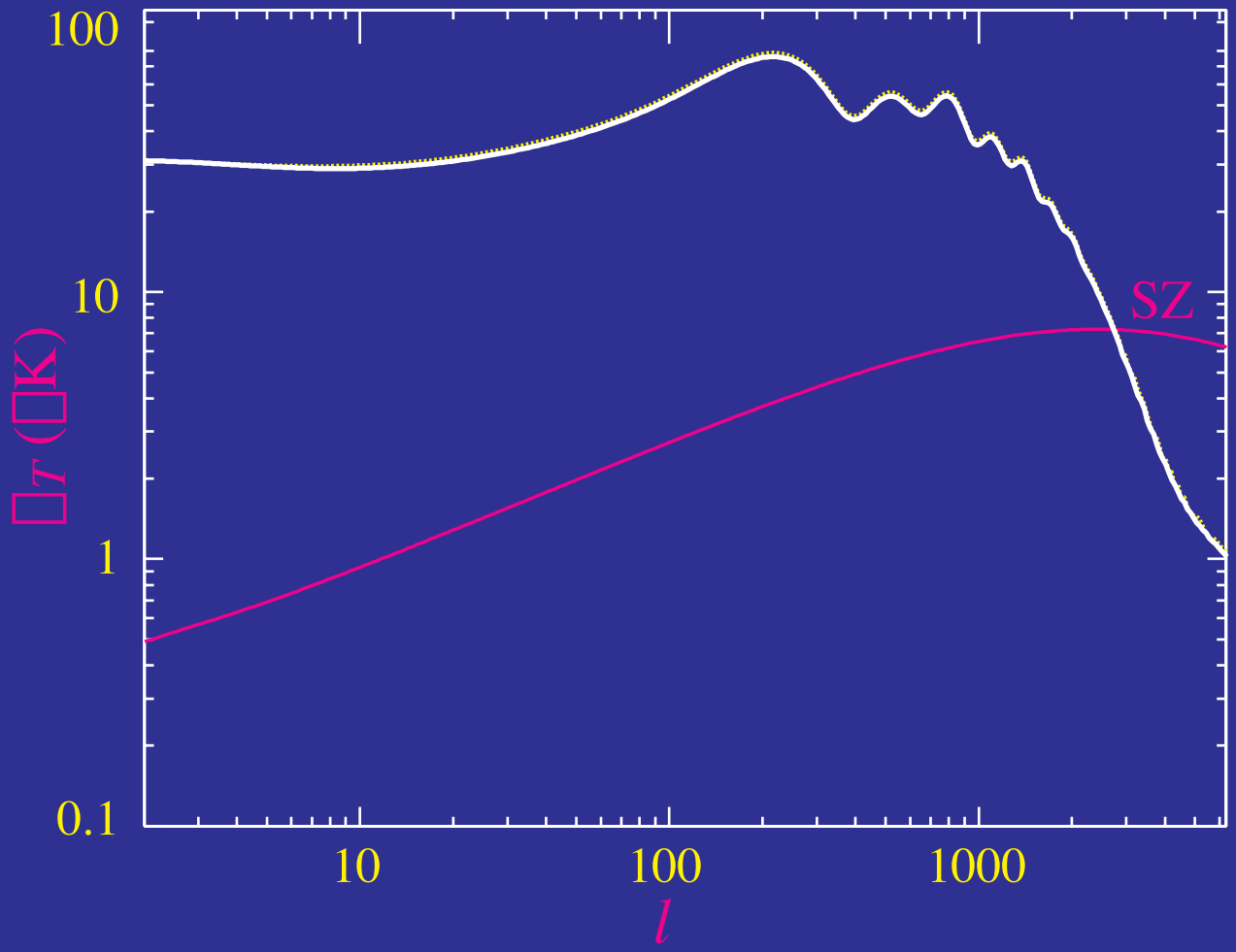

Amplitude of Fluctuations

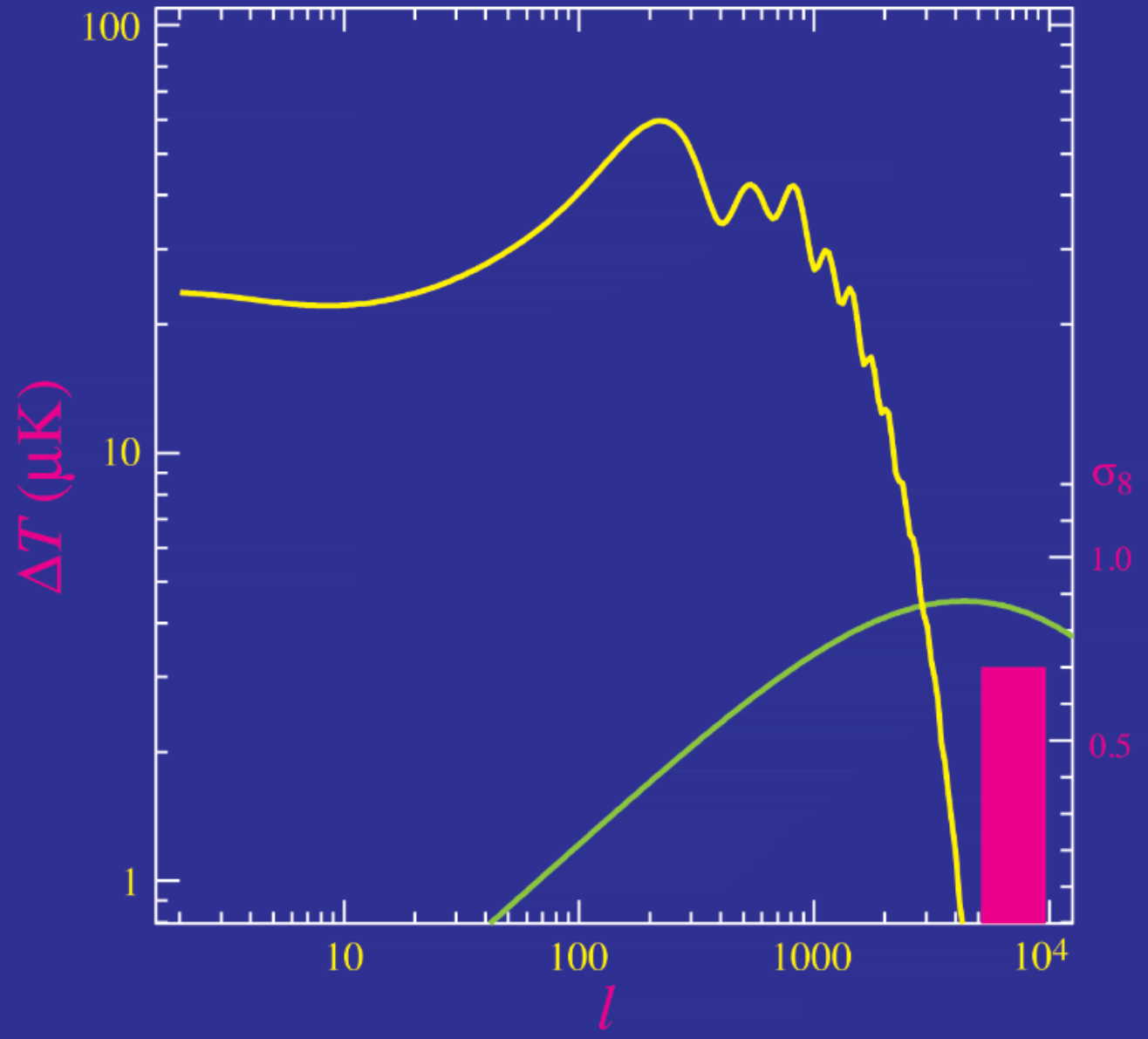

Clusters in Power Spectrum?

- Excess in arcminute scale CMB anisotropy from CBI

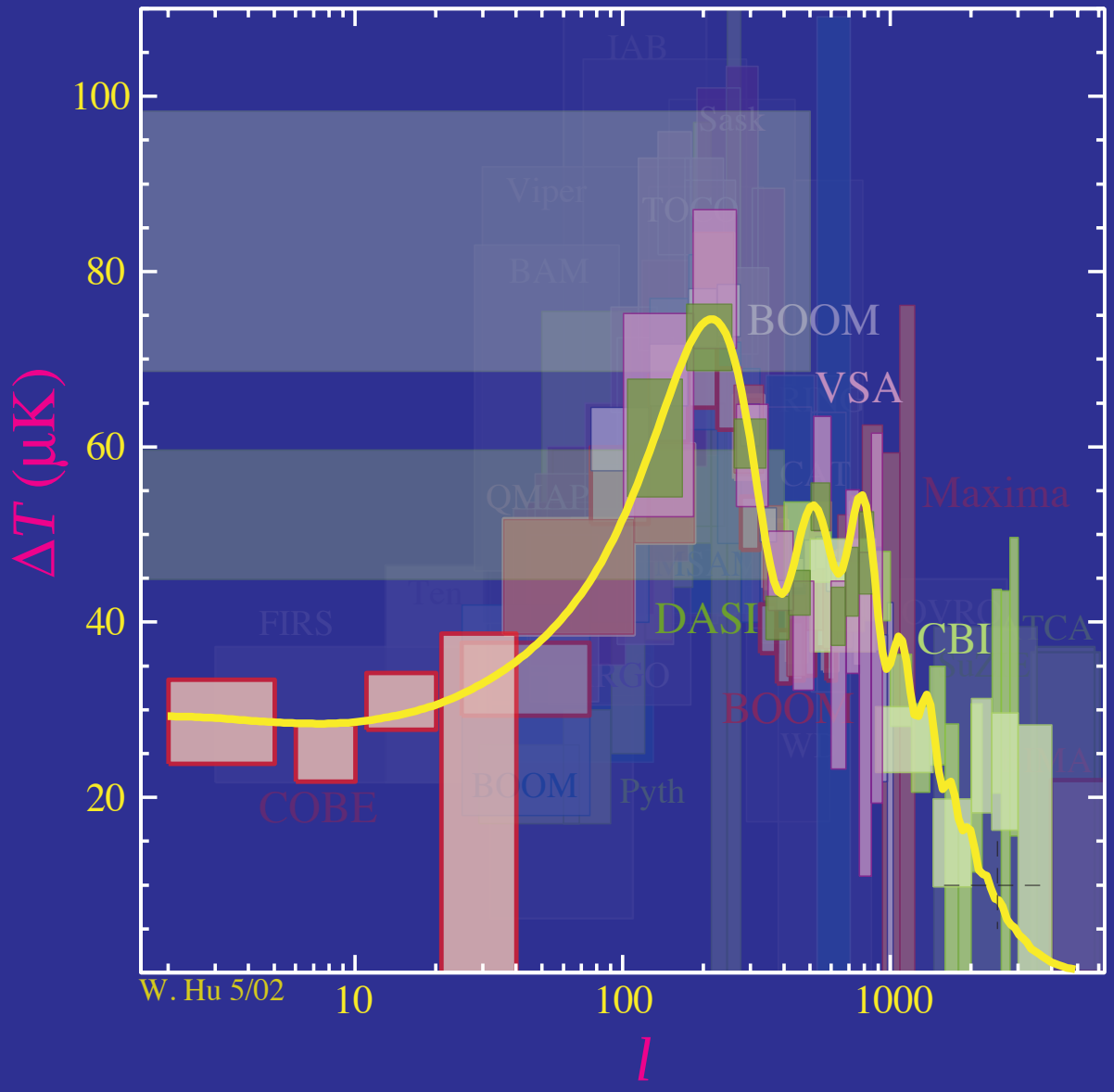

Power Spectrum Present

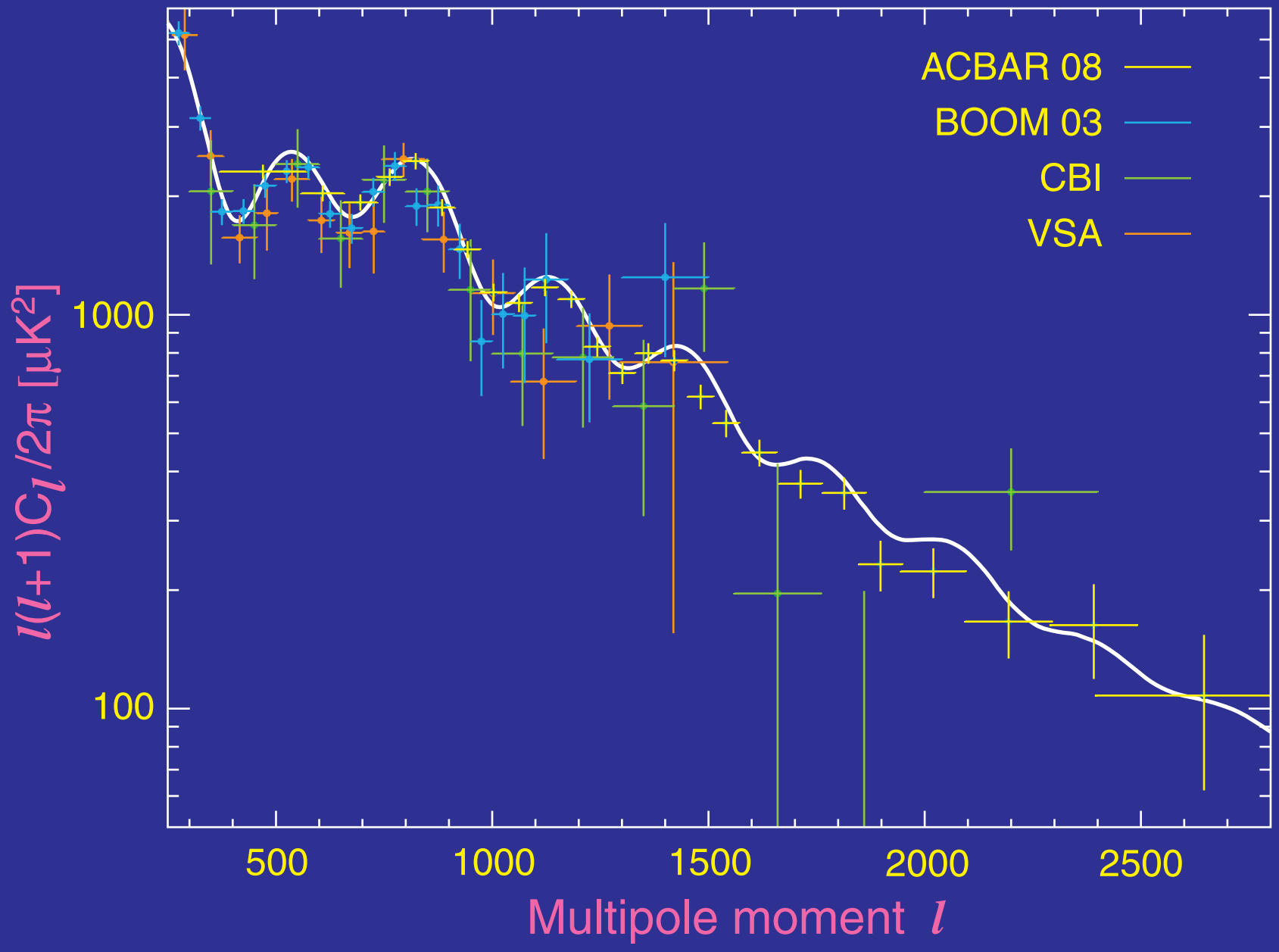

Counting Halos for Dark Energy

- Number density of massive halos extremely sensitive to the growth of structure and hence the dark energy
- Massive halos can be identified by the hot gas they contain

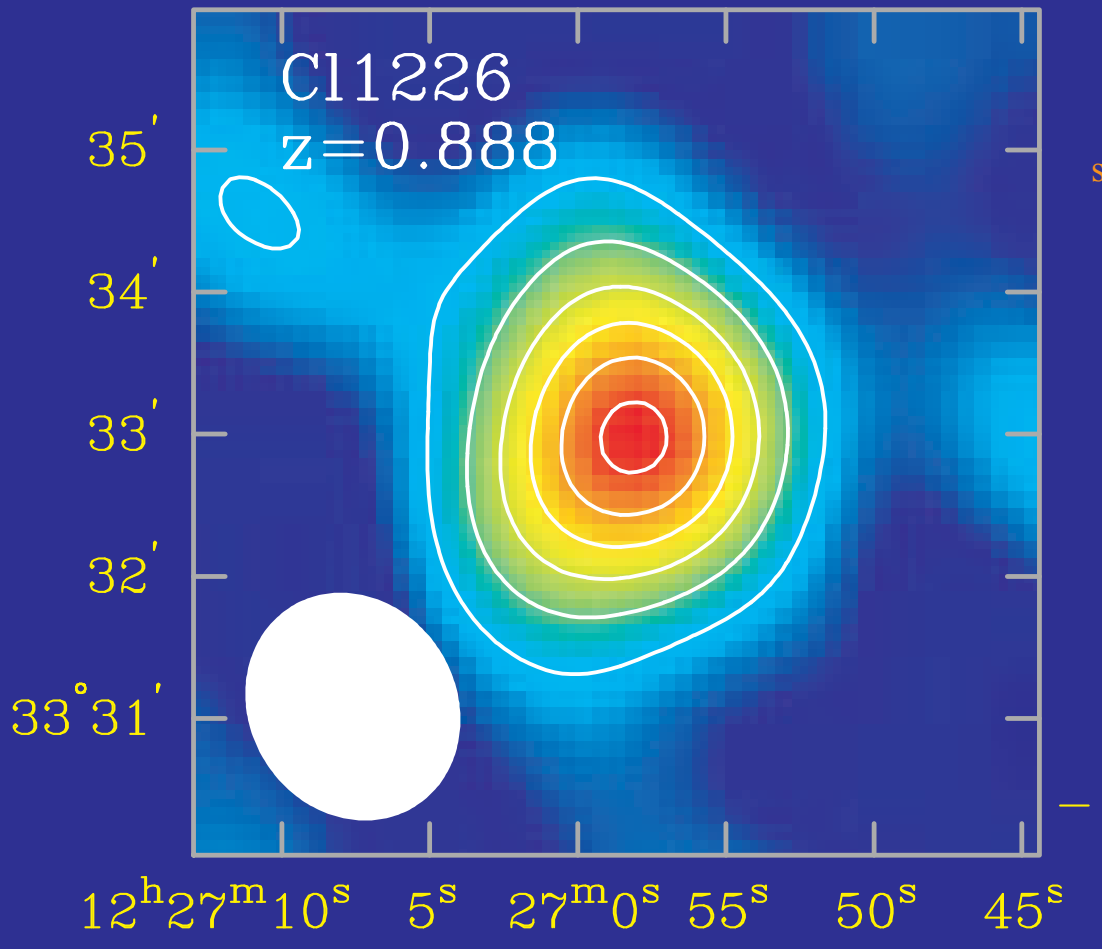

see Jack Sayers' talk

Carlstrom et al. (2001)

SPT Discovered Clusters

- Previously unknown clusters

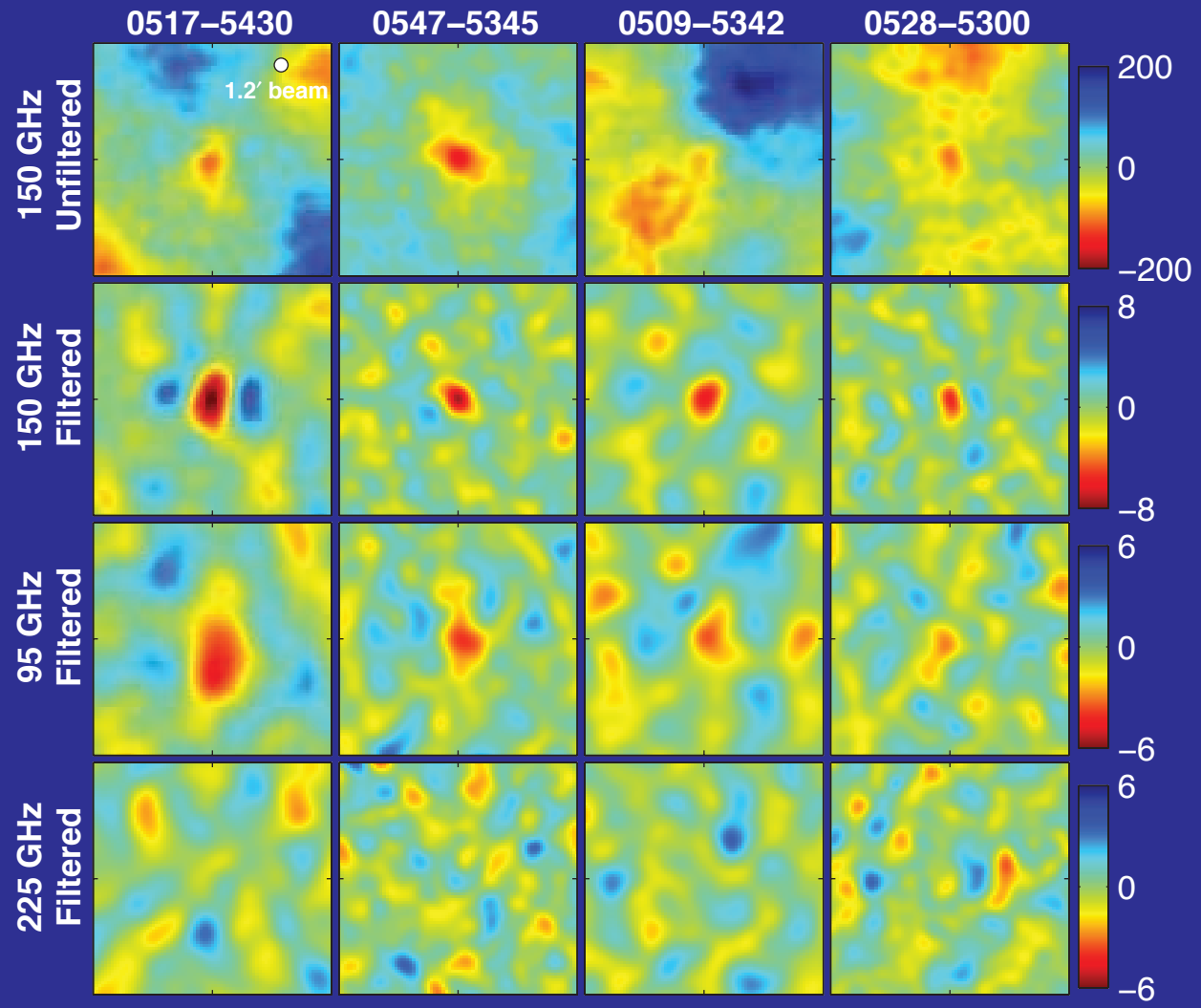

Staniszewski et al (2008)

Mass-Observable Degeneracy

- Uncertainties in bias and scatter cause degeneracies with dark energy

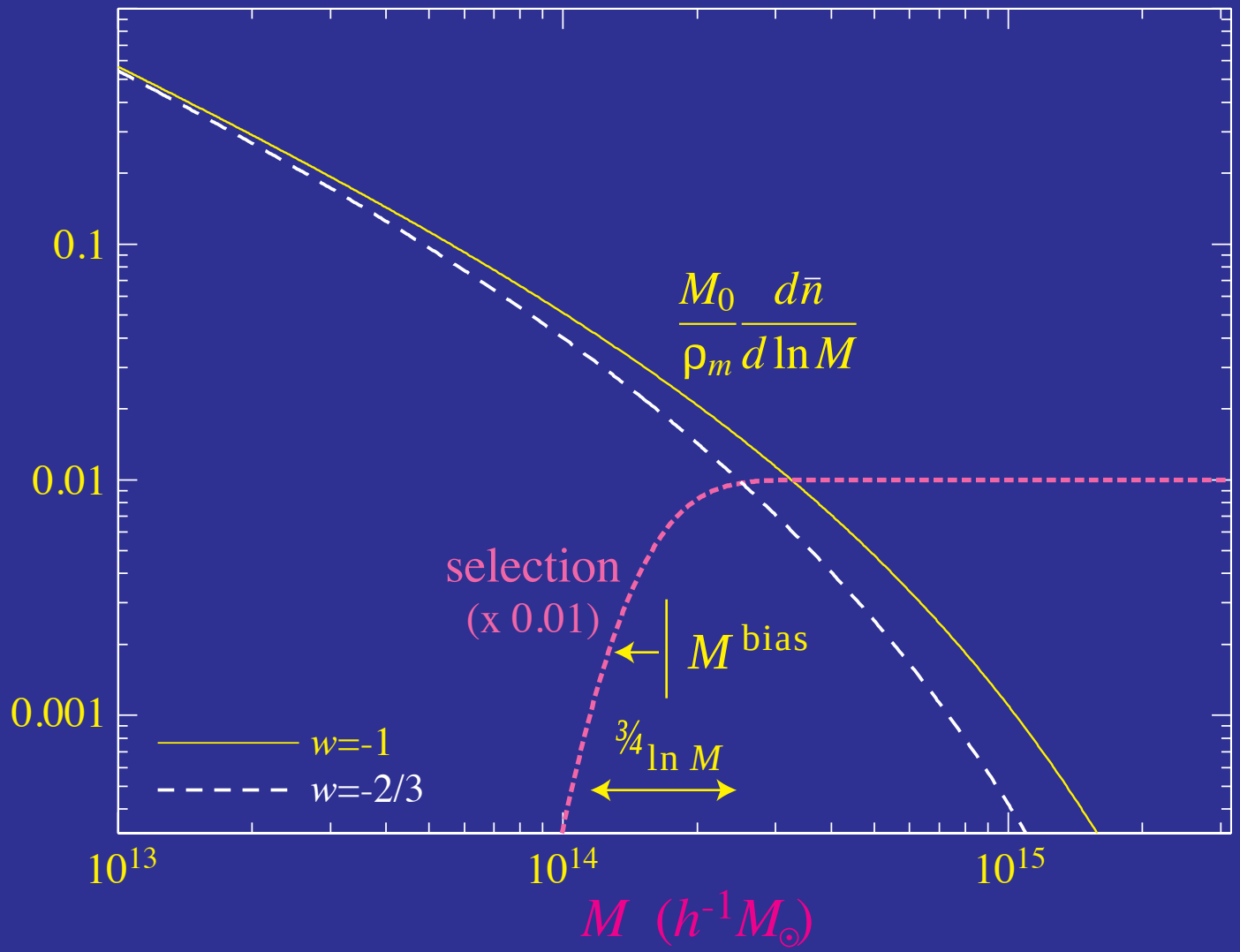

see talks of
Carlos Cunha
Alexie Leauthaud

Fully Calibrated

- Given a completely known observable-mass distribution dark energy constraints are quite tight (4000 sq deg, $z<2$)

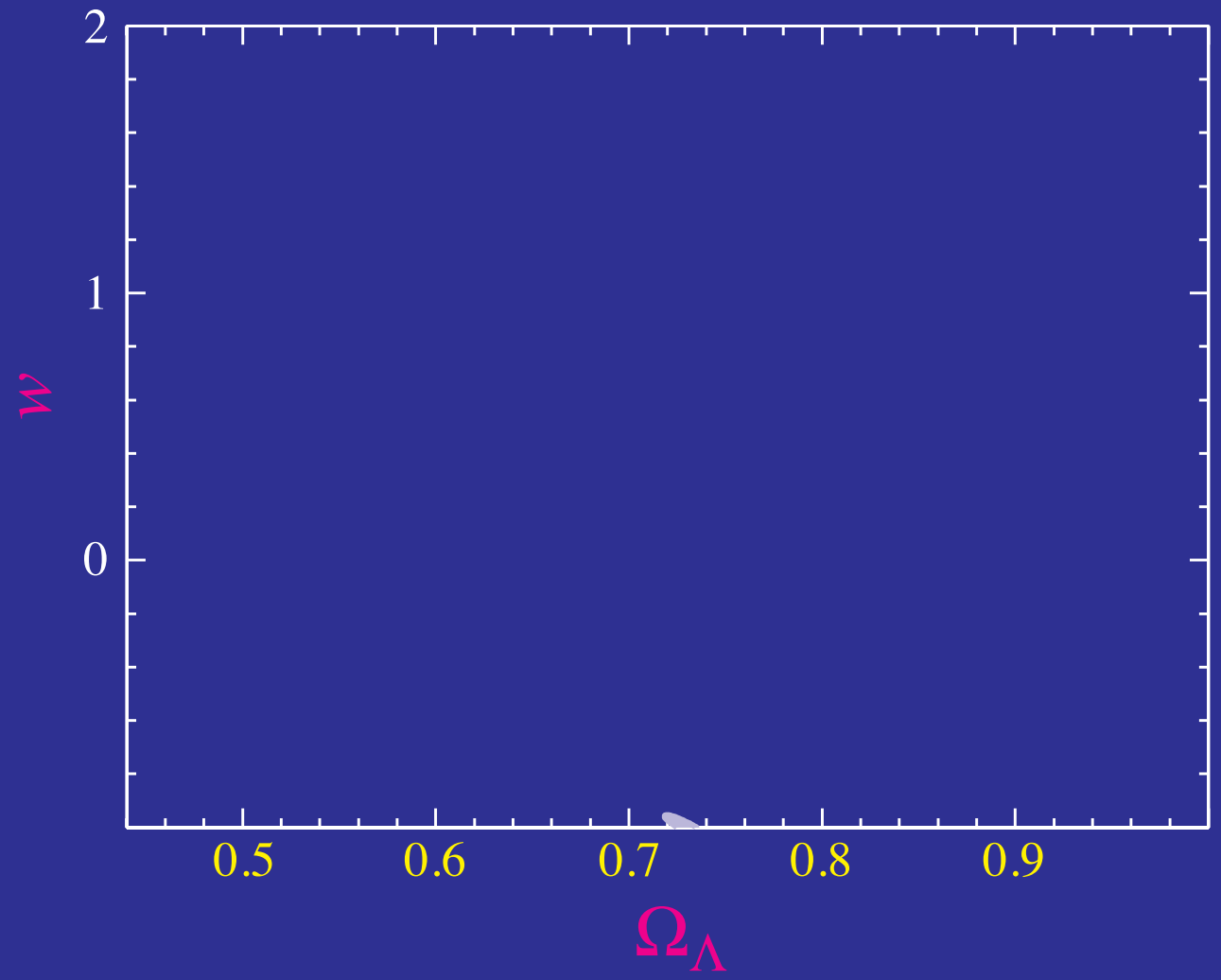

Un-Calibrated

- Marginalizing scatter (linear z evolution) and bias (power law evolution) destroys all dark energy information

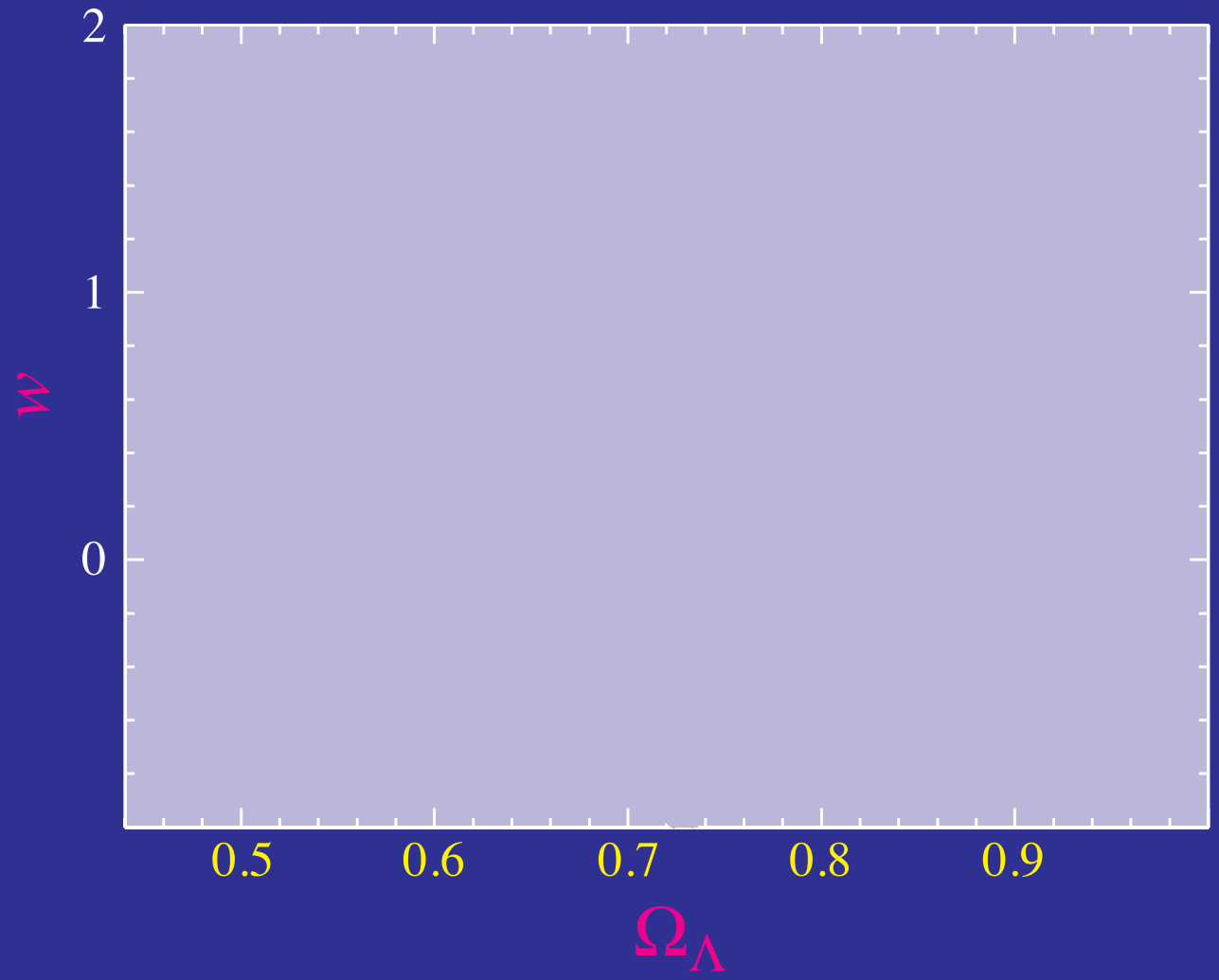

Joint Self-Calibration

- Both counts and their variance as a function of binned observable
- Many observables allows for a joint solution of a mass independent bias and scatter with cosmology

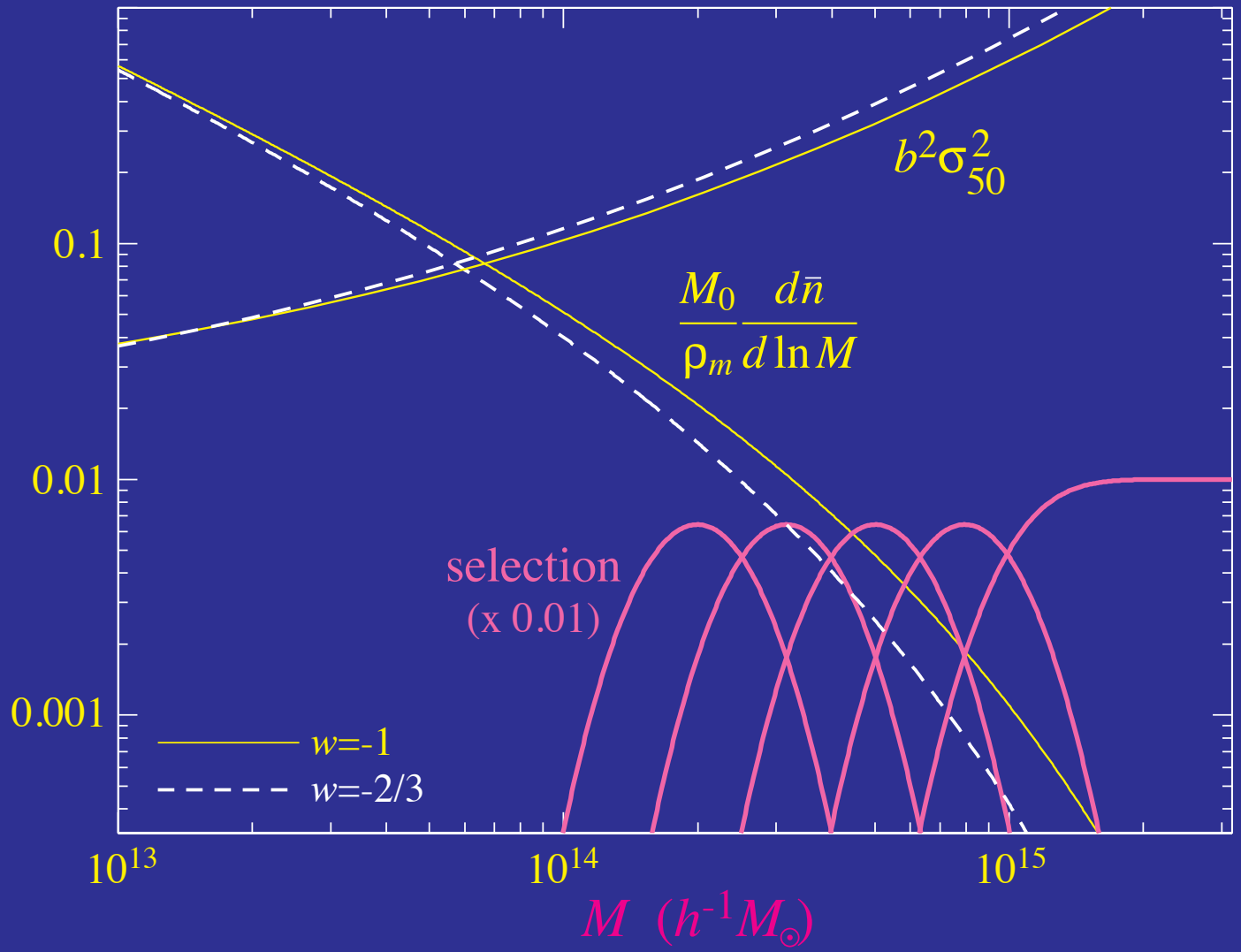

Joint Self Calibration

- Power law evolution of bias and cubic evolution of scatter in z

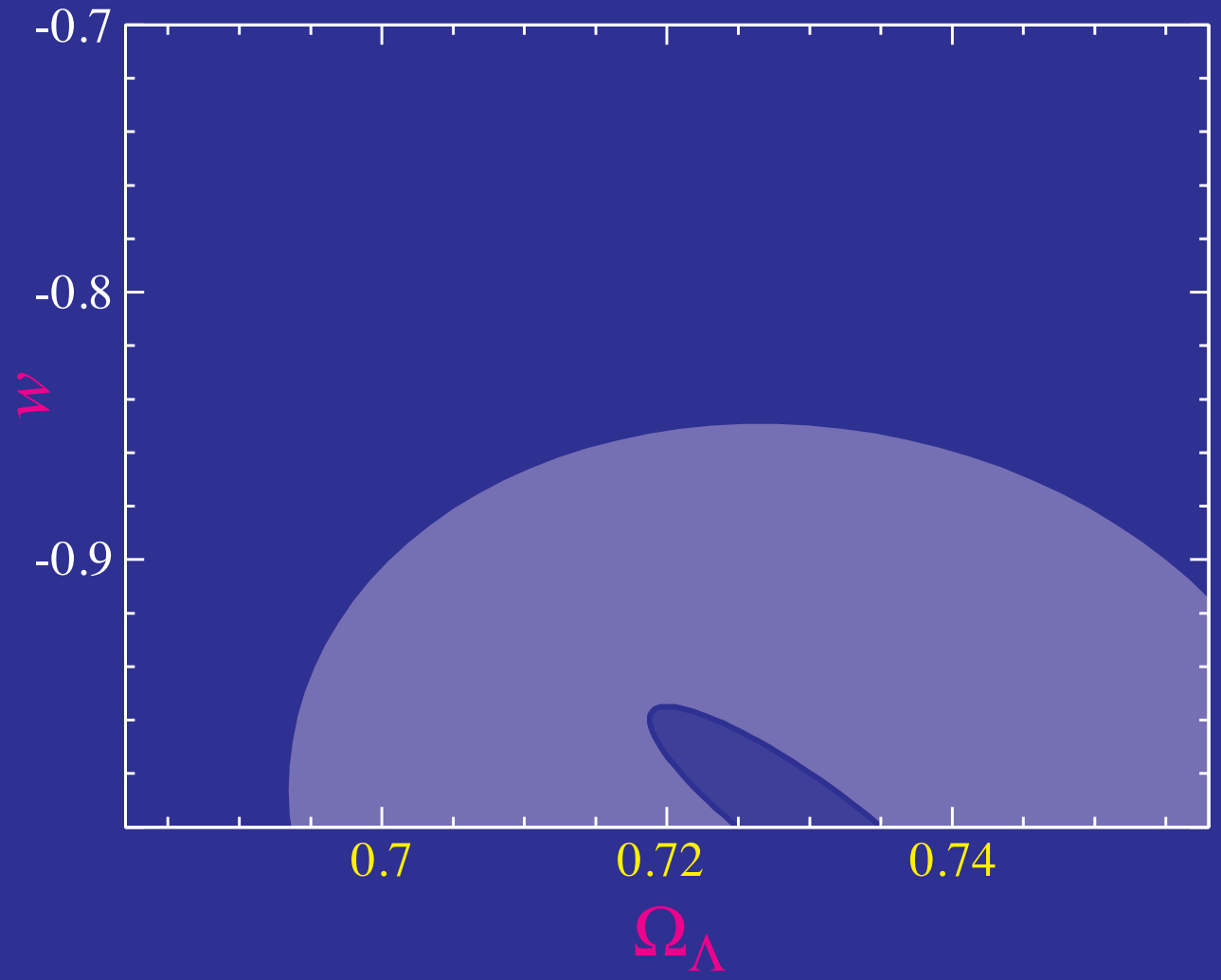

Modified Gravity $f(R)$ Simulations

- For large background field, compared with potential depth, enhanced forces and structure

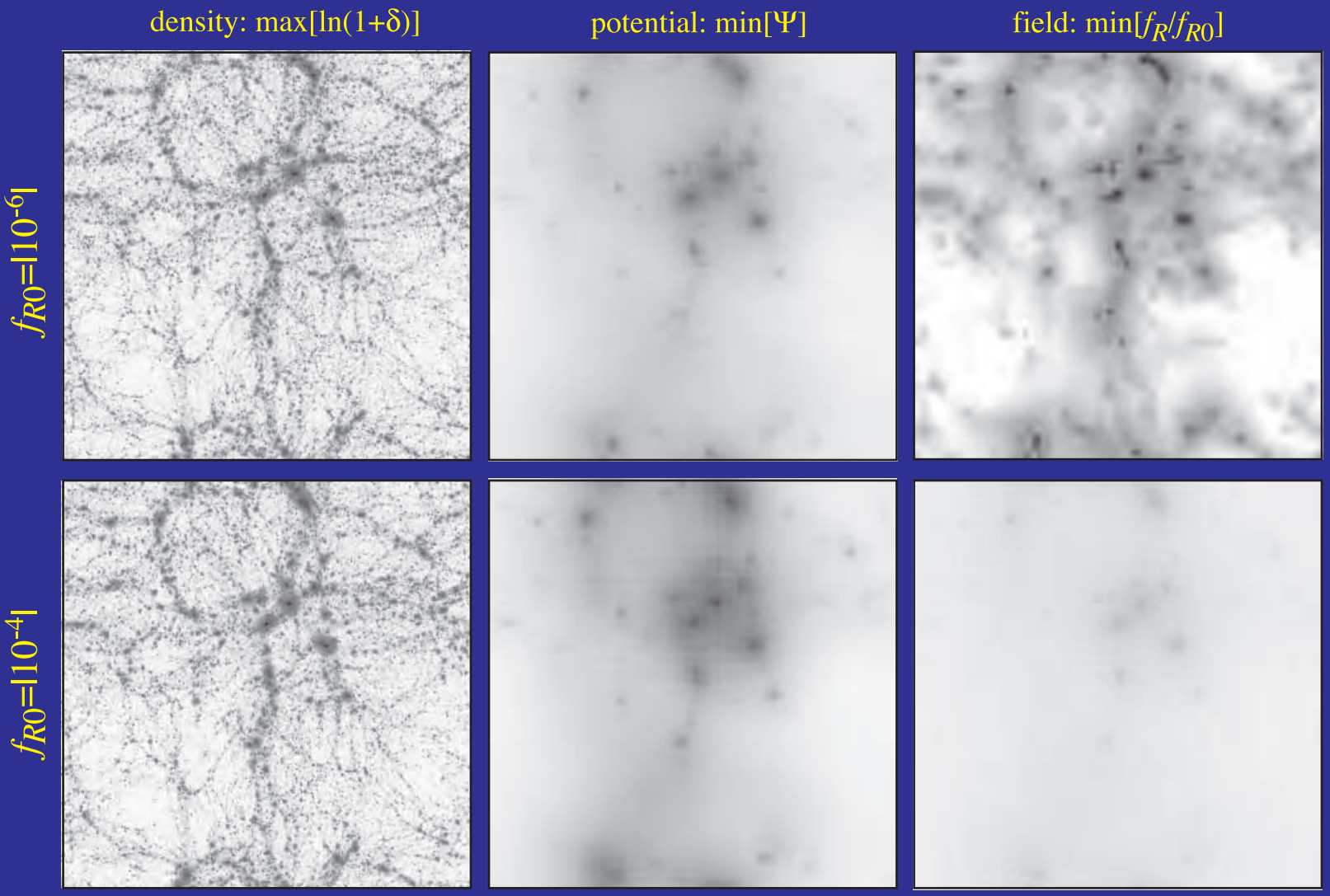

Oyaizu, Lima, Hu (2008)

Mass Function

- Enhanced abundance of rare dark matter halos (clusters) with extra force

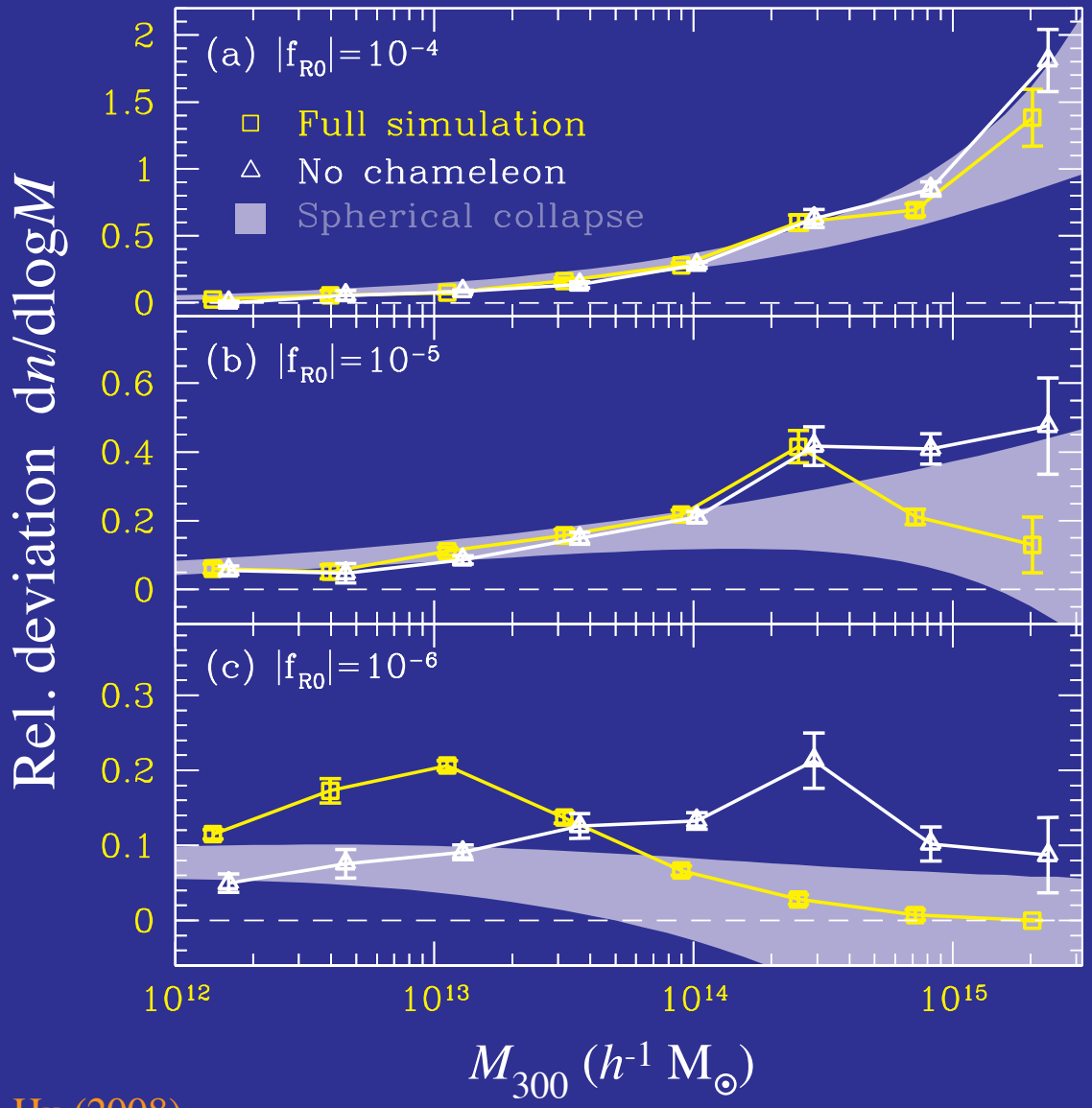

Schmidt, Lima, Oyaizu, Hu (2008)

Summary: Lecture III

- Differential gravitational redshifts from evolving structure causes integrated Sachs-Wolfe (ISW) effect
- Appears on large angles and contributes to quadrupole comparably to primary
- Tests the microphysics of acceleration: clustering of dark energy, modified gravity, dark matter interactions
- Compton scattering leads to energy transfer and thermal SZ effect to second order in velocity
- Unresolved gas clumps generate excess arcminute power
- Resolved clusters provide sensitive test of microphysics of acceleration through counts if masses calibrated